



UNIVERSITY OF TRENTO

International PhD Program in Biomolecular Sciences

XXVIII Cycle

“Cis and Trans, p53 and NF- κ B rules of transactivation”

Tutor

Prof. Alberto Inga
Laboratory of Transcriptional Networks
CIBIO, University of Trento, Italy

Ph.D. Thesis of
Vasundhara Sharma
Laboratory of Transcriptional Networks
CIBIO, University of Trento, Italy

Academic Year 2014-2015

Declaration of Authorship

I, Vasundhara Sharma, confirm that this is my own work and the use of all material from other sources has been properly and fully acknowledged.

Signature of the candidate

Vasundhara Sharma

Acknowledgements

More than three years have been passed since I started my PhD project in Bimolecular Sciences at the University of Trento, Italy. It is difficult to mention the name of each and every person who has contributed in my wonderful journey as a PhD Fellow in their unique manner. Mainly, I would like to thank my tutor Prof. Alberto Inga for supporting me all this time at every possible step and making my PhD journey a fruitful and successful venture. Also, I would like to thank Dr Tali E Haran (Israel Institute of Technology, Israel) with whom I worked for a considerable amount of time at the University of Trento. Additionally, I am grateful Prof. Lucilia Saraiva for hosting me in her laboratory at University of Porto, Portugal, for a period of two months. Also, an equal share of acknowledgment goes to Dr Hector Viadiu and Dr Paola Monti for allowing me to associate with them in their scientific endeavours. On a more personal note, I am thankful to Dr. Yari Ciribilli, Dr. Alessandra Bisio and all the members of Laboratory of Transcriptional Networks and Laboratory of Molecular Cancer Genetics.

I am also grateful to the PhD school for giving me opportunity to be part of a special PhD program.

The non-scientific thanks go to my family and friends who supported me from across the globe each and every day of my stay in Italy.

Abbreviations

5-FOA	5 Flurooratic acid
ChIP	Chromatin Immunoprecipitation
ChIP-Seq	Chromatin Immunoprecipitation sequencing
CORE	<u>C</u> ounter-selectable Marker and <u>R</u> eporter gene
DOXO/DXR	Doxorubicin
DT/DOXO+TNF	Doxorubicin + Tumour Necrosis Factor alpha
FASAY	Functional analysis of separated alleles in yeast
FLUC/RLUC	Firefly Luciferase/Renilla Luciferase
G418	Geneticin
I κ B	Inhibitory Kappa B Protein
IKK	I κ B Kinase
LHS/RHS	Left half site/Right half site
LPS	Lipopolysaccharide
LR/RL	Left Right/ Right Left
MDM2	Mouse Double Minute 2
N-terminal	Amino terminal domain
PBM	Protein binding Microarrays
PeT	Paired end tags
pur/pyr	purine/pyrimidine
qPCR	Quantitative Polymerase chain reaction

RE	Response Element
RHD	Rel homology domain
RTCA	Real time cell analysis
RT-PCR	Reverse transcriptase Polymerase chain reaction
Selex	Systematic Evolution of Ligands By Exponential Enrichment
TA	Transactivation Assay or Transactivation Active (<i>e.g.</i> TAp53)
TF	Transcription factor
TLR	Toll-like receptors
TNF α	Tumor Necrosis Factor alpha
TSS	Transcriptional Start Site

INDEX

ABSTRACT	p.8
<i>Research project 1</i>	p.10
A systematic evaluation of variably organized p53 and NF-κB Response Elements	
INTRODUCTION	
Using yeast as a tool to study human Transcription Factors	p.11
Yeast as a tool to dig on functionality of Response Elements	p.12
<i>Delitto Perfetto</i> : Orchestrating <i>cis</i> regulatory elements inside yeast	p.13
The tumor suppressor p53 and its isoforms	p.16
p53 regulating circuit board	p.17
p53: Sequence specificity as a transcription factor	p.20
Mutant p53 as a tool to study RE-dependent transactivation specificity	p.23
Siblings of p53: p63 and p73	p.25
NF-κB family of transcription factors	p.27
METHODS	p.31
RESULTS	p.36
Part A. p53 studies	
1. “within-RE” sequence code for transactivation capacity	p.36
Impact of consensus changes within the canonical or half site p53 REs on transactivation	
2 “ <i>outside-the-RE</i> ” sequence code for transactivation capacity	p.43
2.1 Impact of sequence flanking the p53 RE on transactivation	
2.2 Impact of sequence flanking the p53 RE on relative transactivation strength of a bidirectional promoter	p.49

Part B. NF- κ B studies

1. Quantitative analysis of transactivation potential and specificity of NF- κ B proteins in yeast and human cell lines	p.58
Publication: Quantitative Analysis of NF- κ B Transactivation Specificity Using a Yeast-Based Functional Assay. Sharma V , Jordan JJ, Ciribilli Y, Resnick MA, Bisio A, Inga A. <i>PLoS One</i> . 2015 Jul 6;10(7):e0130170. doi: 10.1371/journal.pone.0130170. eCollection 2015.PMID:26147604	
DISCUSSION	p.88
<u>Project Target 2</u>	
2. p53 and NF- κ B as partners in crime	p.90
Molecular mechanisms contributing to Doxorubicin and TNF α synergy	
2.1 MATERIALS AND METHODS	p. 93
2.2 RESULTS	
2.2.1 Treatment of A549 cells with doxorubicin + TNF α , synergistically up regulates the genes involved in metastasis, mitosis and kinetochore formation.	p.98
2.2.2 Combined Doxorubicin and TNF α treatments reduce migration potential of A549 cells but enhance the migration of p53 null H1299	p. 101
2.2.3 Impact of Myst family members (HATs), MOF and TIP60 on p53 and NF- κ B transcriptional targets in MCF-7, A549 and H1299 cell lines	p.103
2.2.4 Studying Doxorubicin + TNF α transcriptional synergy with defined promoter fragments from signature genes.	p.109
DISCUSSION	p.111
REFERENCES	p.114
APPENDIX	p.129
Publication: Cooperative interactions between p53 and NF κ B enhance cell plasticity. Bisio A, Zámboorszky J, Zaccara S, Lion M, Tebaldi T, Sharma V , Raimondi I, Alessandrini F, Ciribilli Y, Inga A. <i>Oncotarget</i> . 2014 Dec 15;5(23):12111-25. PMID: 25401416	

ABSTRACT

p53 and NF- κ B families of Transcription Factors (TFs) are among the most studied proteins in tumour biology, typically known to function as antagonists, although recent studies identified example of positive, even cooperative interactions. p53 and NF- κ B act as dimer or dimer of dimers, bind *cis* regulatory elements (referred herein as Response Elements –REs-) of which multiple versions exist in the genome, and coordinate very large networks of target genes, through highly regulated transactivation specificities. TAp53 is a tumour suppressor activated upon genotoxic and physiological stress and involved primarily in deciding senescence, cell cycle arrest or apoptosis as cell fate; the NF- κ B proteins are involved in cell survival, proliferation and innate immunity responses. In our study we tried to elucidate in detail the intrinsic nucleotide preferences of p53 and NF- κ B as sequence specific TFs and their impact on transactivation specificity. Selecting various *in vivo* validated cognate REs and testing various *ad-hoc* sequence permutations, we evaluated the role of identity and positioning of nucleotides in transactivation potential and specificity. To this aim different transcription assays were used, starting from a defined assay in yeast where p53 or NF- κ B protein levels and the sequence of the RE are the only variables.

With human wild type p53, I tested various REs used in co-crystallization studies probing nucleotide positions that are not directly contacted by the p53 DNA binding domain, to explore the effect of DNA conformational shifts on transactivation. Also, we investigated the effect on strength and direction of p53-induced transcription of changes in the nucleotides flanking an RE, selected based on torsional flexibility measurements.

For the NF- κ B family, relA/p65 and NFKB1/p50 were tested as single proteins or when co-expressed using a panel of REs selected based on different DNA binding affinities. The correlation between DNA binding and transactivation potential was examined. Further, the negative modulator I κ B α was co-expressed and its impact measured as a function of NF- κ B protein type, expression level, or RE being tested.

Both for p53 and NF- κ B studies, we confirmed that the hierarchical organization of nucleotides within REs observed with yeast was reasonably well conserved in A549, H1299

or MCF7 human cells using transient transfection and/or treatments to activate endogenous p53 or NF- κ B.

Finally, I contributed to an ongoing study focusing on the interplay between p53 and NF- κ B at the transcriptional level. Using microarrays and quantitative PCR we had observed highly synergistic expression of a group of genes involved potentially in metastasis, cell growth and proliferation upon combined treatment of MCF7 cells with doxorubicin, a chemotherapeutic agent, and TNF α , an inflammatory cytokine. I have studied regions of the promoters of several such synergistic genes carrying putative p53 and NF- κ B binding sites to study *cis*-mediated regulation of gene expression. This led to the investigation of cell type specific effects and the contribution of cofactors in the transcriptional synergy.

Thus the main goals of my thesis work have been:

1. To evaluate the hierarchy of nucleotides in the DNA code read by p53 and NF- κ B as sequence-specific transcription factors.
2. Investigate the conservation of transactivation capacity and specificity between yeast and mammalian systems for the tested panel of REs.
3. Estimate the contribution of physical properties of DNA (torsional rigidity or flexibility) contiguous to a p53 RE in influencing the strength and the direction of transcription.
4. Explore the molecular mechanisms underlying transcriptional synergy in response to Doxorubicin and TNF α treatment

Research Project 1

A systematic evaluation of variably organized
p53 and NF- κ B Response Elements

INTRODUCTION

Using yeast to study human sequence-specific transcription factors

Transcription is a phenomenon involving dynamic, spatial and temporal organization of transcription factors and cofactors on the open chromatin regions scanned by RNA polymerases to synthesize the transcripts. Most of the *trans* factors involved recognize specific DNA codes called Response Elements (REs) within the promoter or enhancer region of a gene to initiate transcription or modulate constitutive transcription rates as part of the responses to specific stimuli. An RE comprises ~6-10 nucleotide motifs with various degree of variability at individual positions resulting in rather loose consensus sequences, usually summarized by weight matrices or logos (1). Hence, TFs can exhibit variable DNA binding affinities towards specific target REs. Many studies have drawn a correlation between the identity of nucleotides at specific positions within an RE and relative binding behaviour of a TF. However, DNA binding affinity may not accurately predicts the transcriptional responsiveness of a promoter, even in defined gene reporter assays, especially for TFs that act as oligomers (dimers or tetramers). The actual contribution of *cis* elements in controlling gene expression *in vivo*, particularly the coordination of large response networks by master genes, can be very elusive (2). Indeed, many *cis*- and *trans*- factors contribute to promoter accessibility, RNA polymerase II recruitment, transcriptional initiation, and elongation.

Considering the primary sequence, enhancer and promoters are composite arrangements of multiple REs. Hence, features like spacer length separating two or more TF binding sites and organization of REs with respect to the transcriptional start site (TSS) impact on binding and transactivation potentials. While various bioinformatics tools and software are available to predict the closeness of input DNA sequences to consensus DNA motifs for transcription factors, such as Jaspar, TOMTOM and TRANSFAC (<http://www.gene-regulation.com/pub/databases.html>), the current tools almost invariably rely on position weight matrices assuming independent contributions of each nucleotide to the score of a binding site. Furthermore, while some tools evaluate co-occurrences of binding sites, there is

little information for predicting the impact of closely spaced binding sites on promoter dynamics.

Yeast as a tool to dig on functionality of Response Elements

The yeast *S. cerevisiae* is a recognized model system for understanding aspects of the biology of human proteins using complementation assays or ectopic expression and functional assays even for the cases where a clear orthologous yeast gene is absent (3-6). For example, techniques such as the Functional Analysis of Separated Alleles in Yeast (FASAY) have been developed and proven to be a reliable tool to evaluate the functional impact of various p53 mutants, one of the most frequently mutated tumour suppressor protein in cancer (7). Briefly, the assay exploits the *ADE2* yeast gene, whose transcription is placed under wild type p53 control by an engineered promoter. Lack of *ADE2* expression resulting from the expression of loss-of-function human p53 cDNA alleles in yeast would lead to small red colonies on plates containing low adenine amounts due to building up of a coloured metabolic intermediate. p53-dependent *ADE2* expression results in yeast cells becoming proficient for adenine biosynthesis giving rise to larger, white colonies. This rapid colour assay is combined with a gap repair approach so that each transformant colony growing on the selective media has captured and constitutively expresses a single p53 cDNA allele, obtained from RT-PCR from human RNA samples, including cancer biopsies, hence the FASAY acronym (8). The basic protocol has been refined over the years, for example introducing a split version of the gap repair assay that evaluates separately two portions of the p53 cDNA and is thus more efficient with low quality RNA, as a shorter cDNA amplicon is needed (9). A second improvement consisted in modified p53-responsive promoters that incorporate different versions of p53 REs that led to the identification of p53 mutants that discriminate binding sites (10, 11). The assay has been used to identify functionally inactivating p53 mutations from clinical samples (12, 13), or to generate mutation spectra after in vitro damage of the p53 cDNA with specific drugs (14). The assay has been further modified to include the co-expression of MDM2, a key negative regulator of p53 (15), or 53BP1, BRCA1, BRCA2, p53 interacting proteins that are important cofactors in the DNA damage response (16-19). A similar experimental approach has been developed more recently to test several other mammalian transcription factors

through their expression in yeast, including Estrogen Receptors, homeodomain NKX2-5, bHLH HAND1/E12/E47 (20, 21).

Delitto Perfetto: Orchestrating *cis* regulatory elements in yeast

Delitto Perfetto is a method that utilizes oligonucleotides or longer donor DNA molecules to target chosen genomic loci in yeast exploiting homologous recombination. With this approach site specific mutations, small or large deletions, or insertions method can be rapidly introduced at chromatin sites by a two-step cloning free protocol (22). The whole technique takes 5-6 days to remove a previously integrated double marker cassette (CORE), containing the genes *KIURA3* (counter-selectable by 5-fluoro-orotic acid, 5FOA) and *kanMX4* (reporter, providing resistance to G418) from a previously targeted yeast locus. In the high-efficient version of the assay, the cassette (termed ICORE) also contains the cDNA for the homing endonuclease I-SceI under an inducible promoter and the unique target site for this enzyme. Hence, prior to transformation of yeast with the targeting molecules, I-SceI expression is induced resulting in a single double strand break at the site of ICORE integration that greatly enhances the frequency of targeting events, which are again selected on 5FOA plates. The replacement of the ICORE cassette can be accomplished using double-strand or even single-strand DNA molecules. Thirty nucleotide of homology at both ends of the donor molecules corresponding to sequences flanking the ICORE cassette integration site are sufficient for the homologous recombination process in wild type yeast (22). Hence, this approach is well-suited to target promoter regions and introduce 10-20 nucleotide-long REs of interest to study TFs. To this end, a yeast reporter strain derived from the FASAY assay has been modified to introduce ICORE upstream of the minimal promoter that can be rendered p53-dependent by the placement at the site of p53 REs (23). In a later development the color *ADE2* reporter gene has been replaced with the quantitative Firefly luciferase cDNA (LUC) to generate yLFM-ICORE that serves as the starting strain for all RE targeting performed in this work. Again, yLFM-ICORE is transformed with synthetic oligonucleotides leading to excision of ICORE cassette from the target locus imparting 5-FOA resistance to the cells. Colonies appearing on 5-FOA plates are then replica plated both on rich YPDA plates and on YPDA plates containing G418. Loss of ICORE would lead to combined 5-FOA resistance and G418

sensitivity (see Figure 1). The colonies unable to grow on G418 are selected from the corresponding position in the YPDA plate replicas, purified and tested using colony PCR to amplify the targeted locus. Sanger sequencing is used to check the correctness of the inserts. Hence, with this approach single or multiple base variants of consensus TF binding sites are integrated in yeast to evaluate their transcriptional strengths in the same chromatin locus without any alterations in the nearby minimal promoter/reporter (*pcyc1-LUC*) or other genomic regions (11). Besides this genome engineering approach, another feature that can assimilate the use of yeast cells for transcription assay to that of an *in vivo* test tube, is the availability of tightly regulated promoter systems for tuneable expression of the desired human transcription factors. Hence, a matrix of analysis can be performed where the only variables are TF protein amount and the nature of its cognate binding in a completely isogenic system (24). As mentioned above, this experimental workflow is enabled also by the conservation of basic components of the transcription machinery between yeast and mammals that allows human TFs to act as transcription factors in yeast (25). While the basic set-up of the experimental system focuses on aspects of *cis*-regulation, including the impact of TF mutations and RE sequence variants, attempts have been made to adapt yeast-based transcription assay to screen for small molecules targeting human TFs (26).

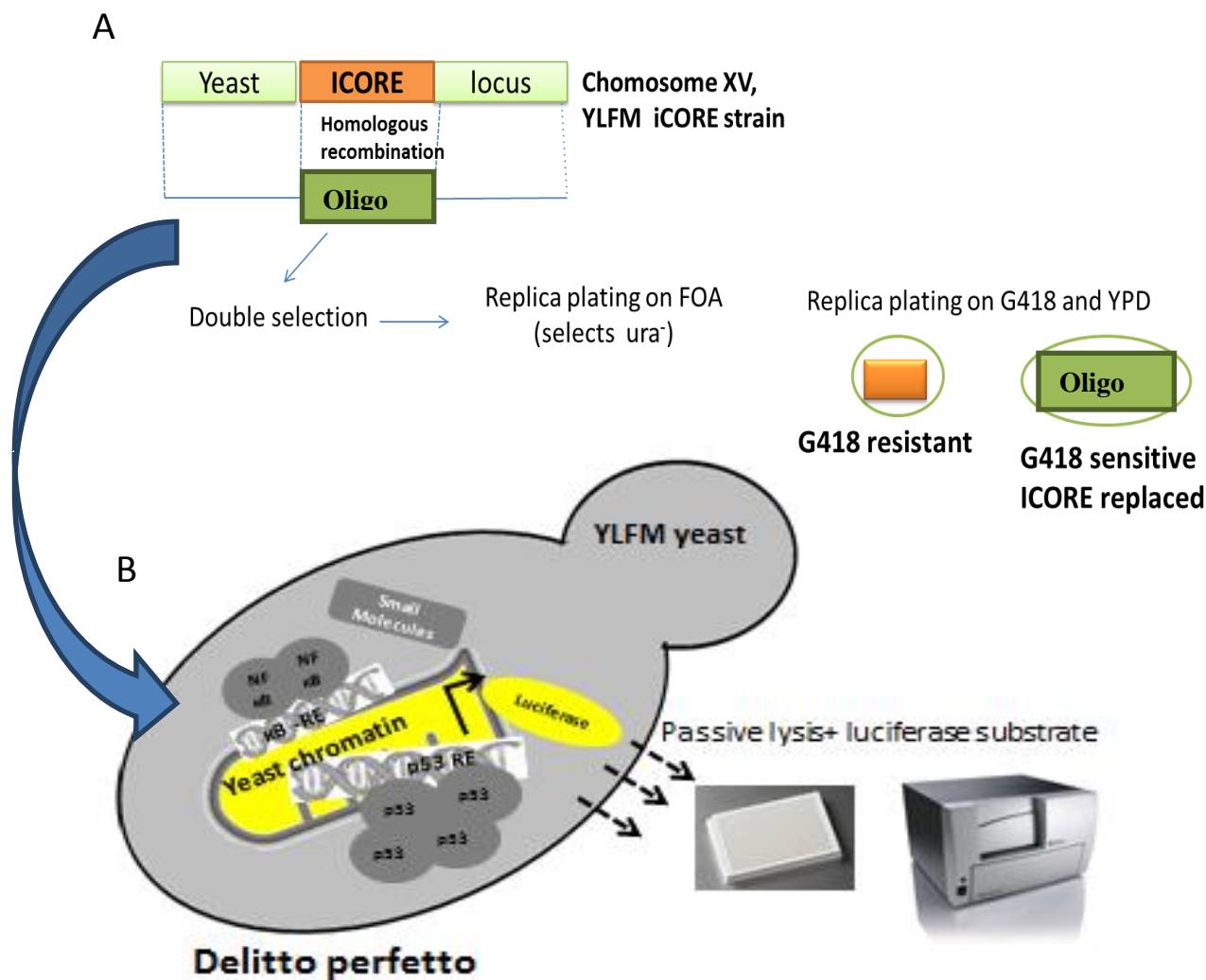


Figure 1: *Delitto perfetto* mediated integration of synthetic oligonucleotide (carrying p53/NF- κ B REs) in yeast chromosome. (A) The yLFM-ICORE yeast strain is transformed with 80nt long oligonucleotide carrying an RE of interest. The pre-integrated ICORE cassette is excised and replaced with the desired oligo DNA through homologous recombination mediated by 30nt homology arms. The ICORE replaced strain becomes G418 sensitive and 5 FOA resistant. **(B)** Yeast serving as an *in vivo* test tube to quantify RE transactivation specificity. The modified yLFM-RE yeast strain is transformed with galactose inducible p53 or NF- κ B expression vectors. The transcriptional strength and specificity of REs is determined comparing the differences in Firefly luciferase activity. Transformed yeast-RE strains are cultured with or without galactose for different time points in a 96-well round-bottom plate. Luciferase activity is measured by transferring in white 384-well plates 10ul of cell culture and permeabilizing cells to the luciferase substrate by adding the same volume of lysis buffer (see results section for more details).

The tumor suppressor p53 and its isoforms

More than 35 years ago, p53 protein was reported as an oncogene in cancer but a decade later it was realized that the original clone was a mutated version of the protein and the function of wild type p53 was redefined as that of a tumour suppressor and subsequently revealed to be largely dependent on sequence-specific DNA binding activity and a role in transcriptional modulation (27-31). Further studies, continuing to this day have revealed p53 as a master gene of cellular responses to an impressively wide array of signalling pathway, regulating an extensive network of target genes resulting in the modulation of cell cycle arrest, apoptosis and DNA repair, from which the honorary title of “guardian of the genome” has been coined (32-35). More recently, p53 functions has been linked to other cellular responses including differentiation, tissue regeneration, senescence, carbon and lipid metabolism, inflammation, ferroptosis and post-apoptosis (36-39).

The tumour suppressor p53 shows a high frequency of mutations in a majority of cancer types, with a prevalence of missense mutations causing aberrant expression of a protein that in some cases exhibits gain-of-function, oncogene-like phenotypes and can lead to a highly dysregulated response gene network (40). The discovery of germline p53 mutations resulting in high penetrance cancer predisposition syndromes (Li-Fraumeni, Li-Fraumeni-like) was very important to establish p53 as a tumour suppressor gene (41). More than 200 different p53 missense mutations have been identified in the germline that when analysed with transcription assays, also in yeast, revealed a range of functional alterations that could be linked to different clinical features (25). This led to the proposition that not all p53 mutants expressed in cancer possess the same impact and potential prognostic value (12).

Various p53 mutants acquire oncogenic properties leading to deleterious outcomes like unrectified cell cycle progression, metastasis, angiogenesis and stemness in tumour cells (25, 42-44). Biochemical studies have established that the p53 protein is functional as a tetramer, composed by a dimer of dimers (45). The protein contains transactivation and protein interaction domains in the amino terminus, a large DNA binding domain with immunoglobulin-like fold and a tetramerization and regulatory domain at the carboxy terminus (46-48).

Many missense mutations cause amino acid substitutions in the p53 DNA binding domain of the protein preventing it from binding specific DNA sequences to modulate target expression (49). Deletion of the entire carboxyl terminal leads to inability to form p53 tetramers, while deletion of just the regulatory domain leads to an apparent slight over-activation of p53 (50). Deletions of the N-terminal domains can lead to complete or partial loss of transactivation ability (51). The vast majority of p53 mutations in cancer occur in the DNA binding domain.

Depending on the stress and in a context-dependent manner, p53 regulates downstream targets at the transcriptional, post transcriptional and translational level (52). The complexity of p53 functions in maintaining genome stability and cell homeostasis further increased with the identification of p53 isoforms expressed in a tissue specific manner, resulting from an alternative promoter usage, alternative translation initiation and alternative splicing (53, 54). So far 9 p53 isoforms have been identified (see Figure 2) from the alternate splicing of full length p53 α transcript (p53 β , p53Y, Δ 40 α , β , Y and Δ p53) or the usage of the alternative promoter in intron four (Δ 133 α , β , Y) (55). Most of these isoforms lack the transactivation domain; some also do not maintain the sequence-specific DNA binding activity of full-length p53 but can inhibit p53 α function, in part through hetero-tetramerization. The functional role of unbalanced expression of p53 isoforms still needs to be fully characterized, but critical roles are emerging for example in senescence, neurodegenerative diseases, premature aging and embryo malformations (54). Notably, p53 regulates the transcription of its own isoforms Δ 133p53 (56, 57). Apparently, another isoform of p53 called Ψ (psi) which stays extra nuclear due to lack of nuclear localization sequence enhances the motility and invasive capacity of cells and lacks the transcriptional abilities (58).

p53 regulating circuit board

Cells in homeostasis maintain p53 at very low levels through its constitutive proteosomal degradation by various negative regulators, of which the ubiquitin ligase MDM2 is the most prominent (59). Intrinsic and extrinsic stress signals leading to loss of fidelity in chromosomal segregation, DNA replication stress or double strand DNA breaks stabilize p53 levels in cells. This stabilization is achieved mainly by post-translational changes inhibiting the interaction

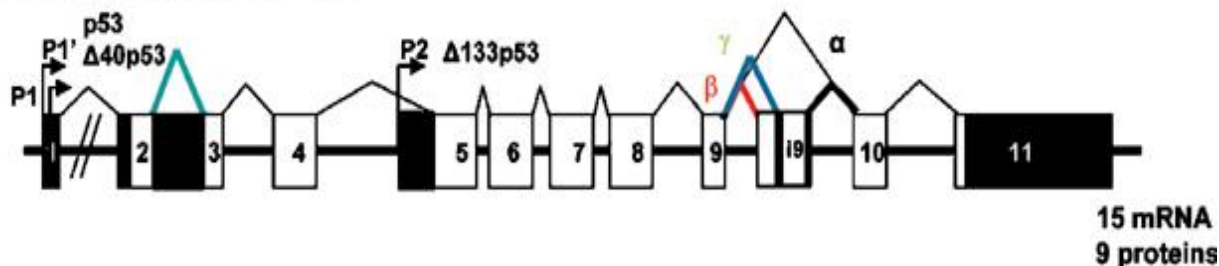
between p53 and its regulators. DNA damaging responses inhibit the interactions between p53 protein and its negative regulators like MDM-2, Cop-1, Pirh-2, delta N p73, cyclin G, Wip-1 and Siah-1 in a specific manner to activate the p53 pathways (60). Many of these negative regulators are under the transcriptional control of p53, thus maintaining negative feedback loops to keep p53 at low levels. On the contrary, p53 controlled genes like PTEN, AKT, p14/19ARF maintain a positive feedback loop to upregulate p53 levels in the cell.

Various strategies are implemented to activate p53 or restore mutant p53 activity in cells as cancer therapy. The non genotoxic drug Nutlin-3A has emerged as one of the most efficient small molecule activator of p53. It relieves p53 from its negative regulator MDM2. Other than the activation of wild type p53, reversion of p53 mutant forms into a transcriptionally active state has also been extensively attempted and considered a valuable treatment strategy (61). In this context, PRIMA-1 has emerged as a drug that can covalently bind p53 mutants (R273H and R175H) to restore at least in part their function *in vitro* as well as *in vivo* (62, 63). Also, mutant p53 Y220C is targetable via compounds PK083 and PK7088, identified through a rational, structure-based approach (64, 65). More recently, the Y220C mutant p53 activating compound has been reported to act also as an inhibitor of heat shock protein Hsp90 (66). Another group has reported tryptophanol derived oxazoloisoindolinone SLMP53-1 as mutant p53 activators (67).

Other than activation and stabilization of p53, various post translational modifications of p53 protein alter its transcriptional specificities. Modifications at particular p53 amino acid residues such as phosphorylation, acetylation and methylation dictate the p53 response to diverse cellular signals and help determine its physiological activities (68, 69) (44, 50). Six acetyl transferases are identified so far which modify p53 at the C terminus or its central DNA binding domain to increase p53 protein stability, binding to low affinity promoters, association with other proteins, antiviral activities etc. (70). The six acetyl transferases can be divided into two groups, one comprising p300/CBP/PCAF the other Tip60/MOF/MOZ (see later section for more information on TIP60 and MOF). There are eight main acetylation sites on human p53 (K120, 164, 370, 372, 373, 381, 382 and 386) and changes of the first three sites from Lysine to Arginine strongly impact on p53 transcriptional function preventing cell

cycle arrest and/or canonical apoptosis, but still resulting in tumor suppression in a mouse model (71).

a Human p53 gene structure



b Putative p53 protein isoforms

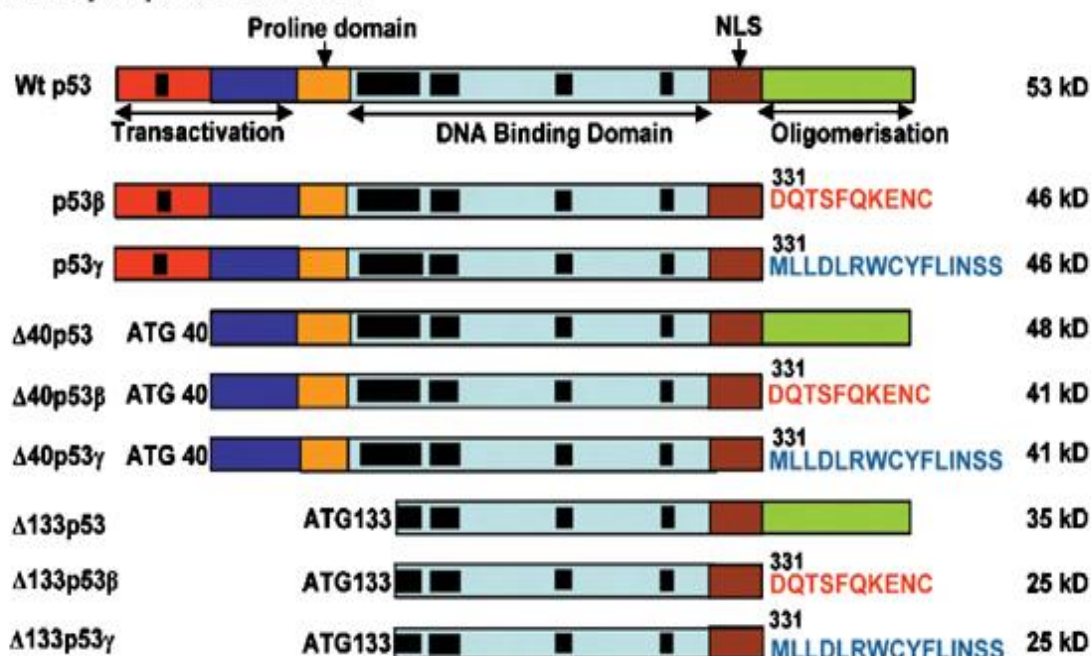


Figure 2: Gene Structure and alternative splicing of TA p53 α transcript. (a) p53 gene structure schematics, alternative splicing and internal promoter are shown (b) Transcripts from promoter P1 give rise to p53 protein isoforms α , β and γ conserved at N-terminal. $\Delta 40$ p53 protein isoforms have lost the conserved N-terminal domain of transactivation but still contain part of the transactivation domain. The internal promoter P2 in intron 4 transcribes $\Delta 133$ isoforms. (53)

p53: Sequence specificity as a transcription factor

The p53 protein belongs to the class of highly sequence-specific transcription factors. It recognizes a palindromic RE of 10 nucleotides (RRRCWWGYYY). Two such motifs, providing interaction with one p53 dimer, can be either adjacent or spaced apart by up to 13 or in some experiments up to ~20 nucleotides without large changes in DNA binding affinity measured in vitro with naked DNA (72). However, more recent studies, using either longer DNA molecules in vitro or measuring p53 occupancy in chromatin using ChIP assays, revealed a preference for adjacent decameric motifs (73). Further, results from functional assays in various systems and competitive DNA binding assays in solution consistently showed higher affinity and transactivation for REs that do not have spacer between the two decameric motifs (74). At the same time, additional variants of the p53 RE have been identified and grouped as non-canonical REs (72, 75, 76). These consist of $\frac{3}{4}$ sites (one decamer plus an adjacent half decamer) or half sites (decamers) and can also mediate p53 binding and gene responsiveness (77) (see below for further details). In terms of location in the genome, p53 REs are generally embedded in the promoter or proximal enhancer regions of established p53 target genes (78), but there are many examples of REs in intronic regions, in distal enhancers, in super-enhancers (79), in repetitive elements (80) and it has been proposed that besides mediating transcriptional regulation, p53 REs may serve as chromatin accessibility factors contributing to p53-mediated genome stability (81)

Since the consensus p53 RE motif is highly degenerate (RRRCWWGYYY)₂, it is implied that individual REs can differ in sequence by one to several nucleotides, potentially impacting on DNA binding affinity. In addition, well-established p53 REs often contain up to three non-consensus bases –herein defined as mismatches– that can further contribute to differences in DNA binding affinity. Hence it has been hypothesized that the specific nature of the p53 RE can directly impact on transactivation specificity to the point that specific types of REs would have been selected in the promoters of p53 target genes implicated in different biological responses, for example cell cycle arrest or apoptosis (82, 83).

Indeed the nucleotide mismatches in CWWG core domain or the flanking purines (RRR) and pyrimidines (YYY) alter the RE transcriptional specificity depending on the expression level of p53 protein. Hundreds of p53 target genes have been identified in the human genome (among which p21, MDM2, BAX, PUMA, GADD45, KILLER, FAS are among the best characterized) (72, 76), and indeed virtually all p53 REs are non-identical in sequence and it appears that high affinity consensus motifs have been negatively selected in evolution, and also that there has been significant evolutionary divergence among p53 REs from different species (84, 85). Various bioinformatics tools are dedicated to specifically scan regulatory regions in genomes to identify p53 REs. The p53 MH algorithm developed by J. Hoh *et al* ranks putative p53 REs by allocating a score as percent similarity to the consensus sequence using a position weight matrix. Out of around 4000 genes registered for the p53 binding sites availability, only 25 genes show perfect match with the consensus p53 recognition DNA binding site.

One of the first study to map p53 occupancy on a genome scale combined chromatin immunoprecipitation ChIP and paired-end ditag (PET) sequencing strategy and revealed specific p53 binding enriched loci in the human genome discovering 98 new p53 binding sites (86) and annotating a total of ~500 p53 bound sites. By treating U2OS cells (osteosarcoma tumour cells) with two anti-cancer drugs, Doxorubicin and Nutlin-3A, differential selectivity of p53 expression and binding patterns through ChIP and high throughput sequencing methodology was established, identifying 149 new p53 target sites in human genome. Validation of weak to strong p53 REs suggested p53 binding to DNA and relative transactivation as two independent events (87).

As summarized above, yeast-based functional assays have been extensively used to compare the transactivation potential of p53 REs. Yeast-based transactivation assays confirm that binding affinity of REs have no significant correlation with the p53 mediated transactivation potentials. Yeast based functional ranking of 26 different p53 REs, out of which four were artificial REs, reveal differential impact of alternations in CWWG core on transactivation potentials in a p53 concentration-dependent manner, establishing the CATG core as the most transcriptionally active motif. As presented above, the construction of many variants of the p53 REs at the same genome location was greatly facilitated by the *delitto perfetto* approach

(23). Furthermore, the functional assay has been exploited to test the most representative p53 missense mutations including most of those found in the germline (12). The results established different classes of p53 mutants; besides loss of function mutations, various p53 mutants, especially when expressed at high concentration showed wild type like transactivation potential, while others were partially functional and even a small group of mutants with increased function were identified –see next section for more details- (8, 11, 19, 88-93). More recently, all the information on the sequence features of p53 REs and resulting transactivation potential were coded in a pattern search algorithm, called p53 REtriever, that maps and then ranks canonical p53 full sites as well as non canonical half sites and $\frac{3}{4}$ sites according to their predicted transactivation potentials. The *in silico* predicted functional and non-functional REs were cross-referenced with data from ChIP-seq, ChIP-exo, expression, and various literature data sources (94). Taken together, all the studies on p53 binding sites establish p53 as a highly pleiotropic master regulator of a vast transcriptional network.

As mentioned above, besides the remarkable degeneration of p53 REs, another unexpected finding has been the relatively high evolutionary divergence of these sequences. A widespread turnover of p53 binding sites through the period of 500 million years has been captured by a study on comparative analysis of functional v/s sequence homology of 47 p53 REs corresponding to 38 genes in a group of 14 species. Also, yeast-based transactivation assays performed with p53 protein isolated from six chordate species provides an outlook of phenotypic divergence or convergence of p53 as a sequence specific transcription factor (85). REs tested with species-specific p53 protein exhibited relative transactivation differences represented as their unique functional fingerprints. Attempts have been made to evaluate the temperature sensitivity of species-specific p53 as TF and to exploit chimeric p53 constructs in understanding the conservation of p53 transactivation specificity or lack thereof (95). For example, PRODH genes carry various putative p53 REs in promoter or intronic regions. However, transactivation assays show negligible conservation of functional p53 REs within PRODH family revealing PRODH2 not as a direct p53 target (96). The conservation of p53 REs is also in effect to features like transposing elements and nucleosome accessibility. Weaker p53 REs are more conserved and found in chromatin accessible regions and p53 occupancy and PWM scores are negatively correlated with the evolutionary conservation and chromatic accessibility (97).

Non canonical p53 binding sites such as half sites or $\frac{3}{4}$ sites are functional depending on the intracellular p53 levels enhancing the dynamicity of p53-mediated regulatory networks. Among the p53 half site (decamer) core (CWWG) variants, CATG show the highest transactivation potential, followed by CTTG, CAAG and CTAG. The spacer elements separating p53 binding sites have been demonstrated to have variable impacts on the transactivation potential depending on the length of the spacer and strength of the REs. Typically, a spacer element between two half sites has been shown to decrease p53-mediated transactivation potential, but non canonical p53 REs can work synergistically upon the presence of a 17nt long spacer between them (77). The transactivation potential of p21 RE decreases depending on the number of nucleotides separating the two half sites. A two-nucleotide separation of p21 half sites already drastically reduces the activity of the RE. The organization of REs in the genome affects the accessibility of binding sites and their interactions with the nearby cis-elements. Variably organized p53 binding sites in the genome exhibit *cis-cis* interactions and non canonical p53 sites can synergize with other half sites such as Estrogen Receptor (ER) $\frac{1}{2}$ sites and, upon estradiol and p53-activating treatments, lead to concerted activation of a target gene (98). Functional single nucleotide polymorphs (SNPs) can also have a significant impact on response elements towards p53 occupancy causing genetic diversity in p53 regulatory network (99). All together, these studies reveal a collective impact of DNA elements and their variations on DNA structure and transcriptional outcomes that can be dissected and studied in details using systems in yeast.

Mutant p53 as tool to study RE-dependent transactivation specificity

As noted above, p53 missense mutations are abundant in cancer and, depending on the amino acid substitution or deletion, the protein shows variably reduced transactivation capacities in a RE specific manner. Depending on the site of mutation, the ability of p53 to form a tetramer, bind the DNA motif or ability to transactivate is abrogated. Yeast-based transactivation assays illustrate the promoter selectivity of distinct L1 loop p53 mutants. C-terminal deletants revealed that mutants with loss of tetramer forming abilities cannot transactivate while deletion of the regulatory region, (after amino acid 368) results in reduced transactivation

potential leading to moderate activation of transcription from half or quarter REs at high levels of mutant protein expression. Certain mutations in the DNA binding domain of p53 lead to super-transactivation phenotype. Potentially, *supertrans* mutants that are not impeded by dominant negative mutations in cells could be very useful for cancer therapy if identified with stronger tumor suppressor abilities (10, 77, 93).

Structural properties of DNA can also influence the transcriptional decisions giving relevance to aspects like shape and geometry of DNA comprising a binding site. For example, the noted difference in transactivation and DNA binding affinity associated with consensus variants of the CWWG core (*e.g.* CATG>CTAG) cannot be directly explained by altered contacts between the p53 DNA binding domain and DNA as the protein does not make base read-out at those positions, according to most structure studies. In vitro experiments proposed that DNA bending might contribute to the specific features of CATG p53 REs (100). Other biophysical parameters have been considered to characterize and correlate sequence and functional properties of p53 REs. Genes containing low cooperativity p53 REs are enriched for cell cycle functions while genes controlled through high cooperativity p53 REs are enriched for apoptotic function (101).

A binding site can be denoted as structurally rigid or flexible and hence affecting the binding of p53 tetramer or dimer based on the identity of nucleotides forming it. The torsional properties of the p53 binding core (CWWG) and pur/pyr (GGG/CCC) flanks impart transactivation strength to an RE. A stretch of three guanines (GGG) on the 5' end of p53 RE is torsionally flexible and enhances the responsiveness of binding sites. A torsionally flexible DNA sequence has a high transactivation potential even at low p53 levels due to low dissociation rates of the protein from DNA binding site. The CATG core remains the most transcriptionally active binding site even at low levels of p53 and binds p53 molecules with low cooperativity as well, meaning that p53 dimers can be independently recruited at such sites. On the contrary CAAG and in CTAG motifs exhibit high cooperativity and tetramer-dependent p53 binding, but lower transactivation potential (102-104).

Siblings of p53: p63 and p73

p63 and p73 are paralogs of p53 and share structural and functional homology (Figure 3). The p63 and p73 proteins are mainly involved in developmental and cell differentiation processes but they share the ability to target at least some of the p53 responsive promoters. p63 and p73 are also tetrameric transcription factors and heterotetramers can be formed with impacts on target site interaction (105, 106). It has been demonstrated that a vast number of genome-wide p53 target sites can also be bound by overexpressed p63 and p73 *in vivo* (73). Also yeast-based assays reveal that p53, p63 and p73 exhibit a similar, but not identical transactivation profile (74). Various splice variants of p63 and p73 also exist (see Figure 4 and 5). A yeast-based study elucidates the impact of p53 mutants on the transactivation abilities of p73 β -isoform (transcriptionally active) signifying the presence of functional interplay between p53, p63 and p73 in their mutant or WT forms. The relative transactivation abilities of p63 and p73 isoforms evaluated using yeast revealed that Δ N-P63 α and TA-P63 α isoforms showed significant differences in terms of transactivation capacity and specificity when tested with an array of REs (107). The same phenotype was not observed for p73. The DNA binding domains of the three proteins has the highest conservation level. For example, corresponding p73 mutations in the L1 loop exhibited equivalent changes in transactivation specificity seen with p53 mutants (93).



Figure 3: Structural conservation between p53, p63 and p73. p63 and p73 are 25% and 29% conserved at the N-terminal Transactivation domain with respect to p53, respectively. The DNA binding domain shows 65% and 63% conservation of p63 and p73. The oligomerization domain is

35% and 38% conserved for the proteins relative to p53 as shown. (source)

http://p53.free.fr/p53_info/p73_p63.html

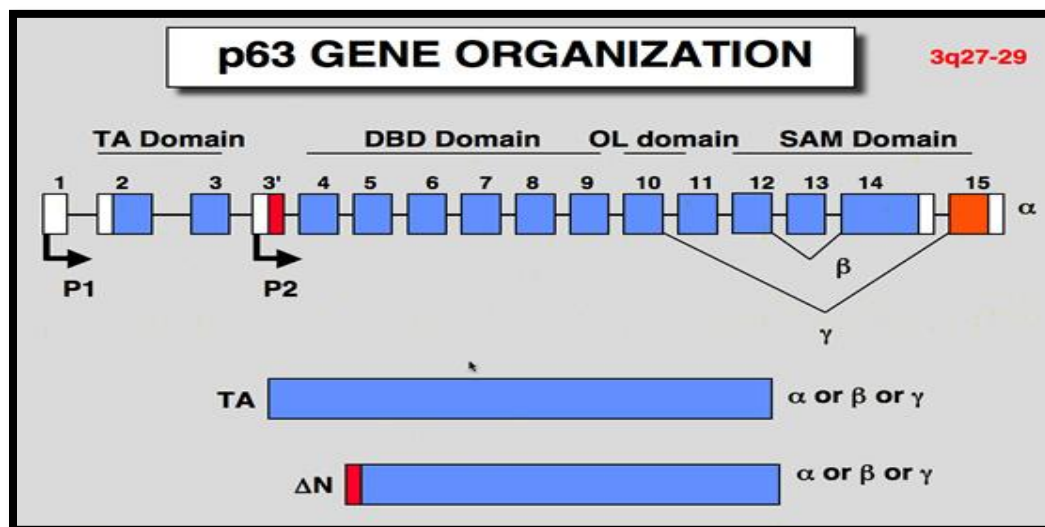


Figure 4: p63 gene transcripts: The transcription from promoter P1 at intron 1 generates transactivation domain carrying isoforms. The alternative splicing form intron 10 till 14 forms either β or γ isoforms. The transcription from promoter 2 generated N-terminal deleted isoforms. (Source):

http://p53.free.fr/p53_info/p73_p63.html

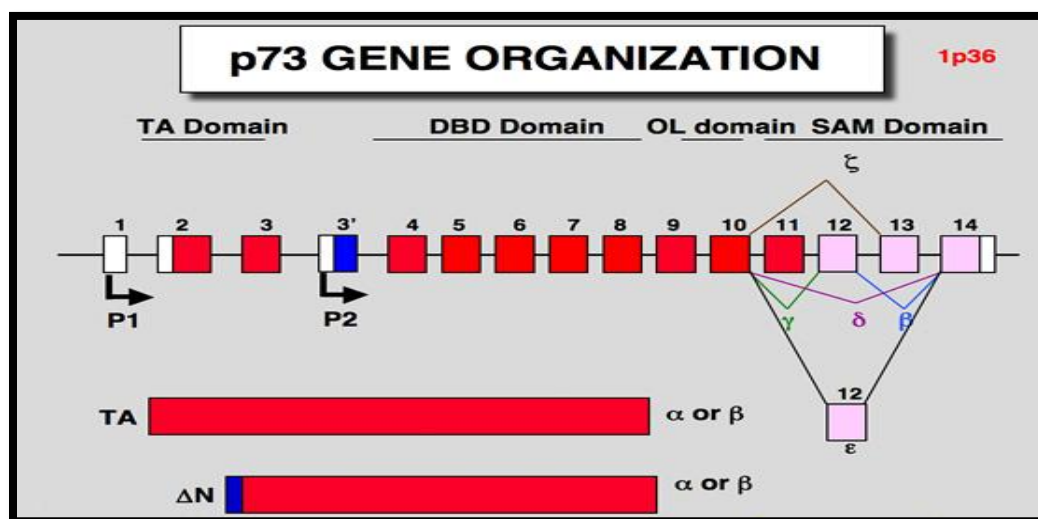


Figure 5: p73 gene transcripts: p73 α transcripts arising from promoter 2 are N-terminal deleted unlike those from promoter 1 which carry the TA domain. Alternative splicing from intron 10 till 12 generates five different isoforms $\beta, \gamma, \delta, \epsilon$ or ζ as shown. (Source):

http://p53.free.fr/p53_info/p73_p63.html

NF-κB family of transcription factors

NF-κB proteins are highly dysregulated in cancer and one of the central players of pro-inflammatory responses in tumours (108). Constitutive expression or lack of expression of NF-κB pathway proteins lead to muscular and neurodegenerative diseases or diabetes (type I and II). NF-κB is constitutively expressed in cells and does not require new protein synthesis upon stimuli to activate a response. It exists as an inactive complex kept in the cytoplasm by the interaction with an inhibitory cofactor, IκB. Such inhibition is relieved by post-translational regulation of IκB that occurs in response to specific stimuli, such as the exposure of cells to inflammatory cytokines, such as TNFα, or molecules associated with pathogen infections (Pathogen Associated Molecular Patterns, PAMPS) and is mediated by the IKK complex (IκB kinase). Interactions of these extracellular factors with their receptors (TNFRSF or TLRs) (109) activates signal transduction pathways leading to IκB phosphorylation and degradation. NF-κB is activated through canonical as well as non canonical pathways (see Fig 6) enabling the protein to relocate to the nucleus to act as a sequence-specific TF (110-115). NF-κB family comprises 5 subunits p50, p52, p65 (REL A), c-rel and relB which form either homo or hetero-dimers to recognize a loosely consensus RE of 10-11 nucleotides “5'-GGGRNWYYCC-3' ” (R = purine, N = any nucleotide= adenine or thymine, and Y = pyrimidine) (116, 117). Some atypical pathways are also known to activate NF-κB in response to stimuli such as genotoxic stress, UV and hypoxia with or without IKK involvement (111). ChIP-seq data suggest that >1000 genes can be regulated by NF-κB proteins such as chemokines, immunoreceptors, stress response genes, regulators of apoptosis, growth factors etc. Approximately 1.5×10^5 NF-κB binding sites have been mapped in the human genome (118). A detailed description of NF-κB activators, inhibitors, diseases and target genes can be found at <http://www.bu.edu/nf-kb/>. The NF-κB family proteins comprise a structurally conserved Rel homology domain (RHD) conferring DNA binding activity. The RHD is formed of ~300 amino acids allowing the dimerization of the subunits and includes a nuclear localization sequence which binds to the IκB protein. Variability exists within the family members at the C-terminus. The transactivation domain (TAD) is localized in the C-terminal region and is not shared by all family members (see Table 1) Mutations in NF-κB proteins in mouse models are associated with various physiological lethal phenotypes (119-121). The

interplay between the NF- κ B family members leads to early or late responsiveness of the target genes in genomic context. Various homo- or hetero-dimers are reported to act in cellular context but p50/p65 complex is the most active and abundant heterodimer found in cells. p50 and p52 proteins lack a transactivation domain and hence cannot function as a homodimers, requiring additional cofactors like BCL3 and BCL6 to transactivate the targets (122, 123).

Various studies established that the nucleotides in a RE define the binding affinities of NF- κ B subunits and that even a single nucleotide variation in a NF- κ B RE can profoundly alter the transactivation capacity of NF- κ B proteins (124, 125). The transactivation capacity of a NF- κ B protein has positive correlation with the RE binding affinity (126, 127). Various non-canonical NF- κ B binding sites have been identified using techniques such as gel-shifts, ChIP-seq and Selex specifically focussing on NF- κ B protein REL A (p65) (128). The degeneracy in NF- κ B consensus RE provides opportunity for complex cis-regulation, transactivation specificity and gene expression tuning (129). Many transcription factors, like Sp1 or NFAT are reported to function with NF- κ B conferring further plasticity (130). Table 1 summarizes concisely features of the biology of NF- κ B family members.

As for the case of p53, there is no clear NF- κ B homolog in yeast, although the RTG family of proteins (RTG1, RTG2 and RTG3) involved in yeast mitochondrial retrograde pathway has been proposed to share structural similarity with NF- κ B (131).

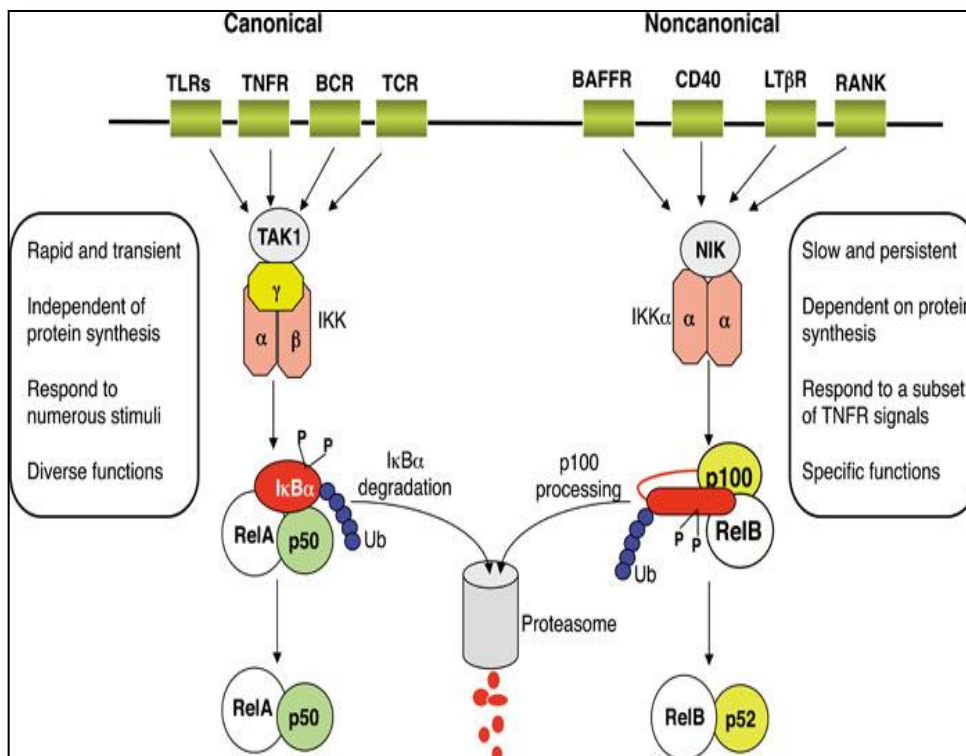


Figure 6: Canonical and non-canonical pathways for NF- κ B activation. The canonical pathway (left side) leads to the activation of RelA-p50 heterodimers. After stimuli such as TNF α or IL-1, the IKK complex containing NEMO, IKK α and IKK β phosphorylates I κ B α on Ser32 and Ser36, inducing ubiquitination and proteasomal degradation of I κ B α , thus releasing RelA-p50 dimers, which then translocate to the nucleus to regulate the target gene transcription. The non-canonical pathway (right side) is responsible for p100 processing and p52 activation. Following stimuli by CD40 or LPS, NIK phosphorylates the IKK α complex. These kinases then phosphorylate p100 on Ser866 and Ser870, leading to its ubiquitination and p100 processing into p52. p52, forming a dimer with RelB, translocate to the nucleus and then can regulate the transcription of target genes. Other combinations of NF- κ B dimerization than RelA-p50 or RelB-p52 are also possible (6).

Family member	Active form/ dimer	<i>In vivo</i> expression, abundance and localization	Presence of Transactivation domain (TAD)	Impact of Loss of Function
RelA/ p65	Dimerizes with p50, most abundant heterodimer and transcription activator	Major and most crucial NF- κ B subunit, highly abundant as heterodimer with p50	Yes	Severe phenotypes such as embryonic lethality observed in mice
p50	Forms a self-dimer (p50/p50) involved in repression of p65 activity	Nearly ubiquitously expressed	No	Defect in their ability to generate a humoral immune response
p52	Forms transcription activating complex with bcl3	Expressed mainly in stomach epithelium and immune cells	No	Slight defect in the splenic and lymph node architecture
c-Rel	Dimerizes with p50 and p52 both	More gene specific expression and responsiveness	Yes	B cell defect like p50.
Rel B	Dimerizes with p52	Localized in dendritic cells and lymphocytes	Yes	defects in both acquired and innate immune response

Table 1: Features of five NF- κ B subunits and effect of their loss in cells. The table summarizes the expression, localization and dimerization of five NF- κ B subunits and the effect of their loss of function in cells.

MATERIALS AND METHODS

Materials and Methods for the NF- κ B project are included in the published manuscript which is presented at the end of the results section. This materials and methods section refers to the procedures employed for the unpublished work described in the Results sections

Construction of yeast reporter strains containing p53 Response Elements regulating the expression of the Firefly cDNA

A panel of isogenic yeast reporter strains containing either single copies of the decameric p53 RE (*i.e.* half site), or a full site consisting of two adjacent identical half sites were constructed using single strand oligonucleotides (synthesized by Eurofins MWG Operon, Ebersberg, Germany), targeted at a modified chromosomal XV locus containing a minimal *CYCI* promoter driving the expression of the Firefly luciferase cDNA. These experiments were developed following a previously published approach (19, 85) that is an adaptation of the “delitto perfetto” system for *in-vivo* site-directed mutagenesis (23, 132) and exploited the yLFM-ICORE strain (19, 85, 99). The protocol utilizes oligonucleotides that contain a desired p53 RE, flanked by two short (30nt) homology tails to direct them to the chosen integration site, and exploits a triple-marker cassette (ICORE) positioned in the yLFM-ICORE strain near the *CYCI* promoter on chromosome XV (*ADE2* gene location). The cassette contains a counter-selectable gene (*URA3*), a reporter gene (*kanMX4*), and the I-SceI homing endonuclease along with its unique 18nt recognition site. Expression of I-SceI is controlled by the *GALI* promoter and leads to the induction of a unique double-strand break (DSB) at the site where the cassette is cloned, which in turn leads to high efficiency homologous recombination and integration of the oligonucleotide. The desired oligonucleotides are transformed into yeast after culturing cells for 4 hours in galactose-containing medium to induce I-SceI expression and the induction of the DSB. The homology tails correspond to the yeast chromosomal sequences flanking the ICORE integration site, while the desired p53 RE is at the centre of the oligonucleotide. Oligonucleotide targeting events are selected exploiting the counter-selectable marker, by plating transformants on medium containing 5-fluorotic acid (1g/L). Colonies appearing on such plates after 3-4 days of incubation at 30°C are streaked or

patched onto rich YPDA plates and then replica plated on both YPDA and YPDA-G418 (0.4mg/ml) plates. Loss of the reporter cassette is assessed by the lack of growth on YPDA-G418. Correct reporter strains' construction is confirmed by colony PCR across the engineered chromosomal region (22), followed by DNA direct sequencing (BMR Genomics, Padua, Italy).

Yeast transformation and luciferase assays

The newly constructed yLFM-p53-RE and yLFM p21 RE strains (see Figure 7 and Table 4 for the list) were transformed with the pLS89 (93) or pTSG-hp53 (92) p53 expression vector using standard LiAc protocol followed by heat shock (133). Both vectors are tryptophan (*TRP1*) selectable. Inducible expression in yeast of p53 WT protein was achieved exploiting *GAL* promoters (galactose inducible) (85). Transformants were then processed for the miniaturized protocol of the luciferase assay (19, 134). Transformant colonies kept on selective glucose plates, lacking tryptophan, were grown for 16 hours, unless otherwise stated, in synthetic tryptophan-deficient liquid media containing raffinose (2%) with or without different concentrations of galactose, which serves as inducer of the *GAL1* promoter driving the expression of the p53 protein. Luciferase activity was measured using the Bright Glo Luciferase assay kit (Promega, Milan, Italy) and expressed either as relative light units (RLU) normalized to optical density ($\lambda=600$ nm), subtracting the luminescence obtained by the cells transformed with an empty vector (pRS314) in each reporter strain, or expressed as fold induction over the empty vector. Experiments included four to seven biological repeats and the results were plotted as mean values and standard errors of the mean.

Cloning of p53 binding motifs in the pGL4.26 mammalian reporter vector

Nine of the half site and full site p53 REs tested in yeast were further tested in the H1299 and A549 human cell lines. To this aim, the RE sequences were cloned upstream of the promoter driving Firefly luciferase gene expression within the commercial pGL4.26 vector (Promega), using a pair of complementary oligonucleotides ligated into KpnI/XhoI double-digested

plasmid DNA. A unique NdeI restriction site was included in the oligonucleotides 5' to the REs to facilitate the identification of ligation products. Plasmids were purified and sequenced across the modified region.

Dual luciferase assays in human cells

The lung cancer derived A549 and H1299 cells were cultured in RPMI media supplemented with 10% FBS 2mM L-Glutamine and 1X Penicillin/ Streptomycin mixture (Pen/Strep). Relevant to our aim, H1299 are p53 null while A549 express wild type p53 protein that can be activated by genotoxic stress or small molecules inhibiting MDM2::p53 interactions. For gene reporter assays, H1299 and A549 cells were transiently transfected at ~80% confluence using TransIT-LT1 Transfection Reagent (Mirus) and Lipofectamine LTX (Invitrogen), respectively, in a 24-well plate. 250 ng of the newly constructed pGL4.26 reporters and 50 ng of the pRL-SV40 control luciferase vector were used. H1299 cells being null for p53 expression, the transfection mix also contained different amounts of a p53 expressing plasmid (CMV-based) and/ or an empty control plasmid always maintaining the total concentration of 500 ng DNA in each well. Each experiment was performed in triplicates and a total of 4 biological replicates were used for analysis. A549 cells were treated with Doxorubicin (1.5 μ M or 3 μ M) and Nutlin-3A (10 μ M) to activate p53. Dual luciferase assay was performed 30 hours post transfection for H1299 using dual luciferase kit (Promega) following the manufacturer's protocol whereas in A549 cells, p53-activating treatments were started 24 hours post transfection and the luciferase activity was captured at 8, 12 or 16 hours post treatment.

Construction of pRS314-RGF bidirectional reporters carrying p53 REs with their genomic or synthetic flanking sequence

A bidirectional reporter plasmid pRS314-RGF containing the 600nt bidirectional, galactose-inducible *GALI,10* promoter transcribing both Firefly and Renilla Luciferase cDNAs,

respectively, from *GALI* and *GALI0* side, was available in the laboratory. The plasmid is tryptophan selective (TRP1) allowing the transformants to grow in tryptophan-lacking media. The *GALI,10* promoter was further modified by introducing p53 REs flanked by 20-nt sequences from each side, exploiting a unique Age I site located at the exact centre of the promoter sequence. To accomplish the integration, sixty-six nucleotides long pairs of complementary oligonucleotides (carrying p53 REs along with contiguous natural or synthetic genomic flanks) were annealed to generate dsDNA with Age I compatible ends that was ligated in Age I digested pRS314-RGF plasmid. The ligation mixes were transformed in DH5-alpha competent *E. coli* cells using the KCM protocol and correct clones containing the oligonucleotides in the desired orientation were identified from miniprep plasmid DNA preparations using restriction digestion tests and PCR with orientation specific primer pairs. The orientation and correct sequence of selected clones was confirmed by Sanger sequencing.

Yeast transformation of bidirectional reporters and measurement of Dual Luciferase activity

pRS314-RGF (TRP1 marked) plasmid containing p53 REs and a p53 expression vector (pLLS-p53, LEU2 marked) (85) were co-transformed in the yIG-397 yeast strain using standard LiAc protocol (133). Transformants were selected and purified using leucine and tryptophan double drop-out media. The luciferase assay was performed essentially as summarized above except that to measure both Firefly and Renilla Luciferase activities the Dual Luciferase assay kit (Promega, Milan, Italy) was utilized. Results were expressed either as Firefly or Renilla relative light units (RLU) normalized to optical density (600 nm), subtracting the luminescence obtained by the cells transformed with an empty p53 expression vector and each bidirectional reporter plasmid, or as fold induction over an empty pRS314-RGF vector in cells expressing p53. Experiments included four to seven biological repeats and the results were plotted as mean values and standard errors of the mean.

Firefly and Renilla promoter inversion in pRS314-RG10F plasmid

As an additional control, the orientation of the *GALI,10* bidirectional promoter was reversed inside the plasmid to test a potential impact of promoter biasness on Firefly and Renilla Luciferase transcription. In fact, we noticed that, depending on the amount of galactose in the medium and time-point, the induction of *GALI* and *GALI0* was not equivalent, with *GALI* being significantly more active than *GALI0* (see Result section). The promoter inversion was achieved by exploiting two Nco I sites present at both sides of the promoter and overlapping with Firefly and Renilla ATG sites. pRS314-RGF plasmids were restricted with Nco I and products resolved on in 1% agarose gel. The plasmid backbone and the ~660 nucleotide long promoter fragments were gel extracted and purified using a commercial kit (Qiagen, gel extraction kit). The two bands were re-ligated and transformed in DH5-alpha cells followed by screening of inverse orientation clones by orientation PCR with the help of appropriate pair of primers. The new constructs now expressing Firefly from *GALI0* and Renilla from the relatively stronger *GALI* promoter were also tested for their dual Luciferase activity as described above.

RESULTS

Part A. p53 studies

1. “*within-RE*” sequence code for transactivation capacity

Impact of consensus changes within the canonical or half site p53 RE on transactivation

We attempted to evaluate p53 transactivation potential towards specific variants of the consensus p53 RE using defined functional assays in yeast and human cells. The same p53 REs were used for co-crystallization studies with the human p53 DNA binding domain (Hector Viadiu, UNAM, Mexico), and they represent *ad-hoc* variations meant to probe the impact of specific changes in the CWWG core and flanking purine or pyrimidines. We compared both half sites (consensus sequence R₁R₂R₃C₄W₅W₆G₇Y₈Y₉Y₁₀ –see Introduction-) and full sites comprising two adjacent half sites without spacer. For these experiments first we took advantage of the yeast-based assay that exploits variable expression of p53 (under *GALI* promoter) and single copy integration of the p53 REs upstream of a minimal *cyc1* promoter at a modified *ADE2* chromosomal location (22). Reporter gene assays were also developed in p53 null H1299 and in p53 wild type A549 human cells using a plasmid reporter system that incorporates the desired p53 REs upstream of a minimal promoter. H1299 cells were cotransfected with variable amounts of p53 expression plasmids, while A549 cells were treated either with doxorubicin or with Nutlin-3A to activate p53 and the level of expression of the reporter was measured at different time points after treatment.

The list of p53 REs tested in the yeast-based assays is presented in Figure 7, along with the relative transactivation measured 16 hours after placing yeast reporter cells in galactose-containing medium to activate human p53 expression. In this assay the amount of p53 protein is proportional to the amount of galactose (11, 85, 135). Results confirmed the expected dramatic difference in transactivation potential between half sites and full sites, the former requiring high levels of p53 to show transactivation (Figure 7). Only half sites with CATG core led to moderate levels of transactivation at high p53 expression. Consensus changes in the purines (*i.e.* G>A) or pyrimidines (*i.e.* C>T), symmetric within the half sites,

can have an impact on RE responsiveness, depending on their position. While such changes at the R₃/Y₈ adjacent to the core had virtually no impact, the same pair of changes in position R₂/Y₉ nearly abolished transactivation even at high p53 levels, consistent with previous observations (85, 135). Also the changes at R₁/Y₁₀ had a rather severe negative impact, although this position is known to be more variable among well-established p53 REs (136, 137) and not directly contacted by the protein, according to crystal structure data (103, 138). Among full site REs, large differences in transactivation potential were apparent at low p53 protein levels, while most REs were nearly equally responsive at high p53 levels, with the striking exception of the full sites with mismatches at the W₅W₆ position or with an inversion of the R and Y code. The latter results confirm that the W₅W₆ bases are essential for p53-dependent transactivation, with TA being the least responsive but only at low p53 levels, even though they do not provide any direct contact with the protein and even in the context of the highest responsive configuration of Rs and Ys (GGG and CCC with two adjacent half sites). Unexpectedly, the asymmetric RE with AAA/CCC flanking the CATG core was highly responsive at low and particularly at high p53 levels, while as a half site this sequence was weakly responsive, consistent with the negative impact of even a single G>A change.

The two most responsive half sites and seven full sites were chosen for the experiments in human cells (Table 2). First we tested the p53 null H1299 cells and cotransfected them with a human p53 expression vector, or empty vector, (25 and 50 ng), along with the Firefly reporter plasmid and a control *Renilla Reniformis* expression vector. Results showed the expected dramatic difference between half-site and full-site responsiveness, and confirmed the slightly higher responsiveness when GGG/CCC flanks the CATG core in a half site. We also confirmed the lack of responsiveness of a full site RE with inverted R and Y code. Transactivation was somewhat proportional to the amount of p53 expression plasmid transfected, although, unlike the case with yeast, these experiments were based on transient transfection and can be influenced by cell-to-cell variability in plasmid uptake. Results with full-site REs confirmed the relatively higher responsiveness when GGG/CCC flanks the CATG core. The higher responsiveness of AT as W₅W₆ dinucleotide was also confirmed, but the TT motif was equally responsive in the transfection experiments with higher levels of p53 expression plasmid. The R₁/Y₁₀ had a more severe negative impact

compared to yeast, and, consistently, the asymmetric RE with AAA/CCC was not highly responsive (Figure 8).

The transient transfection experiments were extended to the A549 cells that express endogenous wild type p53. Results were compared between mock culture condition, *i.e.* at the basal level of endogenous p53 in those cells in standard culture conditions, or after treating them with two different p53-inducing agents: doxorubicin, a genotoxic chemotherapeutic molecule that activates the DNA damage response resulting in p53 stabilization and activation (107), or Nutlin-3A a small molecule inhibitor of MDM2 (139), considered a non genotoxic inducer of p53. Different p53-activating treatments can impact in distinct ways upon p53-dependent functions due to specific post-translational modifications of p53 protein or due to indirect effects (87, 140-142). Since the two treatments also differed in their kinetics of p53 protein stabilization, the gene reporter assays were performed at different time points and in the case of doxorubicin a lower dose was used for the longer time point, which also corresponds to longer time after transfection (Figure 9). The main sequence requirements of full site REs were confirmed also in A549 and with both treatments. Only the GGG/CCC half site (RE 3) showed some responsiveness in this cell line and at the later time point. Most full sites were active also in untreated cells and the activity increased with transfection time. However, the full site RE with GGG/CCC flanking the CATG core (RE 8) was not the most responsive in mock condition nor in treated cells, with the exception of early treatment with Nutlin. The two p53-inducing agents led to a similar ranking of full site p53 REs' transactivation at the later time point, when the REs with TT (RE 9) and AA (RE 5) as W₅W₆ dinucleotides were the most responsive together with the asymmetric RE with AAA/CCC (RE 4) sequences. A negative impact of R₁/Y₁₀ G>A/C>T changes (RE 6) and of the TA as W₅W₆ motif (RE 2) was not apparent, with the exception of the shorter Nutlin treatment.

Name of RE	RE sequence
RE1	AGGCATGCCT
RE3	GGGCATGCC
RE7	(TTTCATGAAA) ₂
RE8	(GGGC AT GCCC) ₂
RE2	(GGGC TA GCCC) ₂
RE6	(AGGCATGCCT) ₂
RE5	(GGGC AA GCCC) ₂
RE9	(GGGC TT GCCC) ₂
RE4	(AAACATGCC) ₂

Table 2: List of p53 REs (full and half sites) tested in A549 and H1299 cell lines.

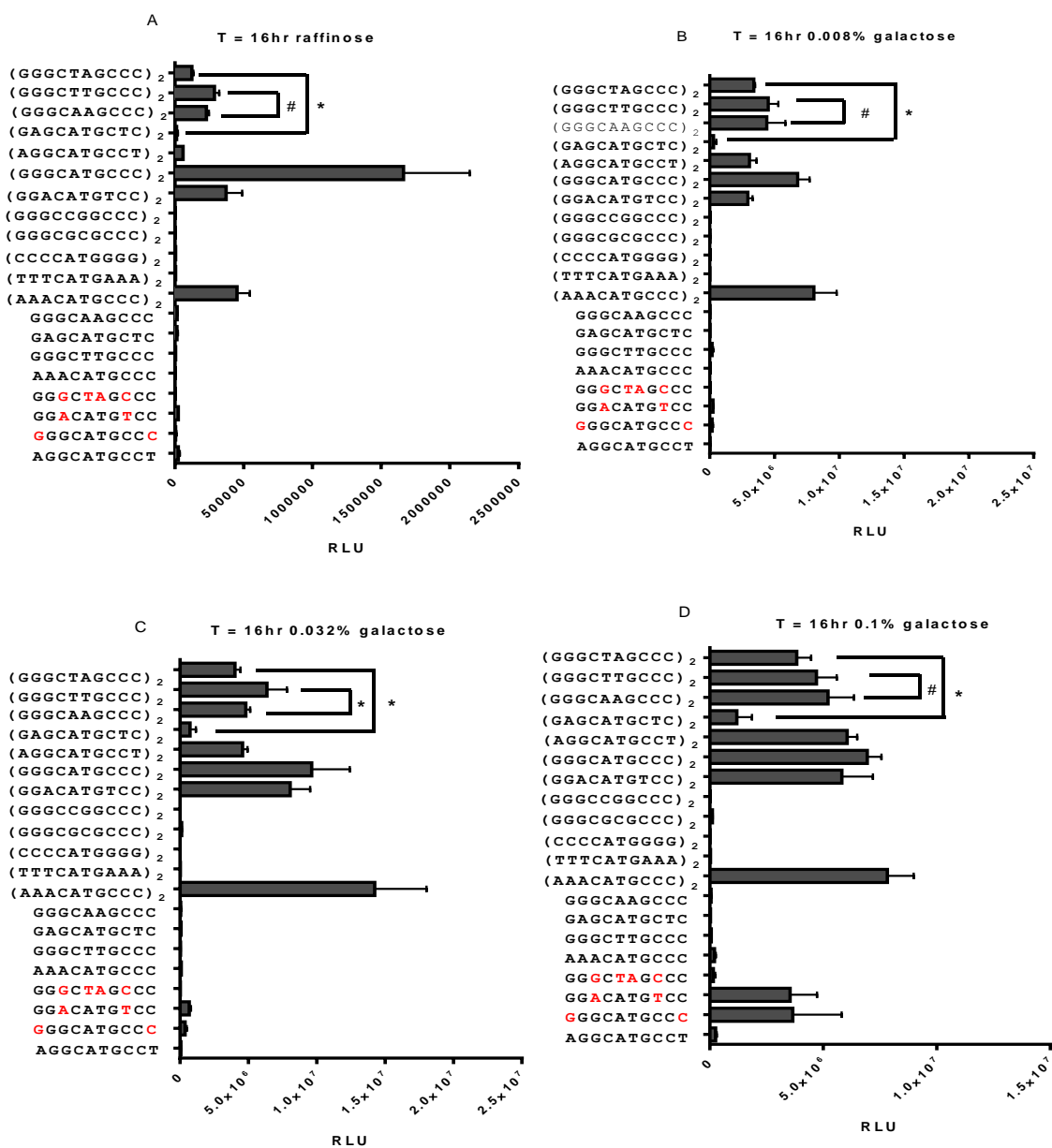


Figure 7: Luciferase activity of p53 full and half sites cloned in yeast yLFM strain. A total of 20 (12 full sites and 8 half sites) p53 RE yeast strains, marked along the y-axis, are tested. Luciferase activity of WT p53 transformed yeast strains is measured sixteen hours post culturing in synthetic selective media in three different galactose concentrations 0.004% (B), 0.008% (C) and 0.032%(D) Raffinose culture (A) without galactose is maintained to determine basal p53 protein activity. Response Elements exhibiting CWWG core permutations viz. RE5 v/s RE9 and RE2 v/s RE8 are compared for statistically significant transactivation differences. * p-value <0.05 for the compared adjacent bars (Student's t-test). # Statistically Non-significant differences

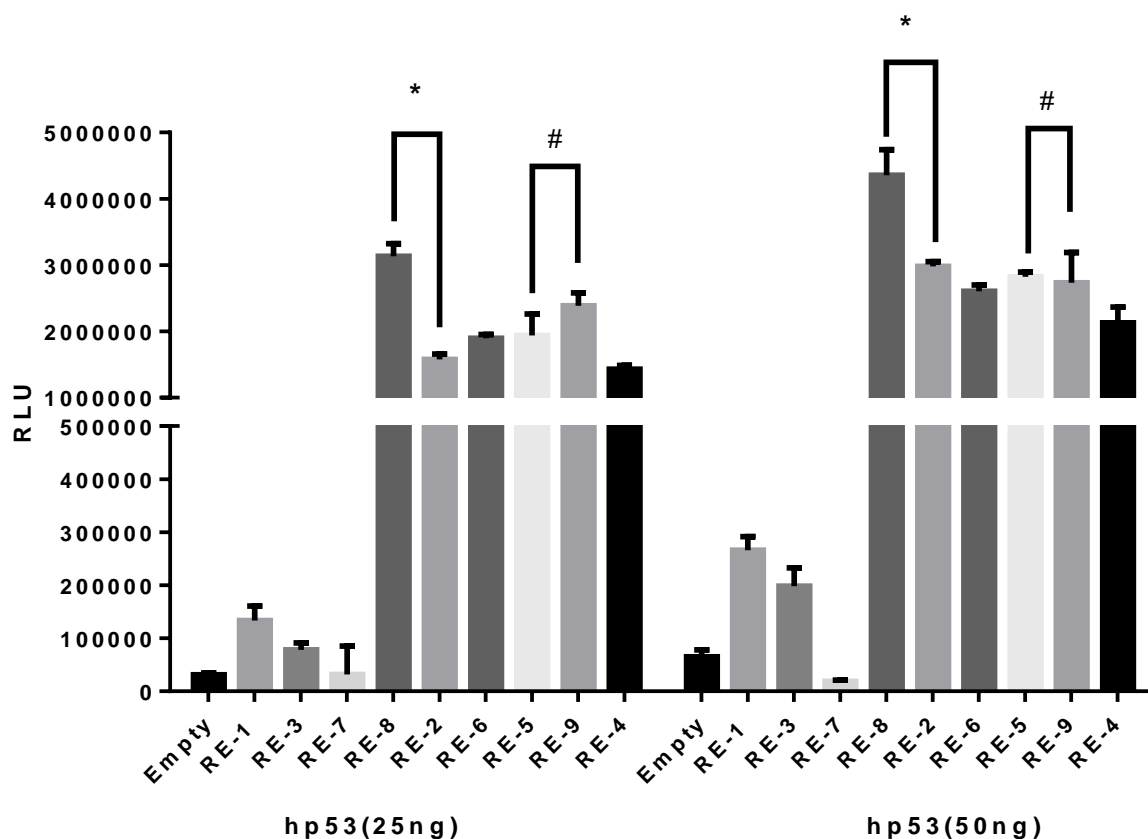


Figure 8: Transactivation potential of p53 full and half sites in H1299 cells expressing variable amounts of p53. p53-null H1299 cells are co-transfected with the list of selected p53 REs (see Table 2), including pGL4.26 empty vector with no RE cloned, and 25ng or 50ng of p53 expressing vector. Empty plasmid backbone without p53 cDNA is also transfected along with all RE constructs in H1299 as a control. Firefly Luciferase activity is measured 36 hours post transfection and the activity of p53 empty plasmid is subtracted from p53-dependent activity of each RE construct type. Response Elements exhibiting CWWG core permutations viz. RE5 v/s RE9 and RE2 v/s RE8 are compared for statistically significant transactivation differences. * p-value <0.05 for the compared adjacent bars (Student's t-test). # Statistically Non-significant differences

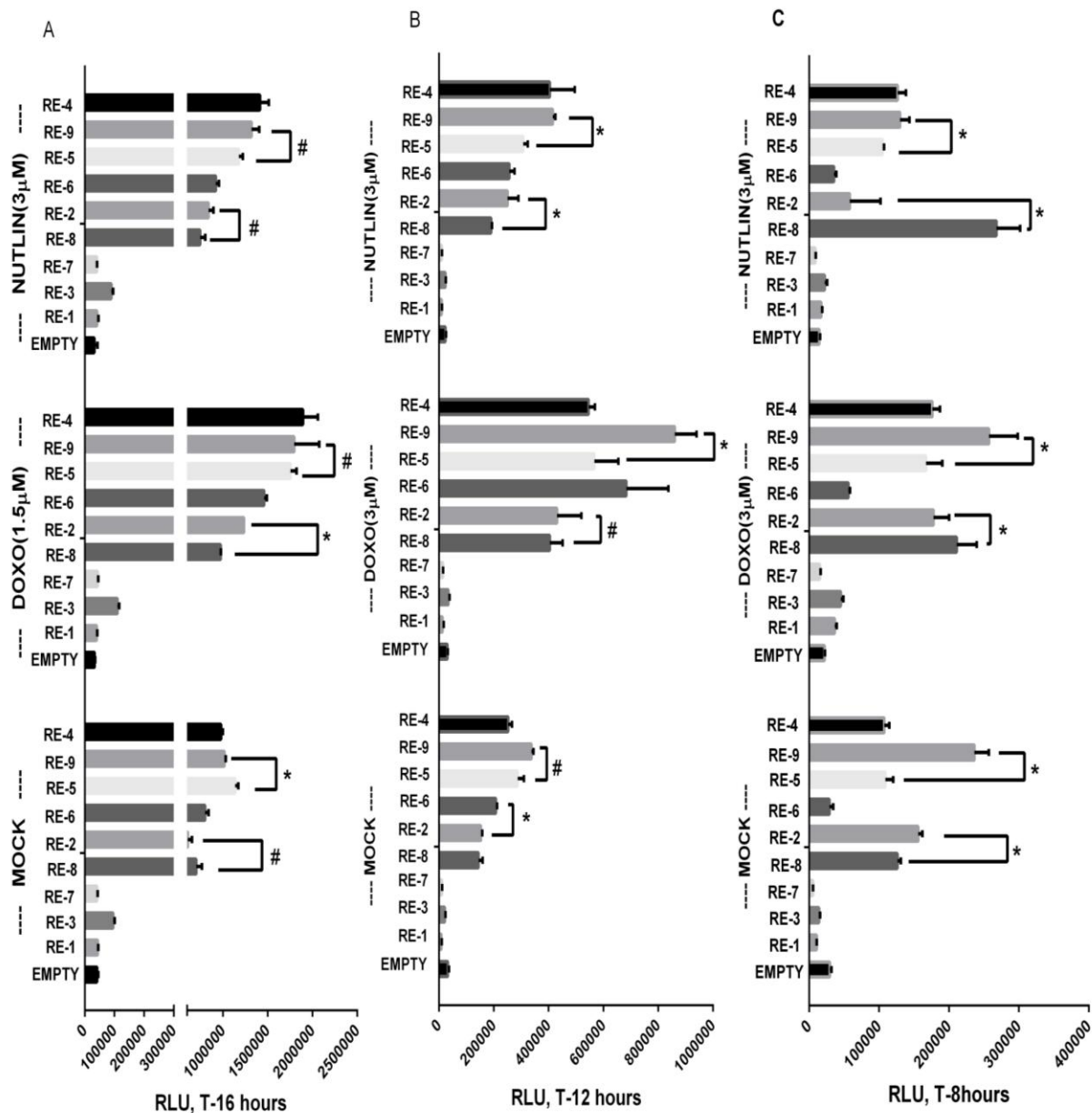


Figure 9: Transactivation potential of selected p53 full and half sites in p53 induced A549 cells. A549 cells transfected with selected p53 REs (see table 2) are measured for Luciferase activity upon treatment with p53 activating drugs doxorubicin (1.5 μ M and 3 μ M) and Nutlin3A (3 μ M) for 16, 12 and 8 hours (A, B, C), respectively. The RE constructs transfected but untreated cells are also measured for activity at all-time points. Response Elements exhibiting CWWG core permutations viz. RE5 v/s RE9 and RE2 v/s RE8 are compared for statistically significant transactivation differences. * p-value <0.05 for the compared adjacent bars (Student's t-test). # Statistically Non-significant differences

2 “*outside-the-RE*” sequence code for transactivation capacity

2.1 Impact of sequence flanking the p53 RE on transactivation

Studies suggest that p53 binding to its RE is regulated by spacer length separating two p53 binding half sites as well as structural properties such as torsional flexibility of the DNA sequence. For example a 10 or 20 bp long spacer element binds more effectively with p53, compared with intermediate spacer lengths (143). Other than influencing p53 binding, the impact that flexibility and rigidity of the DNA sequence constituting an RE site can have on p53-mediated transcriptional strength is a relatively unexplored and intriguing question. Generally, a stretch of thymines is considered structurally rigid while guanines impart flexibility to DNA. We hypothesised that structural organization of an RE and its contiguous flanks characterized by stretch of nucleotides with different rigidity or flexibility can influence p53 tetramer assembly and in turn affect the transcriptional output (see Figure 11). As a first approach, we exploited different structural organizations of a p53 full site RE derived from the p21 promoter, namely the well-established p21-5' RE that is located ~2.2kb upstream of the transcriptional start site (TSS) and that is involved also in the regulation of transcription of the long noncoding RNA PANDA from the opposite DNA strand (144). Yeast reporter strains incorporating the p53 RE and flanking sequences (6-10nt long) were constructed using the previously described method. The two p21-5' RE decamers (half sites) were annotated as Left (L) and Right (R) decamers with respect to the CDKN1A/p21 TSS. These two half sites differ in predicted torsional flexibility as the Right half site scores higher in terms of average flexibility in comparison to the Left half site (Table 3). Average flexibility of each type of p21 flank and the RE (half or full site) is calculated manually by adding up the flexibility score awarded to each dinucleotide pair (145). The natural LR conformation of the p21 RE was also swapped to RL organisation to evaluate the effect on transcriptional strength (22). Also, two tandem copies of the Left (LL) or Right (RR) decamers of p21 were tested. The predicted affinity (K_d) of all p21 RE permutations explored are presented in Table 3.1. The K_d values are calculated using a p53 binding predictor (<http://bioinformatics.ibp.cz:8080/#/en/p53-predictor>). All the REs are embedded in the same chromosomal sequence context. To study the impact of flanking sequence, yeast reporter strains were constructed where the LR or RL REs were flanked by different nucleotide stretches. To reduce experimental variations due to

slight changes in RE position relative to TSS, the flanking sequence changes were introduced only 5' to the RE, except for a strain in which a palindromic nucleotide motif was included on both sides, to obtain a reporter in which the p53 RE is flanked by sequences predicted to possess very similar torsional flexibility. Specifically, we evaluated 10 nucleotides of the natural human upstream sequence to p21 LR RE along with other 10-nucleotide flanks designed to be either more flexible or more rigid in the context of both LR and RL conformation of the p21 RE. See Table 3 for the complete list of p21 RE variants tested.

The panel of reporter strains was transformed with empty or p53 expression vectors and purified clones were tested under variable galactose amounts to induce p53 at different levels and the activity of the reporter was measured at different time points. In these experiments, low levels of p53 were considered more relevant under the assumption that at limiting protein levels p53 will bind a cognate site as individual dimers and tetramers will form at the DNA site. According to a recent study, structural differences of DNA RE sites were proposed to contribute to low off rates and were shown to correlate with transactivation potential only at low p53 levels (146).

The results obtained clearly suggest that LR natural conformation (comprising of natural genomic flank) is the most responsive RE of the panel (Figure 10). This is visible at basal p53 expression (raffinose T0 and T6) and also at low induction levels (0.002% galactose). All the other variants of the 5' flanking sequence do not significantly differ among each other and are lower in activity than the natural flank at T0. Considering instead the p21 RL RE, the rigid flank shows highest activity which is nearly the double of the LR RE activity with rigid flank, followed by neutral, flexible and palindrome in descending order. The trend is maintained at T6 in raffinose medium and also at low induction levels (0.002% galactose). At higher galactose levels, differences level off; except for the construct containing the flexible 5' flanking sequence that remains the weakest. Maintaining constant the flanking sequence (neutral: AATAATACAT) the different version of the p21-5' p53 RE shows differences in transactivation potential. The symmetric LL RE is the most responsive of the series at low p53 protein levels, followed by RL, LR and with RR being the least responsive in all conditions tested.

The predicted $\log K_d$ values in Table 3.1 are somewhat consistent to the transactivation potentials exhibited by p21 full sites. The least active symmetric RR full site also scores the lowest K_d value amongst the other sequences. On the other hand, the average flexibility score obtained by the sequences exhibit roughly an inverse correlation with their relative transactivation potential (see Table 3). Furthermore, for both p21LR and p21RL REs, we establish for the first time that the flanking sequence can impact on transactivation with the presence of a rigid flank leading to higher responsiveness compared to a flexible flank. These features are apparent at low p53 levels and could be relevant for the regulation of p53 targets in unstressed cells.

Name	Sequence	Average Flexibility score
p21 LR (L) HS	GAACATGTCC	1.944444
p21 LR (R) HS	CAACATGTTG	2.544444
RIGID FLANK	TAACTTTTCTT	1.34
FLEX FLANK	GAGTAGTATAC	2.55
PALINDROMIC FLANK	CATATG or GTATAC	3.2
NATURAL FLANK	GGCCGTCAG	2.1
LL	GAACATGTCCGAACATGTCC	1.963158
RR	CAACATGTTGCAACATGTTG	2.505263

Table 3: Flexibility of p21 half or full sites and flanking sequences

Name	Sequence	Predicted log K_d
P21 LR	GAACATGTCCCAACATGTTG	-7.11
P21 RL	CAACATGTTGGAACATGTCC	-7.04
P21 LL	GAACATGTCCGAACATGTCC	-7.38
P21 RR	CAACATGTTGCAACATGTTG	-6.77

Table 3.1: Predicted log K_d values for p21 full sites

Name of p21 RE	Nucleotide Sequence
LR neutral	<u>GAACATGTCCCAACATGTTG</u> LEFT (L) RIGHT (R)
RL neutral	<u>CAACATGTTGGAACATGTCC</u>
LR Natural	<u>GGCCGTCAGGAACATGTCCCAACATGTTG</u> <i>Natural Genomic flank</i>
LR palindrome	<u>CATATGGAACATGTCCCAACATGTTGGTATAC</u> <i>flank</i> <i>flank</i>
RL Palindrome	<u>GTATACCAACATGTTGGAACATGTCCCATATG</u> <i>flank</i> <i>flank</i>
LR Rigid	<u>TAACTTTTCTTGAACATGTCCCAACATGTTG</u> <i>Rigid flank</i>
RL Rigid	<u>AACTTTTCTTCAACATGTTGGGACATGTTC</u> <i>Rigid flank</i>
LR Flexible	<u>GAGTAGTATACGAACATGTCCCAACATGTTG</u> <i>Flexible flank</i>
RL flexible	<u>GAGTAGTATACCAACATGTTGGAACATGTCC</u> <i>Flexible flank</i>
LL neutral	<u>GAACATGTCCGAACATGTCC</u>
RR neutral	<u>CAACATGTTGCAACATGTTG</u>

Table 4: List of p21 REs cloned in yeast yLFM via (*Delitto Perfetto*)

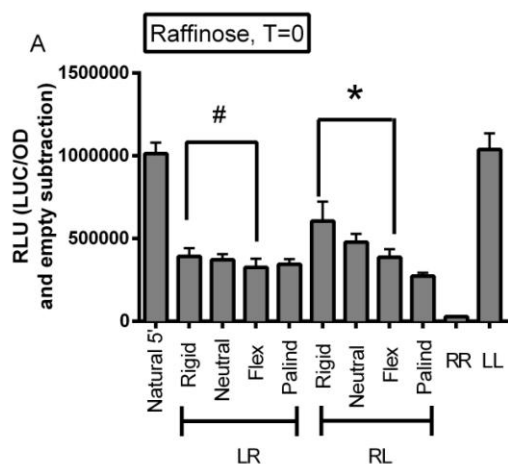
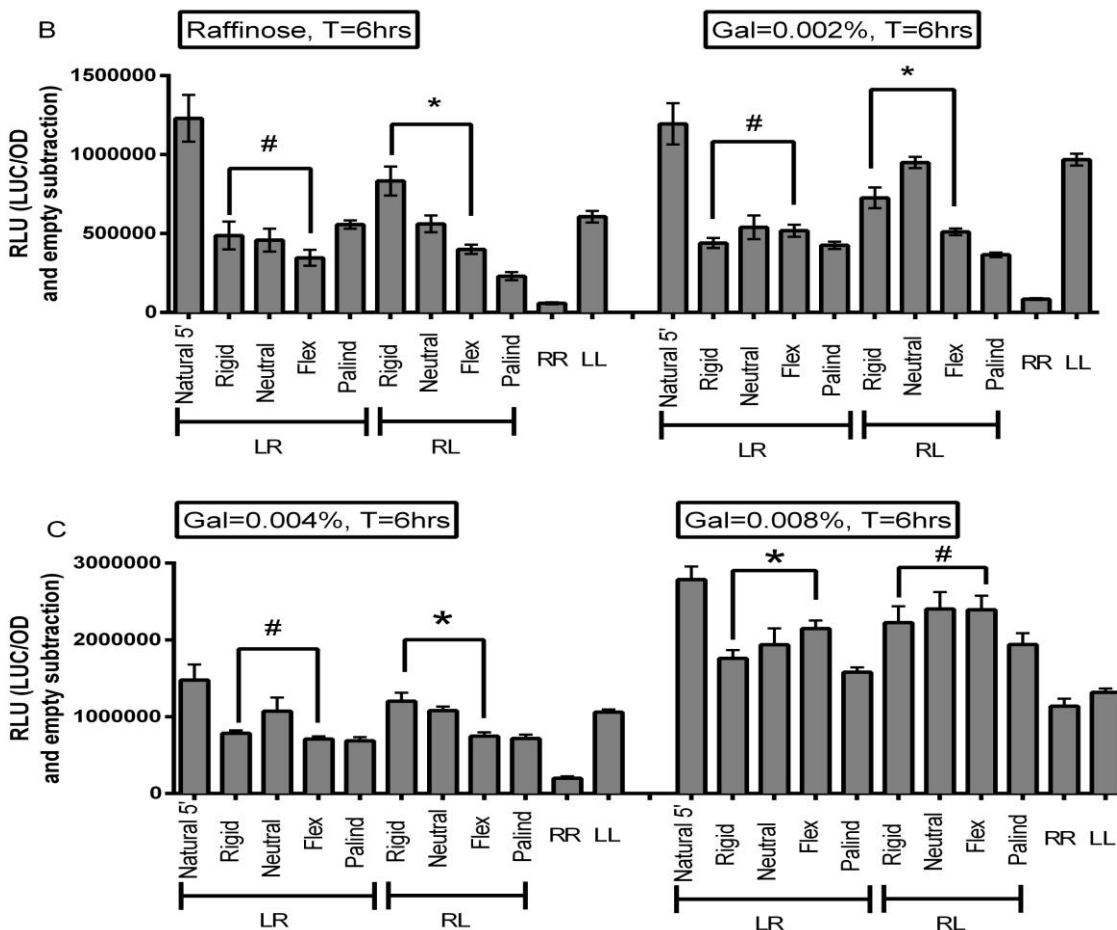


Figure 10: Transactivation potential of p21 RE structural variants in yeast.

Natural LR and swapped RL conformations of p21 RE with genomic (natural) or synthetic rigid, flexible and palindromic flanks was tested for Firefly luciferase activity in yeast yLFM strain. Three concentrations (0.002%, 0.004% and 0.008%) of galactose are used for the induction of p53 protein expression in yeast. A raffinose (no galactose) culture for all strains is maintained in parallel as control. (A) Firefly luciferase is measured at time zero for eleven yeast strains cultured in raffinose. The strains are subtracted for corresponding empty vector activity to plot the graphs. (B) Firefly Luciferase activity measurements at six hours in Raffinose and 0.002% of galactose concentration (C) Luciferase activity in 0.004% and 0.008% galactose concentration at six hours post induction. Differences between transactivation potentials of Rigid and Flex (flexible) flanks are statistically analysed as shown * $p < 0.05$, student's t test. # statistically non-significant

measured at time zero for eleven yeast strains cultured in raffinose. The strains are subtracted for corresponding empty vector activity to plot the graphs. (B) Firefly Luciferase activity measurements at six hours in Raffinose and 0.002% of galactose concentration (C) Luciferase activity in 0.004% and 0.008% galactose concentration at six hours post induction. Differences between transactivation potentials of Rigid and Flex (flexible) flanks are statistically analysed as shown * $p < 0.05$, student's t test. # statistically non-significant



2.2 Impact of sequence flanking the p53 RE on relative transactivation strength of a bidirectional promoter.

These experiments were performed in collaboration with prof. Tali Haran (Technion, Haifa, Israel) who spent a sabbatical period in Trento in 2015.

We implemented another strategy to study the impact of structural properties of the p21 RE and flanking sequences that can also evaluate bidirectional transcription. Both the p21 LR and RL conformations were tested with natural flanks on both sides or with designed flanks that maximize the differences in torsional flexibility at the two sides of the RE. Those *Extra-Flex* or *Extra-Rigid* sequences were chosen examining the natural flanking sites of well-established p53 REs. Hence, the LR-EFR construct contains the p21 LR RE with the extra flexible motif upstream of the L half site and the extra rigid one downstream of the R half site (see Figure 13). On the other hand the RL-EFR construct carries the extra flexible flank upstream of the R half site and a rigid flank downstream to L half site. These constructs were cloned as annealed double strand oligonucleotides at the centre of a bidirectional *GALI,10* promoter, transcribing Firefly and Renilla luciferases from *GALI* and *GALI0*, respectively (see Materials and Methods) (also see Figure 14). The ligation exploited a single Age I restriction site, and clones that incorporated the annealed oligos in both orientation were obtained and characterized, see Table 5 for the list of oligos. For example, for the p21-LR with natural flank construct we obtained two reporters that were labelled p21-LR_LUC, for the case of the forward oligo (5'-3') becoming part of the same strand of *GALI*-Firefly cDNA and p21-LR_REN, for the case of the forward oligo becoming part of the same strand of *GALI0*-Renilla cDNA. Given the bidirectional nature of the *GALI,10* plasmid, the p21-LR_LUC construct contains a p21 RL-reverse strand- acting as enhancer of Renilla transcription (see Figure 12). The same arrangement occurs for the construct containing synthetic flanks, such that when the forward LR_EFR oligo becomes part of the Firefly Luciferase cDNA strand in 5'-3' orientation, the resulting construct is labelled LR_EFR_LUC. For the Renilla reporter then the enhancer will be in conformation extra-Rigid_RL_extra-Flex (see Figure 13). Conversely, when the Reverse LR_EFR oligo (5'-3') becomes part of the same strand of the *GALI*-Firefly cDNA, the construct is labelled LR_EFR_REN as the p21 extra-Flex_LR_Extra-rigid is the enhancer for *GALI0*-Renilla (see Figure 13). All these constructs were developed within the centromeric pRS 314 plasmids

(TRP1) and transformed in the yIG397 yeast strain along with p53 expressing plasmid (LEU2) or empty pRS315 vector as control (see Materials and Methods, and also see Table 5 for the list of p21 oligonucleotides that were cloned). The goal of the experiment was to check if the configuration of the p53 RE and flanking sequence can impact on transactivation strength and/or directionality. As for the previous experiments, variable level of p53 expression was obtained culturing cells in media containing different galactose concentrations and for different time points. An empty dual-luciferase *GAL1,10* reporter plasmid was included as a control to measure the Firefly and Renilla Luciferase activities independent from p53 function as transcription factor at the site.

We observed that p21 REs appended with Synthetic EFR flanks (extra flex/rigid) were much more active than those containing natural genomic flanks (activity of LR/RL EFR > LR natural). The RL_EFR_LUC (flexible flank upstream to Right half site and rigid flank downstream to Left half site close to GAL1 TSS) was the most responsive strain in terms of both Firefly and Renilla luciferases activity whereas RL_EFR_REN (flexible flank downstream to R half site on the GAL10 strand) was the least active. These differences were observed at basal p53 expression (Raffinose) and also at 0.004% and 0.008% galactose concentration after six hours of induction (Figure 15). This informs that for p53-mediated transcription, a torsionally rigid flank is preferred next to the TSS and presence of a flexible flank immediately adjacent to TSS can reduce transactivation. We also calculated the average flexibility score for the p53 REs and flanks appended upstream as well as downstream to the p21 REs (see Table 6). Considering the RE half site (HS) as functional units recruiting p53 dimers, the overall organization Flexible(flank)-Rigid(HS)-Flexible(HS)-Rigid(flank)-TSS results in the highest transcription induction.

One inference drawn from these observations was possibility of promoter biasness as the *GALI* promoter was transcriptionally more active than *GAL10* in our experimental setting. We then reversed the promoter orientation so to place the Firefly cDNA under *GAL10* promoter and Renilla cDNA under *GALI* promoter (see Materials and Methods), for the control plasmid and the p21 series (natural flanks or EFRs: LR_LUC, LR_REN, LR_EFR_LUC, LR_EFR_REN, RL_EFR_LUC, RL_EFR_REN)

Testing those new constructs in yIG397 led to overall higher Renilla Luciferase activity, as expected. We confirmed that the Flexible(flank)-Rigid(HS)-Flexible(HS)-Rigid(flank)-TSS results in the higher transactivation (Figure 16). Furthermore, with the *GAL10*-Firefly *GALI*-Renilla configuration, the impact of this structural feature was simultaneously observed on both directions of transcription. In other words with the RL_EFR_LUC orientation there was a relative gain in Firefly vs Renilla activity whereas the opposite was true for the RL_EFR_REN orientation (Figure 16). Again, these differences were significant only at low p53 expression level.

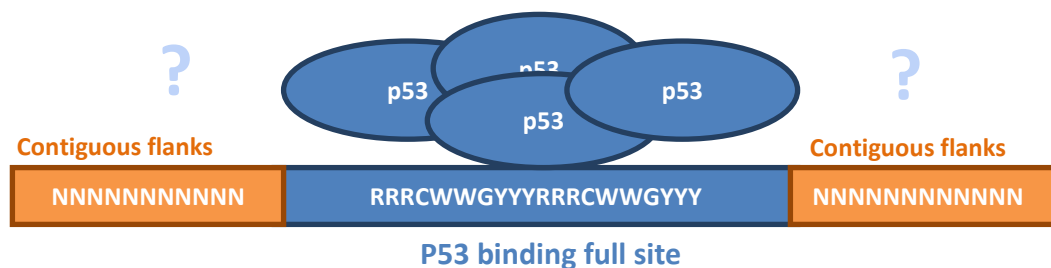
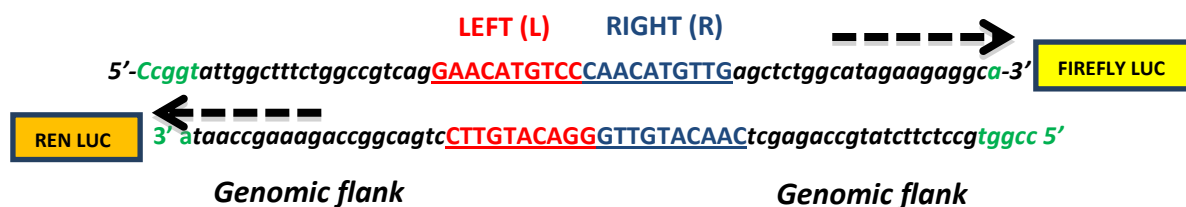


Figure 11: p53 RE in genomic context. A p53 RE is flanked by a stretch of contiguous nucleotides in genome. The interactions between p53 tetramer or dimer and a p53 RE, shown as a full canonical RE in this case, can also be influenced by surrounding nucleotide flanks depending on their physical properties and identity with respect to the genomic context.

P21LR-age_FW facing firefly LUC: (orientation 1)



P21LR-age Rv facing Renilla LUC

Figure 12: Cloning schematics of p21 LR_LUC construct: Sixty six nucleotides long p21 LR Forward and complementary Reverse oligo face Firefly LUC and Renilla LUC in 5'-3' orientation, respectively. The p21 full site contains two palindromic decamers Left (L, in red) and Right (R, in blue). The full site is immediately followed by genomic flanks contiguous to p21 RE in chromatin environment (*in italics*). Both forward and reverse strands carry AgeI restriction overhangs used for cloning in suitable vector (RGF pRS 314). The figure describes orientation 1 of cloning.

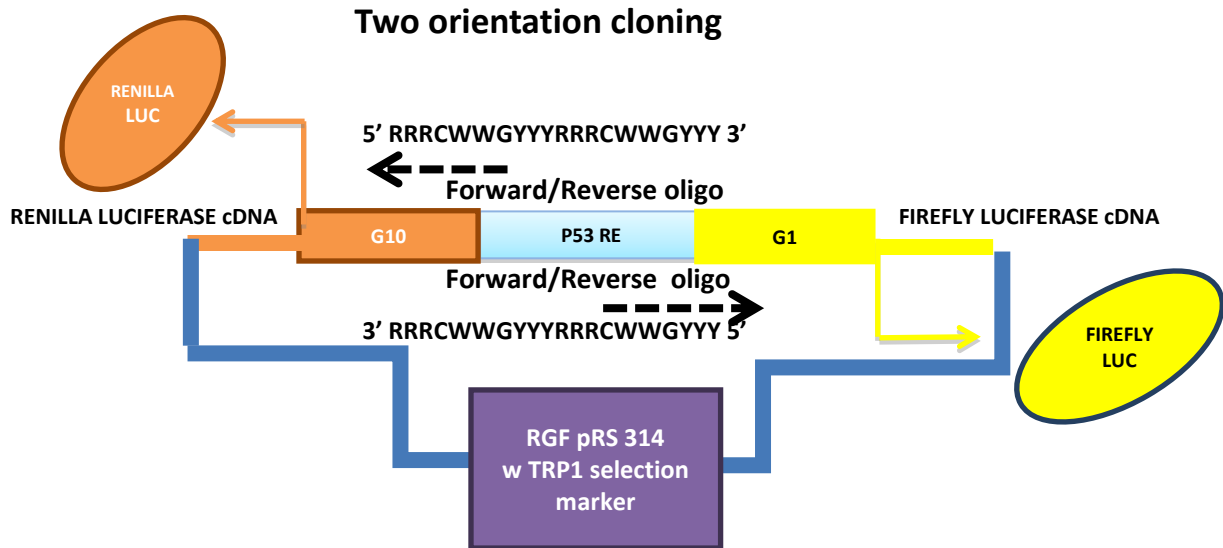


Figure 14: Bidirectional plasmid (RGF pRS 314) transcribing Firefly and Renilla Luciferases from Galactose inducible *GALI* and *GALI0* promoters, respectively. Sixty six nucleotides long phosphorylated double strand DNA oligonucleotide carrying p53 RE is ligated with Age I digested RGF pRS 314 plasmid promoter. The DNA oligos are ligated in both forward and reverse orientation facing Renilla and Firefly Luciferase, respectively.

Name of oligonucleotide	Sequence
P21LR-age_FW	<p>5' ccggtattggctttctggccgtcagGAACATGTCCCAACATGTTGagctctggcatagaagaggca 3'</p> <p>AgeI site Genomic flank LEFT(L) RIGHT(R) Genomic flank</p> <p>P21 canonical Full site</p>
P21LR-age_Rv	<p>5' ccggtgcctcttctatgccagagctCAACATGTTGGGACATGTTTCtgacggccagaaagccaata 3'</p> <p>AgeI site Genomic flank RIGHT(R) LEFT(L) Genomic flank</p> <p>P21 canonical Full site</p>
p21LR-EFR-age_Fw	<p>5' ccggtagcagcacacacacacacacGAACATGTCCCAACATGTTGgctaatttttgaattttta 3'</p> <p>AgeI site Synthetic flexible flank LEFT(L) RIGHT(R) Synthetic Rigid flank</p> <p>P21 canonical Full site</p>
p21 LR-EFR-age_Rv	<p>5' ccggtaaaaaattacaaaattagcCAACATGTTGGGACATGTTTCgtgtgtgtgtgtgtgctgcta 3'</p> <p>AgeI site Synthetic rigid flank RIGHT(R) LEFT(L) Synthetic flexible flank</p> <p>P21 canonical Full site</p>
p215RL-EFR-age_Fw	<p>5' ccggtagcagcacacacacacacacCAACATGTTGGAACATGTCCgctaatttttgaattttta 3'</p> <p>AgeI site Synthetic flexible flank RIGHT(R) LEFT(L) Synthetic Rigid flank</p> <p>P21 canonical Full site</p>
p215RL-EFR-age_Rv	<p>5' ccggtaaaaaattacaaaattagcGGACATGTTCCAACATGTTGgtgtgtgtgtgtgtgctgcta 3'</p> <p>AgeI site Synthetic rigid flank LEFT(L) RIGHT(R) Synthetic flexible flank</p> <p>P21 canonical Full site</p>

Table 5: List of p21 RE variants with flanks cloned in bidirectional RGF plasmid

Position, Features and name of flanking sequence	Sequence (20 nts)	Flexibility score
Upstream genomic flank to a p21 LR Fwd	attggctttctggccgctcag	1.931579
Downstream genomic flank to p21LR Fwd	agctctggcatagaagaggc	1.947368
Extra flexible flank upstream to p21 EFR LR	agcagcacacacacacacac	2.689474
Extra rigid flank downstream to p21 EFR LR	gctaattttgtaattttt	1.521053

Table 6: Calculation of flexibility score for the nucleotides forming p21 RE flank

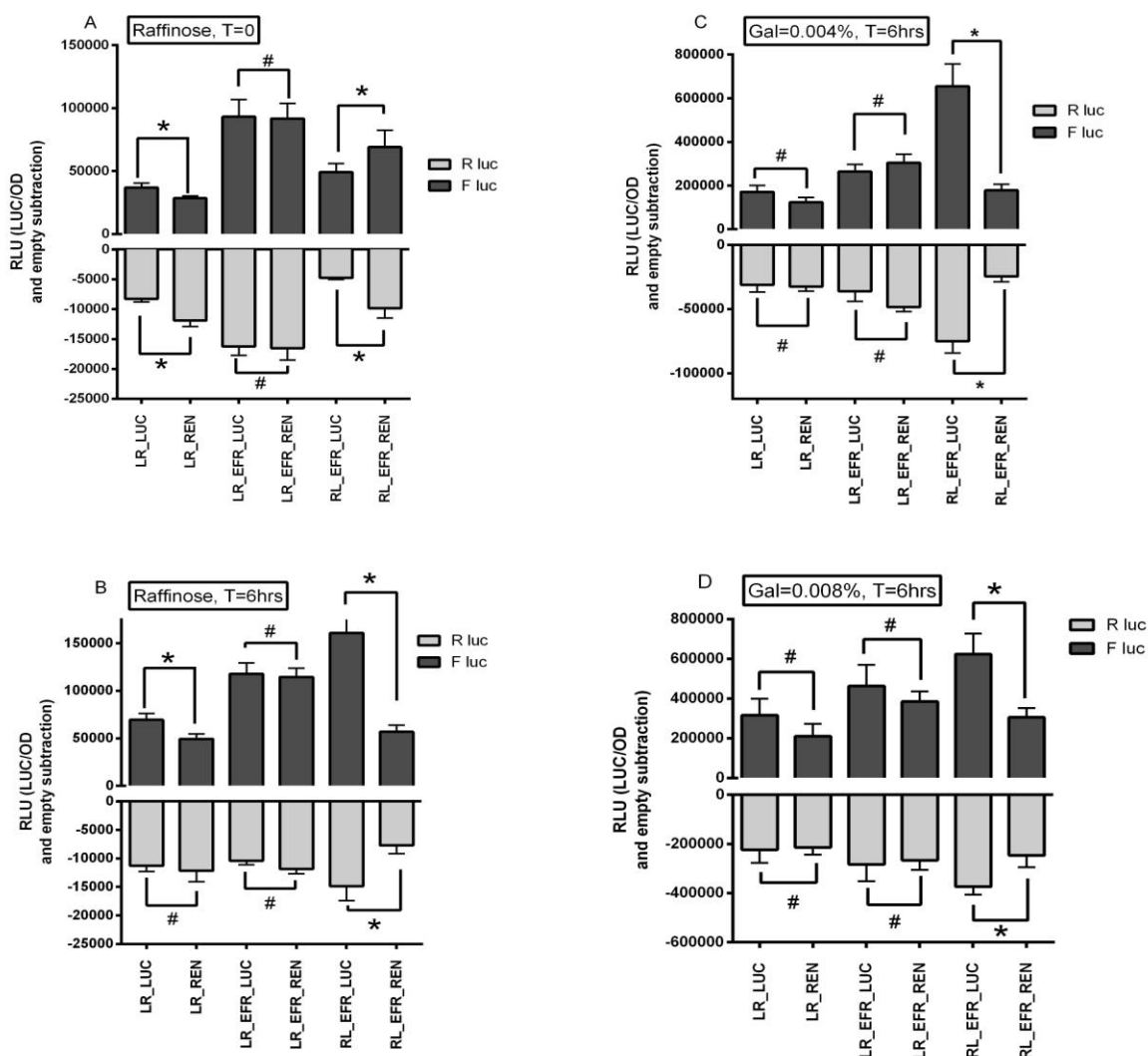


Figure 15: Dual luciferase activity of p53 RE integrated in Bidirectional plasmids in yeast. The yeast cells are transformed with RGF pRS 314 constructs LR_LUC, LR_REN, LR_EFR_LUC, LR_EFR_REN, RL_EFR_LUC and RL_EFR_REN, respectively, along with WT p53 expression plasmid or empty vector pRS 315. The transformed strains are cultured in selective synthetic media in 96 well plates with two concentrations of galactose (0.004% and 0.008%). A parallel raffinose culture (no galactose) is used as a control for all the strains. The dual Luciferase activity of empty vector transformed strains is subtracted from the p53 expressing strains to plot the values as shown above. **(A)** Dual luciferase activity exhibited by bidirectional constructs at time zero in Raffinose media. R Luc signifies Renilla Luciferase readings and F Luc signifies Firefly luciferase. Dual Luciferase is also measured at six hours post culturing the yeast cells in Raffinose media **(B)**, 0.004% galactose **(C)**, and 0.008% galactose **(D)**. * p<0.05 for the compared bars, Student's t-test . # Statistically non-significant differences

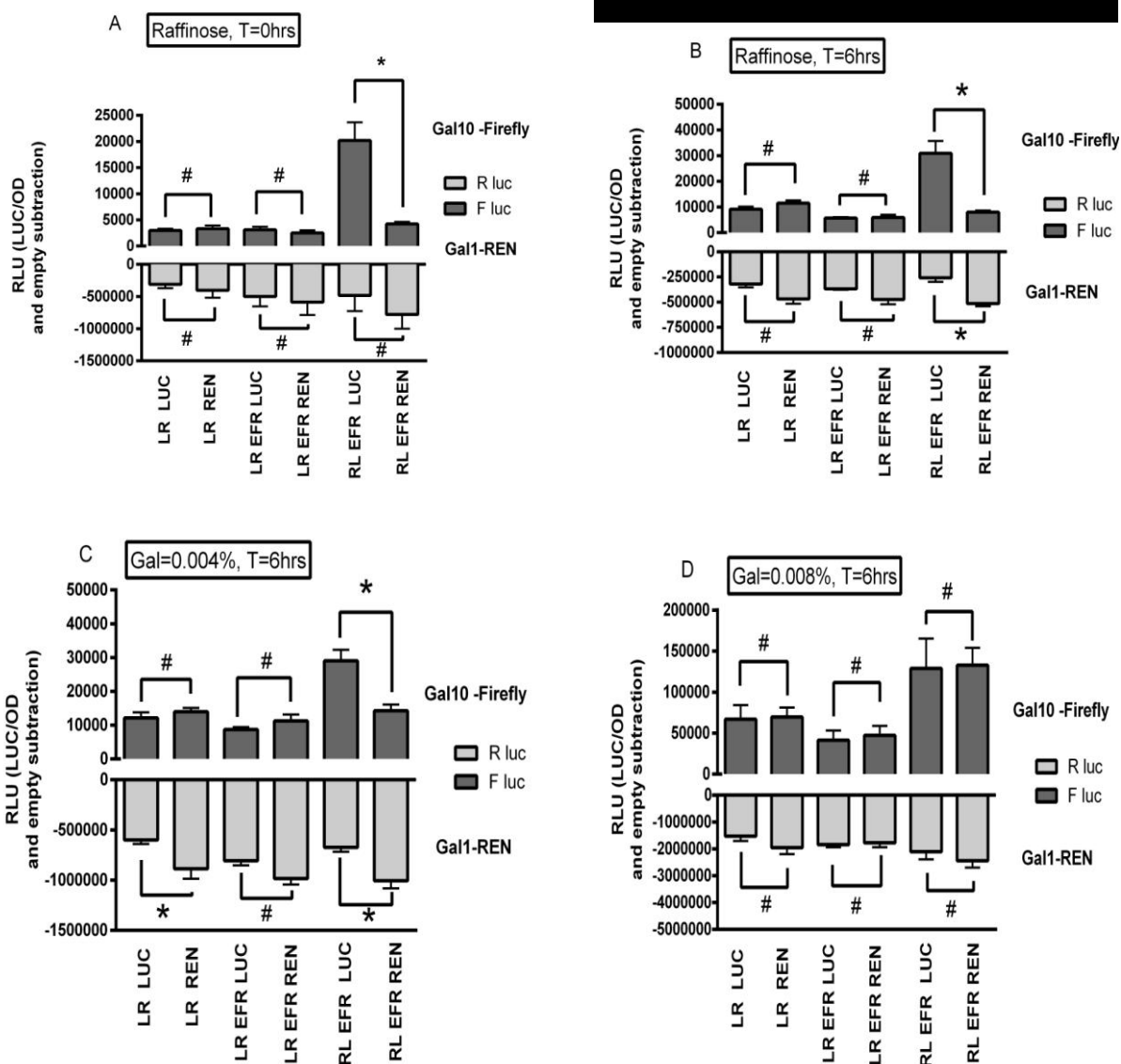


Figure 16: Dual Luciferase activity of reversed galactose inducible bidirectional promoters. Dual luciferase activity of the constructs with reversed promoters is measured at 0.004% (C) and 0.008% (D) galactose concentration six hours post culturing in selective media as described previously. Also, all the cultures are maintained in selective raffinose media (no galactose) and measured for their activity at time zero (A) and six hours post culturing (B). The F luc is Firefly activity from *GAL10* promoter and R luc signifies Renilla transcription from *GAL1* promoter. * $p < 0.05$ for the adjacent compared bars (student's t test), # Statistically non-significant differences.

Part B. NF- κ B studies

1. Quantitative analysis of transactivation potential and specificity of NF- κ B proteins in yeast and human cell lines

These experiments have been presented in a paper published last year, that is appended here, of which I am the first author. The text below summarizes the state of the art, rationale and results of the publication.

Similar to p53, NF- κ B proteins recognize a binding site (κ B-RE) with a rather loose consensus sequence. While p53 is active as a tetramer, NF- κ B acts as a dimer, and both homodimers and heterodimers can be formed between the various family members. Depending on the cell type, the predominant active NF- κ B form may differ (see also Table 1, page 30). Various non-traditional dimer-specific NF- κ B binding sites are identified through protein binding microarrays and surface Plasmon resonance techniques without any knowledge of their transactivation abilities (128, 147). Hundreds of NF- κ B binding sites (canonical as well non canonical) are identified and characterized through EMSA, ChIP-seq, or Selex studies (128, 148-150). Results established a wide range of DNA binding affinities and identified that even single nucleotide changes can impact both on affinity and selectivity of NF- κ B protein interactions (125). In my thesis work, I completed the development of a yeast-based functional assay to examine transactivation potential and specificity of NF- κ B proteins, namely p65 and p50, towards a panel of binding sites. In total, we constructed 17 reporter strains using the methodology of oligonucleotide targeting described in the Methods section and also in the paper included here. The κ B-RE panel included examples of NF- κ B *in vivo* targets, present in the MCP-1, IP-10, and IFN β promoters and others chosen to sample single nucleotide variations in the binding sites resulting in differences in binding affinity (125). We also compared reporters with a single κ B-RE (10mer), and two repeats, either adjacent or spaced.

Inducible expression vectors were constructed for p65/relA and p50. Given that p50 does not possess a transactivation domain, we also constructed a chimeric p50 (p50 fused with a p65 TAD) that enabled us to study relative transactivation potential of p50 homodimers.

The results presented in the paper indicate that p65 and p50TAD chimera (p50 fused with a p65 TAD) exhibited distinct transactivation specificities. The co-expression of p65 and p50TAD led to a change in transactivation specificity. We also tried to test in the assay the impact of trans regulatory factors (small molecules or protein cofactors). We cloned the I κ B α cDNA under a constitutive promoter on a plasmid that is leucine auxotrophy selectable and co-transformed it in the most p65-responsive yeast strain. We observed 50% down regulation in p65 activity in terms of luciferase activity, consistent with a previous study (151), but with the advantage in our settings of inducible expression of p65. Two small molecules, Ethyl Pyruvate and BAY 11-7082, showed a dose dependent impact on NF- κ B transactivation, suggesting a potential use of the assay to screen for small molecules targeting the activity of specific NF- κ B proteins.

Overall, this study confirms that NF- κ B proteins exhibit intrinsic nucleotide preferences as sequence-specific transcription factors and the formation of heterodimers p65/p50 provides for a change in transactivation specificity and that, in principle, small molecules can be identified in a yeast system which alter transactivation specificity. Considering the sequence features of κ B-REs, we confirmed that a change of single nucleotide can increase or decrease transactivation potential of a RE drastically. Although, we noticed an overall low correlation between relative DNA binding affinities measured in vitro and transactivation potential with the yeast-based assays. Finally, considering the contiguous arrangements of multiple κ B-REs, we observed additive or nearly additive interactions, contrary to the case with p53, where cooperative interactions are influenced by the spacer between full site REs (77).

To check if the yeast based NF- κ B transactivation profiles hold significance in mammalian cells as well, we tested 4 κ B-REs. Each of these REs was more active with a different NF- κ B dimer in yeast. The REs were cloned in pGL4.26, upstream of a Firefly luciferase cDNA, and transfected in breast cancer cell line MCF-7, a cell line that can activate the canonical NF- κ B pathway in response to TNF α treatment. Hence, rather than using ectopic expression of different NF- κ B proteins, I treated transfected MCF7 cells with different doses of NF- κ B inducing chemokine TNF α for 4 -8 hours, respectively. I observed that also in MCF7 cells, the order of transactivation potential exhibited by the κ B-REs matches the results in yeast,

suggesting that the reported assay in the lower eukaryotes can be predictive in assessing relative transactivation of κ B-REs. For example, the M2 RE identified as one of the most potent in yeast, is highly active in MCF7 cells. Treatment of transfected cells with NF- κ B inhibitor BAY 11-7082 reduced the RE-mediated transactivation in terms of Firefly luciferase activity confirming that the observed activity is mainly NF- κ B dependent.

RESEARCH ARTICLE

Quantitative Analysis of NF- κ B Transactivation Specificity Using a Yeast-Based Functional Assay

Vasundhara Sharma¹, Jennifer J. Jordan^{1*}, Yari Ciribilli¹, Michael A. Resnick², Alessandra Bisio^{1†*}, Alberto Inga^{1‡*}

1 Laboratory of Transcriptional Networks, Centre for Integrative Biology (CIBIO), University of Trento, Trento, Italy, **2** Chromosome Stability Group; National Institute of Environmental Health Sciences, Research Triangle Park, North Carolina, United States of America

‡ Current address: Department of Biological Engineering, MIT, Boston, MA, USA

† These authors are co-last authors on this work.

* bisio@science.unitn.it (AB); inga@science.unitn.it (AI)



CrossMark
click for updates

OPEN ACCESS

Citation: Sharma V, Jordan JJ, Ciribilli Y, Resnick MA, Bisio A, Inga A (2015) Quantitative Analysis of NF- κ B Transactivation Specificity Using a Yeast-Based Functional Assay. PLoS ONE 10(7): e0130170. doi:10.1371/journal.pone.0130170

Editor: Sue Cotterill, St. Georges University of London, UNITED KINGDOM

Received: November 10, 2014

Accepted: May 18, 2015

Published: July 6, 2015

Copyright: This is an open access article, free of all copyright, and may be freely reproduced, distributed, transmitted, modified, built upon, or otherwise used by anyone for any lawful purpose. The work is made available under the [Creative Commons CC0](https://creativecommons.org/licenses/by/4.0/) public domain dedication.

Data Availability Statement: All relevant data are within the paper and its Supporting Information files.

Funding: This work was funded by intramural project "ADARE" to MAR and Jonathan Freedman (NIH, RFA RM 06 004) and partially supported by the Italian Association for Cancer Research, AIRC (IG 12869 to AI). The funders had no role in study design, data collection and analysis, decision to publish, or preparation of the manuscript.

Competing Interests: The authors have declared that no competing interests exist.

Abstract

The NF- κ B transcription factor family plays a central role in innate immunity and inflammation processes and is frequently dysregulated in cancer. We developed an NF- κ B functional assay in yeast to investigate the following issues: transactivation specificity of NF- κ B proteins acting as homodimers or heterodimers; correlation between transactivation capacity and *in vitro* DNA binding measurements; impact of co-expressed interacting proteins or of small molecule inhibitors on NF- κ B-dependent transactivation. Full-length p65 and p50 cDNAs were cloned into centromeric expression vectors under inducible *GAL1* promoter in order to vary their expression levels. Since p50 lacks a transactivation domain (TAD), a chimeric construct containing the TAD derived from p65 was also generated (p50TAD) to address its binding and transactivation potential. The p50TAD and p65 had distinct transactivation specificities towards seventeen different κ B response elements (κ B-REs) where single nucleotide changes could greatly impact transactivation. For four κ B-REs, results in yeast were predictive of transactivation potential measured in the human MCF7 cell lines treated with the NF- κ B activator TNF α . Transactivation results in yeast correlated only partially with *in vitro* measured DNA binding affinities, suggesting that features other than strength of interaction with naked DNA affect transactivation, although factors such as chromatin context are kept constant in our isogenic yeast assay. The small molecules BAY11-7082 and ethyl-pyruvate as well as expressed I κ B α protein acted as NF- κ B inhibitors in yeast, more strongly towards p65. Thus, the yeast-based system can recapitulate NF- κ B features found in human cells, thereby providing opportunities to address various NF- κ B functions, interactions and chemical modulators.

Introduction

The nuclear factor- κ B (NF- κ B) is a ubiquitously expressed family of transcription factors (TFs) that have critical roles in inflammation, immunity, cell proliferation, differentiation and survival [1]. Constitutive activation of these proteins is related to tumor prevalence and various diseases such as arthritis, immunodeficiency and autoimmunity [2]. These proteins are included in the category of rapidly acting, sequence-specific TFs that are present as inactive proteins in the cell and do not require new protein synthesis for activation. The activities of NF- κ B proteins are tightly regulated at multiple levels and are influenced by several types of external stimuli as well as internal regulators [3,4]. Among the latter group, the I κ B (Inhibitor of NF- κ B) family of proteins is prominent among negative regulators of NF- κ B activity. I κ B associates with NF- κ B through noncovalent, stable interactions forming NF- κ B/I κ B complexes. This interaction masks NF- κ B nuclear localization signals, thereby inhibiting NF- κ B translocation into the nucleus [5]. External stimuli such as IL-1 (interleukin-1), TNF α (tumor necrosis factor- α) and LPS (bacterial lipopolysaccharide) lead to phosphorylation of I κ B by the I κ B kinase (IKK) complex protein and subsequently enable nuclear translocation of NF- κ B and transcription of the target genes [6,7]. Various pharmacological inhibitors act as direct or indirect inhibitors of NF- κ B activity *in vitro* or in mammalian systems. Ethyl pyruvate (EP) directly inhibits NF- κ B transactivation by targeting the DNA binding ability of p65 [8]. The small molecule BAY 11-7082 (BAY) has an indirect effect on NF- κ B by inhibiting the I κ B kinase (IKK) [9,10] or suppressing its activation [11].

The NF- κ B family can be divided into two subfamilies: type I (NF- κ B1/p50 and NF- κ B2/p52) and type II (p65/RELA, RELB and C-Rel). Structurally, the conserved N-terminal region of NF- κ B proteins share a sequence homology across all the subunits that is termed Rel Homology Domain (RHD) [12,13] and is responsible for subunit dimerization, sequence-specific DNA binding and nuclear localization. The carboxy-terminal region comprises the transactivation domain (TAD) but is absent in p50 and p52 subunits. These two TAD deficient subunits can activate transcription only when they form heterodimers with a type II subunit or as homodimers in complex with other co-factors. Therefore, NF- κ B dimers composed only of p50 and/or p52 subunits fail to activate transcription. The five NF- κ B subunits can combine in pairs to produce up to 15 distinct functional NF- κ B dimers [14]. Nevertheless, the physiological existence and relevance of all 15 dimers is not completely understood. The p50/p65 heterodimer is the most prevalent and well-studied NF- κ B family dimer [14]. The p50 subunit can contribute to p65-mediated transcription, while p50 homodimers may have a repressive effect on NF- κ B target gene expression [15]. Some of the NF- κ B dimers are rarely observed *in vivo* such as p65/RelB and c-Rel/RelB [16].

NF- κ B homo- or hetero-dimers target a loose consensus sequence of 9–11 base pairs embedded in promoter or enhancer regions of target genes, referred to as κ B binding site or κ B Response Element (κ B-RE). The general motif of this consensus sequence is 5' -GGGRNWY YCC-3' (R = purine, N = any nucleotide, W = adenine or thymine, and Y = pyrimidine) [13]. Each NF- κ B monomer occupies half of the κ B-RE. NF- κ B homo or heterodimers exhibit distinct DNA binding preferences towards specific κ B-REs. The optimal DNA binding motifs for p50 and p65 homodimers based on *in vitro* selection are GGGGATYCCC and GGGRNTTTC, respectively [17]. Distinct physical contacts along the 10-base-pair κ B RE by NF- κ B p50 homodimer or p65 homodimer have been identified through crystal structure analyses [18],[19]. The exact nature and mechanism of interactions between NF- κ B and κ B-RE sequences responsible for changes in transactivation specificities are not clearly understood. A single nucleotide change within κ B-RE sequences can dramatically alter binding affinity, thereby impacting NF- κ B-dependent target gene expression [20,21]. In a previous study, the transactivation potential of a

κ B-RE was revealed to be strongly influenced by the central base pair, which also impacts recruitment of p52 and p65 homodimers [22]. It has been proposed that NF- κ B family transactivation specificity is not uniquely coded in the κ B-RE sequence, suggesting participation of other cofactors in subunit specificity at NF- κ B target gene promoters [23].

To investigate the role of κ B-RE sequences in mediating transactivation specificity in the absence of other endogenous regulatory regions that might influence κ B-RE and NF- κ B dynamics, we developed a versatile yeast-based NF- κ B functional assay inspired by our previous work on the p53 family of transcription factors [24–26]. Since p50/p65 heterodimer is the most prevalent and well-studied dimer member of NF- κ B family, we focused our attention on these proteins. Using several κ B-REs selected from endogenous target sites, or differing by single nucleotide substitutions, we have employed *in vivo* quantitative analysis to address a) transactivation specificity of NF- κ B proteins acting as homodimers or heterodimers; b) correlation between transactivation capacity and DNA binding measurements *in vitro*; c) impact of protein interactors, namely I κ B α ; and d) impact of small-molecule inhibitors on transactivation by NF- κ B proteins.

Materials and Methods

Construction of yeast reporter strains containing κ B-REs regulating the expression of the Firefly cDNA

A panel of isogenic yeast reporter strain containing different version of single copies of the decameric κ B-RE sequences, or two copies in tandem was constructed using single strand targeting oligonucleotides (Eurofins MWG Operon, Ebersberg, Germany), at the chromosomal XV locus containing a minimal *CYC1* promoter driving the expression of the *Firefly* luciferase cDNA. These experiments were developed following a previously published approach [24,25] that is an adaptation of the “*delitto perfetto*” approach to *in-vivo* site-directed mutagenesis [27,28] and starts with the yLFM-ICORE strain [25,29–31]. The protocol utilizes single-strand oligonucleotides that contain a desired κ B-RE and exploits a triple-marker cassette positioned in the yLFM-ICORE strain near the *CYC1* promoter. The cassette contains a counter-selectable gene (*URA3*), a reporter gene (*kanMX4*), and the I-SceI homing endonuclease along with its unique 18nt recognition site. The latter gene allowed us to engineer a unique double-strand break at the site where the cassette is cloned, which in turn leads to high efficiency oligonucleotide targeting *via* homologous recombination mediated by short (30nt) homology tails in the oligonucleotide sequence. These tails correspond to the sequence flanking the I-SceI target site placed on the chromosome, while the desired κ B-RE sequence is at the center of the oligonucleotide sequence. Oligonucleotide targeting events were selected exploiting the counter-selectable and reporter markers of the ICORE cassette and correct reporter strains’ construction was confirmed by colony PCR across the engineered chromosomal region, followed by DNA direct sequencing (BMR Genomics, Padua, Italy).

Construction of p65 and p50 inducible yeast expression vectors

Inducible expression in yeast of NF- κ B family proteins was achieved with a *GALI-10* promoter using either a pTSG- (TRP1) or a pLSG- based (LEU2) vector [24,30]. Cloned sources of NF- κ B protein cDNAs were a generous gift from Dr. Michael Karin (University of California at San Diego). Plasmid construction was achieved by standard restriction/ligation approaches and clones obtained upon transformation of competent *E. coli* cells were checked by DNA sequencing (BMR Genomics, Padua, Italy). In the case of p50 and RelB, chimeric constructs were also constructed by fusing the region from p65/RelA corresponding to amino acids 302–

549 and containing the transactivation domain, to the C-terminal end of either coding sequences, removing the stop codon. These chimeras were obtained by a PCR-based approach using specific primers amplifying the chosen portion of the p65/RelA cDNA and containing homology tails for a gap-repair approach in yeast [32]. The PCR amplicon was then co-transformed together with the pTSG-p65 or pTSG-RelB plasmids linearized using the SalI or NotI enzymes that are present downstream to the cloned cDNA stop codon. Transformants of this gap-repair assay were cultured to extract genomic and plasmid DNA and then used to transform *E. coli* competent cells to prepare plasmid DNAs that were then checked by restriction digestion and confirmed by DNA sequencing (BMR Genomics). The resulting plasmids were named pTSG-p50TAD and pTSG-RelBTAD. The latter was however inactive in the yeast-based transactivation assays (data not shown). Plasmid pLSG-p50TAD was constructed starting from pTSG-p50TAD (originally derived from pRS314) and pRS315 [33] swapping the portion of the vector containing the selection marker by PvuII restriction and ligation.

I κ B α cDNA cloning into an *ADH1*-based yeast expression vector

Using a designed set of primers containing flanking 5' and 3' homology tails for the *ADH1* promoter region and a *cyc1*-derived terminator sequence, we amplified the human I κ B α coding sequence (953 bp) from cDNA obtained from total RNA extraction of human MCF-7 cells to obtain a PCR amplicon that could be used in a gap repair experiment. As receiving vector for this recombination-based cloning we used the centromeric pRS315-derived pLS-Ad vector [24], containing the *LEU2* selectable marker, the constitutive *ADH1* (alcohol dehydrogenase 1 gene) promoter for expressing cDNA of interest and a terminator sequence from the *CYC1* gene to facilitate transcriptional termination. The pLS-Ad was digested with XhoI and SalI and co-transformed in yeast together with the PCR product using the lithium acetate yeast transformation protocol [34]. Transformants were selected on plates lacking leucine (referred to as SDIA). Randomly selected colonies from SDIA plates were used to recover the expected recombinant plasmid through yeast total DNA extraction protocol, transformation into DH5 α *E. coli* competent cells, subsequent DNA extraction (Qiagen, Milan, Italy), followed by digestion with restriction enzymes to select positive clones, which were further verified by DNA sequencing (BMR Genomics, Padua, Italy). Co-transformants (LiAc protocol) of the correct I κ B vector clone (*LEU2* marked) with an NF- κ B expression vector (*TRP1* marked) into γ LFM-M2 reporter strain were selected on double drop-out plates lacking leucine and tryptophan and containing a high amount of adenine. The empty vector pRS315 was co-transformed along with each of the NF- κ B expression vectors or with pRS314 to generate an appropriate control.

Yeast-based Luciferase assays

The newly constructed γ LFM- κ B-RE strains were transformed with the NF- κ B expression vectors. Transformants were then processed for the miniaturized protocol of the luciferase assay we recently developed [24]. Briefly, transformant colonies kept on selective glucose plates were grown for 16 hours, unless otherwise stated, in synthetic liquid media containing raffinose (2%) with or without different concentrations of galactose, which serves as inducer of the *GAL1* promoter driving the expression of the NF- κ B proteins. Luciferase activity was measured using the Bright Glo Luciferase assay kit (Promega, Milan, Italy) and expressed either as relative light units (RLU) normalized to optical density (600 nm), subtracting the luminescence obtained by the cells transformed with the empty vector in each reporter strain, or as fold-induction over the empty vector. Experiments included four biological repeats and the results were plotted as mean values and the standard errors of the mean.

Gene reporter assays in MCF7 cells

Four κ B-REs were tested in the human MCF7 cell line. Two copies of the decameric motif were cloned in direct orientation upstream of Firefly luciferase gene within the pGL4.26 vector (Promega), using a pair of complementary oligonucleotides ligated into KpnI/XhoI double-digested plasmid. A unique NdeI restriction site was included 5' to the κ B-REs to facilitate the identification of ligation products. Plasmids were purified and sequenced across the modified region. For gene reporter assays, MCF7 cells were transiently transfected at ~80% confluence using FugeneHD (Promega) with the newly constructed pGL4.26 reporters and the pRL-SV40 control luciferase vector. Twenty-four hours after transfection, cells were treated with the immune-cytokine TNF α (either 10ng/ml or 50ng/ml). When needed, the IKK inhibitor BAY11-7082 was added at the final concentration of 20 μ M for a total of 8 hours. Dual luciferase assays were performed 4 hours or 8 hours after TNF α treatment, following the manufacturer's protocol.

Western Blot assays in yeast and human cells

Yeast transformants were grown for 16 hours in selective medium containing the indicated amounts of galactose to induce the expression of NF- κ B cDNAs from the *GALI*-based vectors. An equivalent amount of cells, based on the culture absorbance measurement (corresponding to 2.5 OD measured at OD_{600nm}), was collected by centrifugation. Cells were processed following extraction protocols described previously [35,36] and 15 μ l of extracts were loaded on 12% poly-acrylamide gels. Transfer onto nitrocellulose membranes was achieved using the i-Blot semi-dry system (Invitrogen, Life Technologies, Milan, Italy). Specific antibodies directed against p65/RelA TAD domain (clone C-20 Santa Cruz Biotechnology, Milan, Italy) or p53 (clone DO-1, Santa Cruz Biotechnology) were diluted in 1% non-fat skim milk dissolved in PBS-T. PGK1 (Phospho Glycerate Kinase 1) was used as a loading control and immunodetected with a monoclonal antibody (clone 22C5D8, Life Technologies, Milan, Italy). Nuclear and cytoplasmic protein lysates from human MCF7 cells were prepared using NE-PER Nuclear and Cytoplasmic Extraction Kit (Thermo Fisher, Monza, MB, Italy) and quantified using the BCA assay (Thermo Fisher). 20 μ g of proteins were loaded onto 12% poly-acrylamide gels. p65 (clone C-20), p50 (clone H119, Santa Cruz), GAPDH (cytoplasmic markers; clone 6C5, Santa Cruz) and Histone 3 (nuclear marker, Ab1791, Abcam) were probed. Immuno-reactive bands were detected using the ECL Select reagent (Amersham, GE Health Care, Milan, Italy) and the ChemiDoc XRS+ documentation system through the ImageLab software (BioRad, Milan, Italy).

Results

Development of p65 and p50 expression vectors and reporter yeast strains

We cloned full-length human p65 and p50 cDNAs under the control of the *GALI* promoter in a centromeric yeast expression vector. This promoter was chosen as it enables a wide variation in protein expression in cells cultured in medium containing raffinose (the carbon source) supplemented with various amounts of galactose to induce *GALI* transcription [37]. We were confident that p65 could act as a sequence-specific TF in yeast based on a previous report [38] and on the fact that the protein contains a transactivation domain of the acidic class that is reported to be proficient in contacting the yeast transcriptional machinery [39]. However, given that p50 does not contain a transactivation domain, we also generated a chimeric p50-referred to as p50TAD- where the transactivation domain of p65 was fused to the carboxy-terminus of the

p50 coding sequence. This provided a unique opportunity for an *in vivo* functional assessment of p50 DNA binding specificity.

To develop isogenic κ B reporter strains, we took advantage of the *delitto perfetto* based protocol [24,28] for *in vivo* targeting κ B-REs to a chromosomal locus containing a minimal promoter placed upstream of the Firefly luciferase gene [24,28]. The protocol is described in the Material and Methods. Seventeen κ B-REs were chosen to sample a wide range of DNA binding affinities that had previously been measured by *in vitro* gel shift assays (see sequences in Table A in [S1 File](#)) [21]. The seventeen yeast reporter strains were transformed with p65 or p50 expression vectors and luciferase assays were developed following a miniaturized protocol we previously established for the p53 family of transcription factors [24].

p65 and p50TAD exhibited differences in relative transactivation capacity and specificity

Presented in [Fig 1A](#) are the results of transactivation at the seventeen REs following moderate levels of induction of p65 or p50TAD (0.032% gal, as described in [Fig 1D](#)). p50TAD activated transcription of eight of the seventeen REs ([Fig 1A](#)). This result establishes that p50 can establish specific interactions with target κ B-RE sequences when expressed in yeast. p65 was active towards ten κ B-REs, but the relative transactivation potentials and pattern of specificities differed remarkably from that of p50TAD ([Fig 1A](#)). Five κ B-REs were inactive both with p65 and p50TAD. One RE (LIF) was specifically responsive to p50TAD, while three (RANTES, RE2, M1) were selectively responsive to p65. Some of the κ B-REs are named from the corresponding human NF- κ B target genes. However, in our assay only the decameric κ B motif is studied.

Consensus sequences generated using the web logo tool with the transactivation-proficient and deficient κ B-REs revealed that mismatches at positions 6 but, surprisingly, also changes at the supposedly permissive position 5 of the decameric $G_1G_2G_3R_4N_5W_6Y_7Y_8C_9C_{10}$ κ B-RE impaired transactivation by both proteins ([Fig 1B and 1C](#)). Moreover, p50TAD showed a preference for an A in position 5, while a T at position 8 also negatively impacted transactivation. Taken collectively, the results were in agreement with reported differences in p50 and p65 optimal binding sites determined by SELEX [40]. Overall, p65 was a stronger transcription factor compared to p50TAD (both were expressed at similar levels; [Fig 1D](#)).

Both p50TAD and p65 exhibited weak transactivation cooperativity from adjacent κ B-REs

Having established that both p65 and the chimeric p50TAD could act as sequence specific TFs in yeast, we explored whether two adjacent κ B-REs could lead to synergistic induction of transactivation. Some natural NF- κ B target sites contain pairs of κ B-REs, whose sequence features can impact on gene transcription [20]. Functional interactions between nearby κ B-RE sites have been reported [22] and the potential for cooperative interactions between NF- κ B proteins at clustered binding sites has been inferred [41], but not directly addressed under a defined experimental system. The experiments were performed using two different amounts of galactose to titrate the transactivation response. The M2 and I1 REs, which were highly responsive to p65 and moderately responsive to p50TAD, were chosen. Reporter strains containing two adjacent RE copies had an additive effect when analyzed with p50TAD for both κ B-REs. A higher amount of galactose (0.1%) did not lead to higher transactivation levels with p50TAD, suggesting that the maximal level of responsiveness for these strains was reached at 0.032% galactose. Instead, p65 showed a galactose-dependent transactivation ability and mainly additive effects for one vs two REs number, with the exception of the M2 RE at the lower galactose concentration ([Fig 2A](#)). We also tested RE6 and the combination of RE6 and RE1, which were

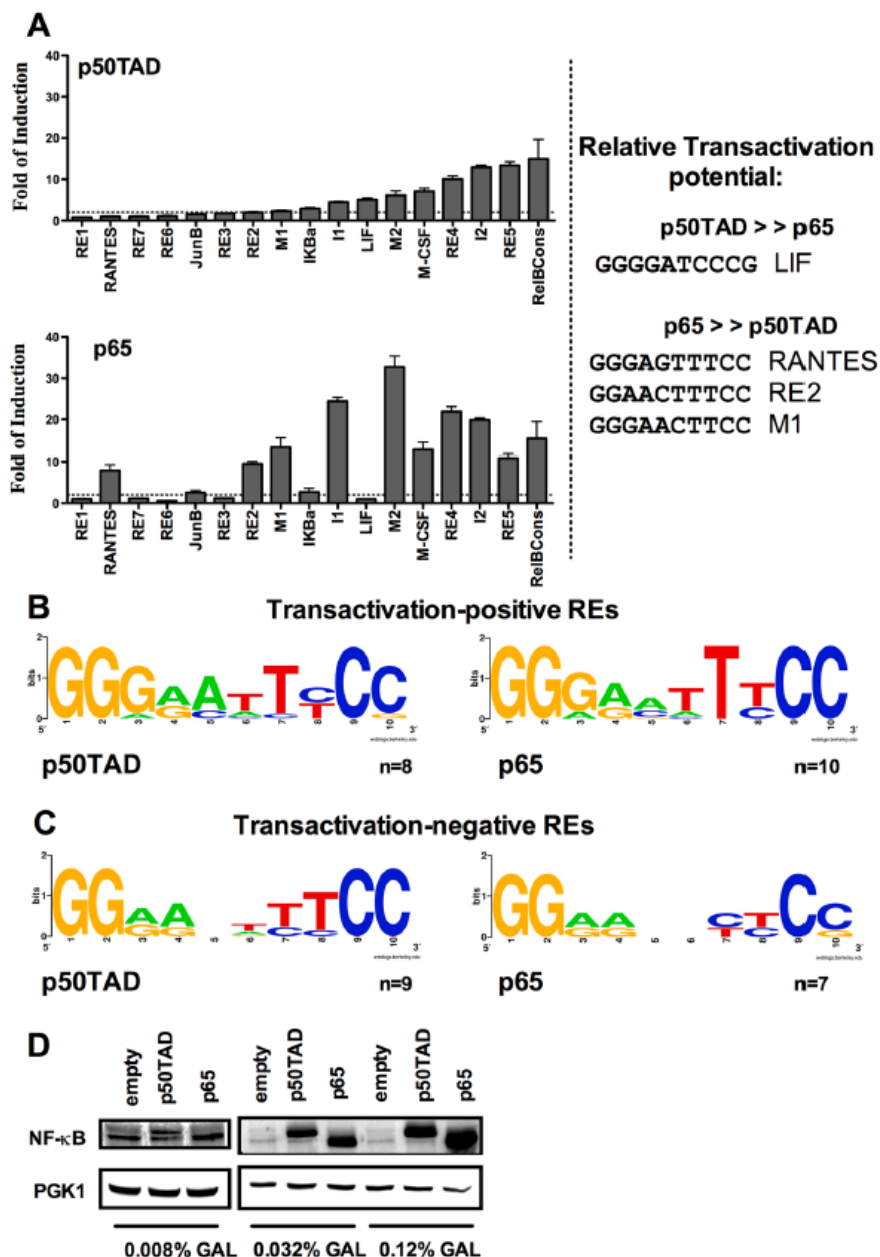


Fig 1. Relative transactivation potential of p50 and p65 homodimers towards a panel of κB Response Elements. **A)** κB target site preferences of p50TAD and p65 homodimers. Luciferase assays were performed to quantify relative transactivation capacity of p50TAD and p65 homodimers towards 17 different κB-REs. Reporter strains were grown in selective media containing 0.032% galactose for 16 hours reaching near stationary phase. For each isogenic reporter strain, the luciferase activity is calculated as fold-induction with respect to the values obtained with empty vector transformants. The average normalized activity and the standard error of four biological repeats are presented. κB-REs are ranked based on increasing transactivation potential with p50TAD. The same rank is used to plot the results obtained with p65 (lower panel). To the right are presented κB-RE sequences that are selectively responsive to either p50TAD or p65 (see text for sequence match to optimized consensus for p50 or p65). **B, C)** Web logo representations of the groups of κB-REs that were active or inactive with p50TAD and p65, respectively. **D)** Western blots presenting the relative expression of p50TAD and p65 proteins at

different amounts of galactose. Yeast cells transformed with the GAL1-based expression vectors for NF- κ B proteins were cultured for 16 hours at the indicated concentrations of galactose. An antibody directed against the p65 transactivation domain, which is also present in the p50TAD construct, was used for immunodetection. PGK1 endogenous protein provides a loading control.

doi:10.1371/journal.pone.0130170.g001

inactive both with p65 and p50TAD when studied separately. Two copies of the non-responsive RE6 did not lead to any transactivation either with p50TAD or p65 even using very high expression levels (1% galactose) (Fig 2B). The same was true for the combination of RE6 and RE1 except for weak responsiveness to p65.

Next, we investigated *cis*-based interactions among different κ B-REs using those from the MCP1 promoter as an example. The responsiveness to NF- κ B of this promoter in human cells is mediated by two closely-spaced REs (M1 and M2) that are separated by 19 nt and are located ~ -2.8kb from the transcriptional start site (TSS) [20,22]. As noted above, the M2 κ B-RE is highly responsive to p65, while M1 exhibited lower responsiveness. On the contrary, the M1 κ B-RE was not responsive to p50, while M2 was weakly responsive. We developed reporter strains containing combinations of M1 and M2 κ B-REs, and also examined the impact of the 19nt spacer sequence between them as well as the effect of the relative positioning of the two κ B-REs with respect to the promoter of the reporter and the TSS. Strains containing two copies of the M1 or M2 κ B-REs were used as controls (Fig 2C).

The non-responsiveness of the M1 RE to p50TAD was confirmed, even when two adjacent copies of this κ B-RE are placed upstream the reporter cassette. The reporter strain containing both M1 and M2 showed responsiveness to p50TAD, similar to what was observed with the M2 strain, while the transactivation by p65 was intermediate between the M1 and M2 strains. The M1 κ B-RE had a stronger negative impact towards p65 than p50TAD. The relative positioning of the M1 and M2 κ B-REs relative to the TSS of the reporter gene did not affect the transactivation potential. Interestingly, the natural 19nt spacer between the M1 and M2 decamers did not impact the transactivation potential. Overall it appears that there is limited functional interaction between adjacent or closely spaced κ B-REs for p50- or p65-dependent transactivation in yeast.

Co-expression of p50 and p65 leads to specific changes in relative transactivation

Since p50 and p65 are normally present at the same time in mammalian cells and the p50/p65 heterodimer is considered a prominent functional complex *in vivo*, we examined p50 and p65 co-expression and transactivation towards the eight κ B-REs described in Fig 3A and 3B. Both genes were expressed under the same GAL1 promoter on different single copy centromere plasmids. Experiments were performed at two levels of NF- κ B protein expression where co-expression of p50TAD and p65 resulted in transactivation levels that were approximately an average of those seen with the expression of either protein, with the exception of the RelBCons κ B-RE. The relative proportion of homodimers and heterodimers was not determined. In fact, p50TAD or p65 alone led to similar levels of RelBCons κ B-RE transactivation but the reporter was much more responsive in the co-expression experiment. The strain with the I1 and I2 κ B-REs exhibited similar responsiveness to both p50TAD and p65, but co-expression of these two proteins did not have an impact on the level of transactivation of this promoter. At higher levels of galactose (Fig 3B), the differences between expression of p65 alone or co-expression were lower, with the RelBCons strain maintaining high responsiveness when the two TFs were co-expressed. The experiment was performed also at different time points of NF- κ B proteins induction with comparable results (Fig A in S1 File).

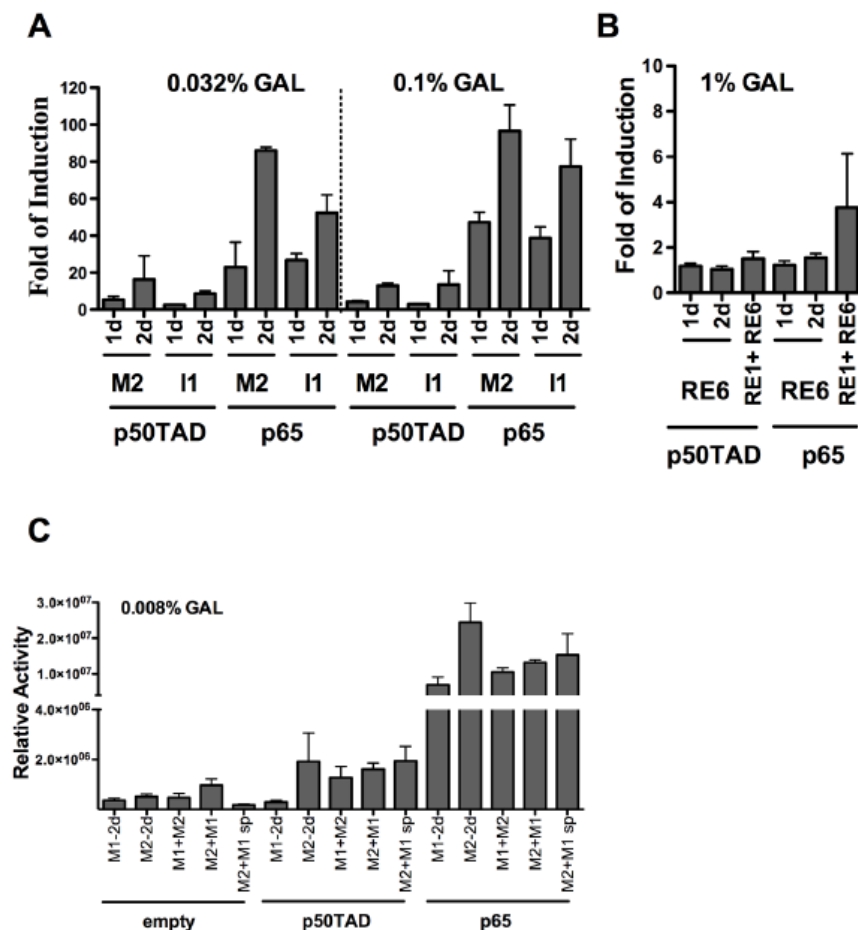


Fig 2. Additive or weak cooperative transactivation between adjacent κ B REs. **A)** Yeast-based luciferase assays were performed at moderate to high expression levels of p50TAD or p65. Results were normalized and plotted as in Fig 1. The impact of tandem duplication (2d) of the decameric (1d) κ B-RE or the indicated combination of two different κ B-REs was evaluated. The REs were chosen based on the results from Fig 1 to include sequences exhibiting different levels of transactivation potentials. **B)** RE1 and RE6 were inactive as decameric κ B-REs and there was no transactivation for two decamers in tandem or high expression of NF- κ B proteins (up to 1% galactose). **C)** Functional interactions between two different κ B-REs derived from the MCP-1 promoter. The M1 and M2 decameric κ B-REs exhibited different responsiveness to p50TAD and p65, when examined separately, but are both derived from the MCP-1 promoter and they are located in close distance (19 nucleotide spacer) in the natural context. The combined responsiveness of the M1 and M2 κ B-REs was examined, taking into account the impact of the distance between the two decamers and orientation relative to the transcriptional start site. Tandem repeats of M1 or M2 were included as controls. Yeast reporter strains, transformed with the indicated expression vector were cultured for 16 hrs with the indicated low amount of galactose. Relative activity refers to the average light units normalized for cell number (measured by optical density at 600nm). Average and standard error of four biological repeats are presented. The NF- κ B-independent reporter activity (empty vector) is also presented as reference. Interestingly, the M2+M1 strains exhibited higher basal level of reporter expression. The M1+M2 sp strain contains the M1 and M2 κ B decamers separated by 18 nt as in the human gene (see Table A in S1 File).

doi:10.1371/journal.pone.0130170.g002

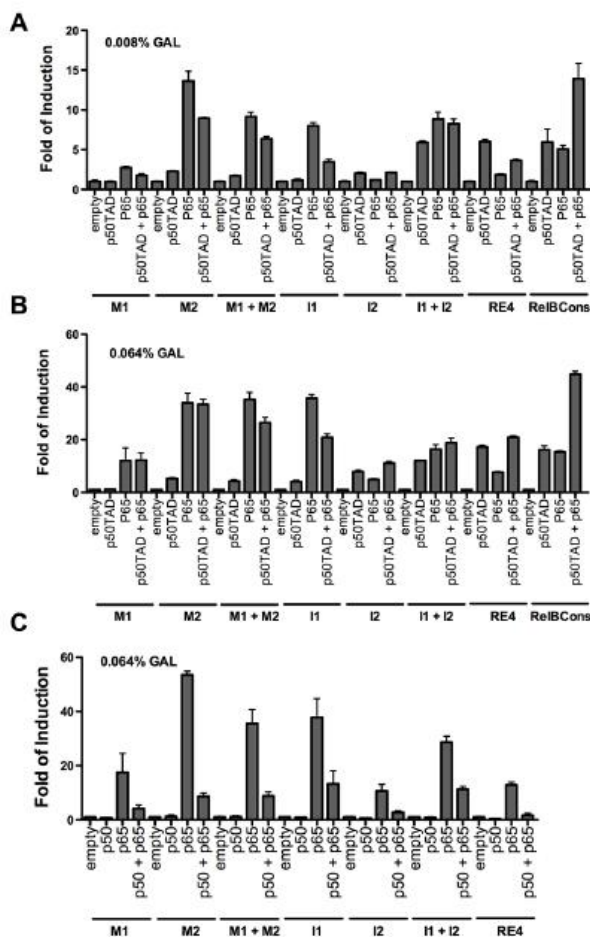


Fig 3. Functional interactions between p50 and p65 towards a panel of κ B-REs. A) and B) Eight different κ B-REs, each comprising two adjacent copies of the decameric κ B sequences were examined for the transactivation potentials of p50TAD, p65 as well as upon co-expression of both proteins. Cells were grown in lower (0.008%, panel A) and high (0.064%, panel B) levels of galactose. C) A non-chimeric p50 construct lacking the TAD domain was also studied at the higher galactose level for all REs, except RelBCons. In all panels, luciferase assays were conducted and results plotted as described in Fig 1.

doi:10.1371/journal.pone.0130170.g003

We also examined the impact of full-length p50 without the chimeric TAD, expressed alone or combined with p65 protein (Fig 3C). As expected, given the lack of a TAD, p50 was inactive as a transcription factor. However, the presence of the full-length p50 actually led to inhibition of p65-dependent transactivation in the co-expression experiments, much more than could be simply accounted for by the anticipated amount of p50 homodimer. This inhibition could be due possibly to competition for the RE site by p50 homodimers, that can be proposed for the case of I2 or RE4 given the transactivation levels with p50TAD homodimers in those strains (see Fig 3B). For other REs, such as M1 and M2 that are weakly if at all responsive to p50TAD homodimers, it could be inferred that in the co-expression experiments, heterodimers would

be preferentially formed and that the p65-p50 dimer would be a weaker transcription factor compared to p65-p50TAD.

The relative transactivation potentials of selected κ B-REs is confirmed in MCF7 cells

To examine whether the differences in transactivation capacity observed in yeast were predictive of variable responsiveness in mammalian cells upon NF- κ B activation, κ B-dependent gene reporter assays were carried out in the human MCF7 cells. We selected 4 different κ B-REs whose transactivation potential driven by co-expressed p65 and p50TAD ranked from high (M2, RelBCons) to medium (RE4) and to low (M1) in yeast. Those κ B-REs were placed upstream of the Firefly luciferase in the pGL4.26 vector for transient transfection experiments. Twenty-four hours post-transfection cells were treated with 10ng/ml (Fig 4A) or 50ng/ml (Fig 4B) TNF α and/or with 20 μ M BAY 11-7082 (BAY) respectively to activate or repress the NF- κ B pathway. Results demonstrated that differences in relative transactivation potential measured in yeast were confirmed in human cells. In fact the M2 κ B-RE was the most responsive, followed by RelBCons, with M1 being the least responsive. Time- and concentration-dependent TNF α responsiveness and repression by BAY were apparent. TNF α treatment led to a strong increase in p65 protein in nuclear extracts, while the p50 protein was already nuclear in mock condition and its abundance did not change significantly after treatment (Fig 4C). This observation suggests that the increase in M2 κ B-RE responsiveness observed already in mock condition might be dependent primarily on p50 homodimers, while the enhanced responsiveness after TNF α treatment would be related to the increase of p65 in the nucleus.

I κ B α and the small molecules BAY 11–7082 and ethyl pyruvate inhibit NF- κ B-dependent transactivation in yeast

Having established that p65 and p50TAD can act as sequence-specific TFs alone or in combination, we asked whether the assay system could be used to monitor the impact of protein or small-molecule inhibitors. In mammalian cells the functions of the canonical NF- κ B pathway are mainly regulated at the level of p65 subcellular localization [42]. In particular, I κ B α can sequester p65 in the cytoplasm by masking the nuclear localization sequences thereby inhibiting its translocation into the nucleus [6,7].

We cloned the human I κ B α cDNA into a constitutive expression vector exploiting the *ADHI* constitutive moderate promoter and the *LEU2* selection marker. This enabled us to select double transformants. The M2 κ B-RE, which was the most responsive to p65 and moderately responsive to p50TAD, was chosen for these experiments. There was a significant reduction in luciferase activity with p65-I κ B α double transformant cells, compared to transformants with p65 alone (Fig 5A). Interestingly, there was no effect of I κ B α on the basal, constitutive level of reporter expression or on the activity of the reporter dependent on p50TAD. Immunoblots indicated that in the presence of the I κ B α expression plasmid, protein levels of both p50TAD and p65 from whole cell extracts were comparable or even higher (Fig 5B), suggesting that the impact of I κ B α might actually be underestimated, and that I κ B α might stabilize p50TAD and especially p65 proteins by forming stable complexes as reported for mammalian cells [43,44].

We also explored the use of the yeast-based assay for assessing the activity of known mammalian NF- κ B inhibitors BAY [9,11,45], ethyl-pyruvate (EP) [8] and parthenolide [46]. Luciferase assays were conducted in M2, RE4 and RelBCons strains as they exhibited different relative responsiveness to either p50TAD or p65 alone or to their co-expression at a low level

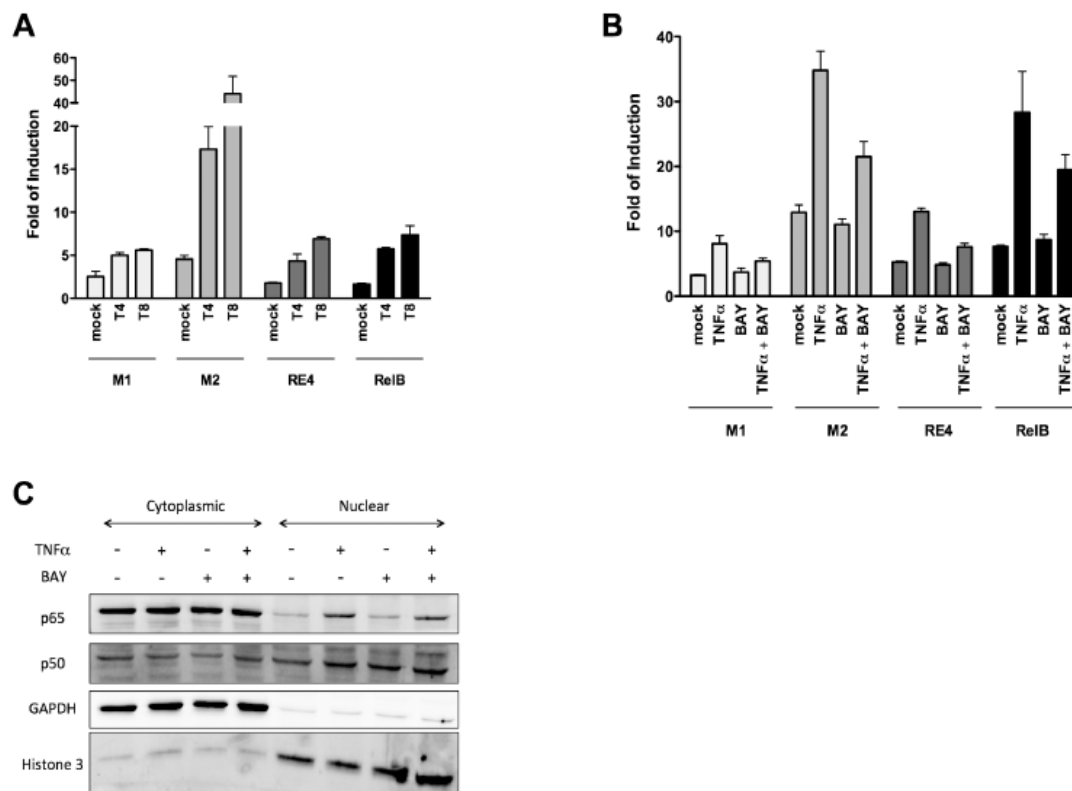


Fig 4. Functional evaluation of four selected κ B-REs in MCF7 cells. A-B) MCF7 cells were transiently transfected with four pGL4.26 derived vectors containing different κ B-REs along with a control pGL4.26 empty vector. Twenty-four hours after transfection cells were treated for 4 or 8 hours with TNF α (10ng/ml for panel A or 50ng/ml for panel B) alone or in combination with BAY 11-7082 (20 μ M for 8 hours, only for panel B). Presented are the average fold-induction relative to the empty pGL4.26 vector and the standard deviation of at least three independent biological replicates. **C)** Western blot analysis showing p50 and p65 protein levels from nuclear-cytoplasmic fractions after the indicated treatments at the following doses: TNF α (50ng/ml) and BAY 11-7082 (20 μ M). GAPDH and Histone 3 were used as reference controls for the cytoplasmic and nuclear fraction respectively.

doi:10.1371/journal.pone.0130170.g004

of galactose (0.008%) (Fig 5). BAY and EP treatments led to a dose-dependent inhibition of p65-mediated transactivation. The effect was less evident with p50TAD (Fig 6). Parthenolide had no impact on p65- or p50TAD-mediated transactivation (Fig B in S1 File). As controls, the effect of the molecules on the NF- κ B-independent, basal expression of the reporter, or on the steady-state levels of p65 or p50TAD proteins was examined (Fig 6D and 6E). To test the generality of the EP effect, we examined its impact on p53-mediated transcription, considering that p53 is expressed in yeast from the same *GAL1* promoter system used for NF- κ B [15,30]. Unlike what was observed with p65 and p50TAD, p53 transactivation was unaffected by EP up to the 5mM dose and only slightly reduced at 10mM, while at the highest dose (20mM) it was completely inhibited. Further, no impact on p53 protein levels was seen after 2.5 or 5mM EP treatment (Fig C in S1 File). Overall, while at high doses, indirect effects could potentially bias the results, the yeast transactivation system provides a tool to study specific small molecule inhibitors of NF- κ B transactivation.

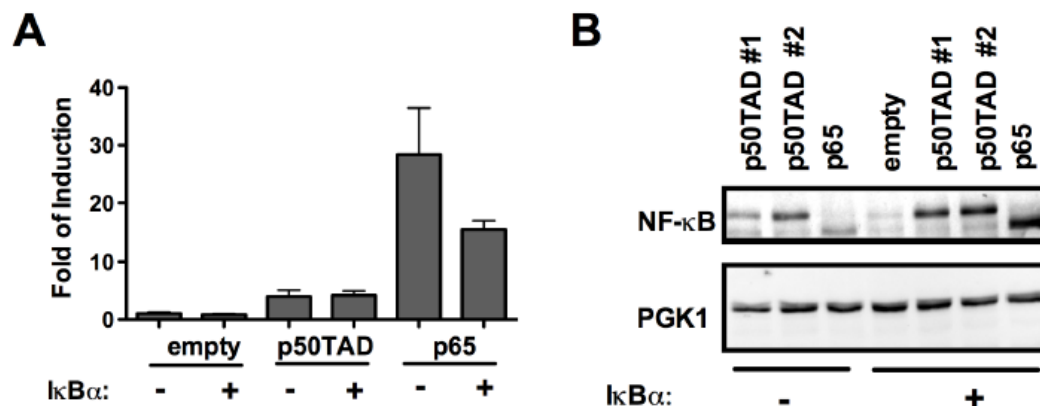


Fig 5. I κ B α inhibits p65-dependent transactivation in yeast. The highly responsive M2 strain was used to test the impact of co-expressing I κ B α with the NF- κ B proteins p50TAD or p65. **A)** Luciferase assays results were obtained and plotted as described in Fig 1. Control transformants lacking the I κ B α expression construct were obtained using the pRS315 empty vector. Cells were cultured in 0.032% galactose for 16 hours to achieve moderate expression of p50TAD or p65. I κ B α is expressed under the constitutive *ADH1* promoter. For all conditions the light units were normalized for the optical density of the cultures. The relative luciferase activity, obtained with cells transformed with empty vectors was set to 1 and used to obtain the fold of reporter induction due to the expression of NF- κ B proteins. Bars plot the average and standard errors of four biological replicates. **B)** A western blot image revealing the impact of I κ B α on p50TAD or p65 protein levels. Transformants with two p50TAD expression vectors that differ for the selection marker gene (LEU2 for p50TAD #1 and TRP1 for p50TAD #2) were included. PGK1 was used as loading control.

doi:10.1371/journal.pone.0130170.g005

Discussion

Using a quantitative luciferase assay system, we investigated the role of κ B-RE sequence in mediating NF- κ B (p50 and p65) transactivation specificity. We devised a chimeric construct (p50TAD) that enabled investigations of relative transactivation specificities of p65 and p50 when expressed alone, and their functional interactions when co-expressed. We were unable to develop an equivalent assay for RelB, even though we developed a chimeric RelB-TAD construct with an equivalent approach to that used for p50 (data not shown). This lack of activity could be due to a lack of relevant cofactors in yeast or to an inability of RelB to be expressed at sufficient levels for transactivation in the yeast nucleus. Previous studies reported the development of a yeast-based assay to measure NF- κ B dependent transactivation and had established that NF- κ B proteins can act as sequence-specific transcription factors in yeast [38] [47]. However, our work has several unique features: variable expression of the transcription factors; creation of a chimeric, transactivation competent p50 construct; use of a chromosomally integrated reporter and a microplate format that was compatible with the analysis of small molecules potentially targeting NF- κ B proteins.

p65 and p50TAD exhibited marked differences in transactivation specificity (Fig 1) and, although limited by the number of κ B-REs examined, co-expression of p65 and p50TAD led to RE-selective changes in transactivation potential. Non-chimeric p50 was inactive as a transcription factor, as expected given its lack of a transactivation domain [42], but its co-expression with p65 led to strong inhibition of p65-dependent transactivation, suggesting that p50 homodimers can compete with p65 homodimers, although we cannot exclude that heterodimers containing only one transactivation domain would be inactive as a transcription factor in yeast. p65 was highly active towards 6 κ B-REs, the highest being M2 (derived from the MCP-1 promoter) followed by I1 and RE4. All three contained the GGAA sequence, predicted to be a preferred binding motif (Table A in S1 File) [20,21]. Co-expression of p50TAD and p65 in

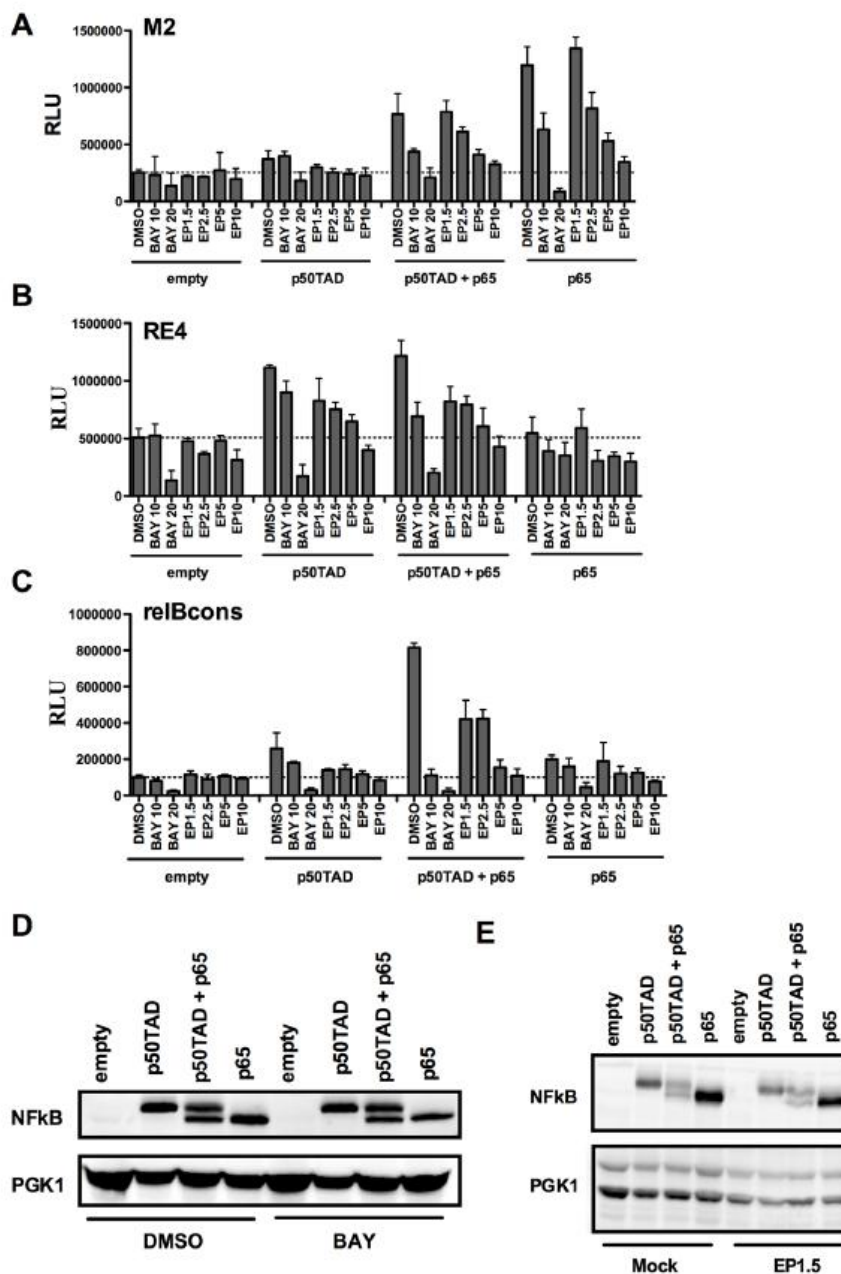


Fig 6. Effect of the small molecules BAY11-7082 and ethyl pyruvate on NF- κ B activity in yeast. The strains containing the REs M2, RE4 and reIBcons were grown overnight (16 hours) in selective media containing low levels of galactose (0.008%) with or without the addition of different concentrations of BAY11-7082 (10 μ M, 20 μ M) and EP (1.5mM, 2.5mM, 5mM, 10mM). **A-C**) Average luciferase assays and standard errors of four biological repeats are presented. Results obtained with cells transfected with an empty expression vector are included to take into account the impact of the small molecules on the NF- κ B-independent, basal expression of the reporter. **D, E**) Western blot images showing p50TAD, p50TAD + p65 and p65 protein levels in BAY and EP treated and untreated cells. PGK1 was used as a loading control.

doi:10.1371/journal.pone.0130170.g006

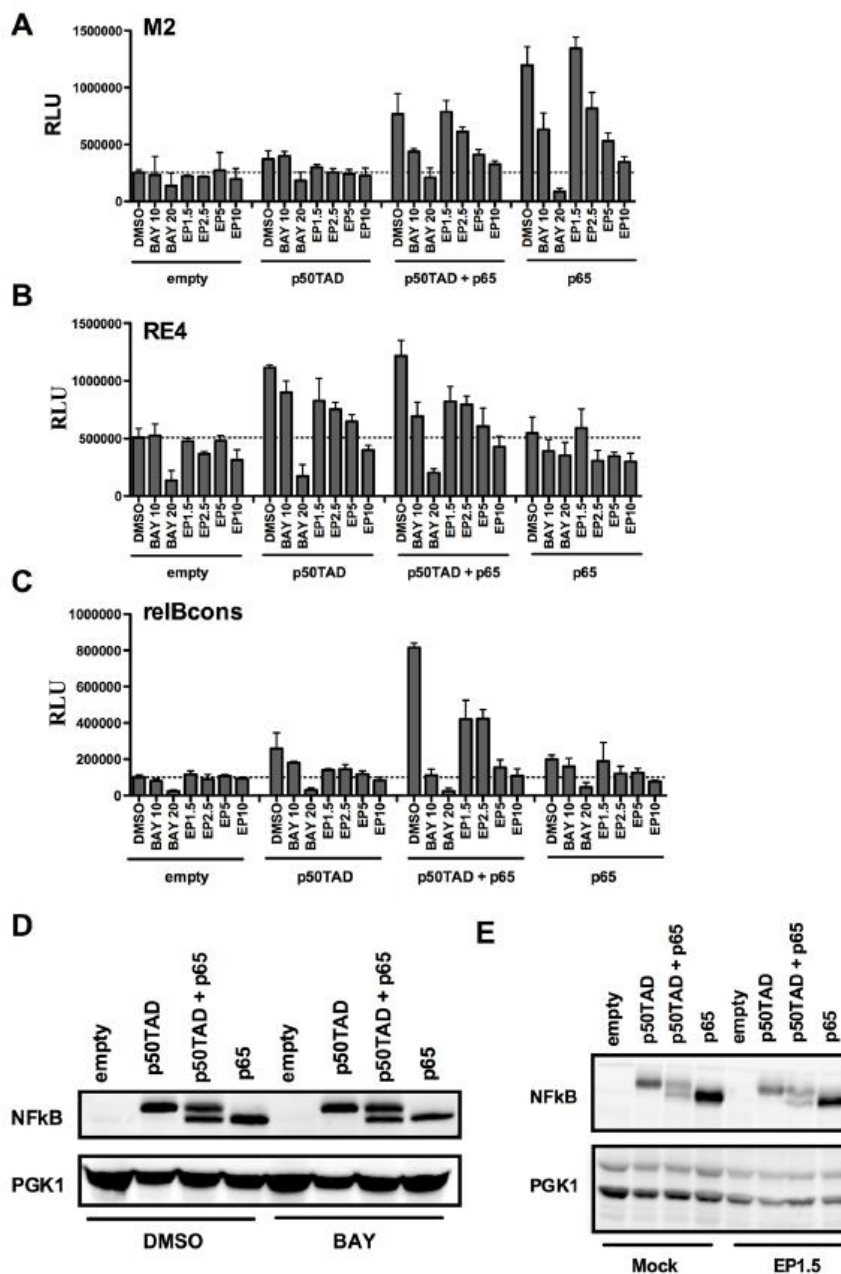


Fig 6. Effect of the small molecules BAY11-7082 and ethyl pyruvate on NF- κ B activity in yeast. The strains containing the REs M2, RE4 and reIBcons were grown overnight (16 hours) in selective media containing low levels of galactose (0.008%) with or without the addition of different concentrations of BAY11-7082 (10 μ M, 20 μ M) and EP (1.5mM, 2.5mM, 5mM, 10mM). **A-C**) Average luciferase assays and standard errors of four biological repeats are presented. Results obtained with cells transfected with an empty expression vector are included to take into account the impact of the small molecules on the NF- κ B-independent, basal expression of the reporter. **D, E**) Western blot images showing p50TAD, p50TAD + p65 and p65 protein levels in BAY and EP treated and untreated cells. PGK1 was used as a loading control.

doi:10.1371/journal.pone.0130170.g006

yeast also demonstrated high activity with 4 κ B-REs (M2, I1, RelBCons and RE4). p50TAD showed higher activity towards the RelBCons, RE5, I2 and RE4, all of which, except for I2, contained a GGGG sequence, reported to be a preferred binding motif.

We compared transactivation potentials with DNA binding affinities measured by *in vitro* gel shift assays [21] or by custom NF- κ B protein binding microarray experiments and surface plasmon resonance analysis [48], as described in Fig 7. We also wanted to address various functional aspects of NF- κ B target sequences, such as interactions between adjacent κ B-REs and the impact of short spacers. Seventeen κ B-REs were chosen for this analysis and the relative transactivation capacities were measured with p65 and p50TAD. These REs were chosen to represent a wide range of DNA binding affinities (~100-fold for p50), based on EMSA assays [21]. There were striking exceptions to an overall correlation trend between relative DNA binding affinity and relative transactivation potential both for p50 and p65+p50. For example, JunB and RE6 were extremely weak in transactivation assays but were reported to be bound with high affinity *in vitro* (Fig D in S1 File). The overall correlation was higher with DNA binding predictions based on protein-binding microarray experiments [48] that were obtained from an online tool (<http://thebrain.bwh.harvard.edu/nfkb>), particularly for p50/p65 heterodimers. There were however differences between the two parameters (e.g. LIF and RANTES for p50, RE2 and RE1 for p65) (Fig 7). These findings further validate our yeast-based approach. A recent study based on a largely unbiased ChIP-sequencing approach in mammalian cells confirmed that the central sequence motif of a κ B-RE plays a critical role in deciding the transcriptional specificity by NF- κ B proteins [22], emphasizing the significance of RE sequence even in an environment where additional *cis*-elements and trans-factors interplay to regulate transcription. Our data confirmed the impact that single nucleotide changes can have on transactivation potential (e.g. RE1 vs RE2, M1 vs M2) (Table A and Fig A in S1 File), consistent with previous reports in mammalian cells [20,21]. For example, a lentiviral-based approach demonstrated that differences in the nucleotide sequence of κ B-REs embedded in about 5 kb of the MCP-1 promoter sequence could dictate the level of responsiveness to NF- κ B activation by TNF α or LPS and the relative activity of different NF- κ B family members [20]. In agreement with our observations in yeast, this study also established p65 as a major factor in MCP-1 promoter transactivation with a limited contribution from p50 and p52. Also, consistent with our results, the replacement of the κ B-REs within MCP-1 with those present in the IP-10 promoter (I1 and I2) led to preferential responsiveness to p50 homo or hetero-dimers. However, the I1 κ B-RE when tested separately exhibited a lower relative responsiveness to p50TAD in yeast.

To address the predictive value of the yeast-based assay for NF- κ B-dependent transactivation in human cells expressing endogenous p65 and p50, four κ B-REs were tested in gene reporter assays in MCF7 cells treated with TNF α . There was generally a good correspondence between transactivation potential in the two systems (Figs 1, 3 and 4).

Clearly, κ B-RE sequences can have a direct role in influencing transactivation specificity of NF- κ B proteins in a manner that is not solely related to DNA binding affinity [49]. A lack of complete correlation between DNA binding affinity and transactivation potential was also observed for the p53 family of TFs in our previous studies [50,51]. For p53, cooperative interactions between adjacent REs and a role for RE structure and kinetic properties were recognized to contribute to transactivation, especially at low expression levels [37,52]. Even a single nucleotide spacer between two half-sites that constitute the canonical p53 RE has a negative impact on p53- and, particularly, p73-dependent transactivation [51,53,54], while a spacer between two full sites has less of an effect and a short spacer could be beneficial, potentially due to steric hindrance [51].

Based on those results we studied interactions between adjacent or closely-spaced κ B-REs and found somewhat more than additive, but not strong cooperative interactions between two

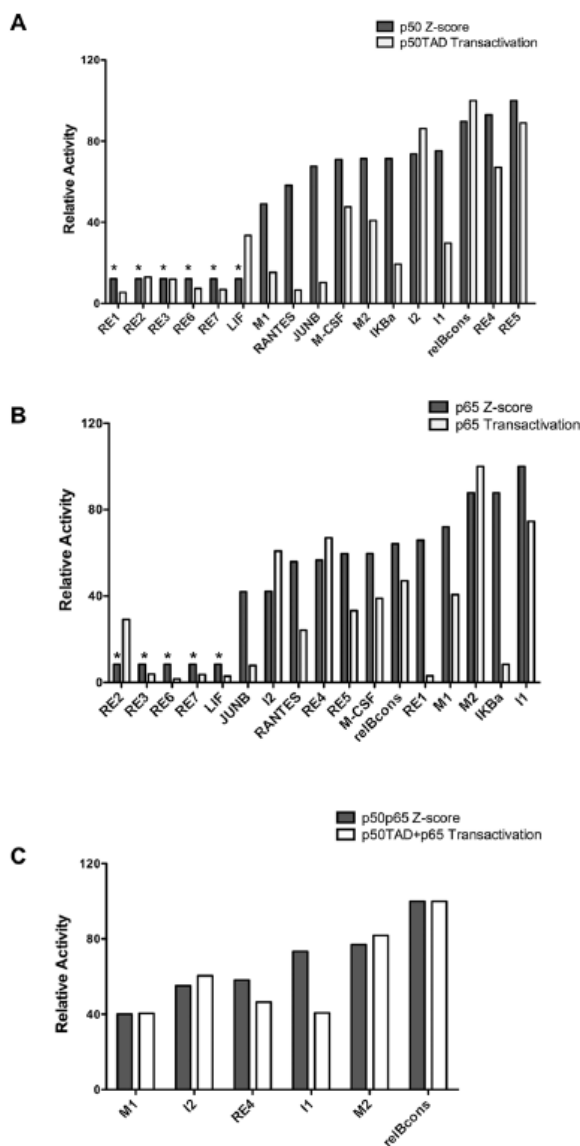


Fig 7. Comparison between predicted DNA binding affinity and yeast-based transactivation. A), B) The relative binding affinities of p50 or p65 towards 17 κB-REs were obtained from (<http://thebrain.bwh.harvard.edu/nfkb>) and compared with the relative transactivation potential measured in yeast at moderate levels of galactose induction. REs are ordered from left to right based on increasing Z-score for DNA binding affinity. The highest affinity RE (RE5 for p50 and I1 for p65) is set to 100. REs with Z-score lower than 4, considered equivalent to background, are labeled by *. **C)** Similarly, Z-scores of the p50-p65 heterodimers and transactivation potentials are compared for the 6 κB-REs that were tested in the co-expression experiments in yeast.

doi:10.1371/journal.pone.0130170.g007

adjacent identical κ B binding half-sites. These results are consistent with a comprehensive recent study in mammalian cells that concluded that NF- κ B acts non-cooperatively at closely-spaced binding sites to provide gradual increase in gene expression [41].

We used the yeast-based assay to explore the possibility to monitor the impact of protein and small molecules inhibitors on transactivation potential and specificity of NF- κ B proteins. Co-expression of I κ B α , a well-known inhibitor of NF- κ B, led to reduced transactivation by p65. This suggests that the assay can be exploited to study crosstalk between NF- κ B and upstream regulators, consistent with a previous report [38]. Interestingly, the effect of I κ B α towards p50TAD was much less evident, suggesting distinct thresholds for I κ B α -dependent regulation of NF- κ B members. Consistently, protein-protein interaction experiments on I κ B α with NF- κ B p50/p65 heterodimers revealed critical interactions between I κ B α and p65 [43]. We also establish that the small molecule BAY-11-7082 causes a dose-dependent inhibition of p65 as well as p50TAD-dependent transactivation. BAY11-7082 is an inhibitor of the IKK kinase that in higher eukaryotes modulates the I κ B α kinase IKK. However, this molecule was shown to inhibit a broad range of protein kinases including tyrosine phosphatases [11,45]. Three different κ B-REs were examined for the effect of BAY treatment. p65 homodimers or p65 co-expressed with p50TAD appeared to be more sensitive to the presence of BAY, but p50TAD homodimers were also inhibited, particularly when the RelBCons RE reporter was used. At the 20 μ M dose, the molecule inhibited the NF- κ B-independent basal transcription of the reporter, suggesting a general repressive effect on constitutive transcription possibly due to some toxicity to yeast cells. While the mechanism of the effect of BAY-11-7082 in yeast resulting in the apparent modulation of p65 and p50 function remains to be elucidated, the effect was independent from I κ B α or the I κ B α kinase IKK. Notably, BAY treatment did not lead to a reduction in p65 or p50 steady state protein levels.

We also tested EP, which may directly target p65 and inhibit *in vitro* DNA binding [8]. Although it reduced both p65- and p50TAD-dependent transactivation in a dose-dependent manner, western blot analysis indicated that this effect could be due to a reduction in protein levels. However, even at high dose EP did not impact basal expression of the reporter or the growth of yeast. EP did not affect p53 transactivation up to the 5mM dose nor it impacted on p53 protein levels at 2.5 or 5mM (Fig C in S1 File). Thus, there may be a specific impact of EP on NF- κ B proteins stability, but the mechanism of action of EP in our assay system remains to be established. Although parthenolide had been shown to inhibit directly and indirectly IKK [46] [55], and possibly also to directly inhibit NF- κ B subunits [56], we did not observe any effect of this molecule on NF- κ B-dependent transactivation in yeast.

In conclusion, our studies highlight the significance of κ B-RE sequence in the transactivation specificity of NF- κ B transcription factors. In fact, the transactivation abilities of p65 and p50 NF- κ B proteins acting as homodimers can be distinguished with respect to κ B-RE sequence specificity, and co-expression of both transcription factors can be particularly effective on selected RE sequences. Importantly, these findings with the yeast system along with the use of the p50TAD provide new opportunities to dissect the transactivation specificity of individual NF- κ B protein members and the role of κ B-REs, including the interaction between closely spaced REs. In addition, our results suggest that small molecules targeting NF- κ B proteins can have a differential impact depending on the κ B-RE being tested. Ideally this could open up the possibility to identify modifiers that can target selected NF- κ B functions, for example by including in the yeast assay cofactors such as Bcl-3, CREB, p300, Tip60 that play important roles in shaping the NF- κ B-directed gene regulatory network [57].

Supporting Information

S1 File. Supporting Figures and Tables. Sequence of the κ B-REs tested in this study (Table A). Transactivation potential of p50TAD and p65 expressed alone or together towards the M1, M2, RE4 and RelBCons κ B-REs at different time points (Figure A). Parthenolide has no effect on NF- κ B activity in yeast (Figure B). Effect of varying the concentrations of BAY11-7082 and ethyl pyruvate on NF- κ B activity (Figure C). A comparison between *in vitro* DNA binding affinity and relative transactivation potential of κ B-REs (Figure D). (PDF)

Acknowledgments

We thank Drs. Daniel Menendez, Gilberto Fronza and Paola Monti for critical evaluation of the manuscript.

Author Contributions

Conceived and designed the experiments: JJJ MAR AI. Performed the experiments: VS AB JJJ YC AI. Analyzed the data: VS AB JJJ YC MAR AI. Wrote the paper: VS MAR AB AI.

References

1. Oeckinghaus A, Ghosh S (2009) The NF- κ B family of transcription factors and its regulation. *Cold Spring Harb Perspect Biol* 1: a000034. doi: [10.1101/cshperspect.a000034](https://doi.org/10.1101/cshperspect.a000034) PMID: [20066092](https://pubmed.ncbi.nlm.nih.gov/20066092/)
2. Courtois G, Gilmore TD (2006) Mutations in the NF- κ B signaling pathway: implications for human disease. *Oncogene* 25: 6831–6843. PMID: [17072331](https://pubmed.ncbi.nlm.nih.gov/17072331/)
3. Perkins ND (2006) Post-translational modifications regulating the activity and function of the nuclear factor κ B pathway. *Oncogene* 25: 6717–6730. PMID: [17072324](https://pubmed.ncbi.nlm.nih.gov/17072324/)
4. Sen R, Baltimore D (1986) Inducibility of κ B immunoglobulin enhancer-binding protein NF- κ B by a posttranslational mechanism. *Cell* 47: 921–928. PMID: [3096580](https://pubmed.ncbi.nlm.nih.gov/3096580/)
5. Jacobs MD, Harrison SC (1998) Structure of an I κ B α /NF- κ B complex. *Cell* 95: 749–758. PMID: [9865693](https://pubmed.ncbi.nlm.nih.gov/9865693/)
6. Karin M (1999) How NF- κ B is activated: the role of the I κ B kinase (IKK) complex. *Oncogene* 18: 6867–6874. PMID: [10602462](https://pubmed.ncbi.nlm.nih.gov/10602462/)
7. Whiteside ST, Israel A (1997) I κ B proteins: structure, function and regulation. *Semin Cancer Biol* 8: 75–82. PMID: [9299585](https://pubmed.ncbi.nlm.nih.gov/9299585/)
8. Han Y, Englert JA, Yang R, Delude RL, Fink MP (2004) Ethyl pyruvate inhibits NF- κ B-dependent signaling by directly targeting p65. *J Pharmacol Exp Ther*.
9. Lee J, Rhee MH, Kim E, Cho JY (2012) BAY 11–7082 is a broad-spectrum inhibitor with anti-inflammatory activity against multiple targets. *Mediators Inflamm* 2012: 416036. doi: [10.1155/2012/416036](https://doi.org/10.1155/2012/416036) PMID: [22745523](https://pubmed.ncbi.nlm.nih.gov/22745523/)
10. Pierce JW, Schoenleber R, Jesmok G, Best J, Moore SA, et al. (1997) Novel inhibitors of cytokine-induced I κ B α phosphorylation and endothelial cell adhesion molecule expression show anti-inflammatory effects *in vivo*. *J Biol Chem* 272: 21096–21103. PMID: [9261113](https://pubmed.ncbi.nlm.nih.gov/9261113/)
11. Strickson S, Campbell DG, Emmerich CH, Knebel A, Plater L, et al. (2013) The anti-inflammatory drug BAY 11–7082 suppresses the MyD88-dependent signalling network by targeting the ubiquitin system. *Biochem J* 451: 427–437. doi: [10.1042/BJ20121651](https://doi.org/10.1042/BJ20121651) PMID: [23441730](https://pubmed.ncbi.nlm.nih.gov/23441730/)
12. Baldwin AS Jr. (1996) The NF- κ B and I κ B proteins: new discoveries and insights. *Annu Rev Immunol* 14: 649–683. PMID: [8717528](https://pubmed.ncbi.nlm.nih.gov/8717528/)
13. Ghosh S, May MJ, Kopp EB (1998) NF- κ B and Rel proteins: evolutionarily conserved mediators of immune responses. *Annu Rev Immunol* 16: 225–260. PMID: [9597130](https://pubmed.ncbi.nlm.nih.gov/9597130/)
14. Gilmore TD (2006) Introduction to NF- κ B: players, pathways, perspectives. *Oncogene* 25: 6680–6684. PMID: [17072321](https://pubmed.ncbi.nlm.nih.gov/17072321/)
15. Schmitz ML, Baeuerle PA (1991) The p65 subunit is responsible for the strong transcription activating potential of NF- κ B. *EMBO J* 10: 3805–3817. PMID: [1935902](https://pubmed.ncbi.nlm.nih.gov/1935902/)

16. Huxford T, Huang DB, Malek S, Ghosh G (1998) The crystal structure of the I κ B/NF- κ B complex reveals mechanisms of NF- κ B inactivation. *Cell* 95: 759–770. PMID: [9865694](#)
17. Kunsch C, Ruben SM, Rosen CA (1992) Selection of optimal kappa B/Rel DNA-binding motifs: interaction of both subunits of NF- κ B with DNA is required for transcriptional activation. *Mol Cell Biol* 12: 4412–4421. PMID: [1406630](#)
18. Ghosh G, van Duyne G, Ghosh S, Sigler PB (1995) Structure of NF- κ B p50 homodimer bound to a kappa B site. *Nature* 373: 303–310. PMID: [7530332](#)
19. Chen FE, Ghosh G (1999) Regulation of DNA binding by Rel/NF- κ B transcription factors: structural views. *Oncogene* 18: 6845–6852. PMID: [10602460](#)
20. Leung TH, Hoffmann A, Baltimore D (2004) One nucleotide in a kappaB site can determine cofactor specificity for NF- κ B dimers. *Cell* 118: 453–464. PMID: [15315758](#)
21. Udalova IA, Mott R, Field D, Kwiatkowski D (2002) Quantitative prediction of NF- κ B DNA-protein interactions. *Proc Natl Acad Sci U S A* 99: 8167–8172. PMID: [12048232](#)
22. Wang VY, Huang W, Asagiri M, Spann N, Hoffmann A, et al. (2012) The transcriptional specificity of NF- κ B dimers is coded within the kappaB DNA response elements. *Cell Rep* 2: 824–839. doi: [10.1016/j.celrep.2012.08.042](#) PMID: [23063365](#)
23. Hoffmann A, Leung TH, Baltimore D (2003) Genetic analysis of NF- κ B/Rel transcription factors defines functional specificities. *Embo J* 22: 5530–5539. PMID: [14532125](#)
24. Andreatti V, Ciribilli Y, Monti P, Bisio A, Lion M, et al. (2011) p53 transactivation and the impact of mutations, cofactors and small molecules using a simplified yeast-based screening system. *PLoS ONE* 6: e20643. doi: [10.1371/journal.pone.0020643](#) PMID: [21674059](#)
25. Ciribilli Y, Monti P, Bisio A, Nguyen HT, Ethayathulla AS, et al. (2013) Transactivation specificity is conserved among p53 family proteins and depends on a response element sequence code. *Nucleic Acids Res*.
26. Raimondi I, Ciribilli Y, Monti P, Bisio A, Pollegioni L, et al. (2013) P53 family members modulate the expression of PRODH, but not PRODH2, via intronic p53 response elements. *PLoS One* 8: e69152. doi: [10.1371/journal.pone.0069152](#) PMID: [23861960](#)
27. Storici F, Resnick MA (2003) Delitto perfetto targeted mutagenesis in yeast with oligonucleotides. *Genet Eng (N Y)* 25: 189–207.
28. Storici F, Resnick MA (2006) The delitto perfetto approach to in vivo site-directed mutagenesis and chromosome rearrangements with synthetic oligonucleotides in yeast. *Methods Enzymol* 409: 329–345. PMID: [16793410](#)
29. Bisio A, De Sanctis V, Del Vescovo V, Denti MA, Jegga AG, et al. (2013) Identification of new p53 target microRNAs by bioinformatics and functional analysis. *BMC Cancer* 13: 552. doi: [10.1186/1471-2407-13-552](#) PMID: [24256616](#)
30. Jegga AG, Inga A, Menendez D, Aronow BJ, Resnick MA (2008) Functional evolution of the p53 regulatory network through its target response elements. *Proc Natl Acad Sci U S A* 105: 944–949. doi: [10.1073/pnas.0704694105](#) PMID: [18187580](#)
31. Tomso DJ, Inga A, Menendez D, Pittman GS, Campbell MR, et al. (2005) Functionally distinct polymorphic sequences in the human genome that are targets for p53 transactivation. *Proc Natl Acad Sci U S A* 102: 6431–6436. PMID: [15843459](#)
32. Monti P, Perfumo C, Bisio A, Ciribilli Y, Menichini P, et al. (2011) Dominant-negative features of mutant TP53 in germline carriers have limited impact on cancer outcomes. *Mol Cancer Res* 9: 271–279. doi: [10.1158/1541-7786.MCR-10-0496](#) PMID: [21343334](#)
33. Sikorski RS, Hieter P (1989) A system of shuttle vectors and yeast host strains designed for efficient manipulation of DNA in *Saccharomyces cerevisiae*. *Genetics* 122: 19–27. PMID: [2659436](#)
34. Gietz RD, Schiestl RH, Willems AR, Woods RA (1995) Studies on the transformation of intact yeast cells by the LiAc/SS-DNA/PEG procedure. *Yeast* 11: 355–360. PMID: [7785336](#)
35. Kushnirov VV (2000) Rapid and reliable protein extraction from yeast. *Yeast* 16: 857–860. PMID: [10861908](#)
36. Monti P, Ciribilli Y, Bisio A, Foggetti G, Raimondi I, et al. (2014) DN-P63alpha and TA-P63alpha exhibit intrinsic differences in transactivation specificities that depend on distinct features of DNA target sites. *Oncotarget* 5: 2116–2130. PMID: [24926492](#)
37. Jordan JJ, Menendez D, Sharav J, Beno I, Rosenthal K, et al. (2012) Low-level p53 expression changes transactivation rules and reveals superactivating sequences. *Proc Natl Acad Sci U S A* 109: 14387–14392. doi: [10.1073/pnas.1205971109](#) PMID: [22908277](#)

38. Epinat JC, Whiteside ST, Rice NR, Israel A (1997) Reconstitution of the NF-kappa B system in *Saccharomyces cerevisiae* for isolation of effectors by phenotype modulation. *Yeast* 13: 599–612. PMID: [9200810](#)
39. Kennedy BK (2002) Mammalian transcription factors in yeast: strangers in a familiar land. *Nat Rev Mol Cell Biol* 3: 41–49. PMID: [11823797](#)
40. Wong D, Teixeira A, Oikonomopoulos S, Humburg P, Lone IN, et al. (2011) Extensive characterization of NF-kappaB binding uncovers non-canonical motifs and advances the interpretation of genetic functional traits. *Genome Biol* 12: R70. doi: [10.1186/gb-2011-12-7-r70](#) PMID: [21801342](#)
41. Giorgetti L, Siggers T, Tiana G, Caprara G, Notarbartolo S, et al. (2010) Noncooperative interactions between transcription factors and clustered DNA binding sites enable graded transcriptional responses to environmental inputs. *Mol Cell* 37: 418–428. doi: [10.1016/j.molcel.2010.01.016](#) PMID: [20159560](#)
42. Karin M (2006) Nuclear factor-kappaB in cancer development and progression. *Nature*. pp. 431–436.
43. Bergqvist S, Ghosh G, Komives EA (2008) The IkappaBalpha/NF-kappaB complex has two hot spots, one at either end of the interface. *Protein Sci* 17: 2051–2058. doi: [10.1110/ps.037481.108](#) PMID: [18824506](#)
44. O'Dea EL, Barken D, Peralta RQ, Tran KT, Werner SL, et al. (2007) A homeostatic model of IkappaB metabolism to control constitutive NF-kappaB activity. *Mol Syst Biol* 3: 111. PMID: [17486138](#)
45. Krishnan N, Bencze G, Cohen P, Tonks NK (2013) The anti-inflammatory compound BAY-11-7082 is a potent inhibitor of protein tyrosine phosphatases. *FEBS J* 280: 2830–2841. doi: [10.1111/febs.12283](#) PMID: [23578302](#)
46. Saadane A, Masters S, DiDonato J, Li J, Berger M (2007) Parthenolide inhibits IkappaB kinase, NF-kappaB activation, and inflammatory response in cystic fibrosis cells and mice. *Am J Respir Cell Mol Biol* 36: 728–736. PMID: [17272824](#)
47. Kamens J, Brent R (1991) A yeast transcription assay defines distinct rel and dorsal DNA recognition sequences. *New Biol* 3: 1005–1013. PMID: [1768648](#)
48. Siggers T, Chang AB, Teixeira A, Wong D, Williams KJ, et al. (2012) Principles of dimer-specific gene regulation revealed by a comprehensive characterization of NF-kappaB family DNA binding. *Nat Immunol* 13: 95–102.
49. Sullivan JC, Wolenski FS, Reitzel AM, French CE, Traylor-Knowles N, et al. (2009) Two alleles of NF-kappaB in the sea anemone *Nematostella vectensis* are widely dispersed in nature and encode proteins with distinct activities. *PLoS One* 4: e7311. doi: [10.1371/journal.pone.0007311](#) PMID: [19806194](#)
50. Inga A, Storici F, Darden TA, Resnick MA (2002) Differential transactivation by the p53 transcription factor is highly dependent on p53 level and promoter target sequence. *Mol Cell Biol* 22: 8612–8625. PMID: [12446780](#)
51. Jordan JJ, Menendez D, Inga A, Nouredine M, Bell D, et al. (2008) Noncanonical DNA motifs as transactivation targets by wild type and mutant p53. *PLoS Genet* 4: e1000104. doi: [10.1371/journal.pgen.1000104](#) PMID: [18714371](#)
52. Beno I, Rosenthal K, Levitine M, Shaulov L, Haran TE (2011) Sequence-dependent cooperative binding of p53 to DNA targets and its relationship to the structural properties of the DNA targets. *Nucleic Acids Res* 39: 1919–1932. doi: [10.1093/nar/gkq1044](#) PMID: [21071400](#)
53. Ethayathulla AS, Tse PW, Monti P, Nguyen S, Inga A, et al. (2012) Structure of p73 DNA-binding domain tetramer modulates p73 transactivation. *Proceedings of the National Academy of Sciences of the United States of America*.
54. Menendez D, Nguyen TA, Freudenberg JM, Mathew VJ, Anderson CW, et al. (2013) Diverse stresses dramatically alter genome-wide p53 binding and transactivation landscape in human cancer cells. *Nucleic Acids Res* 41: 7286–7301. doi: [10.1093/nar/gkt504](#) PMID: [23775793](#)
55. Kwok BH, Koh B, Ndubuisi MI, Elofsson M, Crews CM (2001) The anti-inflammatory natural product parthenolide from the medicinal herb Feverfew directly binds to and inhibits IkappaB kinase. *Chem Biol* 8: 759–766. PMID: [11514225](#)
56. Yeo AT, Porco JA Jr., Gilmore TD (2012) Bcl-XL, but not Bcl-2, can protect human B-lymphoma cell lines from parthenolide-induced apoptosis. *Cancer Lett* 318: 53–60. doi: [10.1016/j.canlet.2011.11.035](#) PMID: [22155272](#)
57. Perkins ND (2012) The diverse and complex roles of NF-kappaB subunits in cancer. *Nat Rev Cancer* 12: 121–132. doi: [10.1038/nrc3204](#) PMID: [22257950](#)

Quantitative Analysis of NF- κ B Transactivation specificity using a Yeast-Based Functional Assay

Vasundhara Sharma *et al.*, Supplementary Figure Legends, Figures and Table.

Fig. A. Transactivation potential of p50TAD and p65 expressed alone or together towards the M1, M2, RE4 and RelBCons κ B-REs at different time points. Panels A), B) Transactivation induced by p50TAD, p65 and p50TAD+p65. Cells were grown in lower (0.008%, panel A) or higher (0.064%, panel B) levels of galactose for 3, 6 and 9 hours respectively. For each isogenic reporter strain, the luciferase activity was calculated as fold of induction with respect to the values obtained with empty vector transformants cultured and assayed in the same conditions. Presented are the average values and the standard deviations of four biological replicates.

Fig. B. Parthenolide has no effect on NF- κ B-dependent transactivation in yeast. Cells were treated with two doses of parthenolide (10 μ M and 20 μ M) for 16 hours while growing in media containing two different galactose concentrations. Presented are the average values and the standard deviations of four biological replicates.

Fig. C. Effect of varying concentrations of BAY11-7082 and ethyl pyruvate on NF- κ B -dependent transactivation. Panel A) M2-RE reporter cells expressing p65 cultured in high galactose (0.032%) are not inhibited by 10 μ M BAY11-7082, contrary to what observed when cells from the same strain were treated in lower galactose. This difference can be related to the higher levels of p65 protein. Higher dose of BAY (10 μ M) reduced p65- but not p50TAD-induced transactivation. High doses of ethyl pyruvate (10mM and 20 mM) completely abolished p65 and p50TAD transactivation activities without affecting the levels of NF κ B-independent luciferase reporter expression (empty). **Panel B)** BAY treatment, or the lower dose of EP did not impact on p53-dependent transactivation. The human p53 cDNA is expressed from the *GAL1* promoter from a plasmid vector equivalent to the one used to express p65 or p50TAD. **Panel C)** A Western blot performed with total protein extracts from yeast cells expressing p50TAD, p50TAD+p65, p65 or p53 and treated with 2.5mM and 5mM EP showed dose-dependent reduction in NF- κ B proteins (left panel), but not in p53 protein levels (right panel).

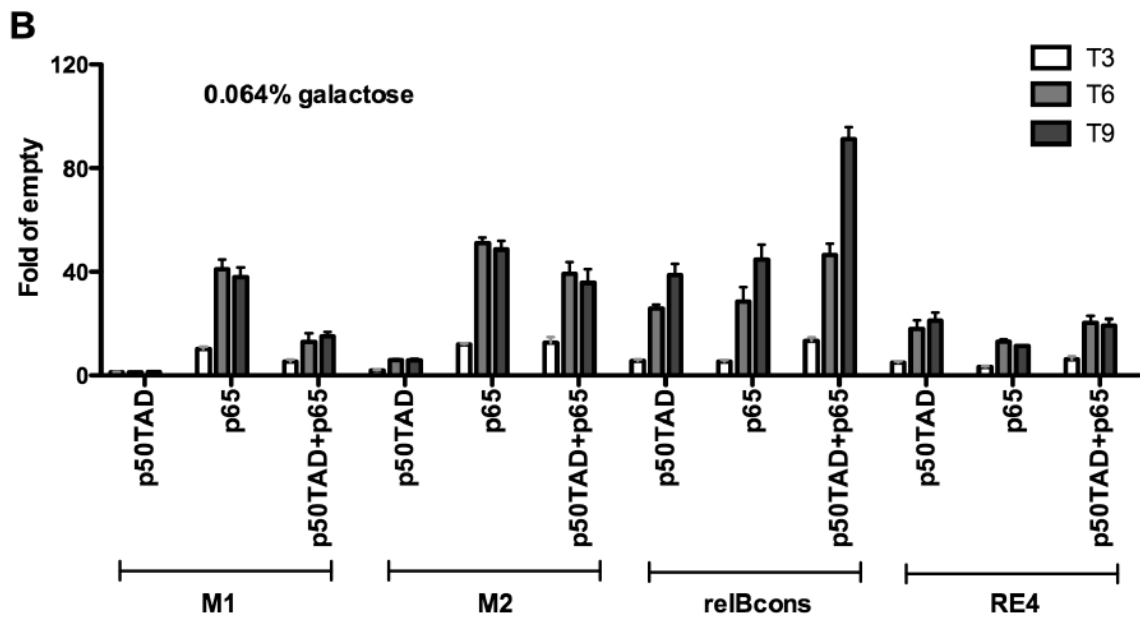
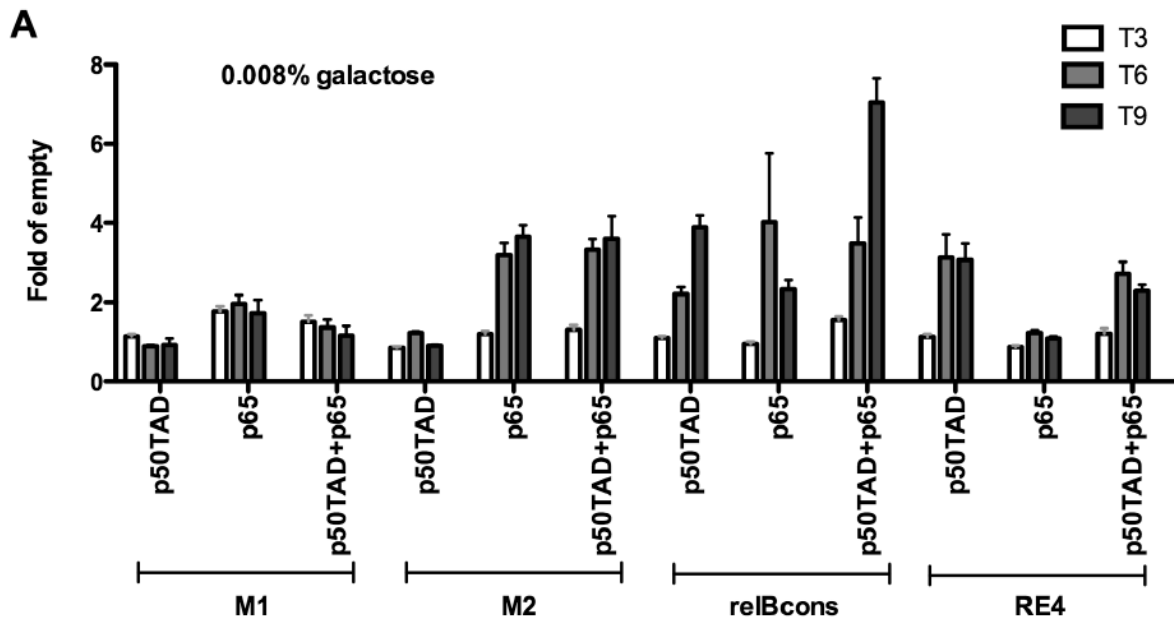
Fig. D. A comparison between *in vitro* DNA binding affinity and relative transactivation potential of κ B-REs. Panel A) The relative binding affinities of p50 towards 16 κ B-REs reported in a previous study [21] were compared with the relative *in vivo* transactivation potentials measured in our study. κ B-REs are ordered from left to right based on predicted DNA binding affinity. The highest affinity was predicted for RE5 and set to 100 in the relative scale, while the most responsive RE in transactivation was RelBCons (also set to 100). **Panel B)** Similarly, DNA binding affinity of the p50/p65

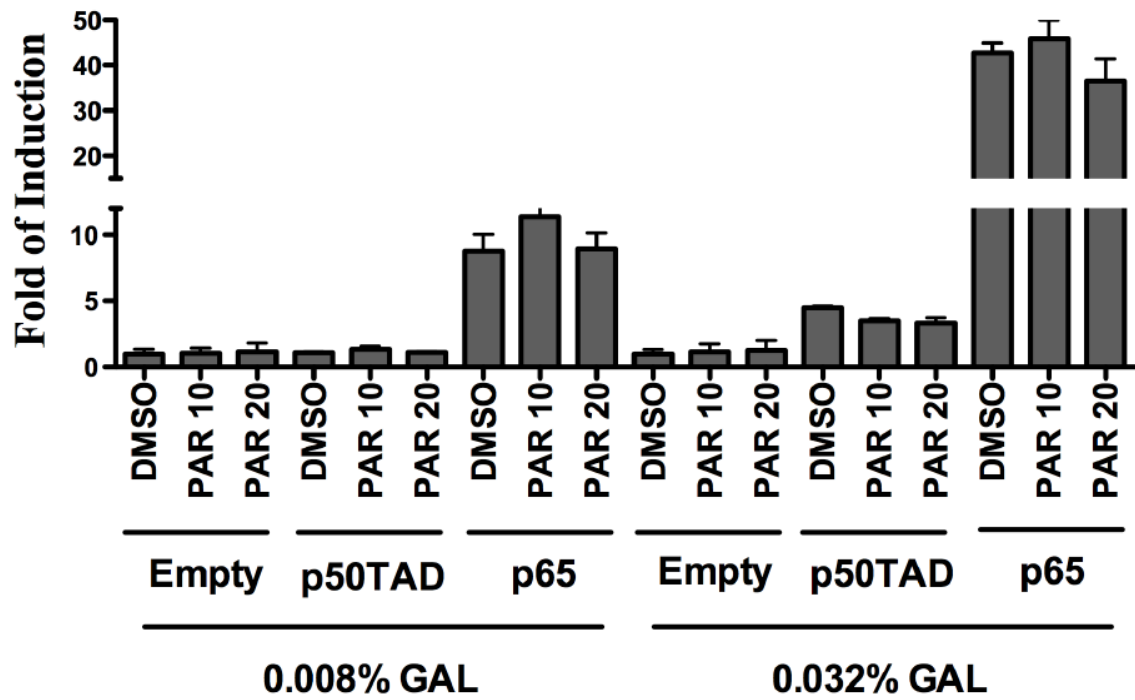
heterodimers was compared to the transactivation data obtained in yeast with the co-expression of p50TAD and p65.

Table A: Sequence of the κ B-REs tested in this study.

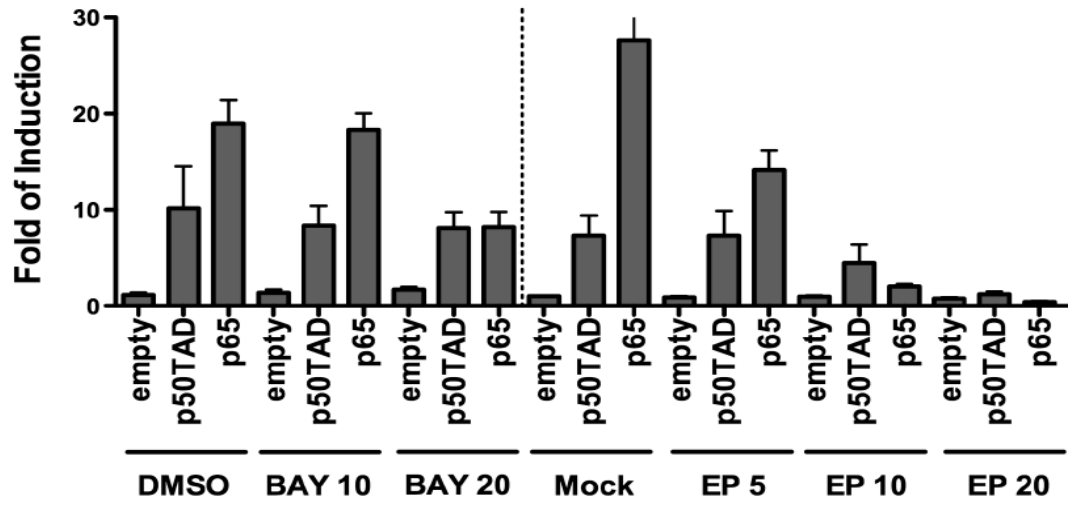
RE NAME	Sequence
RE1	GGAAATTTCC
RE2	GGAACTTTCC
RE3	GGAAGgCTCC
RE4	GGGGAATCCC
RE5	GGGGATTCCC
RE6	GGGATACCCC
M1	GGGAACTTCC
M2	GGGAATTTCC
I1	GGGAAATTCC
I2	GGGACTTCCC
RANTES	GGGAGTTTCC
M-CSF	GGGACTTTCC
relBCons	GGGGATTTCC
I κ B α	GGAAATTTCCC
JUNB	GGGGCTTTCC
RE7	GGAGGATTCC
LIF	GGGGATCCCG
RE8	GGAAATTTCCGGGATACCCC
M1+M2 spacer	GGGAACTTCC-spacer-GGGAATTTCC
I1+I2 spacer	GGGAAATTCC-spacer-GGGACTTCCC
spacer sequence:	aaagctgcctcctcagagt

Supplementary Information

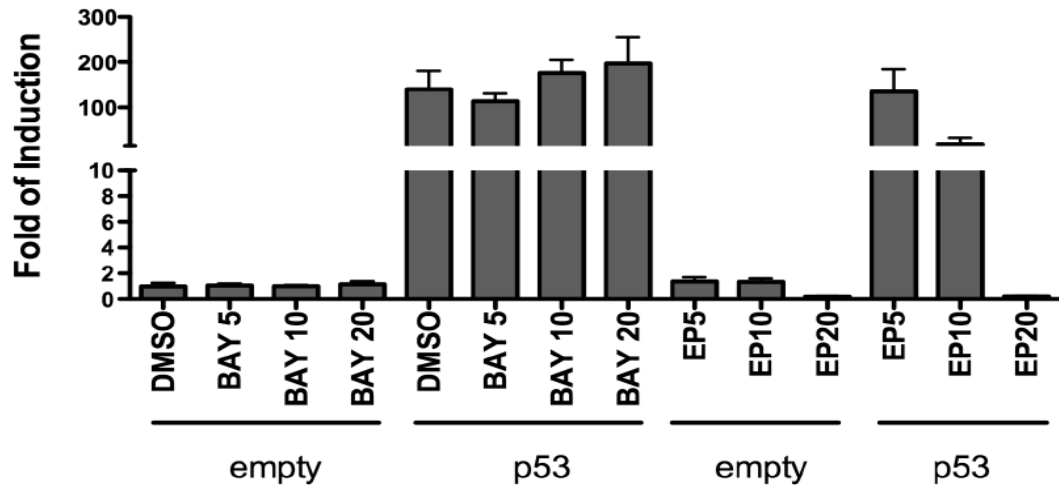




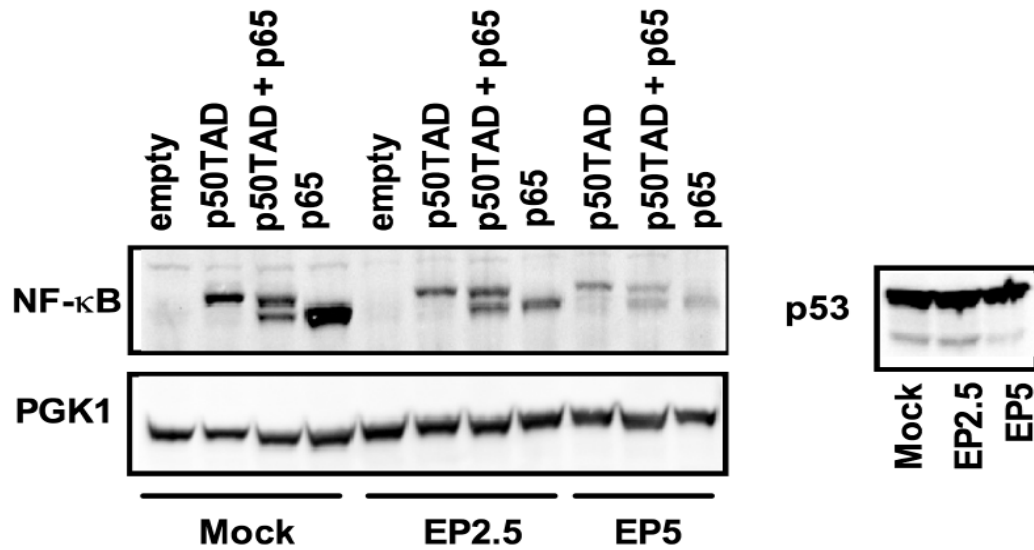
A



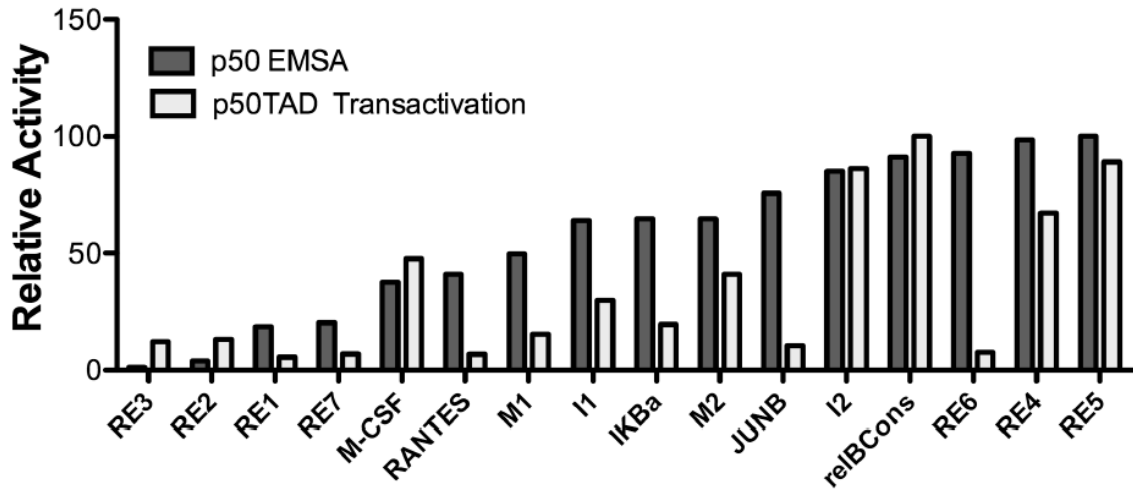
B



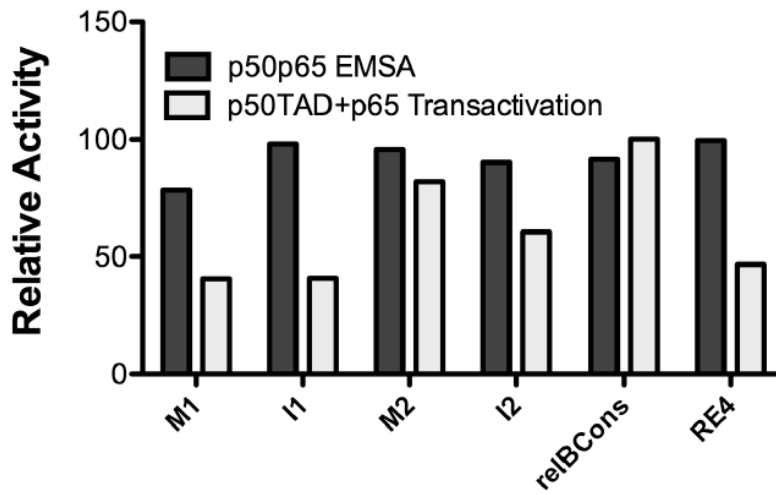
C



A



B



DISCUSSION

Exploiting single nucleotide variants of p53 and NF- κ B REs in yeast as well as human cell lines we established that each nucleotide individually or in cooperation with the adjacent nucleotides contributes to p53 and NF- κ B transactivation specificity. We studied a list of p53 (20 REs) and NF- κ B REs (17 REs) in yeast as well as human cell lines. *Ad-hoc* variation of p53 REs, which were used to probe allosteric changes in p53 DNA binding domain and target DNA conformation by crystallization studies (H. Viadiu, unpublished), were evaluated for their transactivation potential, providing insights on the individual contribution of nucleotides on the transcription function of an RE. p53 and NF- κ B REs studied in yeast chromatin context illustrate a DNA nucleotide code that was at least in part predictive of their function in human cell lines. The correlation was less apparent between transactivation data and measured or predicted DNA binding affinity with naked DNA.

Certain REs are active at low p53 levels whereas others show activity at moderate p53 concentration in cells confirming the correlation between p53 recognition and relative transactivation. This study also confirms that stretch of three guanines (GGG) in the 5' end of RE is structurally flexible and potentiates p53-mediated transactivation. Also, a CATG core within the RE facilitates transcription much more than CTAG, CTTG or CAAG. Surprisingly, the high transactivation potential exhibited by (AAACATGCCC)₂ reveals a positive impact of a stretch of adenines in the 5' end of the decameric RE motif. On the contrary, but as expected, the presence of thymines in the 5' ends of RE adversely affects the strength of an RE in terms of transactivation. Overall, a torsionally flexible 5' end of RE leads to higher transactivation whereas a rigid 5' end of the RE is detrimental for transcription.

Using structural variants of the p21-5' RE also established that physical properties of a RE can modulate transcription. Constructing an artificial p21 RE by swapping the half sites from LR to RL conformation reveals that the natural p21LR conformation is more potent and replacing the genomic flank appended upstream to the p21 RE with an artificial flank reduces the overall transactivation potential of the RE. On the contrary, quantification of transactivation potential of p53 REs in bidirectional plasmid environment reveals that a p21 RE is more potent when appended with synthetic flexible and rigid nucleotide flanks. Natural genomic flanks of the p21 RE present on both sides of the RE are somehow less active in this

case. Also, the dual Luciferase assays reveal artificial p21 RL conformation slightly more active than the LR conformation in galactose-induced yeast cultures suggesting that DNA sequence dependent structural specificity within RE code controls transactivation. Also, it suggests that in addition to nucleotides upstream to a RE, the nucleotides close to a transcription start site (TSS) also affect transactivation differentially. This was confirmed with the bidirectional Firefly and Renilla Luciferase assay performed in both orientations for each p53 RE where a rigid flank next to TSS leads to higher transactivation. Also, arrangement of nucleotides within and outside an RE can control direction of transcription as observed in some cases such as RL_EFR_LUC/REN (see Figure 15).

Overall the study confirms that torsional rigidity or flexibility of nucleotides forming a p53 RE in context with contiguous nucleotides (DNA flanks) alters the transactivation potential of an RE. Also, contiguous genomic flanks to a p53 RE impart structural variability to DNA and partially control strength and direction of transcription.

Further studies are needed to determine how genomic flanks upstream and downstream to a p53 RE can affect the transcriptional decisions to reach definite conclusions. A rigorous analysis of flanks contiguous to other p53 REs in the genomic background has to be assessed. Also, variations in the length and nucleotides can be incorporated in the genomic flanks studied in bidirectional promoter system. Another speculation is the correlation between flexibility scores (see Table 3) of a DNA sequence (upstream flank-LHS-RHS-downstream flank) and relative transactivation potential with respect to p53 concentrations in the vicinity. A generic view describes that alternate flexibility scores (high low high low or low high low high) obtained by half sites and flanks comprising a DNA sequence favour low p53 concentrations to initiate transcription (Raffinose cultured yeast cells). It is also known that p53 as a dimer recognises half site decamers to control transcription. On the contrary, a linear descending flexibility score (high to low) shows maximum transactivation with high p53 levels (yeast cells cultures in the presence of galactose) hinting p53 tetramers as functional TFs in this case. The link between flexibility patterns of a sequence and relative transactivation was addressed previously by Olson et al. As a future direction, we aim to establish more precisely the correlation between flexibility patterns exhibited by a DNA sequence and the relative transactivation potentials.

Research Project 2

2. p53 and NF- κ B: partners in crime

The experiments described here are a follow-up of a published study in which I am a co-author. The paper is presented in the Appendix. Here I summarize unpublished work I developed to further investigate the impact of combined treatment with doxorubicin and TNF α on cell migration and mechanisms of p53 and NF- κ B transcriptional cooperation

Typically, p53 and NF- κ B have antagonistic functions in different cell types and extrinsic and intrinsic stress responses activate p53 and NF- κ B, respectively, to reciprocally regulate each other at cardinal intersections of various pathways (152). Various reports identified or proposed examples of cooperative interactions between the two families of proteins leading to differential regulation of genes involved in cancer. p53 and NF- κ B can act as co regulators of proinflammatory responses driving the expression of IL-6 and CXCL1 in macrophages and this was revealed also after nongenotoxic p53 activation by Nutlin-3A treatment (153). Mutant p53 is also reported to enhance the activity of NF- κ B induced by TNF α in different cancer types affecting tumor aggressiveness and responses to therapy (154, 155). According to other reports, the chemotherapeutic agent doxorubicin enhances NF- κ B's transcriptional activity in a p53 deficient environment whereas the treatment of lung cancer cells with Nutlin-3A down-regulates TNF α -induced NF- κ B pathway in a p53-dependent manner (156, 157). It has also been proposed that p53 and NF- κ B proteins have diverged out from a common ancestral TF involved in cell regulation and apoptosis. Both p53 and NF- κ B interact with ankyrin proteins and recognize a similar DNA sequence as their binding sites share an 80% similarity (158).

In a recent study I contributed to (see Figure 6 and supplementary Figure S3 in Appendix), transcriptome changes were analysed in MCF7 cells treated by doxorubicin or TNF α as single agents or by the combination of the two. The combined treatment leads to a synergistic up regulation of many genes, some previously reported to be involved in cancer and metastasis. Promoter analysis, including ChIP assays, suggested a possible direct interplay between p53 and NF- κ B proteins at the transcriptional level. Also, qPCRs performed on some selected up-regulated genes (PLK3, LAMP3, ETV7, NTN1, UNC5B) established that doxorubicin and TNF α mediated activation in MCF7 cells require p53, as revealed by the used of an MCF7-

shp53 derivative line (159). More recently, another report proposes interplay between p53 and NF- κ B downstream of TLR5 activation, leading to synergistic expression of more than 200 genes. Treatment of cells with TNF α , an activator of NF- κ B, increases cytokines' expression, such as IL6 and CXCL2, in a p53-dependent manner (160). This encouraged us to study p53 and NF- κ B interplay using doxorubicin and TNF α as p53 and NF- κ B activators, respectively.

I developed experiments to examine the regulation of identified, synergistic signature genes in additional cell lines (2.2.1) and evaluated the impact of the treatments on the migration potential of those cells (2.2.2) –see also supplementary data of the publication in Appendix-. Next, I have explored the potential role of trans-factors, namely TIP60 and MOF histone acetylases in the crosstalk between p53 and NF- κ B (2.2.3). Finally, to study more directly the control of selected gene promoters by p53 and NF- κ B, I constructed reporter assays and examined if the transcriptional cooperation could be confirmed and linked to specific *cis*-elements (2.2.4).

Molecular mechanisms contributing to doxorubicin and TNF α synergy

Various intricate molecular mechanisms could underlie the transcriptional synergy upon doxorubicin and TNF α combined treatment, besides the stabilization and nuclear localization of p53 and NF- κ B proteins. These can include a potentially high number of cofactors and molecules that can alter the transcriptome and modify the chromatin landscape (161-163). Given the genetic or pharmacological evidences of an involvement of both p53 and NF- κ B, we decided to investigate a few specific transcription cofactors like histone acetyl transferases (HATs), and histone deacetylases (HDACs) (69, 111, 164, 165). In particular, I began investigating the impact of TIP60 and MOF, two MYST family histone acetyl transferases in regulating doxorubicin+TNF α -mediated transcriptional synergy.

TIP60 (HIV Tat-interacting protein, 60 kDa) was identified as a transactivation enhancer of tat protein at HIV-1 promoter. It acetylates lysine residues in the amino terminal tail peptides of histones H2A, H3 and H4, but not H2B (166). Overall, TIP60 is a cell-type specific transcription co-regulator acting on wide variety of transcription factors such as the androgen receptor, MYC, STAT3, NF- κ B, E2F1 and p53. Also it is involved in various cellular

processes such as cellular signalling, DNA damage repair, cell cycle and checkpoint control and apoptosis (167-169). It is also known as a negative regulator in association with STAT3, p73, CREB (cAMP response element-binding protein) and ZEB (zinc finger E box-binding protein) (170, 171). TIP60 regulates both p53 and NF- κ B transcriptional activity through acetylation of lysine 120 and 310, respectively. TIP60-dependent acetylation of p53 controls the cell fate between cell cycle arrest and apoptosis (172). Reports suggest that K120 acetylation of p53 by TIP60 selectively increases p53 binding to apoptotic gene promoters at sites that exhibit low affinity (173). TIP60 is also involved in NF- κ B pathways through direct protein-protein interactions with RelA/p65, but also indirectly, as proposed for the NF- κ B targets IL6 and IL8 (174, 175).

MOF is another of the MYST HAT that can acetylate p53 at K120 and direct cells towards an apoptotic response. MOF also plays other important roles in gene regulation as the primary acetyltransferase for H4K16 acetylation, which initiates chromatin remodelling and transcriptional regulation (176, 177)

2.1 MATERIAL AND METHODS

Cell lines, culture conditions & drug treatments

A549 cells were obtained from ATCC (Manassas, VA, USA) while H1299 cells were a gift of Dr. Resnick's laboratory (NIEHS, NIH, RTP, NC, USA). Cells were cultured in DMEM or RPMI media supplemented with 10% FBS and Low Serum Growth Supplements (Life Technologies, Milan, Italy). Treatment doses were the following: doxorubicin (Doxo, 1.5 μ M); Nutlin-3A (10 μ M); TNF- α (5ng/mL in MCF7; 10ng/mL in H1299 and A549 based on response tests with gene reporter assays); BAY 11-7082 (20 μ M in H1299 and A549). All compounds were from Sigma-Aldrich (Milan, Italy).

RNA isolation and quantitative qPCR

Total RNA was extracted using Qiagen RNeasy Kit (Qiagen, Milan, Italy). cDNA was converted from 1 μ g of RNA using M-MuLV reverse transcriptase and RevertAid cDNA Synthesis kit (ThermoFisher, Milan, Italy). qPCR was performed on a Bio-Rad CFX384 (Bio-Rad, Milan, Italy). TaqMan gene expression assays (Applied Biosystems, Life Technologies) and Probe MasterMix (Kapa Biosystems, Resnova, Rome, Italy) were used starting with 25ng of cDNA as previously described [56, 61]. GAPDH, B2M or ACTB served as reference genes.

Migration and wound healing assays

The migration potential of A549 and H1299 cells was monitored by a real-time approach using the xCELLigence RTCA Instrument (Acea Biosciences, Euroclone, Milan, Italy) in CIM-16 plates, following manufacturer's instructions. 80% confluent cells were left untreated (mock) or treated with Doxorubicin, TNF α or the combination. 16 hours after the treatments, cells were detached and added to the top chamber in serum-free medium. Migration was detected every 10 minutes for 24 hours. Migration assays were also performed using the Transwell migration kit (Millipore).

Cloning of promoter/enhancer regions of signature genes and Luciferase reporter measurement.

A pair of primers to amplify the promoter/enhancer region of selected genes was designed with appropriate restriction site overhangs (see Table 7 for the list of putative REs in the promoter/enhancer regions cloned and Figure 17 for a schematic view of the cloned fragments and position of the putative REs). The amplified DNA was cloned upstream to Firefly Luciferase cDNA in pGL4.26 vector digested with corresponding enzyme pair using the cloning protocol. The correct clones were selected with restriction digestion patterns and Sanger sequencing. 60% to 70% confluent MCF-7 cells were transfected with 250ng plasmid DNA of each clone type and 50ng of Renilla Luciferase expression plasmid (pRLSV40) for 24 hours using miRUS LT1 transfection agent, followed by Doxorubicin, TNF α , or Doxorubicin + TNF α treatments for another 16 hours. The experiment was performed in triplicates using 24-well plates and the Firefly and Renilla Luciferase activity was measured according to manufacturer's protocol.

GENE promoter/ enhancer	p53 (RE)	NF-κB (RE)
NTN1_PROMOTER+I NTRON1	GCCGGGCATGGAGCTG AGACCGGCTCAGGCATGCCC	AAAGTCCC CGGACTTTCC GGGACTTT
PLK3_PROMOTER	GGGCCAGGCAAGCCAGGCGC TAACATGCCCCGGGCAAAAGCGAGCGC	TGGGAGTTCC GAAATTCCA
DUSP5_PROMOTER	CAACAAGCCCTTGTCTAGTGCGGG	CCTGGGGACC
ETV7 _ INTRON1	AGGCAAGTCC	GGAATTCCCC
LAMP3_PROMOTER	AGGCATGTGCCACCATGCCC	CGGAGTTT TGGAATTTCC
EGR2_INTRON 2	AGACATGTCA	AAGCCCCCAGC TGGAATTTCC
EDN2 INTRON2+EXON2+IN TRON3	CTGCAAGCCCCGGGCATGCCC	GGGACTTT AAAGTCCC
SNAI 1 promoter	GGGCATGCCC	CCAGGGGAGTTTT

Table 7: The table enlists the nucleotide sequence of p53 and NF- κ B Response elements embedded in promoter or enhancer regions of the signature genes. Using TRANSFAC DNA regulatory element pattern search tool, putative p53 and NF- κ B REs with a minimum cut off score of 0.9 were selected.

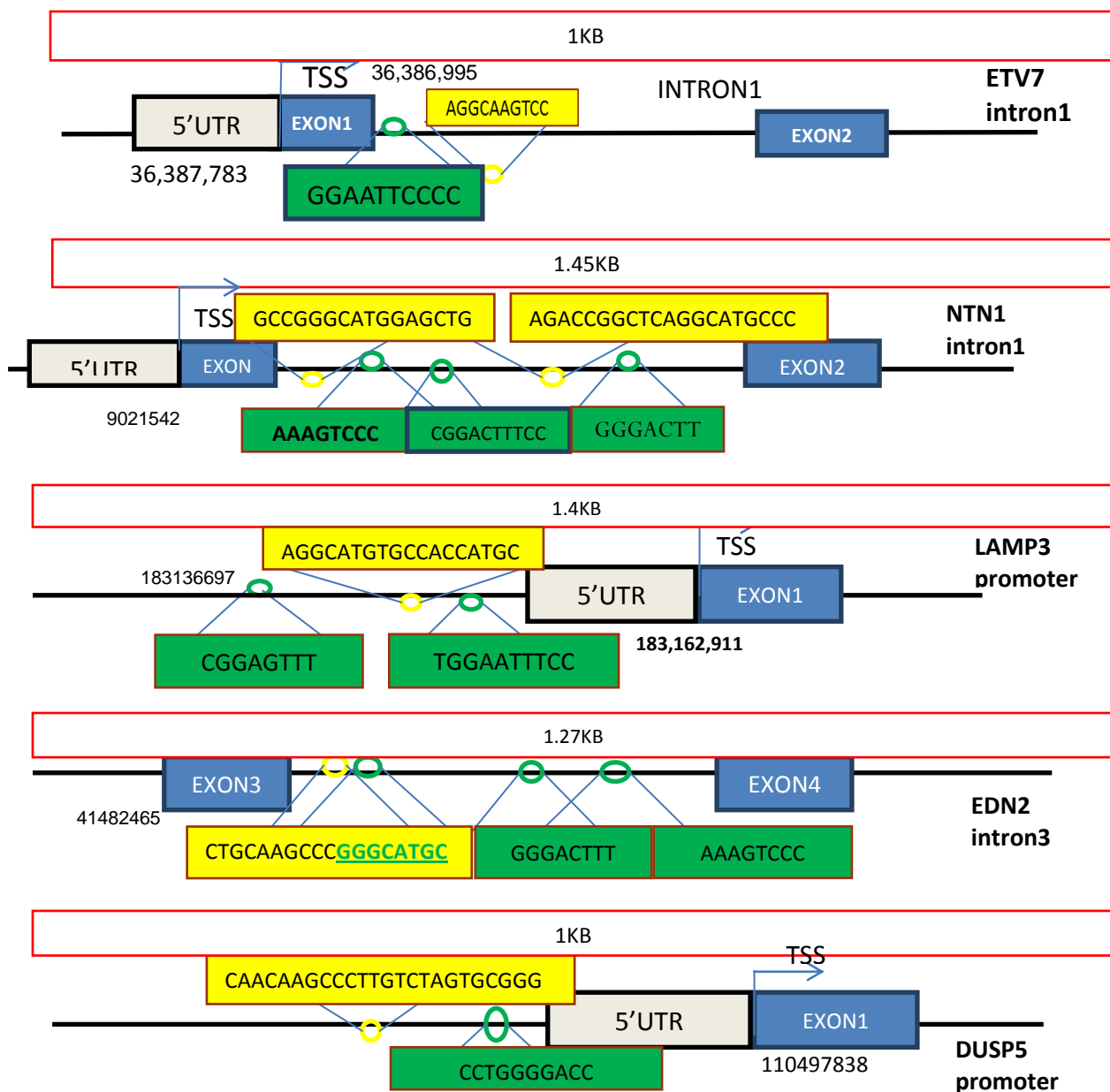


Figure 17: Schematics of putative p53 and NF-κB REs distribution in enhancer /promoter regions of five signature genes. (a) ETV7 intron 1 carries a 10mer NF-κB RE and a p53 half site with mismatches at position one and eight. (b) Intron1 of NTN1 is scored for three NF-κB and two p53 REs. One of the NF-κB sites is a 10mer and the other two are 8mers. The two p53 half sites obtained high PWM score inspite of mismatches. (c) LAMP3 promoter has two NF-κB sites (10 mer and 8 mer) and a p53 full site. (d) EDN2 intron 3 has an overlapping p53 and NF-κB binding site making a full 20mer RE. Also, it has two 8 mer NF-κB REs. (e) DUSP5 promoter has a p53 quarter site and a 10 mer NF-κB site. ■ P53 RE ■ NF-κB RE

Ectopic expression assays.

500ng of TIP60 or MOF expressing plasmids were expressed in 70% to 80% confluent A549, MCF7 and H1299 cells in 6-well plates using Lipofectamine or miRUS LT1 transfection agents. H1299 cells were transfected with 200ng of p53 expressing plasmid for 10^5 seeded cells. Also, empty vector with pSUPER backbone was transfected as a control in all cell lines. 24 hours post transfection, cells were treated with doxorubicin, TNF α or Doxorubicin+TNF α as described earlier.

2.2 RESULTS

2.2.1 Treatment of A549 cells with Doxorubicin + TNF α synergistically up regulates genes involved in metastasis, mitosis and kinetochore formation.

Previously, a transcriptome analysis of MCF7 cells treated with doxorubicin + TNF α identified synergistic upregulation as well as downregulation of numerous genes (defined as differentially expressed genes, DEGs). Transcriptome data was confirmed through qPCR for 12 of 15 selected genes, which were transcriptional targets of either doxorubicin and/or of TNF α treatments and synergistically up-regulated upon Doxo+TNF α double treatment. Five of these genes (ETV7, PLK3, UNC5B, NTN1 and LAMP3) were of particular interest either because of the magnitude of transcriptional changes or due to their functions.

To extend the analysis of synergistic regulation to other cell lines, I explored the impact of doxorubicin and TNF α individually as well as combined on HCT116, A549, and H1299 cell lines. Part of this data was published and is presented in Appendix. Here I present additional unpublished data.

A549 and H1299 are Non-Small Lung carcinoma-derived cell lines, of which the first expresses wild type p53, while the second is considered a true p53 null. Firstly, I performed gene reporter assays to establish the minimal dose of TNF α needed to activate NF- κ B dependent transcription in these cells (10ng/mL) Also, the effective dose of BAY 11-7082 (20 μ M), a known pharmacological inhibitor of NF- κ B activity, was identified.

Next, qPCR was performed using total RNA. A549 cells had exhibited a highly synergistic expression of 3 genes ETV7, LAMP3 and NTN1. For other two genes (UNC5B, PLK3), the responsiveness upon combined treatment was simply additive (see Figure 6 in paper attached in Appendix). Eight additional genes from the initial list of 15 were tested of which EDN2, NPCC and EGR2 were responsive to doxorubicin and PLAU was responsive to TNF α and enhanced by double treatment (Figure 18).

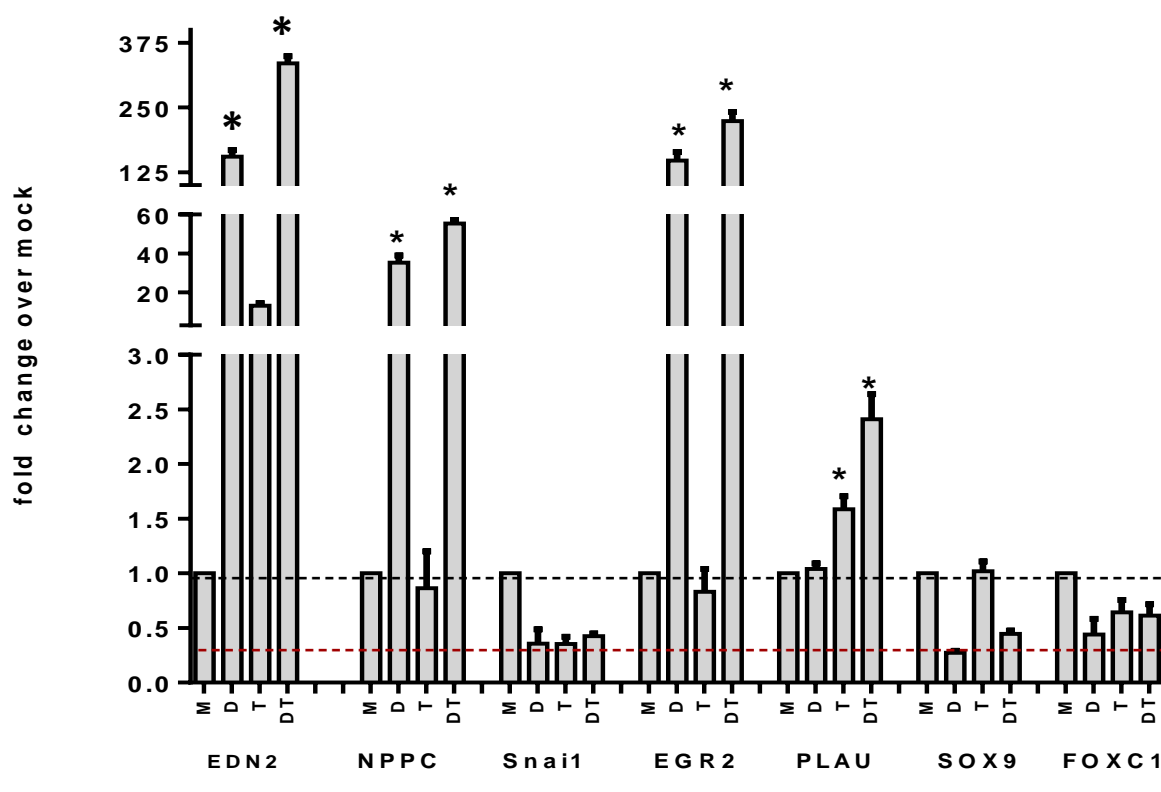


Figure 18: Selective transcriptional synergy of genes in Doxorubicin (D), TNF α (T) and Doxorubicin + TNF α (DT) treated A549 cells. qPCR was performed using RNA extracted from treated (M (mock), D, T, DT) A549 cells to quantify the expression of EDN2, NPPC, Snai1, EGR2, PLAU, SOX9 and FOXC1 genes. Snai1, PLAU, SOX9 and FOXC1 gene expression is not synergistic in combined drug treatment (DT) condition. PLAU gene is TNF α responsive only, whereas EDN2, NPPC and EGR and highly doxorubicin responsive and reveal transcriptional synergy upon combined treatment (DT). * p-value <0.05 for the comparison between single and double treatment for the indicated genes (Student's t-test)

In p53 null H1299 cells, the synergy was absent, suggesting that transcriptional synergy is a p53-dependent phenomenon (see Figure 6 in paper attached in Appendix). We tried to recapitulate p53 and NF- κ B cooperation in H1299 cells after ectopic expression of wild type p53. While p53 overexpression led to activation of p53 target genes such as p21 and PUMA, treatment with doxorubicin did not further stimulate the transcription. Perhaps consistently, no synergistic expression of signature genes (ETV7, LAMP3, NTN1, UNC5B and PLK3) was observed.

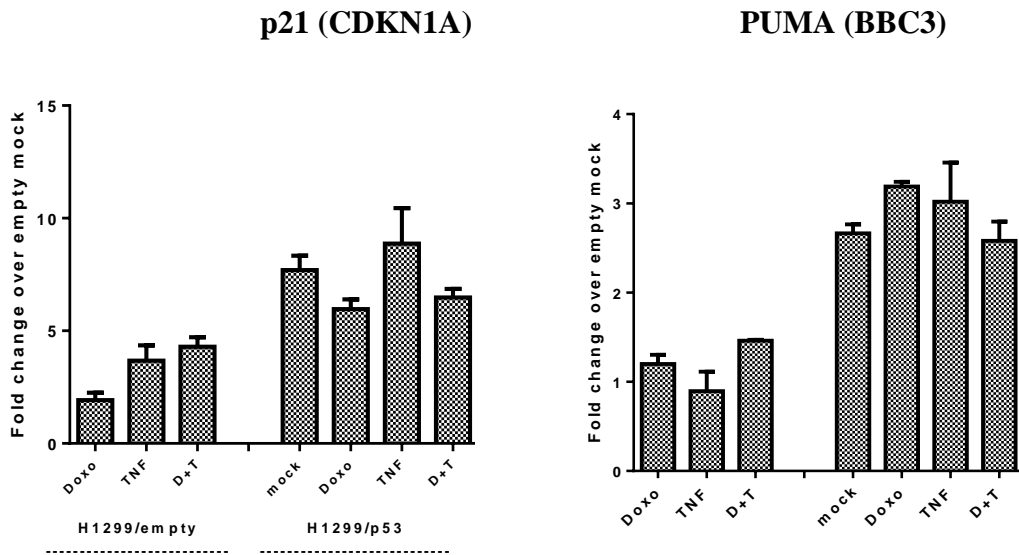


Figure 19: p53 transcriptional targets p21 and PUMA are expressed in p53 transfected H1299 cells. H1299 cells are transfected with low amount of p53 expressing plasmid as well as empty vector and quantified for the expression of p21 and PUMA genes using qPCR. Further Treatment of cells with Doxorubicin (DOXO), TNF α (TNF) and Doxorubicin + TNF α (D+T) does not impact the transcription of two genes.

2.2.2 Combined Doxorubicin and TNF α treatments reduce migration potential of A549 cells, but enhance the migration of p53 null H1299

Cell migration tests for A549 and H1299 cells were performed both using an xCELLigence Real Time Cell Analyzer (RTCA) and a Transwell Migration assay Kit (Figure 20). As previously done for MCF7 cells (see Appendix) both A549 and H1299 cells were treated for 16 hours with Doxorubicin and TNF α individually or combined. Cells were then collected to start migration assays according to manufacturer's protocol (see Materials and Methods). I observed that treatment of cells with TNF α alone enhances the migratory phenotype of A549 cells (more visibly in transwell migration assay, see Figure 20 E). Treatment of cells with Doxorubicin alone reduced the migration by 50% and the combined doxorubicin and TNF α treatment reduced the stimulatory effect of TNF α treatment in A549 cells. On the other hand all treatments and particularly the combined one increases H1299 migration. This suggests that the impact of chemotherapeutic agents is cell line specific and that the synergistic expression of the identified signature genes cannot be directly correlated with cell migration *in vitro*. At the same time, the treatment of p53 null cells with chemotherapeutic agents in the presence of inflammatory signals can alter tumour aggressiveness. Next, we ectopically expressed p53 (with a low amount of transfected plasmid, 200ng for 5×10^5 seeded cells) in H1299 cells to check whether migratory phenotype is affected by p53 expression. As a control, empty pCI-Neomycin vector was transfected. In RTCA experiment, I observed that p53 expression reduces the H1299 migration by 40% but the effect of treatments was not very different from the mock condition in the presence of p53 (see Figure 20 C, D). In transwell migration assay, the treatments further lowered the migration potential of the p53-expressing H1299 cells (Figure 20 F). Expression levels of p65, p53 and p21 proteins were measured in transfected H1299 cells upon all the treatments conditions (Figure 21). The p53 transfected H1299 cells express p53 as well as p21 under treated as well as untreated condition, whereas empty H1299 is null for the expression of p53 while the expression of p21 is slightly increased by the treatments but very weak. The expression of p65 is uniform in all cases.

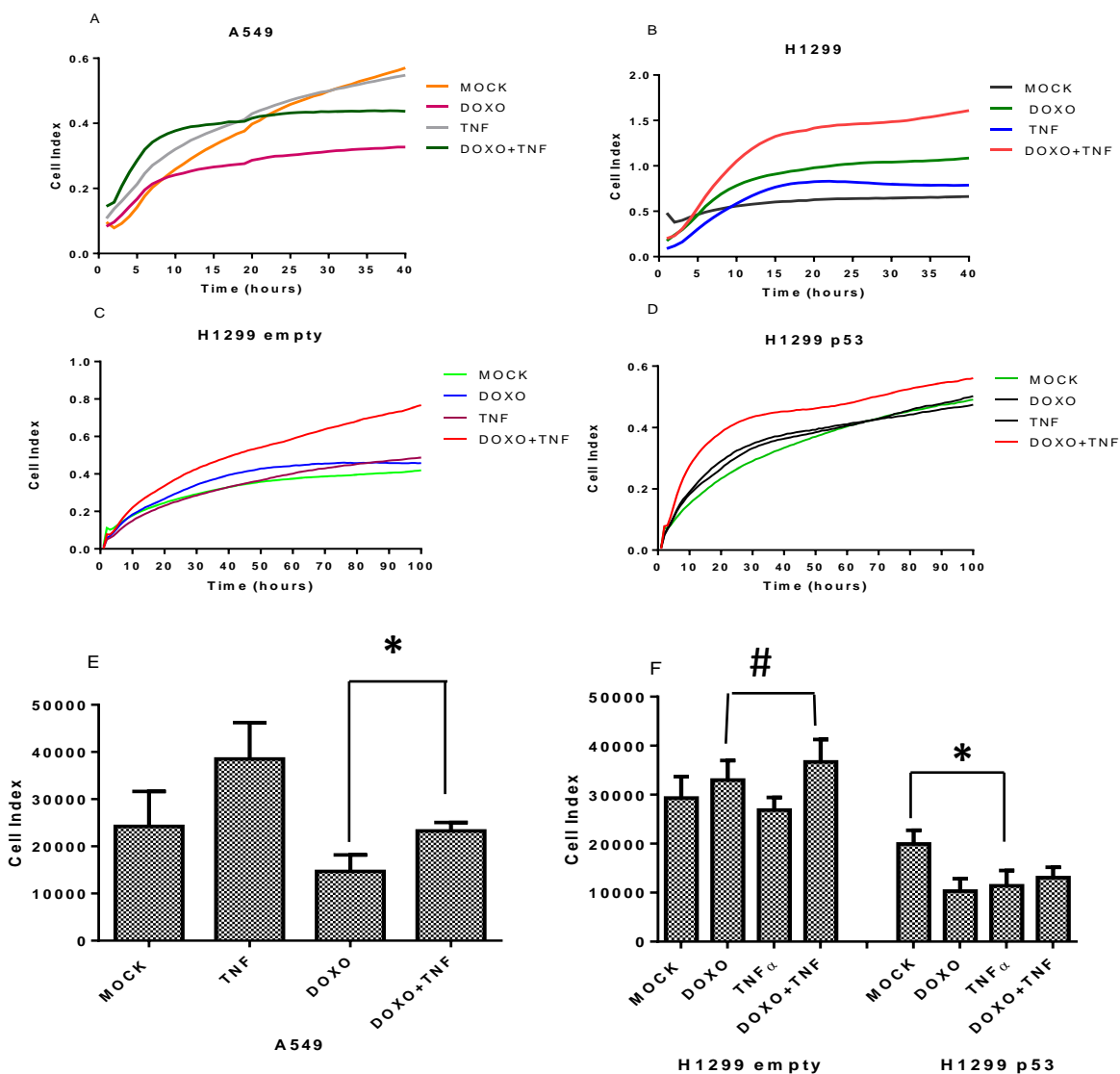


Figure 20: Real time cell migration and Transwell migration analysis. (A, B, C, D) A549, H1299, empty and p53 transfected H1299 cells in (Mock), Doxorubicin (DOXO), TNF α (TNF) and Doxorubicin+TNF α (DOXO+TNF) treated conditions are loaded in equal numbers (four biological replicates) on CIM-16 plates for real time analysis of cell migration till 40-100 hours. Equal number of untreated and treated (E) A549 cells (F) Empty and p53 expressing plasmid transfected in H1299 cells are also loaded in transwell migration plate (three biological replicates) for eight hours to observe the migration. * p-value <0.05 for the compared bars expressing p53 alone or coupled with TNF α treatment (Student's t-test). # Statistically non-significant differences between single or double treatments. In A549 TNF α significantly stimulated migration and doxorubicin as single agent or combined with TNF repressed migration.

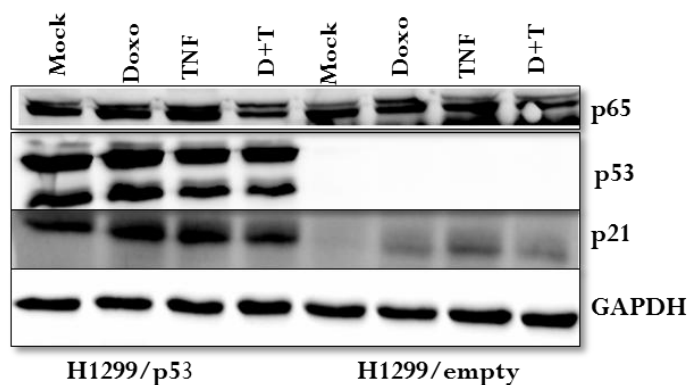


Figure 21: Protein expression in H1299 cells transfected with p53 or empty expression vectors. Transfected cells were also treated with Doxorubicin (Doxo), TNF α (TNF) and Doxorubicin+TNF α (D+T) or left untreated (Mock) and proteins were extracted to quantify the expression of p65, p53 and p21 for all conditions. GAPDH protein expression is used as a loading control

2.2.3 Impact of Myst family members (HATs), MOF and TIP60 on p53 and NF- κ B transcriptional targets in MCF-7, A549 and H1299 cell lines.

TIP60 and MOF are known regulator of both p53 and NF- κ B transcription activity and important hallmarks of tumour. Also, they work in combination with various other cofactors like p300 and CBP in gene regulation (178-180). I wanted to investigate if ectopic expression of TIP60 and MOF contributes in altering the Doxorubicin and TNF α mediated transcription of signature genes (ETV7, LAMP3, NTN1, PLK3 and UNC5B). A549 cells were transfected with plasmids expressing TIP60 and MOF, respectively, followed by 16 hours treatment with doxorubicin and TNF α individually and combined. Post treatment, RNA extraction and RT-qPCR was performed on genes of interest (see Materials and Methods). I observed that TIP60 or MOF expressing cells reveal enhanced transcription of ETV7, NTN1 and LAMP3 in a Doxorubicin-dependent manner in comparison to the cell transfected with empty vector and then treated. Also, TIP60 expression reveals some inhibitory effect on TNF α -dependent transcription of ETV7, NTN1, LAMP3 and PLK3 in A549 cells (Figure 22). No significant effect of TIP60 and MOF on transcription of p21 gene was observed (Figure 23), suggesting doxorubicin-dependent specificity of the two proteins towards our genes of interest. On the other hand, the NF- κ B target MCP-1 was down-regulated upon TNF α treatment of MOF- and particularly TIP60-transfected A549 cells, revealing the two HATs as potential negative regulators on NF- κ B in A549 (Figure 23).

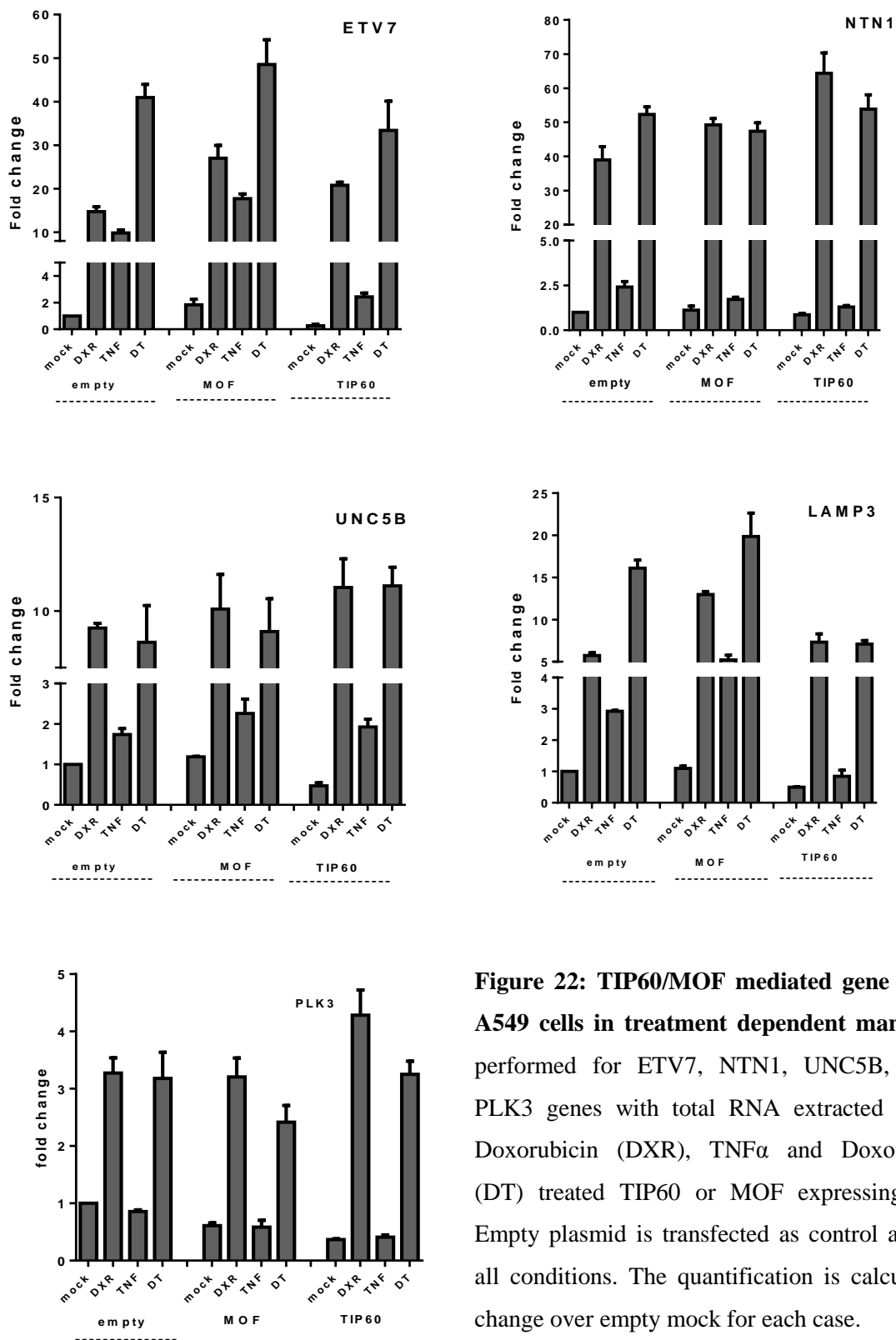


Figure 22: TIP60/MOF mediated gene regulation in A549 cells in treatment dependent manner. qPCR is performed for ETV7, NTN1, UNC5B, LAMP3 and PLK3 genes with total RNA extracted from MOCK, Doxorubicin (DXR), TNF α and Doxorubicin+TNF α (DT) treated TIP60 or MOF expressing A549 cells. Empty plasmid is transfected as control and treated for all conditions. The quantification is calculated as Fold change over empty mock for each case.

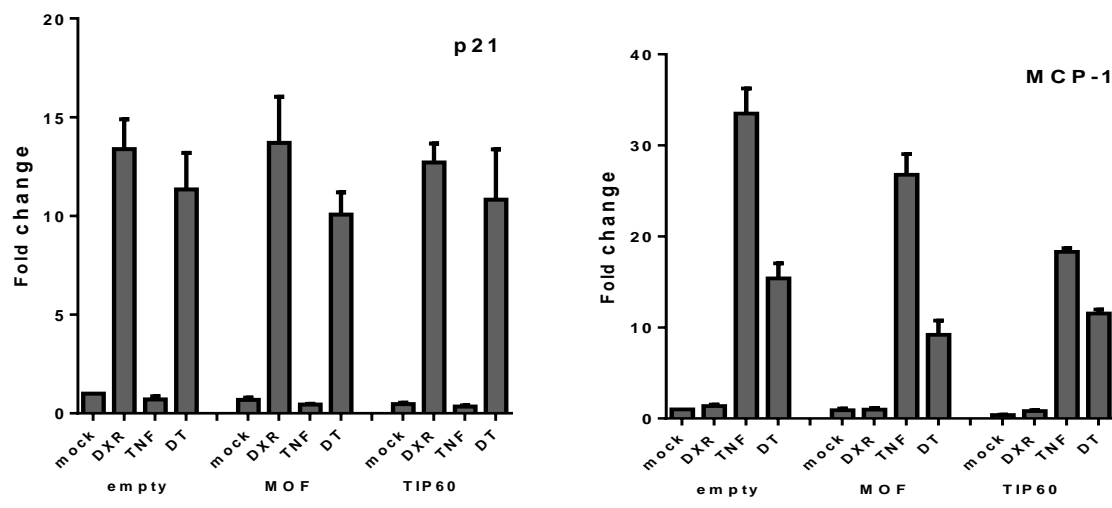


Figure 23: Impact of HATs (TIP60 and MOF) overexpression on transcription of p21 and MCP-1 in A549 cells. qPCR analysis reveals no impact of TIP60 and MOF on transcription of p21 with or without treatment. TIP60 and MOF expression reduces MCP-1 transcription in TNF α -dependent manner.

MCF7 cells upon TIP60 overexpression reveal enhanced transcription of signature genes.

Over-expression of TIP60 in MCF7 cells up regulates the transcription of signature genes in the mock condition (Figure 24). This could be due to the relaxed chromatin state induced upon TIP60-mediated histone acetylation (181). The p21 gene expression is upregulated in Doxorubicin+TNF α treatment condition, whereas the NF- κ B target MCP-1 exhibits TNF α -dependent up regulation in TIP60 overexpressing MCF7 cells (Figure 25). Unlike the case in A549, the LAMP3 and ETV7 signature genes are not negatively regulated by TIP60 ectopic expressing in MCF7 cells treated by TNF α .

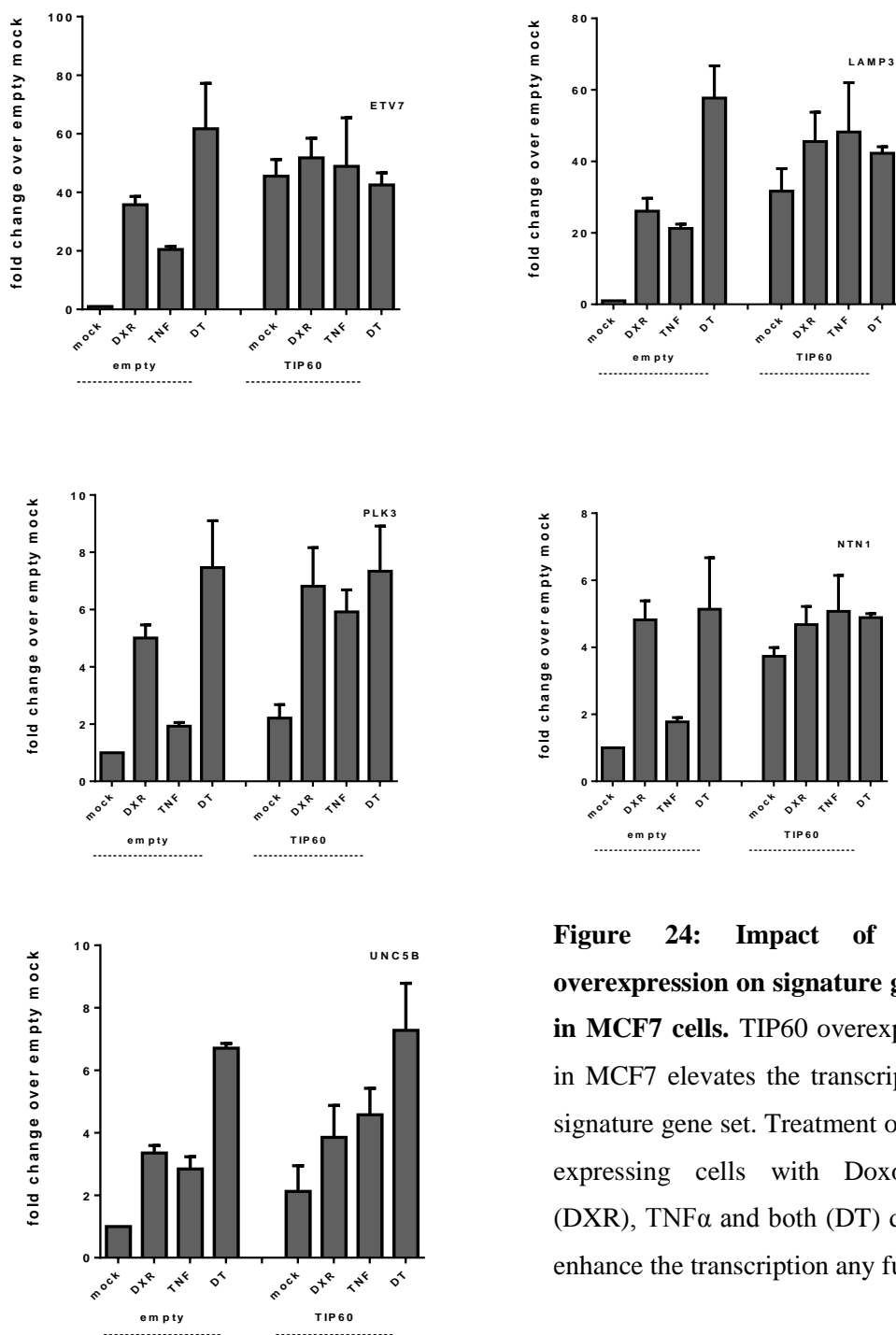


Figure 24: Impact of TIP60 overexpression on signature gene set in MCF7 cells. TIP60 overexpression in MCF7 elevates the transcription of signature gene set. Treatment of TIP60 expressing cells with Doxorubicin (DXR), TNF α and both (DT) does not enhance the transcription any further.

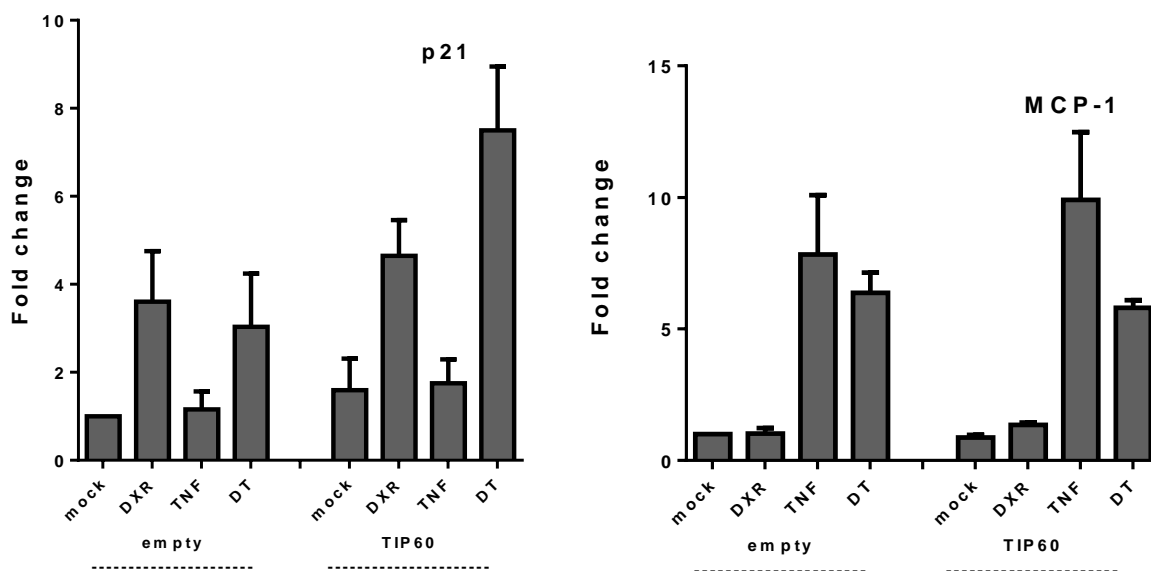


Figure 25: Impact of TIP60 overexpression on p21 and MCP-1 in MCF7 cells. TIP60 overexpression slightly enhances the p21 transcription upon combined treatment (DT) condition in TIP60 dependent manner. A slight increment in MCP-1 expression is observed in TIP60 expressing cells upon TNF α treatment.

Doxorubicin and TNF α combined treatments in p53 null H1299 ectopically expressing TIP60 reveal a striking synergistic expression of ETV7, LAMP3 and PLK3. Also, expression of TIP60 up regulates the transcription of genes in TNF α dependent manner (Figure 26). Treatment of cells with Doxorubicin alone does not induce responsiveness, suggesting TNF α induced signalling as a prerequisite for transcription modulation in this case. Also, one can say that transcriptional synergy observed for ETV7, LAMP3, and PLK3 genes is not really a p53-specific phenomenon for all cell types.

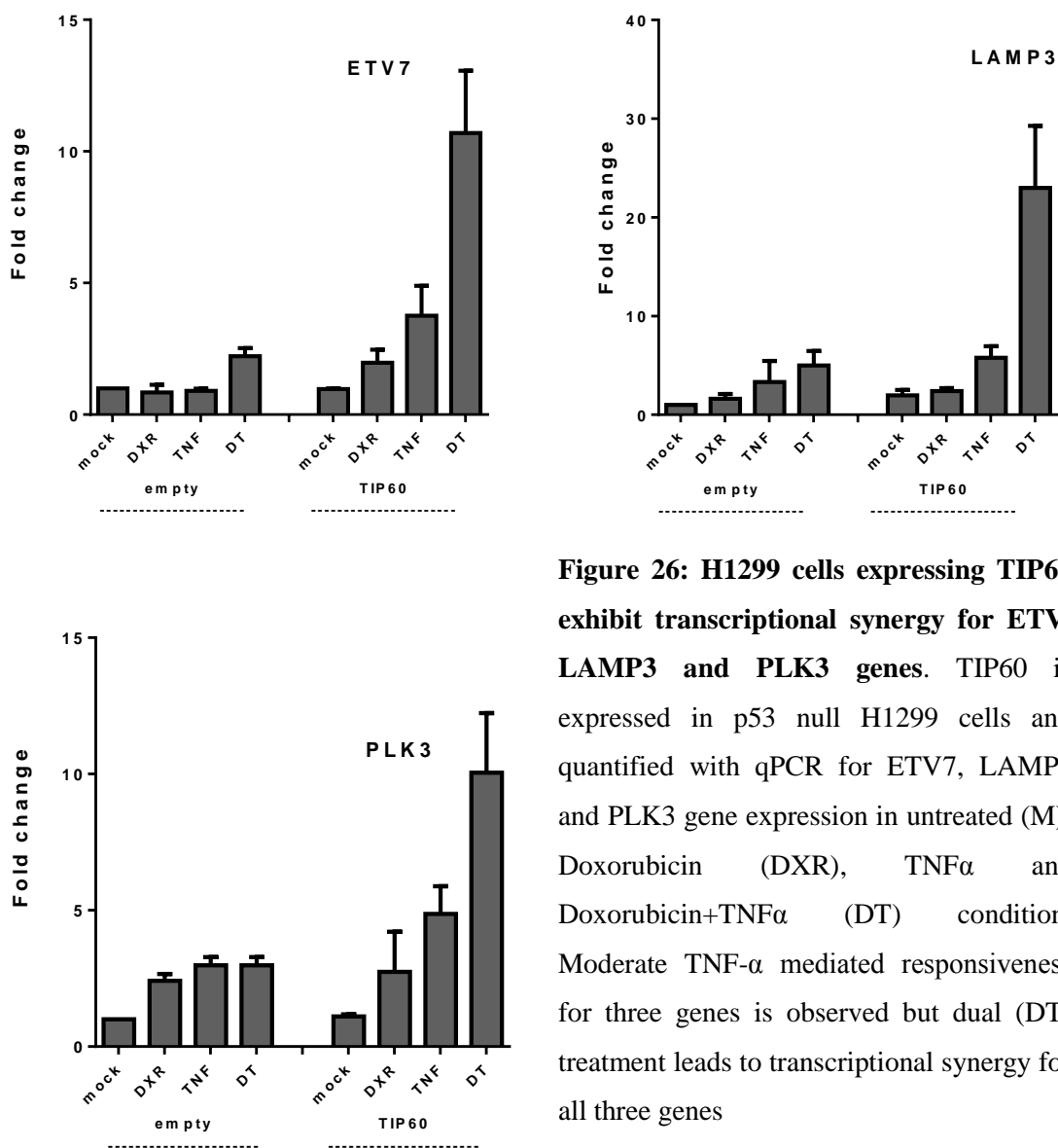


Figure 26: H1299 cells expressing TIP60 exhibit transcriptional synergy for ETV7, LAMP3 and PLK3 genes. TIP60 is expressed in p53 null H1299 cells and quantified with qPCR for ETV7, LAMP3 and PLK3 gene expression in untreated (M), Doxorubicin (DXR), TNF α and Doxorubicin+TNF α (DT) condition. Moderate TNF- α mediated responsiveness for three genes is observed but dual (DT) treatment leads to transcriptional synergy for all three genes

2.2.4 Studying Doxorubicin + TNF α transcriptional synergy with defined promoter fragments from signature genes.

Approximately, 1-1.5 kb long promoter or enhancer regions of eight synergistically upregulated genes carrying variably organized non canonical p53 and NF- κ B REs were selected for cloning upstream of a Firefly luciferase cDNA in pGL4.26 vector, All the REs analysed using TRANSFAC database (<http://www.gene-regulation.com/pub/databases.html>) scored a cutoff value above 0.9, but no information was available regarding their transactivation potentials. Most of the promoter/enhancers carried two to three noncanonical NF- κ B REs which were 8 to 10 nucleotides in length. The p53 REs ranged from half to quarter (3/4th) sites with mismatches in purine and pyrimidine flanks at various positions (see Table 7 in the Materials and Methods section).

I wanted to evaluate if features like proximity between p53 and NF- κ B *cis* elements in human genome and their closeness to transcription start site (TSS) of selective genes (signature genes in our case) can hold some significant impact on transcriptional outcomes. Another target was to find if such REs can synergize with each other at transcriptional level upon doxorubicin and TNF α treatments of cells. Out of eight reporter clones we constructed, five were tested in a preliminary analysis: NTN1, ETV7, LAMP3, DUSP5 and EDN2. The organization of p53 and NF- κ B REs in promoter or enhancer region of the genes is described in Figure 17 (see the Materials and Methods section). All the clones were transfected in MCF7 cells and an empty pGL4.26 vector was used as control. Our results clearly suggest that the identified p53 *cis* elements are active as the cloned constructs were responsive to Doxorubicin treatment with the exception of DUSP5. On the contrary, all constructs were unresponsive to TNF α treatment suggesting that the NF- κ B sites are inactive or not sufficient for transactivation in this type of assay. The combined treatment (Doxorubicin+TNF α) of cells show rather a decline in the luciferase activity in comparison with the Doxorubicin treatment alone, consistent with the lack of effect of TNF α alone (Figure 27). This observation also falls in line with the conventional view of NF- κ B being an antagonistic player in p53-mediated regulation. The *cis* regulatory regions of all the tested genes when explored for their transcriptional activities in extra chromosomal context do not impart much information regarding the rules of transcriptional synergy, but hint towards the presence of context-dependent complex

molecular mechanisms responsible for a highly elevated gene expression upon chemotherapeutic treatments.

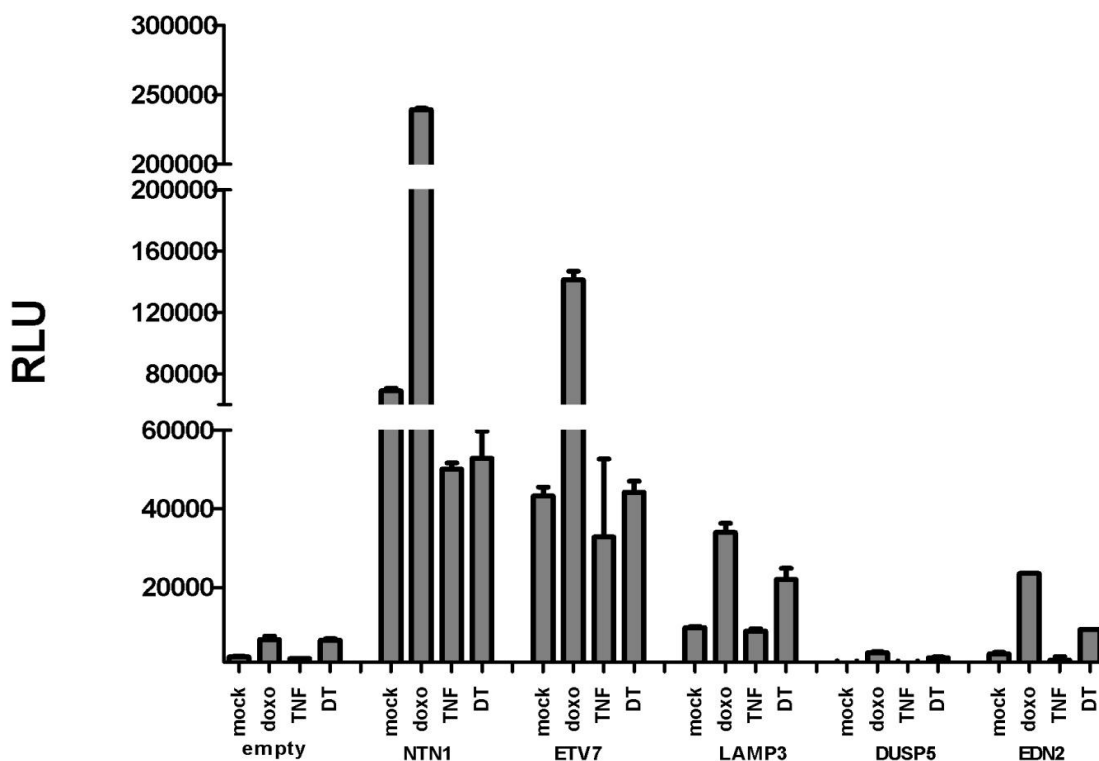


Figure 27: Gene reporter assays evaluate treatment specific transactivation potential of NF- κ B and p53 REs embedded in enhancer regions of five genes. Firefly luciferase activity in MCF-7 cells was quantified as a measure of treatment specific transactivation potential of each reporter clone type. Empty clone without any enhancer/promoter is used as a control and tested for all four conditions (mock, doxo, TNF, DT). Apparently, other than the empty, all other reporter clones exhibit some firefly luciferase activity even in mock condition. NTN1, ETV7, LAMP3 and EDN2 showed responsiveness upon doxorubicin treatments. TNF α treatment does not induce any responsiveness and rather show a repression in Firefly luciferase activity. Also, the combined DT treatment leads to reduced transactivation in comparison to doxorubicin treatment alone.

DISCUSSION

It is quite evident that chemotherapeutic treatments in context of tissue type and tumor microenvironment can concomitantly alter signalling pathways, ultimately impacting on the epigenetic landscape and leading to broad changes in the transcriptome of cancer cells, which can result in vital differences in tumour behaviour in terms of viability, migration and invasiveness (155, 159). In the previous experiment performed in MCF7 cells synergistic upregulation of gene expression was revealed upon combined treatment with doxorubicin and TNF α and correlated with enhanced cell migration *in vitro*. That correlation was not confirmed in A549, where Doxorubicin repressed migration, although the addition of TNF α mitigated the Doxorubicin effect, resulting in higher relative migration potential. Furthermore in p53-null H1299 cells, the combined treatment had virtually no effect on the expression of selected signature genes, yet it led to a clear increase in migration. Combined, these results suggest that the identified genes are not critical determinants of cell migration *in vitro*. The ectopic expression of p53 in H1299 was an attempt to evaluate the role of this transcription factor on both signature gene expression and migration. The ectopic expression of low amounts of p53 in H1299 led to transcriptional activation of p53 target genes like ETV7, NTN1 and UNC5B. Although the treatment of p53 expressing H1299 cells with Doxorubicin and TNF α could not recapitulate the synergy. Also, p53-expressing H1299 cells showed a reduced migratory potential like A549 cells and the treatments further reduced the migration of the cells. While p53 levels can control cell migration behaviour, the virtual synergistic expression of signature genes cannot be directly correlated with the migratory behaviour of these cells.

Various other cofactors and molecules are reported to modulate the interplay of p53 and NF- κ B in a context-dependent manner. Proteins like PI3 kinases, p38 and STAT3 regulate the transcriptional cross talk of p53/NF- κ B at various signalling nodes to control the impact of inflammatory molecules on tumorigenesis. We decided to investigate the impact of epigenetic regulators like histone acetylases or methylases in remodelling the transcriptional landscapes. As a preliminary analysis, we tried to investigate if TIP60 and MOF histone acetyl transferases (HATs), which regulate both p53 and NF- κ B, are involved in the transcription of our target gene set (ETV, LAMP3, NTN1, PLK3 and UNC5B). In A549, transfection of TIP60 and particularly MOF expression vectors led to small changes in the expression of a subset of the

genes by single treatments, but did not significantly modify the impact of the double treatment. In MCF7, TIP60 expression (MOF was not studied) led to dramatic upregulation of the genes' transcription in mock condition, especially for ETV7, LAMP3 and NTN1, but did not further enhance the impact of double treatment. In p53 null H1299, where the impact of single treatment was weak, if at all visible, the TIP60 plasmid led to clear synergistic upregulation in the context of the double treatment. The emerging picture suggests that different subset of molecular players appear to be at play in the regulation of these genes. Given the potential impact on cancer cells of ETV7 or LAMP3 over expression (182, 183), in-depth mechanistic studies are needed to clarify their regulation. More experimental validation is required to establish a defined mechanism that leads to synergy in gene expression. Impact of cofactors like p300, STAT1, STAT3 and CBP in mediating synergistic expression of target genes is to be analysed as yet. Also, silencing of genes like ETV7 and LAMP3 is needed to know their impact on migratory phenotypes of the doxorubicin and TNF α treated cells. Additionally, the function of p53 isoforms like Δ 133p53 is another intriguing aspect which has to be determined. Already it has been reported that p53 isoforms can lead to alterations in behaviour of cancer cells and rather impart oncogenic properties to different tissue types. As another exploratory aspect of this study, I have been trying to knock out p53 in MCF7 and A549 cell lines using CRISPR/Cas9 genome editing methodology to create isogenic p53 null cells to complement their p53-expressing counterparts used throughout the experiments.

cis elements or REs are an important aspect of gene regulation and many studies suggest synergism between two non-canonical *cis* elements to activate the transcription of certain genes (77). For instance the ER α and p53 act synergistically to induce the expression of FLT1 gene by occupying closely spaced REs in its promoter (98). The regulatory regions mapped in our study do not reveal any treatment-specific synergism in gene reporter assays, but we cannot entirely rule out their functionality as mediators of synergistic expression and the endogenous gene level. Studying the transactivation abilities of *cis* regulatory regions in genomic context is more informative due to direct involvement of long-range acting histone modifiers known to reprogram the chromatin landscape and regulate the expression of specific genes. The promoter and enhancer fragments we tested as non-genomic regulatory elements established that p53 REs are more robust in nature and tolerate nucleotide mismatches at various positions whereas NF- κ B REs are comparatively less active. Generally, NF- κ B proteins work as transcription

factors in combination with various other cofactors such as SP1, AP1, STAT3, IRF/ATF etc. to initiate or modulate the transcription (184). It is quite possible that we were not able to include some crucial binding sites needed for NF- κ B mediated gene activation in the tested promoter fragments. Also, we have shown that NF- κ B binding sites function better as a 20mer sequence if exploited outside the genomic context (134). In this regard, the cloning of promoter fragments to establish gene reporter assays revealed that such approach could not recapitulate the synergistic response to doxorubicin and TNF α , although it confirmed the doxorubicin responsiveness in p53 wild type cells. This may also suggest that if the contribution of NF- κ B to the gene regulation is *cis*-element dependent, such sites would be distant from the putative p53 REs.

References

1. Sebastian A, Contreras-Moreira B. The twilight zone of cis element alignments. *Nucleic acids research*. 2013;41(3):1438-49.
2. Das MK, Dai HK. A survey of DNA motif finding algorithms. *BMC bioinformatics*. 2007;8 Suppl 7:S21.
3. Kaeberlein M, Burtner CR, Kennedy BK. Recent Developments in Yeast Aging. *PLoS Genet*. 2007;3(5):e84.
4. Iggo R, Rudewicz J, Monceau E, Sevenet N, Bergh J, Sjoblom T, et al. Validation of a yeast functional assay for p53 mutations using clonal sequencing. *J Pathol*. 2013;231(4):441-8.
5. Scharer E, Iggo R. Mammalian p53 can function as a transcription factor in yeast. *Nucleic acids research*. 1992;20(7):1539-45.
6. Sun SC. Non-canonical NF-kappaB signaling pathway. *Cell research*. 2011;21(1):71-85.
7. Ishioka C, Frebourg T, Yan YX, Vidal M, Friend SH, Schmidt S, et al. Screening patients for heterozygous p53 mutations using a functional assay in yeast. *Nature genetics*. 1993;5(2):124-9.
8. Inga A, Cresta S, Monti P, Aprile A, Scott G, Abbondandolo A, et al. Simple identification of dominant p53 mutants by a yeast functional assay. *Carcinogenesis*. 1997;18(10):2019-21.
9. Weir M, Keeney JB. PCR mutagenesis and gap repair in yeast. *Methods in molecular biology (Clifton, NJ)*. 2014;1205:29-35.
10. Resnick MA, Inga A. Functional mutants of the sequence-specific transcription factor p53 and implications for master genes of diversity. *Proceedings of the National Academy of Sciences of the United States of America*. 2003;100(17):9934-9.
11. Inga A, Storici F, Darden TA, Resnick MA. Differential transactivation by the p53 transcription factor is highly dependent on p53 level and promoter target sequence. *Mol Cell Biol*. 2002;22(24):8612-25.
12. Monti P, Perfumo C, Bisio A, Ciribilli Y, Menichini P, Russo D, et al. Dominant-negative features of mutant TP53 in germline carriers have limited impact on cancer outcomes. *Mol Cancer Res*. 2011;9(3):271-9.
13. Monti P, Ciribilli Y, Jordan J, Menichini P, Umbach DM, Resnick MA, et al. Transcriptional functionality of germ line p53 mutants influences cancer phenotype. *Clin Cancer Res*. 2007;13(13):3789-95.

14. Inga A, Iannone R, Campomenosi P, Molina F, Menichini P, Abbondandolo A, et al. Mutational fingerprint induced by the antineoplastic drug chloroethyl-cyclohexyl-nitrosourea in mammalian cells. *Cancer Res.* 1995;55(20):4658-63.
15. Wu X, Bayle JH, Olson D, Levine AJ. The p53-mdm-2 autoregulatory feedback loop. *Genes Dev.* 1993;7(7A):1126-32.
16. Iwabuchi K, Li B, Massa HF, Trask BJ, Date T, Fields S. Stimulation of p53-mediated transcriptional activation by the p53-binding proteins, 53BP1 and 53BP2. *The Journal of biological chemistry.* 1998;273(40):26061-8.
17. Ward IM, Minn K, van Deursen J, Chen J. p53 Binding protein 53BP1 is required for DNA damage responses and tumor suppression in mice. *Mol Cell Biol.* 2003;23(7):2556-63.
18. Chai YL, Cui J, Shao N, Shyam E, Reddy P, Rao VN. The second BRCT domain of BRCA1 proteins interacts with p53 and stimulates transcription from the p21WAF1/CIP1 promoter. *Oncogene.* 1999;18(1):263-8.
19. Andreotti V, Ciribilli Y, Monti P, Bisio A, Lion M, Jordan J, et al. p53 transactivation and the impact of mutations, cofactors and small molecules using a simplified yeast-based screening system. *PLoS One.* 2011;6(6):e20643.
20. Inga A, Reamon-Buettner SM, Borlak J, Resnick MA. Functional dissection of sequence-specific NKX2-5 DNA binding domain mutations associated with human heart septation defects using a yeast-based system. *Human molecular genetics.* 2005;14(14):1965-75.
21. Wang S, Bovee TF. Estrogen Receptor Agonists and Antagonists in the Yeast Estrogen Bioassay. *Methods in molecular biology (Clifton, NJ).* 2016;1366:337-42.
22. Storici F, Lewis LK, Resnick MA. In vivo site-directed mutagenesis using oligonucleotides. *Nat Biotechnol.* 2001;19(8):773-6.
23. Storici F, Resnick MA. Delitto perfetto targeted mutagenesis in yeast with oligonucleotides. *Genet Eng (N Y).* 2003;25:189-207.
24. Pierrat B, Heery DM, Lemoine Y, Losson R. Functional analysis of the human estrogen receptor using a phenotypic transactivation assay in yeast. *Gene.* 1992;119(2):237-45.
25. Bisio A, Ciribilli Y, Fronza G, Inga A, Monti P. TP53 mutants in the tower of babel of cancer progression. *Human mutation.* 2014;35(6):689-701.
26. Leao M, Gomes S, Bessa C, Soares J, Raimundo L, Monti P, et al. Studying p53 family proteins in yeast: induction of autophagic cell death and modulation by interactors and small molecules. *Experimental cell research.* 2015;330(1):164-77.

27. DeLeo AB, Jay G, Appella E, Dubois GC, Law LW, Old LJ. Detection of a transformation-related antigen in chemically induced sarcomas and other transformed cells of the mouse. *Proceedings of the National Academy of Sciences of the United States of America*. 1979;76(5):2420-4.
28. Kress M, May E, Cassingena R, May P. Simian virus 40-transformed cells express new species of proteins precipitable by anti-simian virus 40 tumor serum. *Journal of virology*. 1979;31(2):472-83.
29. Lane DP, Crawford LV. T antigen is bound to a host protein in SV40-transformed cells. *Nature*. 1979;278(5701):261-3.
30. Melero JA, Stitt DT, Mangel WF, Carroll RB. Identification of new polypeptide species (48-55K) immunoprecipitable by antiserum to purified large T antigen and present in SV40-infected and -transformed cells. *Virology*. 1979;93(2):466-80.
31. Zilfou JT, Lowe SW. Tumor Suppressive Functions of p53. *Cold Spring Harbor Perspectives in Biology*. 2009;1(5).
32. Wang X, Simpson ER, Brown KA. p53: Protection against Tumor Growth beyond Effects on Cell Cycle and Apoptosis. *Cancer Res*. 2015;75(23):5001-7.
33. Nicolai S, Rossi A, Di Daniele N, Melino G, Annicchiarico-Petruzzelli M, Raschella G. DNA repair and aging: the impact of the p53 family. *Aging*. 2015;7(12):1050-65.
34. Brady CA, Attardi LD. p53 at a glance. *Journal of Cell Science*. 2010;123(15):2527-32.
35. Farnebo M, Bykov VJ, Wiman KG. The p53 tumor suppressor: a master regulator of diverse cellular processes and therapeutic target in cancer. *Biochemical and biophysical research communications*. 2010;396(1):85-9.
36. Puzio-Kuter AM. The Role of p53 in Metabolic Regulation. *Genes & Cancer*. 2011;2(4):385-91.
37. Lee C-L, Blum JM, Kirsch DG. Role of p53 in regulating tissue response to radiation by mechanisms independent of apoptosis. *Translational Cancer Research*. 2013;2(5):412-21.
38. Jiang L, Kon N, Li T, Wang S-J, Su T, Hibshoosh H, et al. Ferroptosis as a p53-mediated activity during tumour suppression. *Nature*. 2015;520(7545):57-62.
39. Fridman JS, Lowe SW. Control of apoptosis by p53. *Oncogene*. 0000;22(56):9030-40.
40. Dittmer D, Pati S, Zambetti G, Chu S, Teresky AK, Moore M, et al. Gain of function mutations in p53. *Nature genetics*. 1993;4(1):42-6.

41. Bougeard G, Renaux-Petel M, Flaman JM, Charbonnier C, Fermey P, Belotti M, et al. Revisiting Li-Fraumeni Syndrome From TP53 Mutation Carriers. *Journal of clinical oncology : official journal of the American Society of Clinical Oncology*. 2015;33(21):2345-52.
42. Dong P, Karaayvaz M, Jia N, Kaneuchi M, Hamada J, Watari H, et al. Mutant p53 gain-of-function induces epithelial-mesenchymal transition through modulation of the miR-130b-ZEB1 axis. *Oncogene*. 2013;32(27):3286-95.
43. Di Fiore R, Marcatti M, Drago-Ferrante R, D'Anneo A, Giuliano M, Carlisi D, et al. Mutant p53 gain of function can be at the root of dedifferentiation of human osteosarcoma MG63 cells into 3AB-OS cancer stem cells. *Bone*. 2014;60:198-212.
44. Vogelstein B, Lane D, Levine AJ. Surfing the p53 network. *Nature*. 2000;408(6810):307-10.
45. Stenger JE, Mayr GA, Mann K, Tegtmeyer P. Formation of stable p53 homotetramers and multiples of tetramers. *Molecular carcinogenesis*. 1992;5(2):102-6.
46. Oren M. The p53 cellular tumor antigen: gene structure, expression and protein properties. *Biochimica et biophysica acta*. 1985;823(1):67-78.
47. Wang P, Reed M, Wang Y, Mayr G, Stenger JE, Anderson ME, et al. p53 domains: structure, oligomerization, and transformation. *Mol Cell Biol*. 1994;14(8):5182-91.
48. Hulboy DL, Lozano G. Structural and functional analysis of p53: the acidic activation domain has transforming capability. *Cell growth & differentiation : the molecular biology journal of the American Association for Cancer Research*. 1994;5(10):1023-31.
49. Zhang W, Funk WD, Wright WE, Shay JW, Deisseroth AB. Novel DNA binding of p53 mutants and their role in transcriptional activation. *Oncogene*. 1993;8(9):2555-9.
50. Maxwell SA, Roth JA. Posttranslational regulation of p53 tumor suppressor protein function. *Critical reviews in oncogenesis*. 1994;5(1):23-57.
51. Ohki R, Kawase T, Ohta T, Ichikawa H, Taya Y. Dissecting functional roles of p53 N-terminal transactivation domains by microarray expression analysis. *Cancer science*. 2007;98(2):189-200.
52. Truant R, Xiao H, Ingles CJ, Greenblatt J. Direct interaction between the transcriptional activation domain of human p53 and the TATA box-binding protein. *The Journal of biological chemistry*. 1993;268(4):2284-7.
53. Murray-Zmijewski F, Lane DP, Bourdon JC. p53/p63/p73 isoforms: an orchestra of isoforms to harmonise cell differentiation and response to stress. *Cell death and differentiation*. 2006;13(6):962-72.

54. Joruz SM, Bourdon JC. p53 Isoforms: Key Regulators of the Cell Fate Decision. Cold Spring Harbor perspectives in medicine. 2016.
55. Marcel V, Dichtel-Danjoy ML, Sagne C, Hafsi H, Ma D, Ortiz-Cuaran S, et al. Biological functions of p53 isoforms through evolution: lessons from animal and cellular models. Cell death and differentiation. 2011;18(12):1815-24.
56. Arai N, Nomura D, Yokota K, Wolf D, Brill E, Shohat O, et al. Immunologically distinct p53 molecules generated by alternative splicing. Mol Cell Biol. 1986;6(9):3232-9.
57. Bourdon JC, Fernandes K, Murray-Zmijewski F, Liu G, Diot A, Xirodimas DP, et al. p53 isoforms can regulate p53 transcriptional activity. Genes Dev. 2005;19(18):2122-37.
58. Senturk S, Yao Z, Camiolo M, Stiles B, Rathod T, Walsh AM, et al. p53Psi is a transcriptionally inactive p53 isoform able to reprogram cells toward a metastatic-like state. Proceedings of the National Academy of Sciences of the United States of America. 2014;111(32):E3287-96.
59. Lee JT, Gu W. The multiple levels of regulation by p53 ubiquitination. Cell death and differentiation. 2010;17(1):86-92.
60. Harris SL, Levine AJ. The p53 pathway: positive and negative feedback loops. Oncogene. 2005;24(17):2899-908.
61. Secchiero P, Bosco R, Celeghini C, Zauli G. Recent advances in the therapeutic perspectives of Nutlin-3. Current pharmaceutical design. 2011;17(6):569-77.
62. Peng X, Zhang MQ, Conserva F, Hosny G, Selivanova G, Bykov VJ, et al. APR-246/PRIMA-1MET inhibits thioredoxin reductase 1 and converts the enzyme to a dedicated NADPH oxidase. Cell death & disease. 2013;4:e881.
63. Tessoulin B, Descamps G, Moreau P, Maiga S, Lode L, Godon C, et al. PRIMA-1Met induces myeloma cell death independent of p53 by impairing the GSH/ROS balance. Blood. 2014;124(10):1626-36.
64. Liu X, Wilcken R, Joerger AC, Chuckowree IS, Amin J, Spencer J, et al. Small molecule induced reactivation of mutant p53 in cancer cells. Nucleic acids research. 2013;41(12):6034-44.
65. Boeckler FM, Joerger AC, Jaggi G, Rutherford TJ, Veprintsev DB, Fersht AR. Targeted rescue of a destabilized mutant of p53 by an in silico screened drug. Proceedings of the National Academy of Sciences of the United States of America. 2008;105(30):10360-5.
66. Abbasi M, Sadeghi-Aliabadi H, Hassanzadeh F, Amanlou M. Prediction of dual agents as an activator of mutant p53 and inhibitor of Hsp90 by docking, molecular dynamic simulation and virtual screening. Journal of molecular graphics & modelling. 2015;61:186-95.

67. Soares J, Raimundo L, Pereira NA, dos Santos DJ, Perez M, Queiroz G, et al. A tryptophanol-derived oxazolopiperidone lactam is cytotoxic against tumors via inhibition of p53 interaction with murine double minute proteins. *Pharmacol Res.* 2015;95-96:42-52.
68. Meek DW, Anderson CW. Posttranslational modification of p53: cooperative integrators of function. *Cold Spring Harbor Perspectives in Biology.* 2009;1(6):a000950.
69. Kruse JP, Gu W. Modes of p53 regulation. *Cell.* 2009;137(4):609-22.
70. Gu W, Roeder RG. Activation of p53 sequence-specific DNA binding by acetylation of the p53 C-terminal domain. *Cell.* 1997;90(4):595-606.
71. Tang Y, Zhao W, Chen Y, Zhao Y, Gu W. Acetylation is indispensable for p53 activation. *Cell.* 2008;133(4):612-26.
72. Menendez D, Inga A, Resnick MA. Potentiating the p53 network. *Discov Med.* 2010;10(50):94-100.
73. Smeenk L, van Heeringen SJ, Koeppel M, van Driel MA, Bartels SJ, Akkers RC, et al. Characterization of genome-wide p53-binding sites upon stress response. *Nucleic acids research.* 2008;36(11):3639-54.
74. Ciribilli Y, Monti P, Bisio A, Nguyen HT, Ethayathulla AS, Ramos A, et al. Transactivation specificity is conserved among p53 family proteins and depends on a response element sequence code. *Nucleic acids research.* 2013;41(18):8637-53.
75. Nouredine MA, Menendez D, Campbell MR, Bandele OJ, Horvath MM, Wang X, et al. Probing the functional impact of sequence variation on p53-DNA interactions using a novel microsphere assay for protein-DNA binding with human cell extracts. *PLoS Genet.* 2009;5(5):e1000462.
76. Menendez D, Inga A, Resnick MA. The expanding universe of p53 targets. *Nat Rev Cancer.* 2009;9(10):724-37.
77. Jordan JJ, Menendez D, Inga A, Nouredine M, Bell DA, Resnick MA. Noncanonical DNA motifs as transactivation targets by wild type and mutant p53. *PLoS Genet.* 2008;4(6):e1000104.
78. el-Deiry WS, Kern SE, Pietenpol JA, Kinzler KW, Vogelstein B. Definition of a consensus binding site for p53. *Nature genetics.* 1992;1(1):45-9.
79. Sammons MA, Zhu J, Drake AM, Berger SL. TP53 engagement with the genome occurs in distinct local chromatin environments via pioneer factor activity. *Genome research.* 2015;25(2):179-88.

80. Wylie A, Jones AE, D'Brot A, Lu WJ, Kurtz P, Moran JV, et al. p53 genes function to restrain mobile elements. *Genes Dev.* 2016;30(1):64-77.
81. Rubbi CP, Milner J. p53 is a chromatin accessibility factor for nucleotide excision repair of DNA damage. *The EMBO journal.* 2003;22(4):975-86.
82. Wang T, Zeng J, Lowe CB, Sellers RG, Salama SR, Yang M, et al. Species-specific endogenous retroviruses shape the transcriptional network of the human tumor suppressor protein p53. *Proceedings of the National Academy of Sciences of the United States of America.* 2007;104(47):18613-8.
83. Allen MA, Andrysiak Z, Dengler VL, Mellert HS, Guarnieri A, Freeman JA, et al. Global analysis of p53-regulated transcription identifies its direct targets and unexpected regulatory mechanisms. *Elife.* 2014;3:e02200.
84. Horvath MM, Wang X, Resnick MA, Bell DA. Divergent evolution of human p53 binding sites: cell cycle versus apoptosis. *PLoS Genet.* 2007;3(7):e127.
85. Jegga AG, Inga A, Menendez D, Aronow BJ, Resnick MA. Functional evolution of the p53 regulatory network through its target response elements. *Proceedings of the National Academy of Sciences of the United States of America.* 2008;105(3):944-9.
86. Wei CL, Wu Q, Vega VB, Chiu KP, Ng P, Zhang T, et al. A global map of p53 transcription-factor binding sites in the human genome. *Cell.* 2006;124(1):207-19.
87. Menendez D, Nguyen TA, Freudenberg JM, Mathew VJ, Anderson CW, Jothi R, et al. Diverse stresses dramatically alter genome-wide p53 binding and transactivation landscape in human cancer cells. *Nucleic acids research.* 2013;41(15):7286-301.
88. Jordan JJ, Menendez D, Sharav J, Beno I, Rosenthal K, Resnick MA, et al. Low-level p53 expression changes transactivation rules and reveals superactivating sequences. *Proceedings of the National Academy of Sciences of the United States of America.* 2012;109(36):14387-92.
89. Jordan JJ, Inga A, Conway K, Edmiston S, Carey LA, Wu L, et al. Altered-function p53 missense mutations identified in breast cancers can have subtle effects on transactivation. *Mol Cancer Res.* 2010;8(5):701-16.
90. Menendez D, Inga A, Resnick MA. The biological impact of the human master regulator p53 can be altered by mutations that change the spectrum and expression of its target genes. *Mol Cell Biol.* 2006;26(6):2297-308.
91. Monti P, Campomenosi P, Ciribilli Y, Iannone R, Inga A, Abbondandolo A, et al. Tumour p53 mutations exhibit promoter selective dominance over wild type p53. *Oncogene.* 2002;21(11):1641-8.

92. Inga A, Resnick MA. Novel human p53 mutations that are toxic to yeast can enhance transactivation of specific promoters and reactivate tumor p53 mutants. *Oncogene*. 2001;20(26):3409-19.
93. Inga A, Monti P, Fronza G, Darden T, Resnick MA. p53 mutants exhibiting enhanced transcriptional activation and altered promoter selectivity are revealed using a sensitive, yeast-based functional assay. *Oncogene*. 2001;20(4):501-13.
94. Tebaldi T, Zaccara S, Alessandrini F, Bisio A, Ciribilli Y, Inga A. Whole-genome cartography of p53 response elements ranked on transactivation potential. *BMC genomics*. 2015;16:464.
95. Lion M, Raimondi I, Donati S, Jousson O, Ciribilli Y, Inga A. Evolution of p53 transactivation specificity through the lens of a yeast-based functional assay. *PLoS One*. 2015;10(2):e0116177.
96. Raimondi I, Ciribilli Y, Monti P, Bisio A, Pollegioni L, Fronza G, et al. P53 family members modulate the expression of *PRODH*, but not *PRODH2*, via intronic p53 response elements. *PLoS One*. 2013;8(7):e69152.
97. Su D, Wang X, Campbell MR, Song L, Safi A, Crawford GE, et al. Interactions of chromatin context, binding site sequence content, and sequence evolution in stress-induced p53 occupancy and transactivation. *PLoS Genet*. 2015;11(1):e1004885.
98. Menendez D, Inga A, Resnick MA. Estrogen receptor acting in cis enhances WT and mutant p53 transactivation at canonical and noncanonical p53 target sequences. *Proceedings of the National Academy of Sciences of the United States of America*. 2010;107(4):1500-5.
99. Tomso DJ, Inga A, Menendez D, Pittman GS, Campbell MR, Storici F, et al. Functionally distinct polymorphic sequences in the human genome that are targets for p53 transactivation. *Proceedings of the National Academy of Sciences of the United States of America*. 2005;102(18):6431-6.
100. Nagaich AK, Zhurkin VB, Durell SR, Jernigan RL, Appella E, Harrington RE. p53-induced DNA bending and twisting: p53 tetramer binds on the outer side of a DNA loop and increases DNA twisting. *Proceedings of the National Academy of Sciences of the United States of America*. 1999;96(5):1875-80.
101. Schlereth K, Heyl C, Krampitz AM, Mernberger M, Finkernagel F, Scharfe M, et al. Characterization of the p53 cistrome--DNA binding cooperativity dissects p53's tumor suppressor functions. *PLoS Genet*. 2013;9(8):e1003726.
102. Beno I, Rosenthal K, Levitine M, Shaulov L, Haran TE. Sequence-dependent cooperative binding of p53 to DNA targets and its relationship to the structural properties of the DNA targets. *Nucleic acids research*. 2011;39(5):1919-32.

103. Kitayner M, Rozenberg H, Kessler N, Rabinovich D, Shaulov L, Haran TE, et al. Structural basis of DNA recognition by p53 tetramers. *Molecular cell*. 2006;22(6):741-53.
104. Weinberg RL, Veprintsev DB, Fersht AR. Cooperative binding of tetrameric p53 to DNA. *Journal of molecular biology*. 2004;341(5):1145-59.
105. Levrero M, De Laurenzi V, Costanzo A, Gong J, Melino G, Wang JY. Structure, function and regulation of p63 and p73. *Cell death and differentiation*. 1999;6(12):1146-53.
106. Dotsch V, Bernassola F, Coutandin D, Candi E, Melino G. p63 and p73, the ancestors of p53. *Cold Spring Harbor Perspectives in Biology*. 2010;2(9):a004887.
107. Monti P, Ciribilli Y, Bisio A, Foggetti G, Raimondi I, Campomenosi P, et al. N-P63alpha and TA-P63alpha exhibit intrinsic differences in transactivation specificities that depend on distinct features of DNA target sites. *Oncotarget*. 2014;5(8):2116-30.
108. Oeckinghaus A, Ghosh S. The NF-kappaB family of transcription factors and its regulation. *Cold Spring Harbor Perspectives in Biology*. 2009;1(4):a000034.
109. Lawrence T. The Nuclear Factor NF- κ B Pathway in Inflammation. *Cold Spring Harbor Perspectives in Biology*. 2009;1(6).
110. Shukla S, MacLennan GT, Fu P, Patel J, Marengo SR, Resnick MI, et al. Nuclear factor-kappaB/p65 (Rel A) is constitutively activated in human prostate adenocarcinoma and correlates with disease progression. *Neoplasia*. 2004;6(4):390-400.
111. Perkins ND. Post-translational modifications regulating the activity and function of the nuclear factor kappa B pathway. *Oncogene*. 2006;25(51):6717-30.
112. Jacobs MD, Harrison SC. Structure of an IkappaBalpha/NF-kappaB complex. *Cell*. 1998;95(6):749-58.
113. Sen R, Baltimore D. Inducibility of kappa immunoglobulin enhancer-binding protein Nf-kappa B by a posttranslational mechanism. *Cell*. 1986;47(6):921-8.
114. Whiteside ST, Israel A. I kappa B proteins: structure, function and regulation. *Seminars in cancer biology*. 1997;8(2):75-82.
115. Karin M. How NF-kappaB is activated: the role of the IkappaB kinase (IKK) complex. *Oncogene*. 1999;18(49):6867-74.
116. Ghosh S, May MJ, Kopp EB. NF-kappa B and Rel proteins: evolutionarily conserved mediators of immune responses. *Annual review of immunology*. 1998;16:225-60.

117. Kunsch C, Ruben SM, Rosen CA. Selection of optimal kappa B/Rel DNA-binding motifs: interaction of both subunits of NF-kappa B with DNA is required for transcriptional activation. *Mol Cell Biol.* 1992;12(10):4412-21.
118. Natoli G, Sacconi S, Bosisio D, Marazzi I. Interactions of NF-kappaB with chromatin: the art of being at the right place at the right time. *Nature immunology.* 2005;6(5):439-45.
119. Gilmore TD. Clinically relevant findings. *The Journal of clinical investigation.* 1997;100(12):2935-6.
120. Gapuzan ME, Yufit PV, Gilmore TD. Immortalized embryonic mouse fibroblasts lacking the RelA subunit of transcription factor NF-kappaB have a malignantly transformed phenotype. *Oncogene.* 2002;21(16):2484-92.
121. Gapuzan ME, Schmah O, Pollock AD, Hoffmann A, Gilmore TD. Immortalized fibroblasts from NF-kappaB RelA knockout mice show phenotypic heterogeneity and maintain increased sensitivity to tumor necrosis factor alpha after transformation by v-Ras. *Oncogene.* 2005;24(43):6574-83.
122. Schmitz ML, Baeuerle PA. The p65 subunit is responsible for the strong transcription activating potential of NF-kappa B. *The EMBO journal.* 1991;10(12):3805-17.
123. Ghosh G, van Duyne G, Ghosh S, Sigler PB. Structure of NF-kappa B p50 homodimer bound to a kappa B site. *Nature.* 1995;373(6512):303-10.
124. Leung TH, Hoffmann A, Baltimore D. One nucleotide in a kappaB site can determine cofactor specificity for NF-kappaB dimers. *Cell.* 2004;118(4):453-64.
125. Udalova IA, Mott R, Field D, Kwiatkowski D. Quantitative prediction of NF-kappa B DNA-protein interactions. *Proceedings of the National Academy of Sciences of the United States of America.* 2002;99(12):8167-72.
126. Wang VY, Huang W, Asagiri M, Spann N, Hoffmann A, Glass C, et al. The transcriptional specificity of NF-kappaB dimers is coded within the kappaB DNA response elements. *Cell reports.* 2012;2(4):824-39.
127. Hoffmann A, Leung TH, Baltimore D. Genetic analysis of NF-kappaB/Rel transcription factors defines functional specificities. *The EMBO journal.* 2003;22(20):5530-9.
128. Siggers T, Gilmore TD, Barron B, Penvose A. Characterizing the DNA binding site specificity of NF-kappaB with protein-binding microarrays (PBMs). *Methods in molecular biology (Clifton, NJ).* 2015;1280:609-30.
129. Sullivan JC, Wolenski FS, Reitzel AM, French CE, Traylor-Knowles N, Gilmore TD, et al. Two alleles of NF-kappaB in the sea anemone *Nematostella vectensis* are widely dispersed in nature and encode proteins with distinct activities. *PLoS One.* 2009;4(10):e7311.

130. Sif S, Gilmore TD. Interaction of the v-Rel oncoprotein with cellular transcription factor Sp1. *Journal of virology*. 1994;68(11):7131-8.
131. Srinivasan V, Kriete A, Sacan A, Jazwinski SM. Comparing the yeast retrograde response and NF-kappaB stress responses: implications for aging. *Aging cell*. 2010;9(6):933-41.
132. Storici F, Resnick MA. The delitto perfetto approach to in vivo site-directed mutagenesis and chromosome rearrangements with synthetic oligonucleotides in yeast. *Methods Enzymol*. 2006;409:329-45.
133. Gietz RD, Schiestl RH, Willems AR, Woods RA. Studies on the transformation of intact yeast cells by the LiAc/SS-DNA/PEG procedure. *Yeast*. 1995;11(4):355-60.
134. Sharma V, Jordan JJ, Ciribilli Y, Resnick MA, Bisio A, Inga A. Quantitative Analysis of NF-kappaB Transactivation Specificity Using a Yeast-Based Functional Assay. *PLoS One*. 2015;10(7):e0130170.
135. Jordan JJ, Menendez D, Inga A, Nourredine M, Bell D, Resnick MA. Noncanonical DNA motifs as transactivation targets by wild type and mutant p53. *PLoS Genet*. 2008;4(6):e1000104.
136. Transcriptional control of human p53-regulated genes, (2008).
137. Algorithm for prediction of tumour suppressor p53 affinity for binding sites in DNA, (2008).
138. Kitayner M, Rozenberg H, Rohs R, Suad O, Rabinovich D, Honig B, et al. Diversity in DNA recognition by p53 revealed by crystal structures with Hoogsteen base pairs. *Nat Struct Mol Biol*. 2010;17(4):423-9.
139. Khoo KH, Verma CS, Lane DP. Drugging the p53 pathway: understanding the route to clinical efficacy. *Nat Rev Drug Discov*. 2014;13(3):217-36.
140. Mechanisms of regulatory diversity within the p53 transcriptional network, (2008).
141. Lion M, Bisio A, Tebaldi T, De Sanctis V, Menendez D, Resnick MA, et al. Interaction between p53 and estradiol pathways in transcriptional responses to chemotherapeutics. *Cell Cycle*. 2013;12(8):1211-24.
142. Zaccara S, Tebaldi T, Pederiva C, Ciribilli Y, Bisio A, Inga A. p53-directed translational control can shape and expand the universe of p53 target genes. *Cell death and differentiation*. 2014;21(10):1522-34.
143. Vyas P, Beno I, Xi Z, Kessler N, Kitayner M, Crothers D, et al. 29 Structural and binding properties of DNA response elements bound to p53 proteins and the role of spacer sequences in p53-DNA interactions. *Journal of biomolecular structure & dynamics*. 2015;33 Suppl 1:16-7.

144. Baldassarre A, Masotti A. Long non-coding RNAs and p53 regulation. *Int J Mol Sci.* 2012;13(12):16708-17.
145. Olson WK, Gorin AA, Lu XJ, Hock LM, Zhurkin VB. DNA sequence-dependent deformability deduced from protein-DNA crystal complexes. *Proceedings of the National Academy of Sciences of the United States of America.* 1998;95(19):11163-8.
146. Menendez D, Resnick MA, Haran T. Transactivation by low and high levels of human p53 reveals new physical rules of engagement and novel super-transactivation sequences. *Cell Cycle.* 2012;11(23):4287-8.
147. Siggers T, Chang AB, Teixeira A, Wong D, Williams KJ, Ahmed B, et al. Principles of dimer-specific gene regulation revealed by a comprehensive characterization of NF-kappaB family DNA binding. *Nature immunology.* 2012;13(1):95-102.
148. Gu G, Wang T, Yang Y, Xu X, Wang J. An improved SELEX-Seq strategy for characterizing DNA-binding specificity of transcription factor: NF-kappaB as an example. *PLoS One.* 2013;8(10):e76109.
149. Du W, Gao J, Wang T, Wang J. Single-nucleotide mutation matrix: a new model for predicting the NF-kappaB DNA binding sites. *PLoS One.* 2014;9(7):e101490.
150. Wong D, Teixeira A, Oikonomopoulos S, Humburg P, Lone IN, Saliba D, et al. Extensive characterization of NF-kappaB binding uncovers non-canonical motifs and advances the interpretation of genetic functional traits. *Genome Biol.* 2011;12(7):R70.
151. Epinat JC, Gilmore TD. Diverse agents act at multiple levels to inhibit the Rel/NF-kappaB signal transduction pathway. *Oncogene.* 1999;18(49):6896-909.
152. Ak P, Levine AJ. p53 and NF-kappaB: different strategies for responding to stress lead to a functional antagonism. *FASEB J.* 2010;24(10):3643-52.
153. Lowe JM, Menendez D, Bushel PR, Shatz M, Kirk EL, Troester MA, et al. p53 and NF-kappaB coregulate proinflammatory gene responses in human macrophages. *Cancer research.* 2014;74(8):2182-92.
154. Weisz L, Damalas A, Lontos M, Karakaidos P, Fontemaggi G, Maor-Aloni R, et al. Mutant p53 enhances nuclear factor kappaB activation by tumor necrosis factor alpha in cancer cells. *Cancer Res.* 2007;67(6):2396-401.
155. Di Minin G, Bellazzo A, Dal Ferro M, Chiaruttini G, Nuzzo S, Bicciato S, et al. Mutant p53 reprograms TNF signaling in cancer cells through interaction with the tumor suppressor DAB2IP. *Molecular cell.* 2014;56(5):617-29.

156. Dalmases A, Gonzalez I, Menendez S, Arpi O, Corominas JM, Servitja S, et al. Deficiency in p53 is required for doxorubicin induced transcriptional activation of NF-small ka, CyrillicB target genes in human breast cancer. *Oncotarget*. 2014;5(1):196-210.
157. Dey A, Wong ET, Bist P, Tergaonkar V, Lane DP. Nutlin-3 inhibits the NFkappaB pathway in a p53-dependent manner: implications in lung cancer therapy. *Cell Cycle*. 2007;6(17):2178-85.
158. Dreyfus DH, Nagasawa M, Gelfand EW, Ghoda LY. Modulation of p53 activity by IkappaBalpha: evidence suggesting a common phylogeny between NF-kappaB and p53 transcription factors. *BMC Immunol*. 2005;6:12.
159. Bisio A, Zamborszky J, Zaccara S, Lion M, Tebaldi T, Sharma V, et al. Cooperative interactions between p53 and NFkappaB enhance cell plasticity. *Oncotarget*. 2014;5(23):12111-25.
160. Shatz M, Shats I, Menendez D, Resnick MA. p53 amplifies Toll-like receptor 5 response in human primary and cancer cells through interaction with multiple signal transduction pathways. *Oncotarget*. 2015;6(19):16963-80.
161. Pang B, Qiao X, Janssen L, Velds A, Groothuis T, Kerkhoven R, et al. Drug-induced histone eviction from open chromatin contributes to the chemotherapeutic effects of doxorubicin. *Nature communications*. 2013;4:1908.
162. Klajic J, Busato F, Edvardsen H, Touleimat N, Fleischer T, Bukholm I, et al. DNA methylation status of key cell-cycle regulators such as CDKNA2/p16 and CCNA1 correlates with treatment response to doxorubicin and 5-fluorouracil in locally advanced breast tumors. *Clin Cancer Res*. 2014;20(24):6357-66.
163. Hermsdorff HH, Mansego ML, Campion J, Milagro FI, Zulet MA, Martinez JA. TNF-alpha promoter methylation in peripheral white blood cells: relationship with circulating TNFalpha, truncal fat and n-6 PUFA intake in young women. *Cytokine*. 2013;64(1):265-71.
164. Dechend R, Hirano F, Lehmann K, Heissmeyer V, Ansieau S, Wulczyn FG, et al. The Bcl-3 oncoprotein acts as a bridging factor between NF-kappaB/Rel and nuclear co-regulators. *Oncogene*. 1999;18(22):3316-23.
165. Reed SM, Quelle DE. p53 Acetylation: Regulation and Consequences. *Cancers*. 2014;7(1):30-69.
166. Kimura A, Horikoshi M. Tip60 acetylates six lysines of a specific class in core histones in vitro. *Genes to cells : devoted to molecular & cellular mechanisms*. 1998;3(12):789-800.
167. Brady ME, Ozanne DM, Gaughan L, Waite I, Cook S, Neal DE, et al. Tip60 is a nuclear hormone receptor coactivator. *The Journal of biological chemistry*. 1999;274(25):17599-604.

168. Hlubek F, Lohberg C, Meiler J, Jung A, Kirchner T, Brabletz T. Tip60 is a cell-type-specific transcriptional regulator. *Journal of biochemistry*. 2001;129(4):635-41.
169. Sapountzi V, Logan IR, Robson CN. Cellular functions of TIP60. *The international journal of biochemistry & cell biology*. 2006;38(9):1496-509.
170. Xiao H, Chung J, Kao HY, Yang YC. Tip60 is a co-repressor for STAT3. *The Journal of biological chemistry*. 2003;278(13):11197-204.
171. Kim JW, Song PI, Jeong MH, An JH, Lee SY, Jang SM, et al. TIP60 represses transcriptional activity of p73beta via an MDM2-bridged ternary complex. *The Journal of biological chemistry*. 2008;283(29):20077-86.
172. Tang Y, Luo J, Zhang W, Gu W. Tip60-dependent acetylation of p53 modulates the decision between cell-cycle arrest and apoptosis. *Molecular cell*. 2006;24(6):827-39.
173. Sykes SM, Mellert HS, Holbert MA, Li K, Marmorstein R, Lane WS, et al. Acetylation of the p53 DNA-binding domain regulates apoptosis induction. *Molecular cell*. 2006;24(6):841-51.
174. Kim JW, Jang SM, Kim CH, An JH, Kang EJ, Choi KH. New molecular bridge between RelA/p65 and NF-kappaB target genes via histone acetyltransferase TIP60 cofactor. *The Journal of biological chemistry*. 2012;287(10):7780-91.
175. Kim CH, Kim JW, Jang SM, An JH, Seo SB, Choi KH. The chromodomain-containing histone acetyltransferase TIP60 acts as a code reader, recognizing the epigenetic codes for initiating transcription. *Bioscience, biotechnology, and biochemistry*. 2015;79(4):532-8.
176. Li X, Wu L, Corsa CA, Kunkel S, Dou Y. Two mammalian MOF complexes regulate transcription activation by distinct mechanisms. *Molecular cell*. 2009;36(2):290-301.
177. Dou Y, Milne TA, Tackett AJ, Smith ER, Fukuda A, Wysocka J, et al. Physical association and coordinate function of the H3 K4 methyltransferase MLL1 and the H4 K16 acetyltransferase MOF. *Cell*. 2005;121(6):873-85.
178. Kasper LH, Thomas MC, Zambetti GP, Brindle PK. Double null cells reveal that CBP and p300 are dispensable for p53 targets p21 and Mdm2 but variably required for target genes of other signaling pathways. *Cell Cycle*. 2011;10(2):212-21.
179. Lee CW, Ferreone JC, Ferreone AC, Arai M, Wright PE. Graded enhancement of p53 binding to CREB-binding protein (CBP) by multisite phosphorylation. *Proceedings of the National Academy of Sciences of the United States of America*. 2010;107(45):19290-5.
180. Saha S, Bhattacharjee P, Guha D, Kajal K, Khan P, Chakraborty S, et al. Sulphur alters NFkappaB-p300 cross-talk in favour of p53-p300 to induce apoptosis in non-small cell lung carcinoma. *Int J Oncol*. 2015;47(2):573-82.

181. Hong S, Dutta A, Laimins LA. The acetyltransferase Tip60 is a critical regulator of the differentiation-dependent amplification of human papillomaviruses. *Journal of virology*. 2015;89(8):4668-75.
182. Nagelkerke A, Sieuwerts AM, Bussink J, Sweep FC, Look MP, Foekens JA, et al. LAMP3 is involved in tamoxifen resistance in breast cancer cells through the modulation of autophagy. *Endocr Relat Cancer*. 2014;21(1):101-12.
183. Nagelkerke A, Mujcic H, Bussink J, Wouters BG, van Laarhoven HWM, Sweep FCGJ, et al. Hypoxic regulation and prognostic value of LAMP3 expression in breast cancer. *Cancer*. 2011;117(16):3670-81.
184. Oeckinghaus A, Hayden MS, Ghosh S. Crosstalk in NF- κ B signaling pathways. *Nat Immunol*. 2011;12(8):695-708.

Cooperative interactions between p53 and NFκB enhance cell plasticity

Alessandra Bisio¹, Judit Zámboorszky^{1,3}, Sara Zaccara¹, Mattia Lion^{1,4}, Toma Tebaldi², Vasundhara Sharma¹, Ivan Raimondi¹, Federica Alessandrini¹, Yari Ciribilli¹, Alberto Inga¹

¹Laboratory of Transcriptional Networks, Centre for Integrative Biology, CIBIO, University of Trento, Trento, 38123, Italy

²Laboratory of Translational Genomics, Centre for Integrative Biology, CIBIO, University of Trento, Trento, 38123, Italy

³Institute of Enzymology, Research Centre for Natural Sciences, Budapest, Hungary

⁴Department of Genetics, Massachusetts General Hospital, Boston, MA, USA

correspondence to:

Yari Ciribilli, **e-mail:** ciribilli@science.unitn.it

Alberto Inga, **e-mail:** inga@science.unitn.it

Keywords: p53, NFκB, chemotherapy, doxorubicin, TNFα, EMT, synergy, breast cancer

Received: June 25, 2014

Accepted: October 01, 2014

Published: October 21, 2014

ABSTRACT

The p53 and NFκB sequence-specific transcription factors play crucial roles in cell proliferation and survival with critical, even if typically opposite, effects on cancer progression. To investigate a possible crosstalk between p53 and NFκB driven by chemotherapy-induced responses in the context of an inflammatory microenvironment, we performed a proof of concept study using MCF7 cells. Transcriptome analyses upon single or combined treatments with doxorubicin (Doxo, 1.5μM) and the NFκB inducer TNF-alpha (TNFα, 5ng/ml) revealed 432 up-regulated (log₂ FC > 2), and 390 repressed genes (log₂ FC < -2) for the Doxo+TNFα treatment. 239 up-regulated and 161 repressed genes were synergistically regulated by the double treatment. Annotation and pathway analyses of Doxo+TNFα selectively up-regulated genes indicated strong enrichment for cell migration terms. A panel of genes was examined by qPCR coupled to p53 activation by Doxo, 5-Fluoruracil and Nutlin-3a, or to p53 or NFκB inhibition. Transcriptome data were confirmed for 12 of 15 selected genes and seven (PLK3, LAMP3, ETV7, UNC5B, NTN1, DUSP5, SNAI1) were synergistically up-regulated after Doxo+TNFα and dependent both on p53 and NFκB. Migration assays consistently showed an increase in motility for MCF7 cells upon Doxo+TNFα. A signature of 29 Doxo+TNFα highly synergistic genes exhibited prognostic value for luminal breast cancer patients, with adverse outcome correlating with higher relative expression. We propose that the crosstalk between p53 and NFκB can lead to the activation of specific gene expression programs that may impact on cancer phenotypes and potentially modify the efficacy of cancer therapy.

INTRODUCTION

Cancer cells are continuously exposed to a number of signaling cues that reflect the distinct nature of the microenvironment at primary tumor site, metastatic lesions and potentially also during circulation in the blood stream [1–4]. Therapeutic intervention strategies can result in acute changes in microenvironment signaling, acting also through non-transformed cellular components resident at the primary tumor site [3, 5]. Cellular responses

to changes in the microenvironment requires coordinated activation of sequence-specific transcription factors [6], among which NFκB and p53 have a prominent role and often opposing functions [7].

The p53 tumor suppressor gene is activated in response to a large number of cellular stress signals, including genotoxic stress, carbon and oxygen deficiencies, excessive proliferation signals [8, 9]. There are >150 established p53 target genes that link p53 to many different biological outcomes [10–14].

The NFκB family of sequence-specific transcription factors consists of essential regulators of immune, inflammatory, proliferative and apoptotic responses [15], and their activation generally results in the onset of pro-survival signals [16]. The most common form of the NFκB complexes is the p50/RELA (p65) heterodimer. p53 and NFκB activation occurs simultaneously in response to diverse stress conditions, including genotoxic stress and NFκB proteins are frequently de-regulated in cancer, resulting in constitutive activation [17]. Competition between p53 and NFκB for a common limiting cofactor such as p300 can result in mutual inhibition [17, 18]. However, examples of positive interactions have also been reported. For example, it was shown that p65 can induce the p53 target gene p21 by direct binding to its promoter [19] and participates in p53-dependent apoptosis [20]. Several human Toll-like receptors (TLRs), whose signaling leads to NFκB activation [21], were identified as direct p53 target genes both in cancer cells and primary cells [22] and it was demonstrated that p53 and NFκB can cooperate in the activation of pro-inflammatory genes in primary human monocytes and macrophages [23].

To investigate more globally the transcriptional crosstalk between p53 and NFκB we performed a proof of concept study using breast cancer-derived MCF7 cells treated with Doxorubicin, Tumor Necrosis Factor alpha (TNFα) and a combination of the two compounds (Doxo+TNFα). Our results demonstrated a synergistic interaction between p53 and NFκB transcription factors, which can lead to the reprogramming of cell fate and enhanced migratory potential. Seven genes (PLK3, LAMP3, ETV7, UNC5B, NTN1, DUSP5, SNAI1) were established as synergistically up-regulated after Doxo+TNFα and dependent both on p53 and NFκB. A 29-gene signature of highly synergistic genes up-regulated by Doxo+TNFα appeared to have prognostic value in a cohort of luminal breast cancer patients [24].

RESULTS

Striking transcriptome changes upon the combination of Doxorubicin and TNFα treatment of MCF7 cells

We first investigated the potential crosstalk between Doxorubicin (Doxo) and TNFα treatment using gene reporter assays in the human breast adenocarcinoma-derived MCF7 cells (Figure S1A). p53-dependent responsiveness of the P21 and MDM2 promoter plasmid constructs was observed following Doxo treatment and confirmed by p53 silencing. The transactivation of the P21 and MDM2 constructs was reduced upon addition of TNFα to Doxo, suggesting possible inhibition of p53 activity by NFκB. Mutual inhibition of the p53 and p65/RELA proteins has been previously shown on p21 [17], while both inhibition and cooperation were reported at the

BAX gene [18, 20]. However, this effect was not observed at the level of the endogenous P21 and MDM2 genes (Figure S1B), which showed similar level of activation in response to either Doxo alone or Doxo+TNFα. An NFκB reporter construct was responsive to both Doxo and TNFα as single treatments and showed a strong increase following the double treatment that was unaffected by p53 silencing. On the contrary, the endogenous TNFα and MCP1 NFκB target genes were weakly responsive to Doxo alone, highly induced by TNFα treatment, and showed intermediate induction levels upon double treatment. Hence, canonical p53 or NFκB target genes did not exhibit synergistic transcriptional responses to the combined treatment with doxorubicin and TNFα.

Next we performed a genome-wide transcriptome analysis after Doxo, TNFα, or the combination of the two compounds using the Agilent 4 × 44k array and single color labeling. Differentially expressed genes (DEGs) were selected based on rank product test, setting a threshold of 0.05 on the percentage of false positives (pfp) and a threshold of 2 on the absolute log₂ fold changes. The double treatment more than doubled the number of DEGs (Figure 1). The vast majority of DEGs resulting from the single treatments were also differentially expressed in the double treatment. Gene Ontology (GO) as well as pathway and upstream regulators analyses (DAVID, <http://david.abcc.ncifcrf.gov/>; IPA, <http://www.ingenuity.com/>) confirmed activation of p53 signaling upon Doxo treatment as most significant pathway, and apoptosis induction as the most significantly enriched GO terms among up-regulated DEGs (Figure 1A-C). TNFα treatment also resulted in gene annotation terms consistent with NFκB activation, such as regulation of T cell activation. The gene annotation of DEGs resulting from the double treatment was enriched for terms typical of the two single treatments (*e.g.* T cell activation and apoptosis regulation among the up-regulated DEGs). TP53 as an upstream regulator was less significant in the double treatment compared to the Doxo single treatment, while p65/RELA, NFKBIA, IRF7 and STAT1 appeared to be even more enriched in the double treatment compared to TNFα single treatment (Figure 1B). The double treatment not only led to a higher number of DEGs, but resulted in quantitative differences in gene expression levels compared to the single treatments. We applied a rigorous filter and identified 212 repressed, 361 induced DEGs that were synergistically regulated by the double treatment Doxo+TNFα (see Methods) (Figure 1D). Notably, this subgroup of up-regulated DEGs was enriched for cell migration GO biological process along with the expected canonical terms for p53 and NFκB. Collectively, our systematic analysis indicates a vast network of genes that can be mutually affected by combined activation of p53- and NFκB-dependent responses.

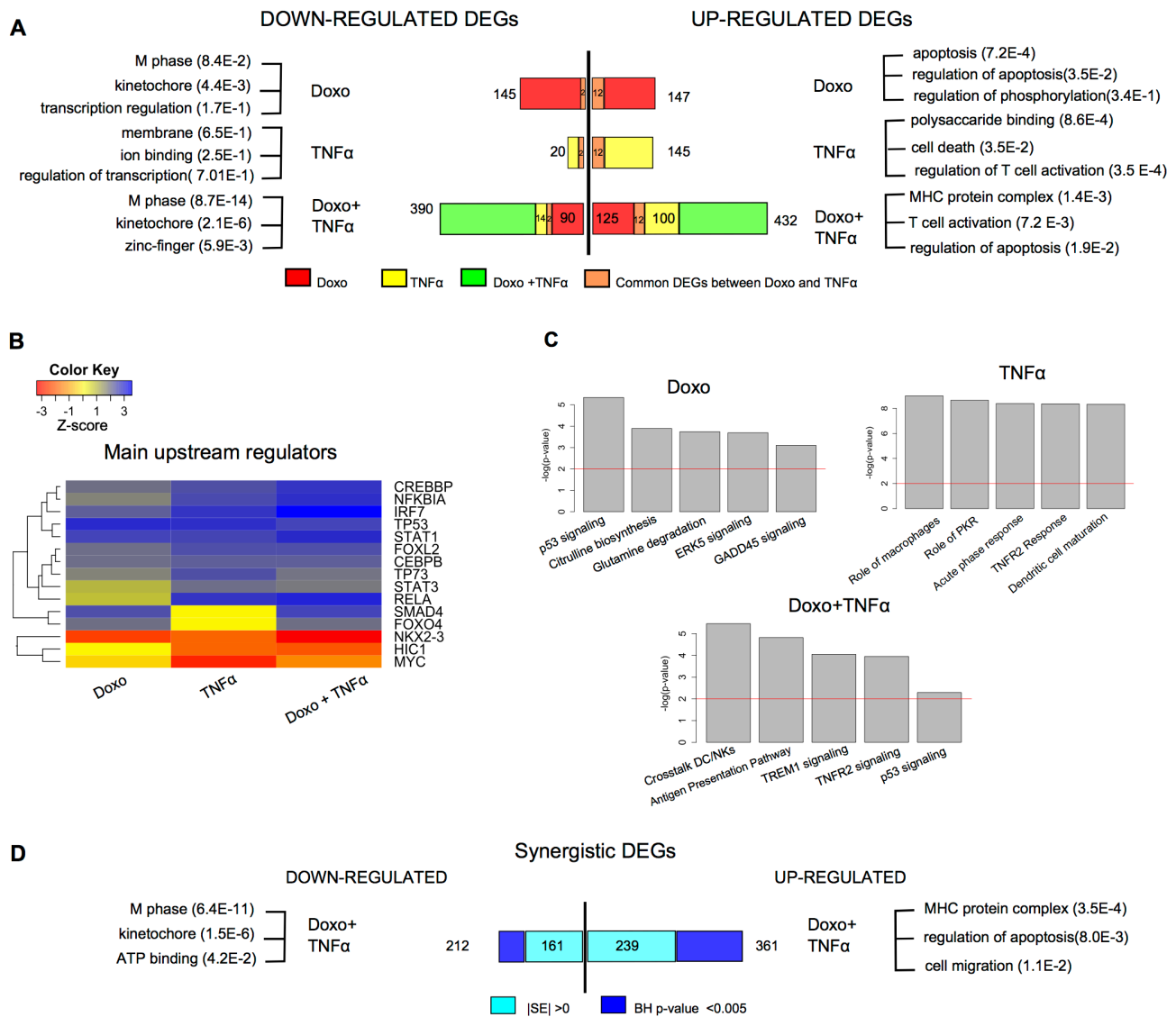


Figure 1: A vast array of genes responds selectively to Doxorubicin and TNF α in MCF7 cells. (A) Number of DEGs identified after single or combined treatment (see Methods for statistical filters). Most significant gene ontology terms of down- or up-regulated DEGs, according to DAVID (<http://david.abcc.ncifcrf.gov>). **(B)** Predicted upstream regulators of the DEGs for the indicated treatments, according to IPA (IPA, <http://www.ingenuity.com>). The color code reflects the enrichment or depletion of the listed transcription factors targeting the DEGs from the array analysis. **(C)** Statistically relevant pathways predicted to be modulated in response to the indicated treatments according to IPA. **(D)** Number of DEGs that are synergistically regulated by the double treatment according to two different statistical filters (see Materials and Methods). The most significant gene ontology terms are also indicated.

Doxorubicin + TNF α transcriptional synergy identifies new direct p53 and NF κ B target genes

We selected fifteen genes for validation experiments based on (a) statistical analysis of synergistic up-regulated DEGs, (b) prior knowledge on direct regulation by either p53 or NF κ B, (c) availability of ChIP-seq data for both transcription factors, and (d) gene functions in relation to cancer biology. The selected list contains genes encoding players of the control of various cellular processes, e.g. cell proliferation (PLK3, DUSP5, PLAU, GBX2,

ETV7, EDN2), apoptosis (TNFRSF10B, UNC5B), inflammation (LAMP3, EGR2), development (GBX2, SOX9, NPPC, FOXC1) and cell migration (SNAI1, PLAU, UNC5B, NTN1, EDN2).

For twelve of the 15 genes we confirmed a synergistic response to the Doxo+TNF α treatment by qPCR (Figure 2A). Most of them were independently reported as putative targets of either p53, p65 or both according to published ChIP-seq data (for p65, <http://genome.ucsc.edu/ENCODE>) [14, 25]. A potential direct contribution of NF κ B on the observed gene expression

changes was evaluated using the small molecule inhibitor BAY 11-7082 (BAY) used as single agent or in combination with Doxo or/and TNF α (Figure 2B). Eight of the twelve validated synergistic DEGs were tested and for five of them BAY markedly inhibited the effect of Doxo+TNF α , or of TNF α alone. TNF α treatment led to higher levels of nuclear p65, while Doxo alone or in the combined treatment did not significantly impact p65 nuclear protein levels. BAY treatment led to a slight reduction of p65 nuclear levels, which was paralleled by an increase in the cytoplasm (Figure 2C). p53 protein levels were induced to similar levels by the different treatment combinations (Figure S2).

The five genes that showed more convincing p65 dependence on the synergistic response to Doxo+TNF α (PLK3, NTN1, UNC5B, ETV7, LAMP3) were investigated more deeply to establish a direct role of wild type p53 in their transcription. MCF7 cells were treated with the chemotherapeutic agent 5-Fluorouracil (5FU) or with the MDM2 inhibitor Nutlin-3a, alone or in combination with TNF α . Both p53-inducing molecules were at least additive with TNF α in the responsiveness of the five genes (Figure 2D). Although the magnitude of the synergistic response was higher with Doxo, the fact that three different p53-activating treatments led

to up-regulation of these five genes strongly suggested a direct role of p53. We next employed an MCF7 clone with stable knock-down of p53 and the HCT116 p53^{-/-} cell line, to further establish p53-dependence of the five genes expression upon Doxo treatment. Matched MCF7 vector and HCT116 p53^{+/+} were used as a comparison (Figure 2E, F). Invariably, Doxo responsiveness was strongly reduced in the p53-defective cells. Previous reports in the literature demonstrated or suggested p53-dependent regulation of PLK3, NTN1 and UNC5B. Our results confirm those findings and establish, for the first time, the possibility of synergistic regulation by NF κ B. PLK3, a polo-like kinase, is an important regulator of the cell cycle and it is involved in the control of hypoxia signaling pathway [26]. NTN1 is ligand for both DCC1 and UNC5B receptors whose signaling can potentially modulate p53 activity, impacting on the decision between cell survival and cell death [27]. LAMP3 is a lysosomal membrane associated protein important in dendritic cells and potentially involved in tumor invasion [28], while ETV7 is a transcription factor associated to cell proliferation and tumorigenesis [29].

Given the lack of definitive evidence for LAMP3 and ETV7 being direct p53 targets and since our finding of synergistic responsiveness, we examined p53 and

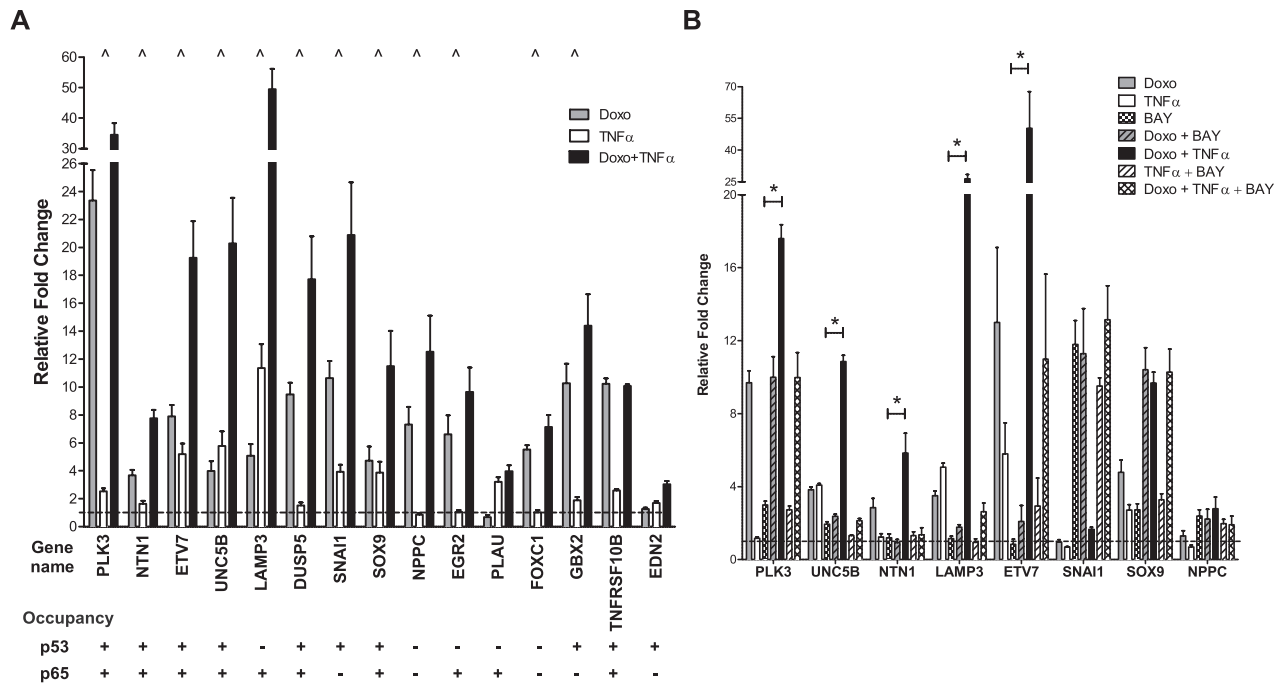


Figure 2: p53- and p65-dependent up-regulation of selected synergistic DEGs. (A) Twelve out of fifteen selected synergistic DEGs were validated by qPCR. Plotted are the average fold change relative to the mock condition and three reference genes (GAPDH, B2M, ACTB) and the standard deviations of three biological replicates. “^” marks genes responding in synergistic manner to the double treatment. p53 and p65 occupancy data from available ChIP-seq datasets are summarized below each gene name. (B) Impact of the NF κ B inhibitor BAY 11-7082 on the synergistic gene expression response plotted as in panel A. “*” Significant inhibition of by BAY when combined to Doxo + TNF α (t-test, p<0.01). NPPC and SNAI1 were also tested but their expression levels were not affected by BAY treatment.

(Continued)

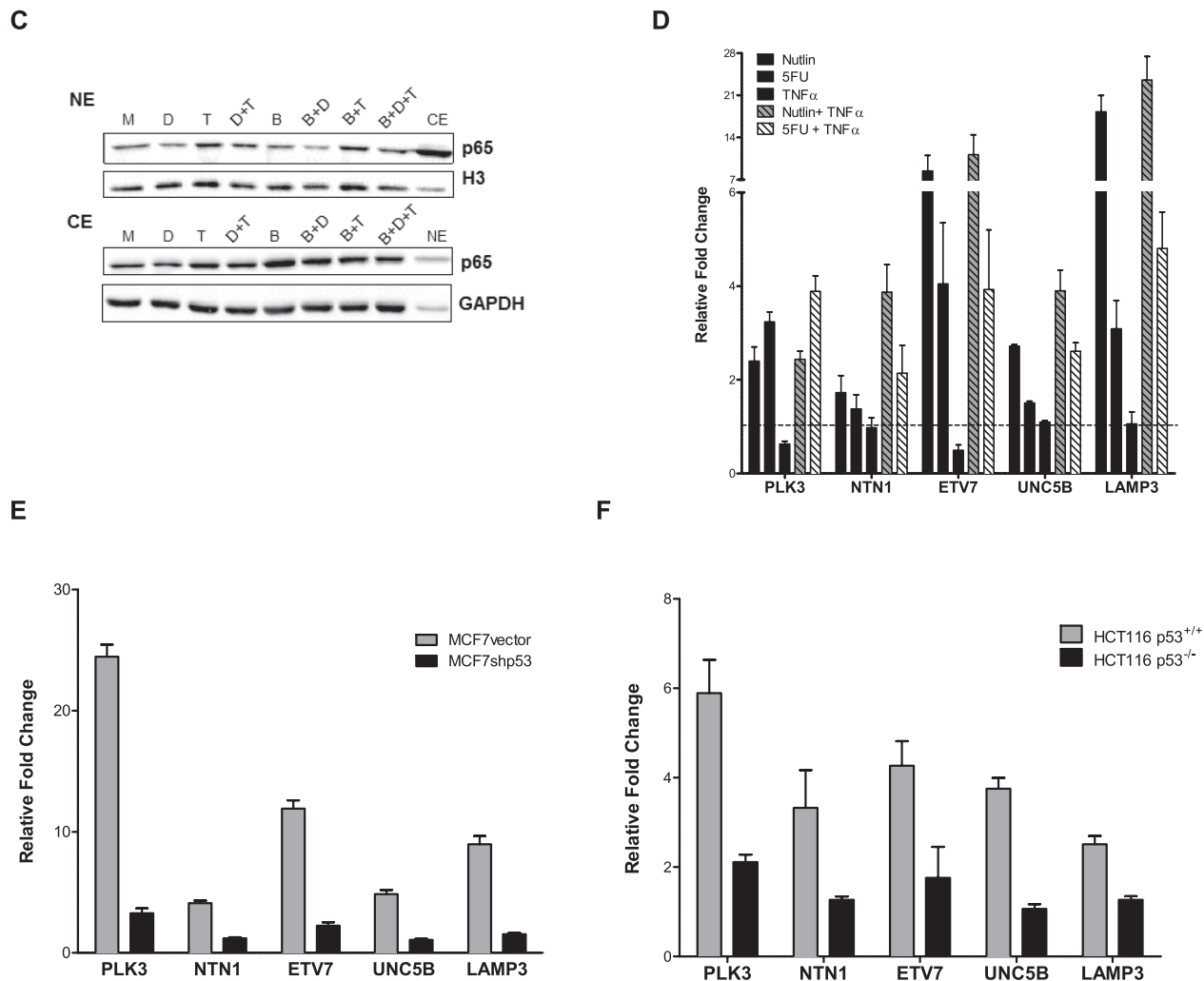


Figure 2: (C) p65 nuclear (NE) and cytoplasmic (CE) relative protein levels under the different treatments used in panel B. M = mock; D = Doxo; T = TNF α ; B = BAY. Proteins were fractionated as described in Materials and Methods. GAPDH and histone 3 (H3) served as controls for cytoplasmic and nuclear fraction respectively. As controls, a cytoplasmic mock fraction sample (CE) is loaded together with the nuclear proteins and vice versa a nuclear mock sample (NE) is included in the cytoplasmic blot. (D) 5-fluorouracil and Nutlin-3a induced expression of 5 selected DEGs alone or in combination with TNF α . Results were obtained and are plotted as in A. (E), (F) The relative expression of the 5 selected genes shown in panel C was tested in doxorubicin treated matched cell lines differing for p53 status (MCF7 vector and shp53, D; HCT116 p53^{+/+} and p53^{-/-}, E).

p65 occupancy in MCF7 cells treated with Doxo or TNF α (Figure 3). p53 occupancy was detected both for ETV7 and LAMP3 as well as for the positive control P21, in Doxo treated cells. For ETV7 p53 occupancy appeared to increase also after TNF α treatment. P21 was the only target for which p53 appeared to be bound also in the mock condition, a result consistent with previous data [30]. p53 occupancy levels were not distinguishable between Doxo and Doxo+TNF α treatment.

Both LAMP3 and ETV7 exhibited p65 occupancy in TNF α treated cells, although to a lower extent compared to the positive control MCP1. For the three promoter regions, occupancy was increased also by Doxo treatment alone, but no additive effect of the double treatment was

apparent, except for a trend with LAMP3. On the contrary lower occupancy at MCP1 was detected in double treated cells. This latter result is consistent with the MCP1 mRNA expression changes (Figure S1B).

Hence, we identified genes whose expression is co-regulated by Doxo and TNF α . The gene expression studies conducted with different p53-activating molecules, the use of cells lines with different p53 status, and the chromatin immune-precipitation studies collectively established a direct role for p53 and p65 on the transcriptional regulation of PLK3, NTN1, ETV7, UNC5B and LAMP3. However, we did not find a direct correlation between occupancy levels at predicted promoter binding sites and gene expression changes.

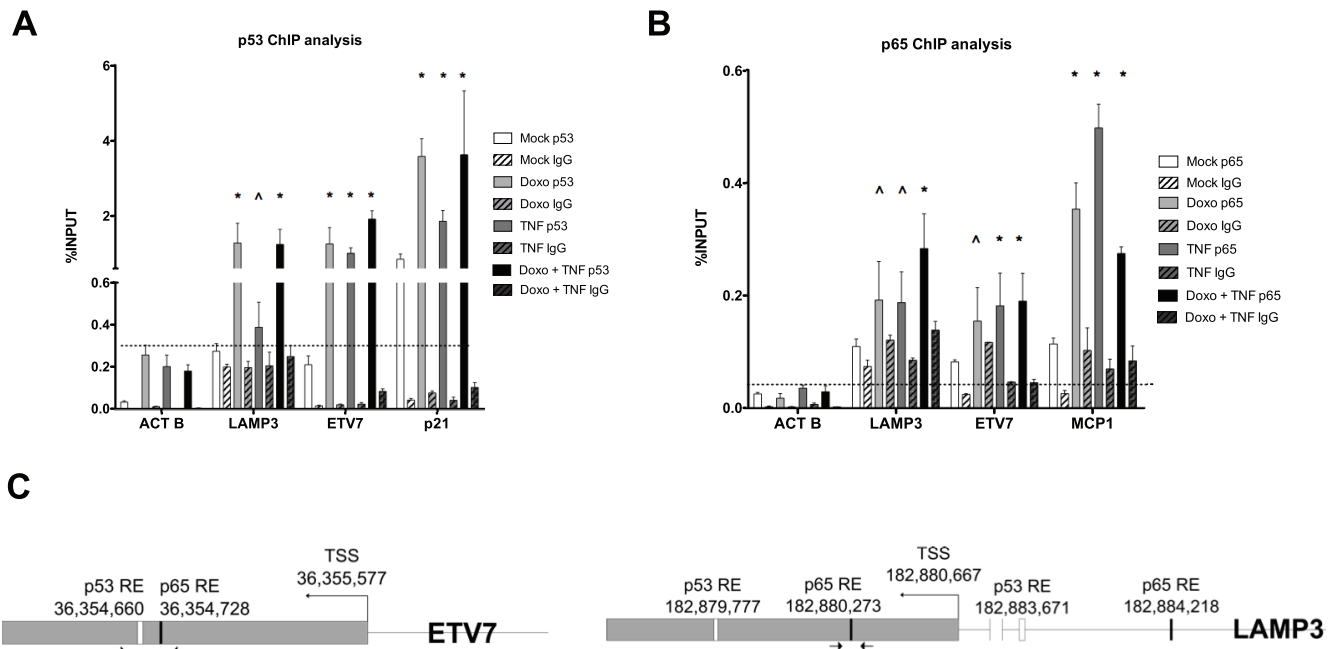


Figure 3: Occupancy analysis establishes ETV7 and LAMP3 as direct p65 and/or p53 target genes. (A) Relative quantification of immune-precipitated gene fractions by qPCR from MCF7 cells subjected to Doxo or TNF α single treatments and to the double treatment. The antibodies used for the immune-precipitations are listed. P21 was used as positive control, while ACTB was used as a negative control. Plotted are the average percentages relative to input signals. Error bars represent the standard errors of at least three biological replicates. (B) as in A, but probing p65 occupancy. MCP1 was used as positive control. The IgG antibody controls were anti-mouse (A) or anti-rabbit (B) to match the specific primary antibodies. (C) The position of the primers used for the qPCR and the location of predicted p53 and p65 binding sites in the ETV7 and LAMP3 genes are depicted.

Doxorubicin + TNF α treatment enhances the migration potential of MCF7 cells

Both the gene ontology enrichments of synergistic DEGs and the known function of the fifteen genes chosen for validation suggested the possible activation of gene expression programs influencing cell motility, epithelial mesenchymal transition (EMT) or even stem-like phenotypes. Projected to an *in vivo* context, the crosstalk of signals present in an inflammatory microenvironment could have a negative impact on the efficacy of chemotherapy, possibly by enhancing tumor cell plasticity. To begin exploring this hypothesis, we investigated migration and invasion potential of MCF7 cells treated with Doxo, TNF α or both. Three different experimental approaches consisting in real-time cell migration analysis (Figure 4A), transwell migration test (Figure 4B) and wound healing assay (Figure 4D) consistently showed higher migration potential of double-treated MCF7 cells, while the invasion phenotype was unaffected by all three types of treatment (Figure 4C).

Several studies suggest that EMT not only enhances the motility and invasiveness of cancer cells, but also provides additional aggressive features such as stemness and therapeutic resistance [31]. Indeed, several of the 15 synergistic DEGs we validated are directly or indirectly

associated with acquisition of stem-like phenotypes in normal or cancer cells, particularly SNAI1 [32, 33], SOX9 [34] and GBX2 [35]. Different lines of evidence indicate that breast cancer stem cells (BCSCs) display increased cell motility, invasion, and overexpress genes that promote metastasis [36] and can be traced by CD44⁺/CD24^{-low} surface marker expression [37]. We asked if the Doxo+TNF α treatment could enhance the stem-like subpopulation of the MCF7 cell line (Figure 4E). FACS analysis showed that the CD44⁺/CD24⁻ subpopulation virtually disappeared after all treatments. Therefore, the higher motility observed upon double treatment cannot be directly related to the expression of these surface markers, hence to putative stem-like features.

Prognostic value of Doxorubicin + TNF α synergistic DEGs

Since luminal type breast cancer, of which MCF7 is considered as a model, frequently retains wild type p53 and NF κ B responsiveness, we asked if Doxo+TNF α synergistic DEGs could be endowed with prognostic significance. Up-regulated DEGs were further filtered by selecting genes that were strongly responsive to the double treatment but minimally responsive to the single ones (see Materials and Methods). A signature list of

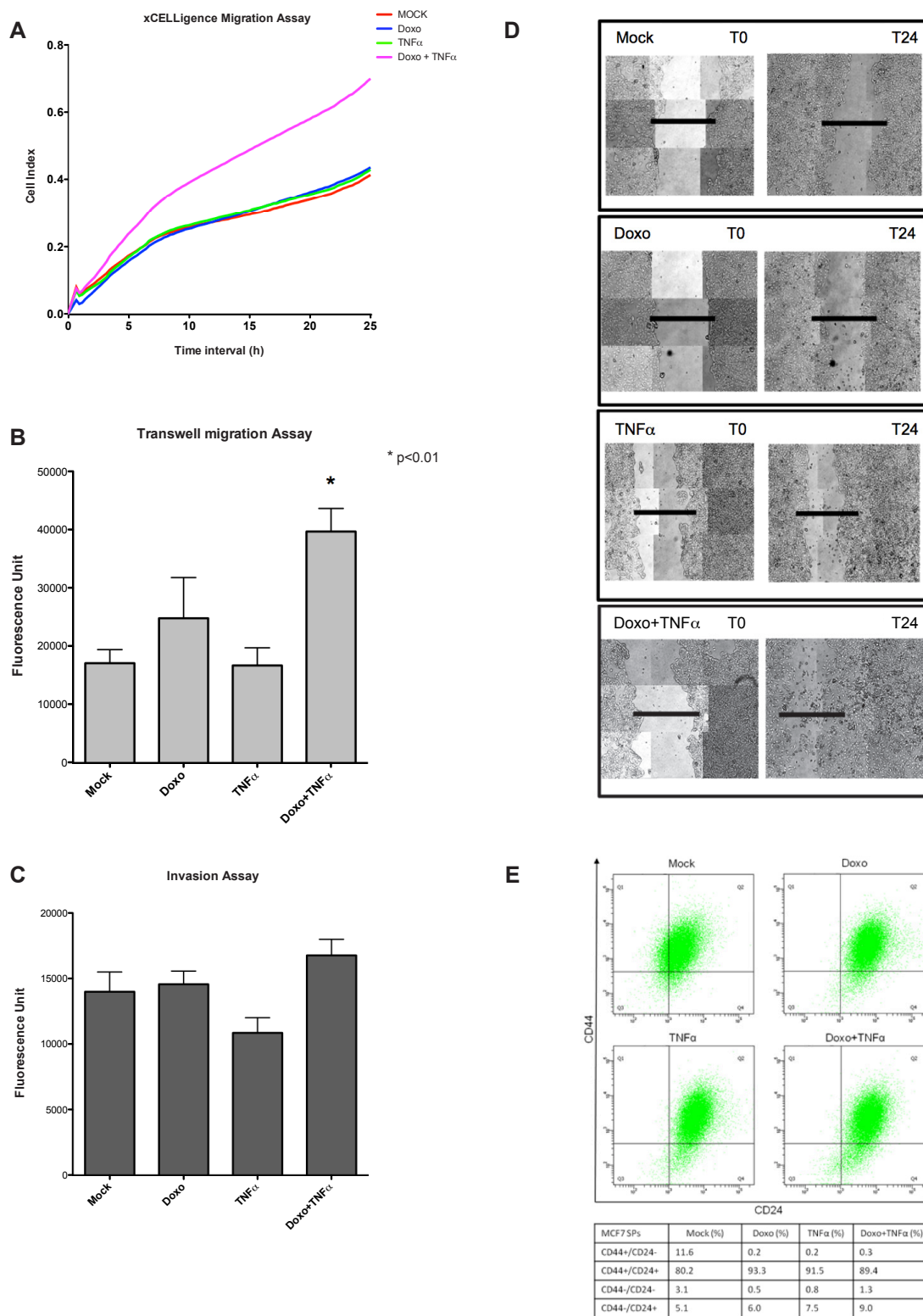


Figure 4: Doxo+TNF α leads to enhanced MCF7 motility but ablates the stem-like side population. (A) Real-time migration assays examined by xCELLigence. Plotted are the average results of four biological repeats. Cell Index is proportional to the number of cells migrating through a hole in the culture plate. The treatments relative to the different curves are indicated. (B) Relative transwell migration values quantified by a fluorescence readout (see Materials and Methods). Average and standard deviation of triplicate biological replicates are presented. The applied treatments are listed on the x-axis. (C) As for B, but measuring the invasion potential of MCF7. (D) Images of a wound healing assay obtained at T0 or T24. Composite (3 \times 3) images were acquired using an automated Zeiss microscope and the AxioVision3.1 software. (E) Cell sorting results based on intensity of CD44 and CD24 surface markers on 30000 cells. Q1 individuates the CD44⁺/CD24^(low) cells, considered as stem-like. The percentages in the four quadrants after the various treatments are presented in the table.

29 genes (DT29) was generated (Figure 5A) and used to interrogate clinical data using the KM plotter tool [38]. Interestingly, breast cancer patients with luminal type A diagnosis who underwent chemotherapy and exhibited higher relative expression of DT29 genes showed poorer prognosis (Figure 5B). The same was true for luminal A patients with lymph node infiltration or luminal A grade 2 (Figure 5C, D).

Analysis of Doxorubicin and TNF α crosstalk in lung cancer-derived and HUVEC cells

We extended our analysis to another pair of cancer cell lines that differ for p53 status. A549 (p53 wild type) and H1299 (p53 null) lung cancer derived cells were treated with Doxo or/and TNF α or/and BAY. Expression of PLK3, NTN1, ETV7, UNC5B and LAMP3 was measured by qPCR (Figure 6A-E). The impact of the various treatments on p65 nuclear and cytoplasmic, p53 and p21 protein levels was also evaluated (Figure 6F, 6G). In the p53 null H1299 cells the relative expression changes of all the genes was invariably much lower compared to A549 cells. However, NTN1 was weakly TNF α inducible

and ETV7 was weakly Doxo+TNF α responsive. Instead in A459 cells NTN1, ETV7 and LAMP3 were synergistically up-regulated by Doxo+TNF α , while PLK3 and UNC5B were additive. The magnitude of induction upon Doxo was often one order of magnitude higher compared to TNF α alone. Transient transfection assays with the κ B luciferase reporter construct were performed using different concentrations of TNF α or BAY (Figure S3). Based on the results, 10ng/ml TNF α and/or 20 μ M BAY were chosen for the qPCR experiments, although the reduction of TNF α -induced reporter activity was modest, albeit significant. At the endogenous gene level in A549 cells we did not observe the inhibitory effect of BAY on either TNF α -induced changes or Doxo+TNF α , with the possible exception of UNC5B (Figure 6A-E). However, BAY treatment reduced the Doxo responsiveness of these genes, which might be dependent on its effect on the activation of NF κ B by endogenous production of TNF α . In the p53 wild type A549 cells, p53 and p21 protein levels were induced by Doxo and not affected by the treatment with TNF α . Total p65 levels were unaffected by all treatments in both cell lines (Figure 6F). Nuclear p65 protein levels were increased in response to TNF α or

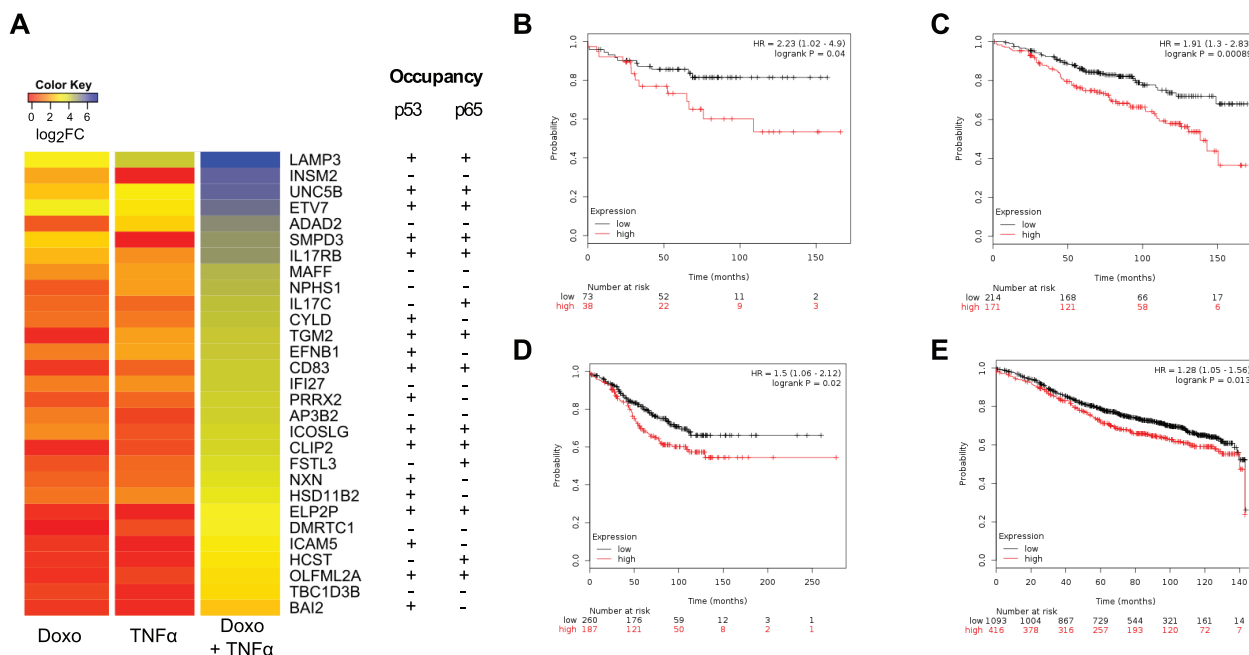


Figure 5: Prognostic significance of a 29-gene list of synergistic Doxo+TNF α DEGs. (A) Top list of 29 genes (DT-29) exhibiting minimal responsiveness to Doxo or TNF α as single agents, but strong synergy upon combined treatment. A heat map view of the gene expression results is presented (see Materials Methods for statistical filters). Occupancy of both for p65 and p53 in the vicinity of the transcription start sites of these genes has been summarized from ChIP-seq data available in the literature. (B-E) Kaplan-Meier plots stratifying a breast cancer patient cohort based on the relative expression of the DT-29 gene list and relapse free survival. Graphs were generated with the KM-plotter tool (ref). Patients' numbers are listed below the graph. Hazardous Ratio and the statistical analysis is reported for selected patients subgroups: (B) luminal A patients who underwent chemotherapy treatment (n = 111); (C) luminal A patients with a Grade 2 cancer at diagnosis (n = 385); (D) luminal A patients with lymph node infiltration at diagnosis (n = 447) and (E) the entire cohort of luminal A patients (n = 1509). Patients with a diagnosis of Luminal A breast cancer subtype were selected as the p53 status is not available in KM plotter, but this subgroup of breast cancer is expected to be strongly enriched for cases retaining wild type p53 protein.

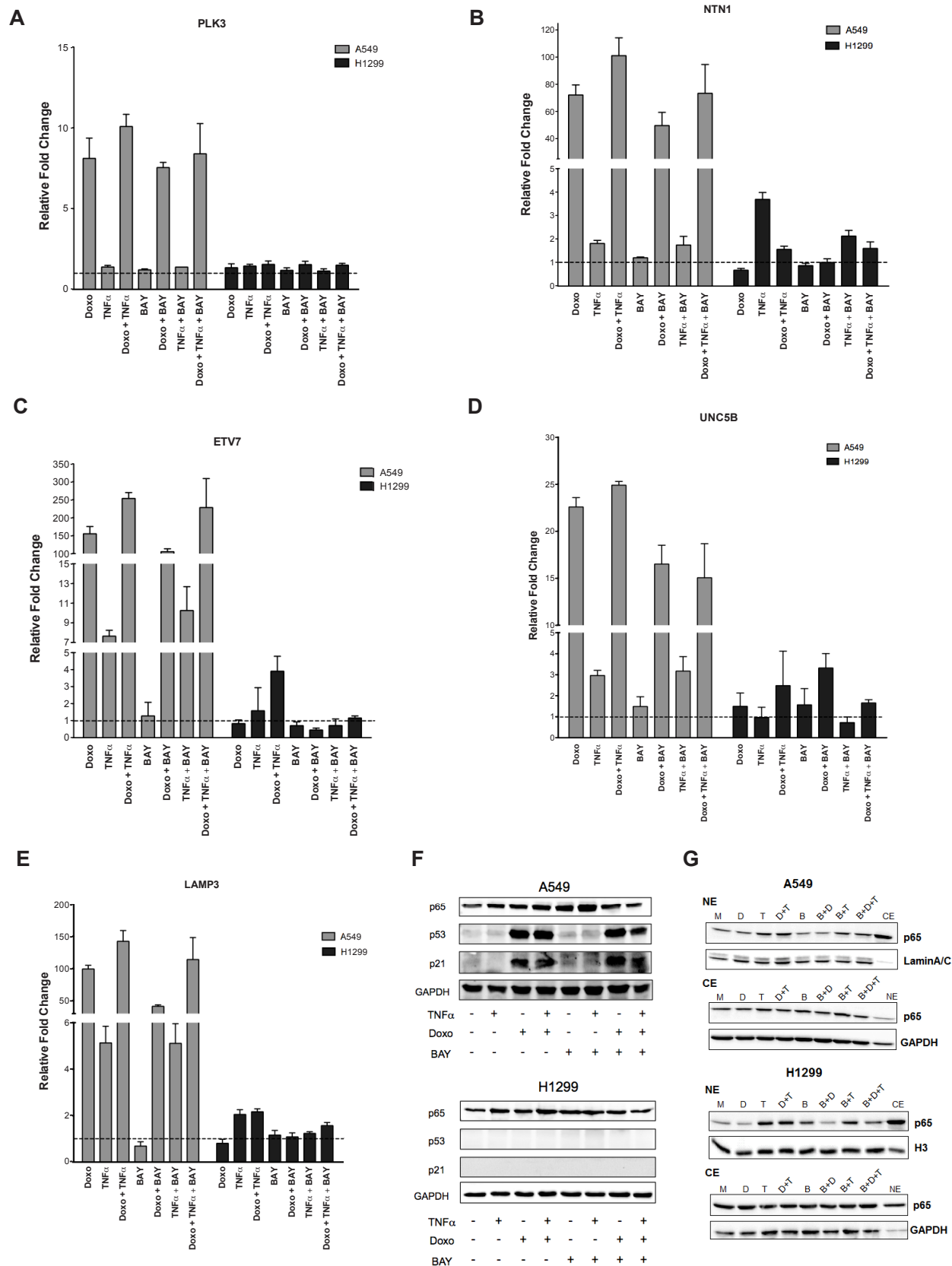


Figure 6: PLK3, NTN1, ETV7, UNC5B and LAMP3 responsiveness in lung cancer cell lines. (A-E) Relative fold change expression of the indicated genes and after the listed treatments in A549 (p53 wild type) and H1299 (p53 null) cells, measured by qPCR. Average and standard deviations of three biological replicates are presented. **(F)** Western blot of total p65, p53 and the p53 target p21. GAPDH was used as loading control. **(G)** Western blot of nuclear and cytoplasmic protein fractions were performed as for Figure 2C.

Doxo+TNF α in both A549 and H1299 cells (Figure 6G). Interestingly, BAY treatment alone or in combination led to a reduction in p65 nuclear accumulation (Figure 6G).

HUVEC primary cells were also subjected to Doxo and TNF α single or double treatment and the expression of the same panel of five genes was tested by qPCR (Figure S4). Results among biological repeats varied, but in the majority of tests, all genes with the exception of LAMP3 were Doxo responsive; NTN1 and ETV7 were also TNF α responsive. No synergistic up-regulation by the double treatment could be consistently established. p53 and p65 protein levels confirmed i) the activation of p53, with a similar level of p53 protein in the double treatment, and ii) the p65 proficiency of this cell line.

DISCUSSION

Wild type p53 functions are intricately related to multiple tumor suppressor pathways, primarily acting in cell autonomous manner to restrain cell proliferation and including cell death and senescence in response to genotoxic and many other types of cellular stresses [8, 9]. Furthermore, p53 also contributes to modulate the microenvironment in a non-cell autonomous manner [39]. p53 has also been linked to inhibition of EMT, for example through an indirect stimulation of E-cadherin expression [40]. At the same time, paracrine signaling in mice triggered by Doxorubicin were found to stimulate EMT and metastatic potential of cancer cells, in part through NF κ B activation [3]. Many studies have highlighted the potential contribution of NF κ B-induced signaling in the acquisition of cancer cell traits conducive to chemoresistance and higher metastasis risk [2] [41]. While, the canonical functions of p53 and NF κ B are consistent with the co-occurrence of p53 inactivation and NF κ B hyper-activation that is frequent in cancer [7], recent studies provided examples of positive cooperation between p53 and NF κ B that would occur in specific cell types, such as antigen presenting cells or macrophages, and contribute to physiological responses, such as for example in the process of innate immunity and inflammation [12, 22, 23, 42].

Here we modeled the impact of a first line chemotherapeutic drug leading to genotoxic stress and p53 activation, using exposure to the immune cytokine and NF κ B activator molecule TNF α as a variable, mimicking the effect of an inflammatory microenvironment. We used transcriptome analysis as primary endpoint and uncovered a vast network of differentially expressed genes that selectively responds to combined treatment with Doxorubicin and TNF α . Furthermore, genes that were synergistically up-regulated by both treatments appeared to endow cells with higher motility potential *in vitro*. Analyses of the annotated gene functions related to the aforementioned genes also revealed the possibility of an induced epithelial mesenchymal transition upon

combination of the treatments. For example, SNAI1 appeared to be regulated in more than additive manner by the double treatment, as well as LAMP3, a lysosomal protein previously associated with metastasis risk [28, 43]. Multiple cytokines and secreted factors, including IL6, IL17, IL15 and its receptor, S100A8 and S100A9, CXCL12 and several Serpins were also identified as synergistic DEGs (Table S1). The presence of S100A8, S100A9 and CXCL12 among synergistic DEGs raises the possibility that, unlike the case of the triple negative cell line MDA-MB-231 for which S100A8-mediated signaling appeared to require heterotypic cell interactions [3] contributing to metastasis potential, in MCF7 cells this signaling could become homotypic or even autocrine. A marked difference in secreted factors and associated signaling among MDA and MCF7 cells was elegantly shown in recent studies [4].

A direct contribution of p65/RELA and p53 in the observed gene expression changes elicited by Doxorubicin and TNF α was inferred for some of the synergistic DEGs by modulating pharmacologically or genetically p65 or p53 activities. However, we cannot exclude at this stage a (Doxo+TNF α)-dependent, but p53- or NF κ B- independent gene expression changes. For example, NF κ B can functionally interact with AP-1 [44–46] or ER [47], which in turn can modulate p53-dependent responses [48] [49] [50].

Among the most synergistic genes, 29 appear to be prognostic in luminal A breast cancer patients who underwent chemotherapy, where their higher expression correlated with adverse outcome. The majority of luminal A breast cancers are wild type for p53 [51], although data is not available to stratify patients for p53 status in the KM plotter tool [24]. Based on available ChIP-seq data [14, 25, 52, 53], 20 of these 29 genes are putative targets of either p53 or p65 and 10 of them are putative targets of both factors (Figure 5). This result raises the possibility of an unexpected negative outcome of chemotherapy in the context of an inflammatory microenvironment. The prognostic significance of this gene signature needs in-depth evaluation in independent patients cohorts. If confirmed, the results would further support the value of combining treatments activating p53 and repressing NF κ B [7].

Given that the crosstalk between Doxorubicin and TNF α and the interplay between p53 and NF κ B would occur in cells residing or infiltrating the tumor microenvironment, the ultimate *in vivo* outcome of these functional interactions may vary and cannot be directly predicted from our study using a pure culture of MCF7 cells *in vitro*. Here we have explored Doxo+TNF α impact on HUVEC cells and also on a p53 wild type lung adenocarcinoma-derived cancer cell line. Although limited by the number of genes tested, the results suggest that a positive crosstalk between Doxorubicin and TNF α can be a general characteristic of different cell types and is

at least in part p53-dependent, based on the results with a p53 null lung cancer cell line. Furthermore, while we have addressed here the functional interactions between two small molecules, cells are constantly exposed to a complex milieu of signaling factors. However, both p53 and NFκB are master regulators, often contributing a dominant trait in gene expression changes to their target genes. Nuclear receptors, including Estrogen Receptors (ERs) can also modulate NFκB as well as p53 functions [54–56] and have critical roles in breast cancer etiology. We also explored the impact of ER function in the transcriptional programs responding to Doxorubicin and TNFα exposure, using estrogen-depleted culture conditions and adding 17β-estradiol (10⁻⁹M, E2) as variable (Table S2 and GSE24065). However, the combination of E2 to Doxo and TNFα resulted only in 15 and 11 selective up- and down-regulated DEGs, respectively (Table S3). A hierarchical cluster analysis of all the treatments confirmed graphically the large difference between TNFα- and Doxo-induced transcriptomes and also the significant impact of TNFα when combined to Doxo, while E2 had a minor effect both in the combination with Doxo and with Doxo + TNFα (Figure S5).

With this study we established an example of positive cooperation between p53 and NFκB, in the context of the responses of an epithelial cancer cell to standard chemotherapy but in the presence of active signaling by a pleiotropic inflammatory cytokine, such as TNFα. A signature gene of the consequent transcriptional reprogramming appears to be prognostic in breast cancer patients. Associated gene functions indicate the potential acquisition of enhanced cell plasticity and motility and provide a rationale to investigating mechanisms resulting in acquired chemoresistance, particularly for luminal A breast cancer, but potentially with general implication for p53 wild type tumors of different tissue types, and for overcoming such resistance by targeting NFκB. The unexpected positive crosstalk between p53 and NFκB emerging from our and other very recent studies [23] may represent an evolutionary consequence of anti-viral and infection responses towards which NFκB is an established master regulator [57], but the p53 and p73 family member are emerging as important/critical contributors [42, 58, 59].

MATERIALS AND METHODS

Cell lines and culture conditions

MCF7 (p53 wild type, expressing p65 and positive for ERs) and HUVEC (Human Umbilical Vein Endothelial Cells) cells were obtained from ICLC (Genoa, Italy), while A549 from ATCC (Manassas, VA, USA). H1299 cells were a gift of Dr. Resnick's laboratory (NIEHS, NIH, RTP, NC, USA); HCT116 p53^{+/+} and p53^{-/-} of Dr. Vogelstein's (John Hopkins Kimmel Cancer Center, Baltimore, MD, USA).

MCF7-shp53 or control MCF7-vector cells were provided by Dr. Agami (Netherlands Cancer Institute, Amsterdam, The Netherlands). Cells were cultured in DMEM or RPMI media supplemented with 10% FBS, or Medium 199 (Lonza Milan, Italy) supplemented with 50 units/ml Low Serum Growth Supplements (Life Technologies, Milan, Italy) in the case of HUVEC cells that were also cultured on 0.1% gelatin pre-coated plastics. Media were supplemented by 2mM L-Glutamine and 1X Penicillin/Streptomycin mixture (Pen/Strep), and Puromycin (0.5 μg/ml) in the case of MCF7-shp53 and -vector cells. When appropriate, cells were maintained in DMEM without Phenol Red (Lonza) supplemented with Charcoal/Dextran treated FBS (Hyclone, GE Healthcare, South Logan, UT, USA).

Drug treatments

Doxorubicin (Doxo, 1.5 μM), 5-Fluorouracil (5FU, 375 μM), Nutlin-3a (10 μM) were used to stabilize p53 protein. When needed TNFα (5ng/ml in MCF7 and 10ng/ml in H1299, A549 and HUVEC cells –based on dose-response tests with gene reporter assays) or BAY11-7082 (10μM or 20μM in H1299 and A549) were added to the culture medium. All compounds were from Sigma-Aldrich (Milan, Italy).

Microarray experiment and data analysis

Total RNA was extracted from 4 biological replicates using the Agilent Total RNA Isolation Mini Kit (Agilent Technologies, Santa Clara, CA, USA). Samples with RNA Integrity Number (RIN) above 9 (Agilent 2100 BioAnalyzer) were processed. Details are provided with the Gene Expression Omnibus (GEO) (www.ncbi.nlm.nih.gov/geo) submission (GSE24065) and in [56]. The output of Feature Extraction (Agilent standard protocol GE1_107_Sep09) was analyzed with the R software for statistical computing and the Bioconductor library of biostatistical packages. Probes with low signals were removed in order to filter out the unexpressed genes and keep only probes with acceptable signals in most of the replicates. Signal intensities across arrays were normalized by quantile normalization. Signal intensities from probes associated with the same gene were averaged. This procedure resulted in quantitative signals for 14095 HGNC genes. To identify potential target genes of Doxorubicin and TNFα, we compared the signals after the double treatment (Doxo+TNFα) and the two single treatments relative to the untreated control (mock). DEGs were selected applying a statistical test based on rank products implemented in RankProd Bioconductor package, setting a threshold of 0.05 on the percentage of false positives (pfp) and a threshold of 2 on the absolute log₂ fold changes [60]. Every treatment was compared to the mock condition (Table S1, S2 and Figure S5).

To select genes with synergistic effect, i.e. genes whose expression variations were more than additive in the double treatment with respect to single treatments, a further comparison between the double treatment samples and all the remaining samples (single treatments and control samples) was performed (double treatment vs all). Synergistic DEGs were selected applying an additional pfp filter ($pfp < 0.005$) derived from this comparison, to the list of DEGs resulting from the “double treatment vs mock” comparison. A more stringent criterion was obtained by calculating the synergistic effect (SE) of the double treatment as the observed difference between the fold change of the double treatment and the sum of the fold changes of the single treatments ($SE = \log_2 FC \text{ double treatment} - (\log_2 FC \text{ Doxorubicin} + \log_2 FC \text{ TNF}\alpha)$). We filtered genes with $SE > 0$ for up-regulated DEGs, $SE < 0$ for down-regulated genes (Figure 1). To select genes where the up-regulation contribution of each single treatment was low respect to the up-regulation of the double treatment, the ratio of the single/double treatments was calculated, applying a 0.25 filter on them ($FC \text{ Doxorubicin}/FC \text{ double treatment} < 0.25$ and $FC \text{ TNF}\alpha/FC \text{ double treatment} < 0.25$) (see Table S1, S2).

RNA isolation and quantitative qPCR

Total RNA was extracted using Qiagen RNeasy Kit (Qiagen). cDNA was converted from 1 μg of RNA using M-MuLV reverse transcriptase and RevertAid cDNA Synthesis kit (ThermoFisher, Milan, Italy). qPCR was performed on a Bio-Rad CFX384 (Bio-Rad, Milan, Italy). TaqMan gene expression assays (Applied Biosystems, Life Technologies) and Probe MasterMix (Kapa Biosystems, Resnova, Rome, Italy) were used starting with 25ng of cDNA as previously described [56, 61]. GAPDH, B2M or ACTB served as reference genes.

Western blot

Protein extraction and immunodetections were performed as previously described [62], using ECL Select detection reagent (GE Healthcare) and anti-p53 (DO-1) anti-RelA/p65 (C-20) anti-p21 (C19), anti-GAPDH (6C5) (Santa Cruz Biotechnology, Heidelberg, Germany). When appropriate, nuclear and cytoplasmic fractionation was performed. MCF7, A549 and H1299 cell lines were seeded on 100mm Petri dishes and treated at 80% confluence with Doxo, TNF α , BAY or the combination of the drugs for 16 hours. Cells were harvested and cytoplasmic and nuclear proteins were extracted using NE-PER Nuclear and Cytoplasmic Extraction Kit (Pierce, ThermoFisher Scientific), following the instructions provided by the manufacturer. 20 μg of nuclear and cytoplasmic extracts were loaded on a 12% poly-acrylamide gel and transferred to nitrocellulose membranes. Antibodies used for detection were: anti-Histone H3 (clone #: ab1791, AbCam, Milan,

Italy) and anti-Lamin A/C (clone #: 2032, Cell Signaling, Milan, Italy) used as nuclear loading control, and anti-GAPDH used as cytoplasmic loading control.

Chromatin immunoprecipitation assay

We used previously described protocols [63, 64]. The following antibodies were used: anti-p53 (DO-1), anti-p65 (C-20) and IgG (sc-2025 or sc-2027) (Santa Cruz Biotechnology). ChIP-qPCR experiments were performed using Sybr MasterMix (Kapa Biosystems) and 2 μl of enriched DNA. Results were analyzed by the comparative Ct method (ΔCt) and normalized as % of input. Regions in the promoter of GAPDH or ACTB and p21 or MCP1 genes served as negative and positive controls, respectively. Primers were selected using Primer 3 (<http://primer3.ut.ee/>).

Migration and wound healing assays

The migration potential of MCF7 cells was monitored by a real-time technique using the xCELLigence Instrument (Acea Biosciences, Euroclone) and CIM-16 plates, following manufacturer's instructions. Prior to the analysis, cells were grown in estrogen-free medium for two days and left untreated (mock) or treated with Doxo, TNF α or the combination. 16 hours after the treatments, cells were detached and added to the top chamber in serum-free medium. Migration was detected every 10 minutes for 24 hours. We used 0.5% and 5% FBS as chemo-attractant. Migration and Invasion were also measured by QCM™ Fluor 24-Well Cell Migration and Cell Invasion kits (Merck-Millipore, Milan, Italy), according to manufacturer's instructions. For wound healing, cells were seeded in 12-well plates and treated with Doxo, TNF α or the combination. After 16 hours a scratch was introduced using a 10 μl pipette tip. Images of the same field were acquired immediately (T0) and after 24 hours (T24) using an automated Zeiss microscope and the AxioVision3.1 software in multidimensional mode with mosaic (3x3) acquisition.

Flow cytometry

MCF7 cells, seeded and treated as described above, were washed with PBS and harvested by 0.05% trypsin/0.025% EDTA. The cells were washed again with PBS containing 2% FBS before being subjected to antibody binding, a combination of fluorochrome-conjugated monoclonal antibodies against human CD44 (APC) and CD24 (FITC) or their respective isotype controls (BD Biosciences, Milan, Italy) and incubated on ice in the dark for 30 minutes. Cells were then washed twice with PBS/2% FBS and resuspended in PBS. Flow cytometry analysis was conducted using a FACSCanto II instrument (BD Biosciences).

ACKNOWLEDGEMENTS

We thank Dr. Valentina Adami (CIBIO High-throughput screening facility), Dr. Isabella Pesce (CIBIO Cell Separation facility), Ms. Sonia Leonardelli, Mr. Dennis Pedri for technical support. This work was supported by the Italian Association for Cancer Research, AIRC (IG grant # 12869 to AI). IR is supported by a Fellowship from the Pezcoller Foundation.

Competing interests

The authors declare no conflict of interest.

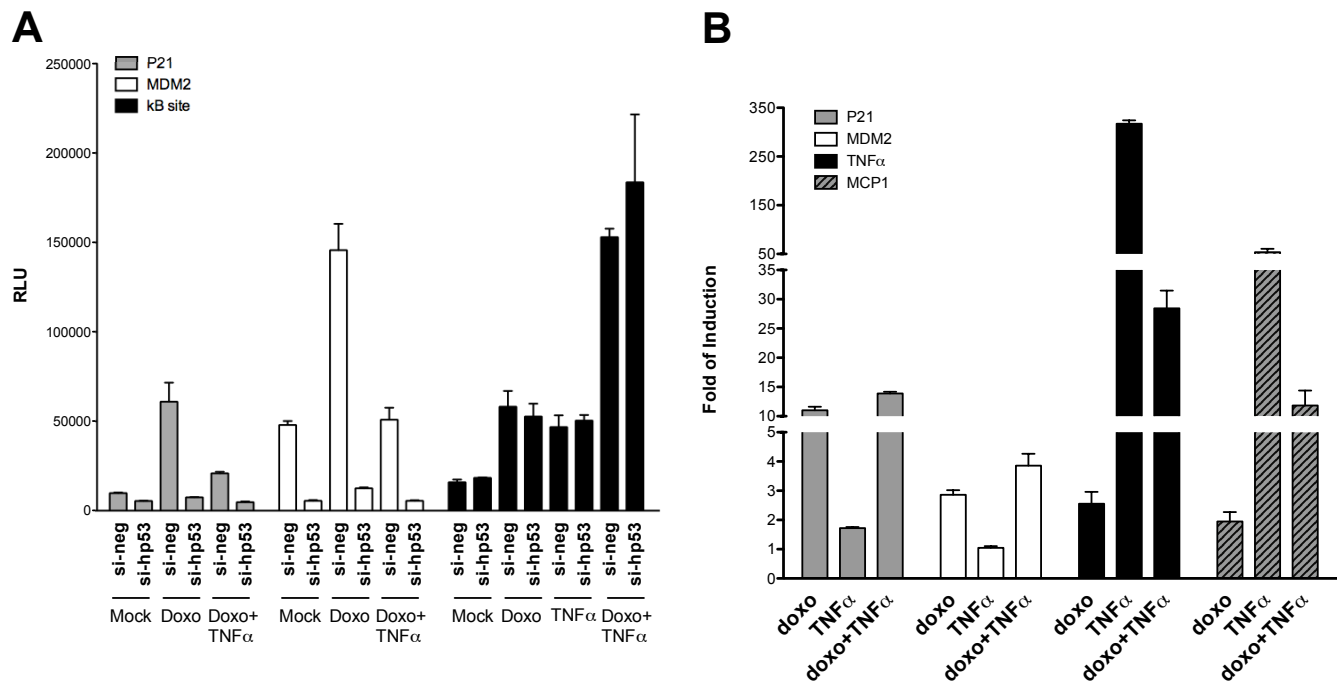
REFERENCES

1. Hanahan D, Weinberg RA. Hallmarks of cancer: the next generation. *Cell*. 2011; 144:646–674.
2. Labelle M, Begum S, Hynes RO. Direct signaling between platelets and cancer cells induces an epithelial-mesenchymal-like transition and promotes metastasis. *Cancer Cell*. 2011; 20:576–590.
3. Acharyya S, Oskarsson T, Vanharanta S, Malladi S, Kim J, Morris PG, Manova-Todorova K, Leversha M, Hogg N, Seshan VE, Norton L, Brogi E, Massague J. A CXCL1 paracrine network links cancer chemoresistance and metastasis. *Cell*. 2012; 150:165–178.
4. Kuznetsov HS, Marsh T, Markens BA, Castano Z, Greene-Colozzi A, Hay SA, Brown VE, Richardson AL, Signoretti S, Battinelli EM, Mc Allister SS. Identification of luminal breast cancers that establish a tumor-supportive macroenvironment defined by proangiogenic platelets and bone marrow-derived cells. *Cancer Discov*. 2012; 2:1150–1165.
5. Cooke VG, Le Bleu VS, Keskin D, Khan Z, O'Connell JT, Teng Y, Duncan MB, Xie L, Maeda G, Vong S, Sugimoto H, Rocha RM, Damascena A, Brentani RR, Kalluri R. Pericyte depletion results in hypoxia-associated epithelial-to-mesenchymal transition and metastasis mediated by met signaling pathway. *Cancer Cell*. 2012; 21:66–81.
6. Darnell JE Jr. Transcription factors as targets for cancer therapy. *Nat Rev Cancer*. 2002; 2:740–749.
7. Dey A, Tergaonkar V, Lane DP. Double-edged swords as cancer therapeutics: simultaneously targeting p53 and NF-kappaB pathways. *Nat Rev Drug Discov*. 2008; 7:1031–1040.
8. Vogelstein B, Lane D, Levine AJ. Surfing the p53 network. *Nature*. 2000; 408:307–310.
9. Vousden KH, Prives C. Blinded by the Light: The Growing Complexity of p53. *Cell*. 2009; 137:413–431.
10. Espinosa JM. Mechanisms of regulatory diversity within the p53 transcriptional network. *Oncogene*. 2008; 27:4013–4023.
11. Riley T, Sontag E, Chen P, Levine A. Transcriptional control of human p53-regulated genes. *Nat Rev Mol Cell Biol*. 2008; 9:402–412.
12. Vousden KH. Outcomes of p53 activation--spoilt for choice. *J Cell Sci*. 2006; 119(Pt 24):5015–5020.
13. Menendez D, Inga A, Resnick MA. The expanding universe of p53 targets. *Nat Rev Cancer*. 2009; 9:724–737.
14. Nikulenkov F, Spinnler C, Li H, Tonelli C, Shi Y, Turunen M, Kivioja T, Ignatiev I, Kel A, Taipale J, Selivanova G. Insights into p53 transcriptional function via genome-wide chromatin occupancy and gene expression analysis. *Cell Death Differ*. 2012.
15. Karin M. Nuclear factor-kappaB in cancer development and progression. *Nature*. 2006; 441:431–436.
16. Chen LF, Greene WC. Shaping the nuclear action of NF-kappaB. *Nat Rev Mol Cell Biol*. 2004; 5:392–401.
17. Webster GA, Perkins ND. Transcriptional cross talk between NF-kappaB and p53. *Mol Cell Biol*. 1999; 19:3485–3495.
18. Kawauchi K, Araki K, Tobiume K, Tanaka N. Activated p53 induces NF-kappaB DNA binding but suppresses its transcriptional activation. *Biochem Biophys Res Commun*. 2008; 372:137–141.
19. Ma S, Tang J, Feng J, Xu Y, Yu X, Deng Q, Lu Y. Induction of p21 by p65 in p53 null cells treated with Doxorubicin. *Biochim Biophys Acta*. 2008; 1783:935–940.
20. Ryan KM, Ernst MK, Rice NR, Vousden KH. Role of NF-kappaB in p53-mediated programmed cell death. *Nature*. 2000; 404:892–897.
21. Kawai T, Akira S. Signaling to NF-kappaB by Toll-like receptors. *Trends in molecular medicine*. 2007; 13:460–469.
22. Menendez D, Shatz M, Azzam K, Garantziotis S, Fessler MB, Resnick MA. The Toll-like receptor gene family is integrated into human DNA damage and p53 networks. *PLoS Genet*. 2011; 7:e1001360.
23. Lowe JM, Menendez D, Bushel PR, Shatz M, Kirk EL, Troester MA, Garantziotis S, Fessler MB, Resnick MA. p53 and NF-kappaB Coregulate Proinflammatory Gene Responses in Human Macrophages. *Cancer Res*. 2014; 74:2182–2192.
24. Györfy B, Lanczky A, Eklund AC, Denkert C, Budczies J, Li Q, Szallasi Z. An online survival analysis tool to rapidly assess the effect of 22,277 genes on breast cancer prognosis using microarray data of 1,809 patients. *Breast Cancer Res Treat*. 2010; 123:725–731.
25. Menendez D, Nguyen TA, Freudenberg JM, Mathew VJ, Anderson CW, Jothi R, Resnick MA. Diverse stresses dramatically alter genome-wide p53 binding and transactivation landscape in human cancer cells. *Nucleic Acids Res*. 2013; 41:7286–7301.
26. Xu D, Yao Y, Lu L, Costa M, Dai W. Plk3 functions as an essential component of the hypoxia regulatory pathway by direct phosphorylation of HIF-1alpha. *J Biol Chem*. 2010; 285:38944–38950.

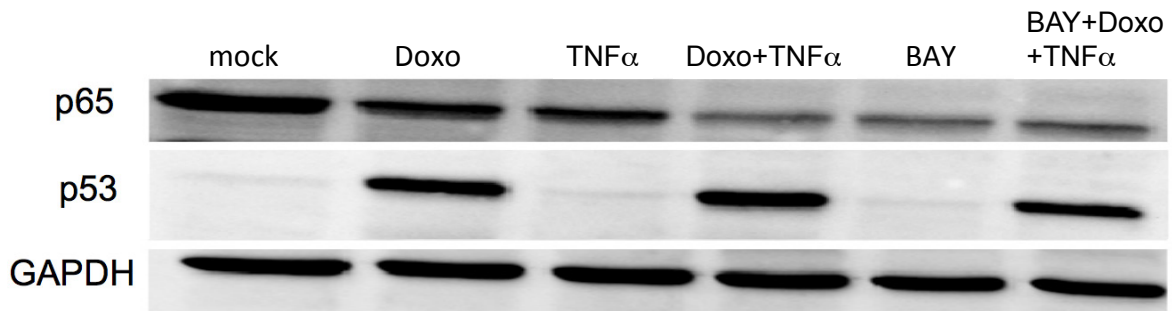
27. Arakawa H. Netrin-1 and its receptors in tumorigenesis. *Nat Rev Cancer*. 2004; 4:978–987.
28. Nagelkerke A, Bussink J, Mujcic H, Wouters BG, Lehmann S, Sweep FC, Span PN. Hypoxia stimulates migration of breast cancer cells via the PERK/ATF4/LAMP3-arm of the unfolded protein response. *Breast Cancer Res*. 2013; 15:R2.
29. Cardone M, Kandilci A, Carella C, Nilsson JA, Brennan JA, Sirma S, Ozbek U, Boyd K, Cleveland JL, Grosveld GC. The novel ETS factor TEL2 cooperates with Myc in B lymphomagenesis. *Mol Cell Biol*. 2005; 25:2395–2405.
30. Espinosa JM, Verdun RE, Emerson BM. 2003; p53 functions through stress- and promoter-specific recruitment of transcription initiation components before and after DNA damage. *Mol Cell*. :1015–1027.
31. Gupta PB, Chaffer CL, Weinberg RA. Cancer stem cells: mirage or reality? *Nat Med*. 2009; 15:1010–1012.
32. Lim S, Becker A, Zimmer A, Lu J, Buettner R, Kirfel J. SNAI1-mediated epithelial-mesenchymal transition confers chemoresistance and cellular plasticity by regulating genes involved in cell death and stem cell maintenance. *PLoS One*. 2013; 8:e66558.
33. Deep G, Jain AK, Ramteke A, Ting H, Vijendra KC, Gangar SC, Agarwal C, Agarwal R. SNAI1 is critical for the aggressiveness of prostate cancer cells with low E-cadherin. *Molecular cancer*. 2014; 13:37.
34. Sun L, Mathews LA, Cabarcas SM, Zhang X, Yang A, Zhang Y, Young MR, Klarmann KD, Keller JR, Farrar WL. Epigenetic regulation of SOX9 by the NF-kappaB signaling pathway in pancreatic cancer stem cells. *Stem cells*. 2013; 31:1454–1466.
35. Tai CI, Ying QL. Gbx2, a LIF/Stat3 target, promotes reprogramming to and retention of the pluripotent ground state. *J Cell Sci*. 2013; 126(Pt 5):1093–1098.
36. Shipitsin M, Campbell LL, Argani P, Weremowicz S, Bloushtain-Qimron N, Yao J, Nikolskaya T, Serebryiskaya T, Beroukhim R, Hu M, Halushka MK, Sukumar S, Parker LM, Anderson KS, Harris LN, Garber JE, et al. Molecular definition of breast tumor heterogeneity. *Cancer Cell*. 2007; 11:259–273.
37. Al-Hajj M, Wicha MS, Benito-Hernandez A, Morrison SJ, Clarke MF. Prospective identification of tumorigenic breast cancer cells. *Proc Natl Acad Sci U S A*. 2003; 100: 3983–3988.
38. Gyorfy B, Lanczky A, Szallasi Z. Implementing an online tool for genome-wide validation of survival-associated biomarkers in ovarian-cancer using microarray data from 1287 patients. *Endocrine-related cancer*. 2012; 19: 197–208.
39. Lujambio A, Akkari L, Simon J, Grace D, Tschaharganeh DF, Bolden JE, Zhao Z, Thapar V, Joyce JA, Krizhanovsky V, Lowe SW. Non-cell-autonomous tumor suppression by p53. *Cell*. 2013; 153:449–460.
40. Muller PA, Vousden KH, Norman JC. p53 and its mutants in tumor cell migration and invasion. *J Cell Biol*. 2011; 192:209–218.
41. Dalmasas A, Gonzalez I, Menendez S, Arpi O, Corominas JM, Servitja S, Tusquets I, Chamizo C, Rincon R, Espinosa L, Bigas A, Eroles P, Furiol J, Lluch A, Rovira A, Albanell J, et al. Deficiency in p53 is required for doxorubicin induced transcriptional activation of NF-small ka, CyrillicB target genes in human breast cancer. *Oncotarget*. 2014; 5:196–210.
42. Wang B, Niu D, Lai L, Ren EC. p53 increases MHC class I expression by upregulating the endoplasmic reticulum aminopeptidase ERAP1. *Nat Commun*. 2013; 4:2359.
43. Kanao H, Enomoto T, Kimura T, Fujita M, Nakashima R, Ueda Y, Ueno Y, Miyatake T, Yoshizaki T, Buzard GS, Tanigami A, Yoshino K, Murata Y. Overexpression of LAMP3/TSC403/DC-LAMP promotes metastasis in uterine cervical cancer. *Cancer Res*. 2005; 65:8640–8645.
44. Fujioka S, Niu J, Schmidt C, Sclabas GM, Peng B, Uwagawa T, Li Z, Evans DB, Abbruzzese JL, Chiao PJ. NF-kappaB and AP-1 connection: mechanism of NF-kappaB-dependent regulation of AP-1 activity. *Mol Cell Biol*. 2004; 24:7806–7819.
45. Redhu NS, Saleh A, Halayko AJ, Ali AS, Gounni AS. Essential role of NF-kappaB and AP-1 transcription factors in TNF-alpha-induced TSLP expression in human airway smooth muscle cells. *American journal of physiology Lung cellular and molecular physiology*. 2011; 300:L479–485.
46. Westwick JK, Weitzel C, Minden A, Karin M, Brenner DA. Tumor necrosis factor alpha stimulates AP-1 activity through prolonged activation of the c-Jun kinase. *J Biol Chem*. 1994; 269:26396–26401.
47. Sas L, Lardon F, Vermeulen PB, Hauspy J, Van Dam P, Pauwels P, Dirix LY, Van Laere SJ. The interaction between ER and NFKappaB in resistance to endocrine therapy. *Breast Cancer Res*. 2012; 14:212.
48. Shaulian E, Karin M. AP-1 in cell proliferation and survival. *Oncogene*. 2001; 20:2390–2400.
49. Sayeed A, Konduri SD, Liu W, Bansal S, Li F, Das GM. Estrogen receptor alpha inhibits p53-mediated transcriptional repression: implications for the regulation of apoptosis. *Cancer Res*. 2007; 67:7746–7755.
50. Lion M, Bisio A, Tebaldi T, De Sanctis V, Menendez D, Resnick MA, Ciribilli Y, Inga A. Interaction between p53 and estradiol pathways in transcriptional responses to chemotherapeutics. *Cell Cycle*. 2013; 12:1211–1224.
51. Cancer Genome Atlas N: Comprehensive molecular portraits of human breast tumours. *Nature*. 2012; 490:61–70.
52. Consortium EP. A user's guide to the encyclopedia of DNA elements (ENCODE). *PLoS biology*. 2011; 9:e1001046.

53. Wang B, Niu D, Lam TH, Xiao Z, Ren EC. Mapping the p53 transcriptome universe using p53 natural polymorphs. *Cell Death Differ.* 2014; 21:521–532.
54. Quaedackers ME, van den Brink CE, van der Saag PT, Tertoolen LG. Direct interaction between estrogen receptor alpha and NF-kappaB in the nucleus of living cells. *Molecular and cellular endocrinology.* 2007; 273:42–50.
55. Thomas C, Gustafsson JA. The different roles of ER subtypes in cancer biology and therapy. *Nat Rev Cancer.* 2011; 11:597–608.
56. Lion M, Bisio A, Tebaldi T, De Sanctis V V, Menendez D, Resnick MA, Ciribilli Y, Inga A. Interaction between p53 and estradiol pathways in transcriptional responses to chemotherapeutics. *Cell Cycle.* 2013; 12.
57. Vallabhapurapu S, Karin M. Regulation and function of NF-kappaB transcription factors in the immune system. *Annual review of immunology.* 2009; 27:693–733.
58. Yang A, Walker N, Bronson R, Kaghad M, Oosterwegel M, Bonnin J, Vagner C, Bonnet H, Dikkes P, Sharpe A, Mc Keon F, Caput D. p73-deficient mice have neurological, pheromonal and inflammatory defects but lack spontaneous tumours. *Nature.* 2000; 404:99–103.
59. Menendez D, Shatz M, Resnick MA. Interactions between the tumor suppressor p53 and immune responses. *Curr Opin Oncol.* 2013; 25:85–92.
60. Breitling R, Armengaud P, Amtmann A, Herzyk P. Rank products: a simple, yet powerful, new method to detect differentially regulated genes in replicated microarray experiments. *FEBS Lett.* 2004; 5733:83–92.
61. Raimondi I, Ciribilli Y, Monti P, Bisio A, Pollegioni L, Fronza G, Inga A, Campomenosi P. P53 family members modulate the expression of PRODH, but not PRODH2, via intronic p53 response elements. *PLoS One.* 2013; 8:e69152.
62. Ciribilli Y, Monti P, Bisio A, Nguyen HT, Ethayathulla AS, Ramos A, Foggetti G, Menichini P, Menendez D, Resnick MA, Viadiu H, Fronza G, Inga A. Transactivation specificity is conserved among p53 family proteins and depends on a response element sequence code. *Nucleic Acids Res.* 2013; 41:8637–8653.
63. Ciribilli Y, Andreotti V, Menendez D, Langen JS, Schoenfelder G, Resnick MA, Inga A. The coordinated p53 and estrogen receptor cis-regulation at an FLT1 promoter SNP is specific to genotoxic stress and estrogenic compound. *PLoS One.* 2010; 5:e10236.
64. Bisio A, De Sanctis V V, Del Vescovo V, Denti MA, Jegga AG, Inga A, Ciribilli Y. Identification of new p53 target microRNAs by bioinformatics and functional analysis. *BMC Cancer.* 2013; 13:552.

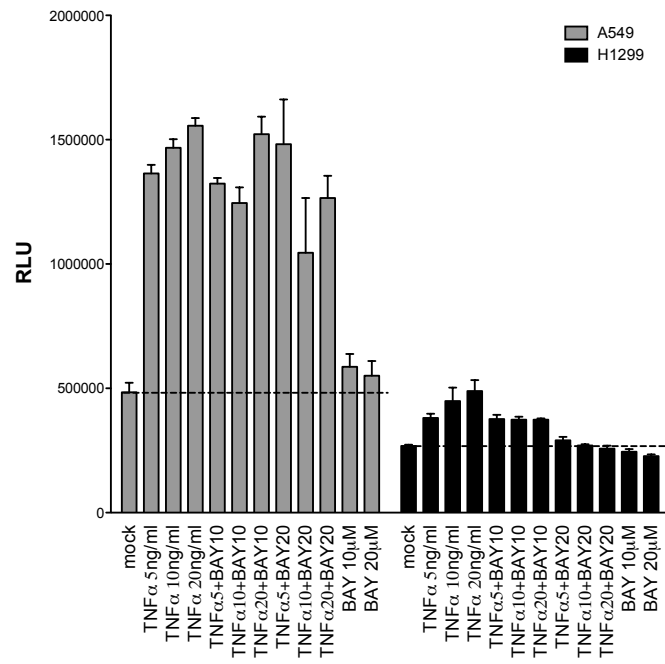
SUPPLEMENTARY FIGURES AND TABLES



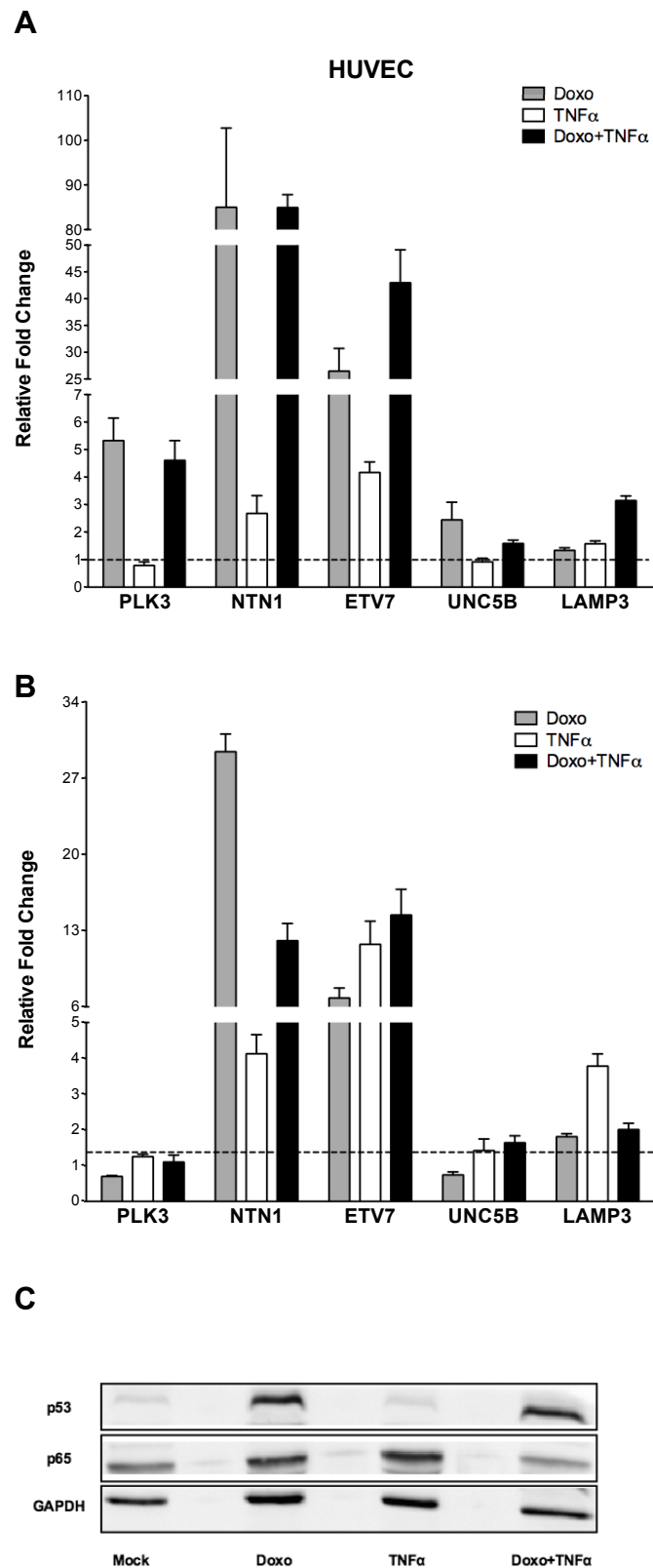
Supplementary Figure S1: Gene reporter and qPCR assays to probe p53 and p65 activity in MCF7 cells. (A) **Gene reporter assays.** To test p53 and NF κ B responsiveness and effect of co-activation on reporter activity, MCF7 cells were seeded onto 24-well plates 24 hours before transfection. 250ng of pGL3 promoter based reporters, containing portion of p21 and MDM2 promoter (harboring p53 response elements) or a p65 responsive repeat of kB responsive sequence plasmids, were co-transfected along with 50 ng of pRL-SV40 vector, to normalize for transfection efficiency. When appropriate, 25nM of siRNA double strand oligonucleotides (Qiagen, Milan, Italy) against human p53 (si-hp53) were added to the transfection mixture. A scramble siRNA with no match in human coding RNA (25nM) was used as control (Qiagen). Cells were transiently transfected using the HighPerFect transfection reagent (Qiagen). Twenty-four hours after transfection, cells were treated with Doxo (1.5 μ M) increasing concentration of TNF α (1, 5, 10 ng/ml) and with a combination of the two compounds. Sixteen hours post-treatment cells were washed with PBS and lysed with Passive Lysis Buffer 1X and luciferase activity was analyzed using the Dual-Luciferase Reporter Assay System (Promega, Milan, Italy). MCF7 cells were transiently transfected with pGL3-based reporter vectors containing fragments of the p53 responsive MDM2 intron 1, p21 promoter or a p65 responsive repeat of kB response elements. A control vector expressing the Renilla luciferase was cotransfected to normalize for transfection efficiency. Short ds-RNA oligonucleotides targeting the p53 mRNA or a scramble control were also co-transfected. 24 hours after the transfection cells were treated as indicated. Dual luciferase assays were performed 16 hours after the treatment. Presented in the graph are the average relative light units and the standard deviations of three biological replicates. (B) **qPCR assays.** Relative changes in the expression of the P21, MDM2, TNF α , and MCP1 genes were measured by qPCR in MCF7 cells treated with Doxo (1.5 μ M), TNF α (5 ng/ml) or the combination of the two drugs. mRNA was isolated 16 hours after treatment, as described in the Methods Section. Bars plot the average fold of induction relative to the mock condition and error bars plot the standard deviations of three technical replicates. The entire experiment was repeated two times with consistent results.



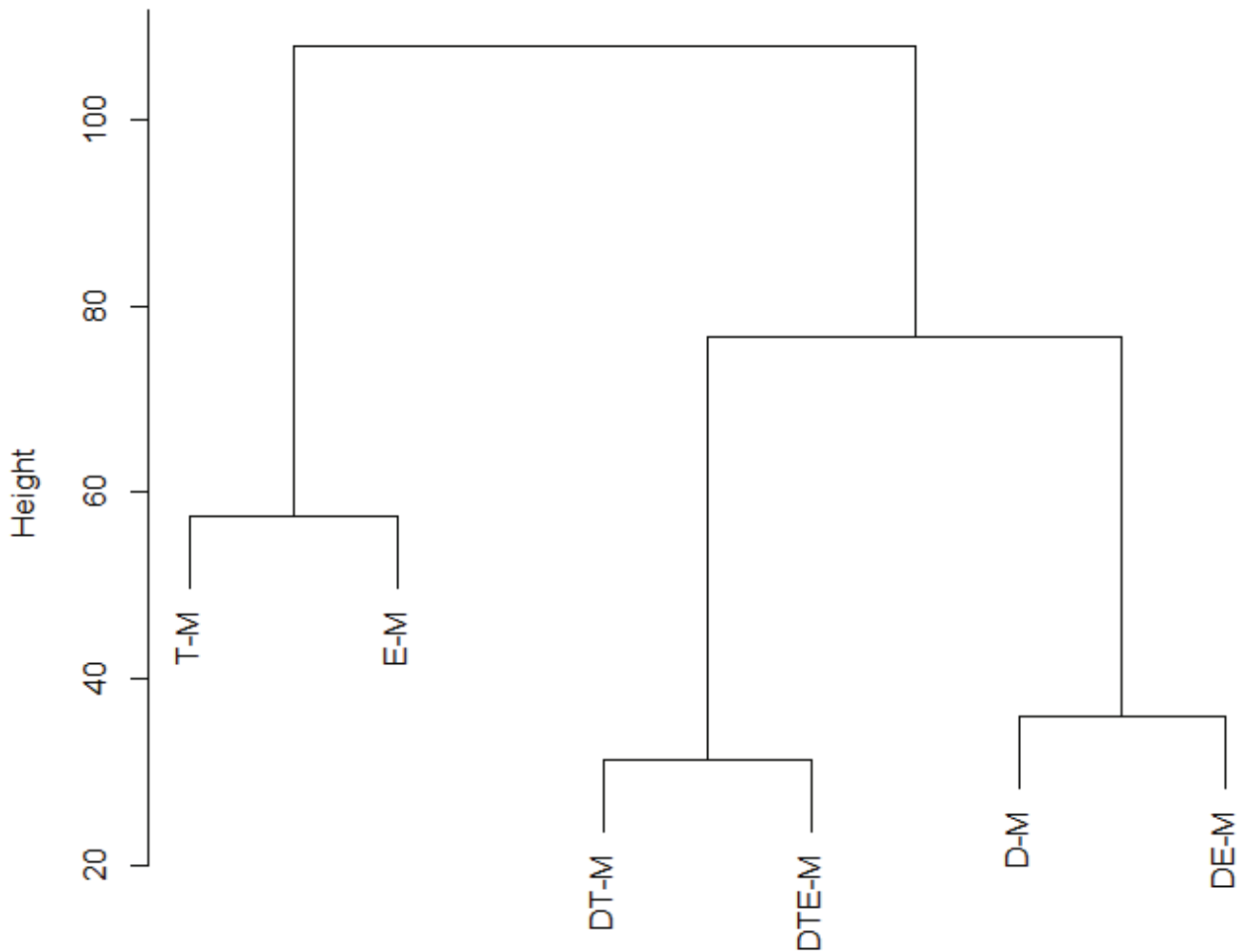
Supplementary Figure S2: p53 and p65 protein levels in MCF7 cells treated with Doxo, or/and TNF α , or/and BAY 11-7082. Immunodetection of p65, p53 and the GAPDH loading control, from total MCF7 protein extracts prepared from cell treated with the indicated molecules. See Methods for details on the antibodies used.



Supplementary Figure S3: Gene reporter assay in A549 and H1299 cells. The experiment was performed as described for Figure S1. The different concentrations of TNF α and BAY are indicated.



Supplementary Figure S4: PLK3, NTN1, ETV7, UNC5B and LAMP3 responsiveness varied among biological repeats in HUVEC cells. (A, B) Relative fold change expression of the indicated genes measured by qPCR. The two panels are representative of two different results each obtained in two biological replicates. (C) Western blot and immune-detection of p53, p65 and the GAPDH loading control.



Supplementary Figure S5: Hierarchical cluster analysis. Hierarchical cluster analysis of all the treatments performed in MCF7 cells and profiled with microarrays, based on the fold changes of 1099 genes whose expression resulted to be significantly changed in at least one of the treatments (Euclidean distances and Ward clustering method). D-M (doxo vs mock); T-M (TNF α vs mock); E-M (E2 vs mock); DT-M (Doxo + TNF α vs mock); DE-M (Doxo + E2 vs mock); DTE-M (Doxo + TNF α + E2 vs mock).